AD-A152 344 SES-200 (SURFACE EFFECT SHIP) TECHNICAL EVALUATION TEST 1/3
REPORT(U) MARITIME DYNAMICS INC TACOMA WA
J D ADAMS ET AL. JAN 84 MD-R-1199-2 USCG-D-1-85
UNCLASSIFIED N00167-83-C-0047 F/G 13/10 NL

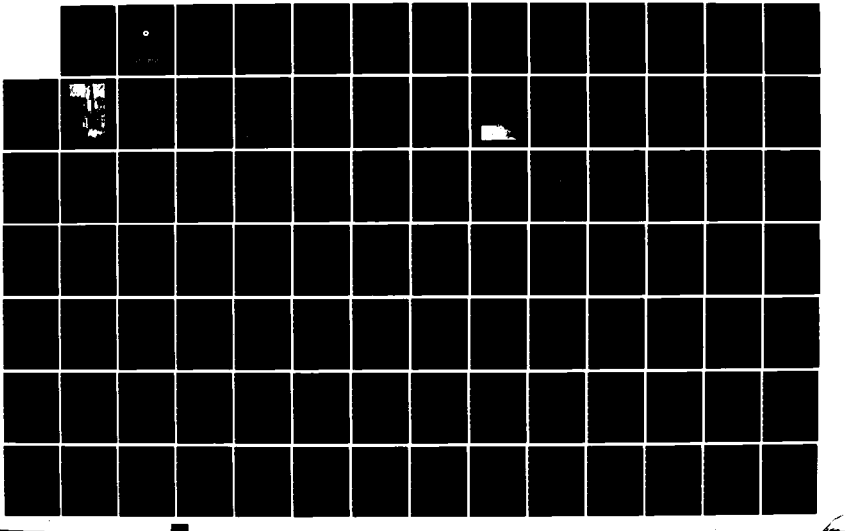

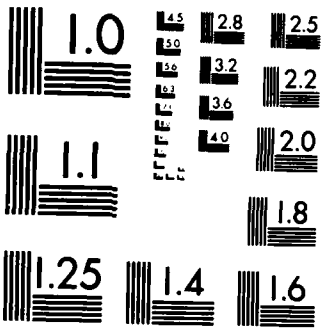

MICROCOPY RESOLUTION TEST CHART
NATIONAL BUREAU OF STANDARDS-1963-A

Report No. CG-D-1-85

SES-200 TECHNICAL EVALUATION TEST REPORT

JANUARY 1984

FINAL REPORT

Prepared for

DEPARTMENT OF TRANSPORTATION
UNITED STATES COAST GUARD
Office of Research and Development
Washington, D.C. 20593

NOTICE

This document is disseminated under the sponsorship of the Department of Transportation in the interest of information exchange. The United States Government assumes no liability for its contents or use thereof.

The contents of this report do not necessarily reflect the official view or policy of the Coast Guard; and they do not constitute a standard, specification, or regulation.

This report, or portions thereof may not be used for advertising or sales promotion purposes. Citation of trade names and manufacturers does not constitute endorsement or approval of such products.

Technical Report Documentation Page

1. Report No.	2. Government Accession No.	3. Recipient's Catalog No.
CG-D-1-85		

4. Title and Subtitle	5. Report Date
SES-200 TECHNICAL EVALUATION TEST REPORT	January 1984
	6. Performing Organization Code
7. Author(s)	8. Performing Organization Report No.
John D. Adams, A. W. Ernest, J. H. Lewis	MD-R-1199-2
9. Performing Organization Name and Address	10. Work Unit No. (TRAIS)
Maritime Dynamics, Inc. 8100 27th Street West, Tacoma, WA 98466 1169 East Ash Avenue, Fullerton, CA 92631	11. Contract or Grant No. N00167-83-C-0047
	13. Type of Report and Period Covered
12. Sponsoring Agency Name and Address	Final Report April-December 1983
United States Coast Guard Headquarters G-DMT-2/54 Washington, D. C. 20593	14. Sponsoring Agency Code

15. Supplementary Notes

16. Abstract

An extensive technical evaluation of the SES-200 High Length-to-Beam (L/B) Surface Effect Ship was conducted. Performance and maneuvering tests were conducted in the Chesapeake Bay and seakeeping tests were conducted in the Atlantic Ocean 200 miles off Cape Hatteras, North Carolina. This report presents a detailed analysis of the test data.

17. Key Words	18. Distribution Statement
Surface Effect Ship Ride Control SES-200 SES Test and Evaluation Seakeeping Maneuvering	Document is available to the public through the National Technical Information Service, Springfield, Virginia 22161

19. Security Classif. (of this report)	20. Security Classif. (of this page)	21. No. of Pages	22. Price
Unclassified	Unclassified	202	

TABLE OF CONTENTS

TABLE OF CONTENTS (Cont.)

TABLE OF CONTENTS (Cont.)

TABLE OF CONTENTS (Cont.)

LIST OF FIGURES

LIST OF FIGURES (Cont.)

LIST OF FIGURES (Cont.)

LIST OF FIGURES (Cont.)

LIST OF FIGURES (Cont.)

Between these hump speeds (Figure 4-4) and at speeds above the primary hump (Figure 4-5), the wave drag is lower as the cushion wave profile does not tilt the resultant force as much.

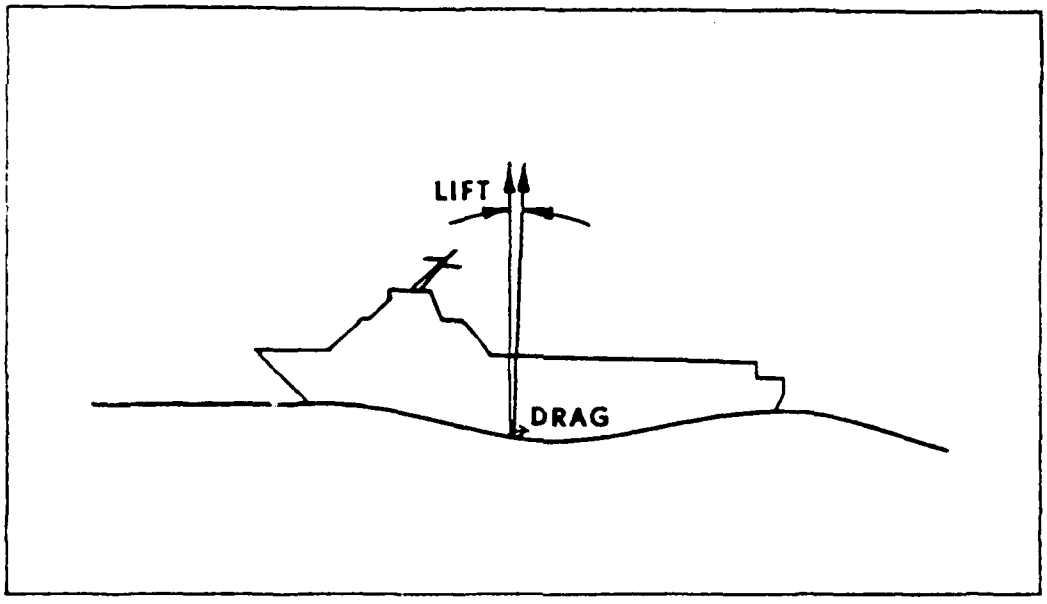

Figure 4-4 CUSHION WAVE PROFILE BETWEEN HUMP SPEEDS

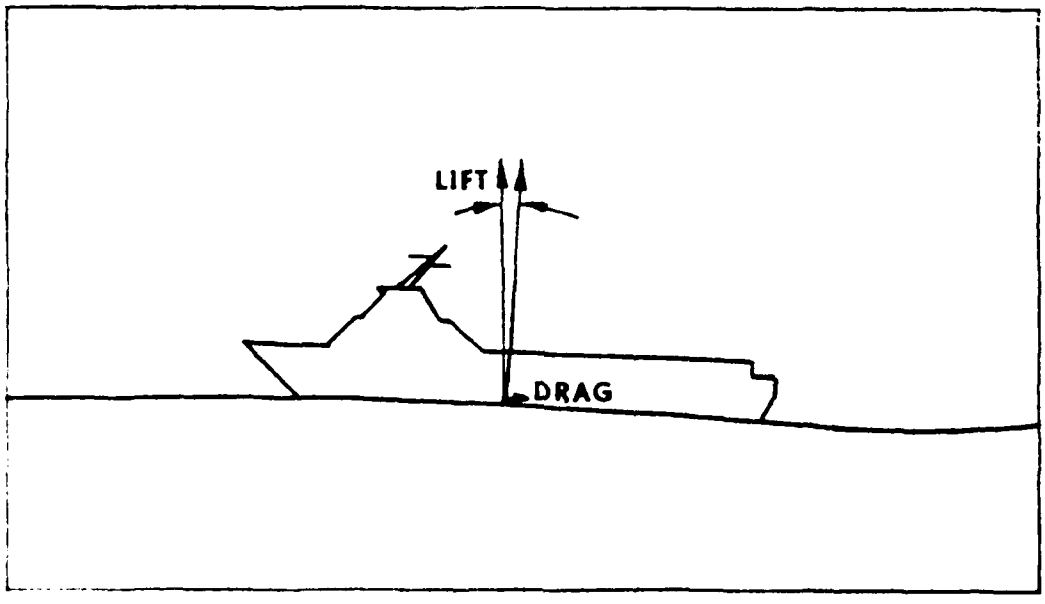

Figure 4-5 CUSHION WAVE PROFILE ABOVE PRIMARY HUMP SPEED

As shown in Figure 4-2, cushion air pressure distorts the water surface which tilts the resultant force that the cushion exerts on the water. This produces a drag force known as cushion wave making resistance since the water surface distortion creates waves. These waves travel at speeds which depend on the distance between successive crests. At the primary and secondary hump speeds, the wavelengths maximize the inclination of the resultant force (see Figures 4-2 and 4-3) and this produces the peaks or humps in the drag curve at these speeds.

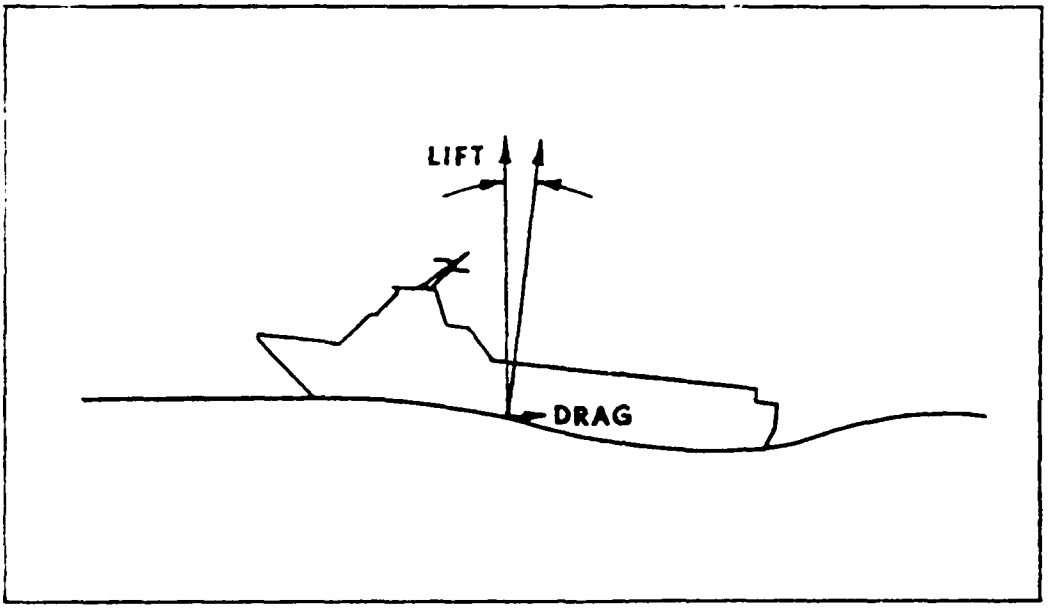

Figure 4-2 CUSHION WAVE PROFILE AT PRIMARY HUMP SPEED

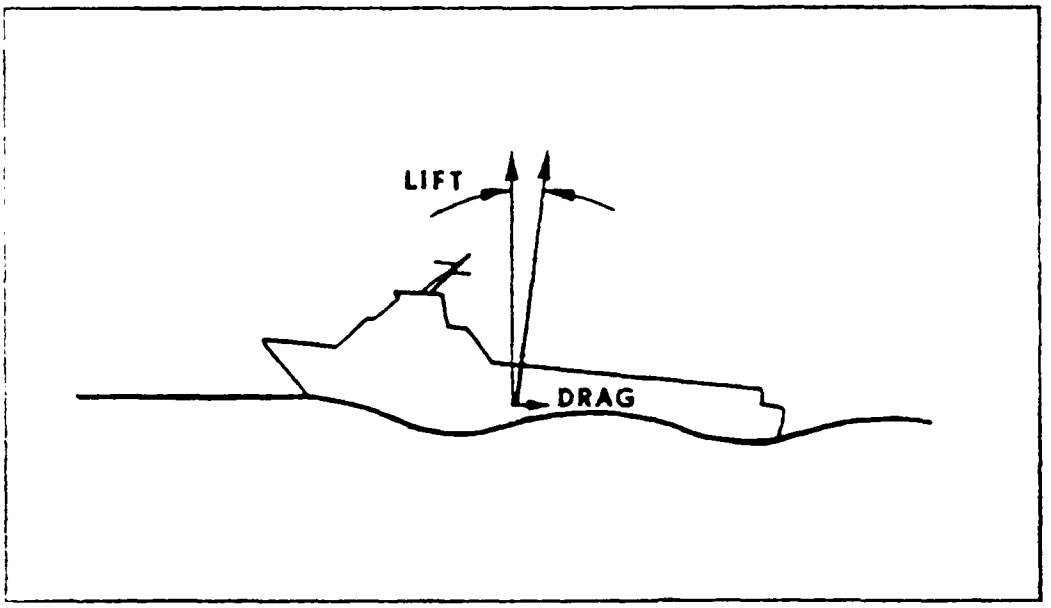

Figure 4-3 CUSHION WAVE PROFILE AT SECONDARY HUMP SPEED

4. TEST SUMMARY

A general discussion of the influence of length-to-beam proportions on SES resistance is presented in Section 4.1. This discussion is useful in understanding the results of the performance tests which are summarized in Section 4.2. Section 4.3 presents the major results of the seakeeping tests and Section 4.4 summarizes results of the maneuvering and stability tests.

4.1 RESISTANCE

An SES's resistance is made up of the components illustrated in Figure 4-1. The two principal components are: sidehull drag and cushion wave making resistance.

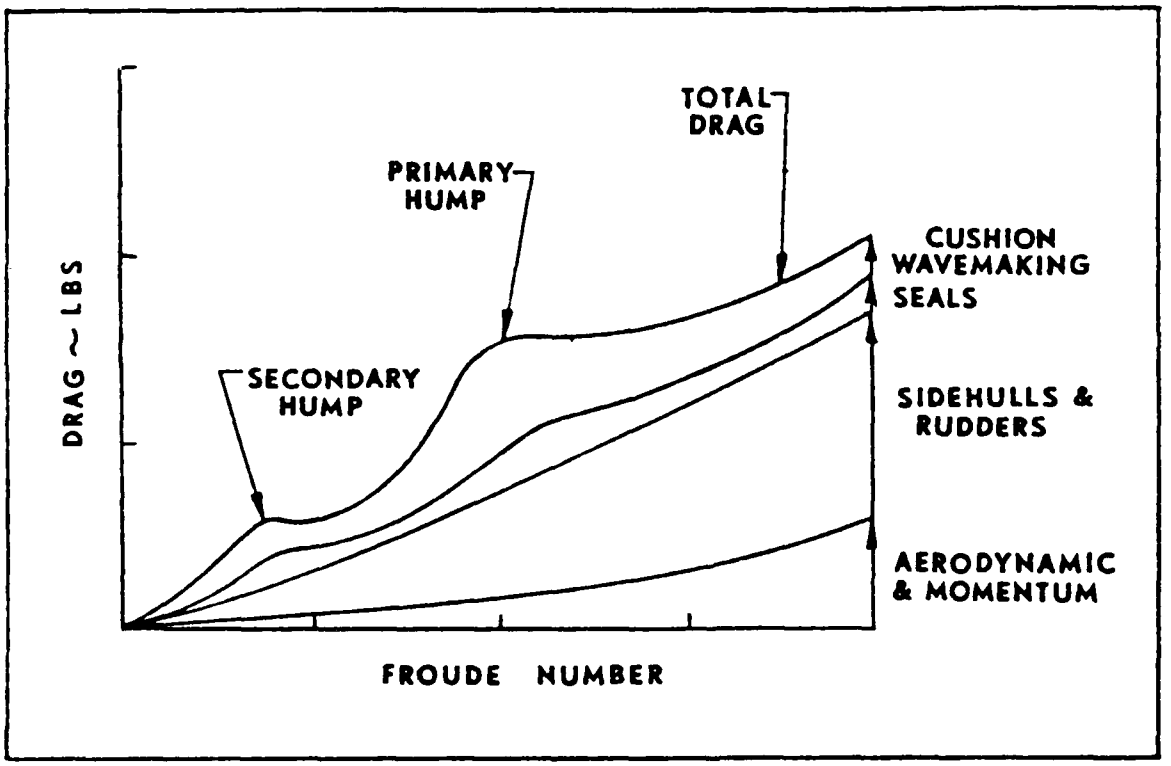

Figure 4-1 SES DRAG COMPONENTS

Sidehull drag typically increases with speed; however, cushion wave drag has one small peak referred to as secondary hump and one large peak referred to as primary hump. The magnitude of these peaks and the Froude numbers at which they occur depends on the length-to-beam ratio of the air cushion. Ratios of 2 to 3 are typically designated as "low" while ratios of 4 to 8 are referred to as "high".

Figure 3-4

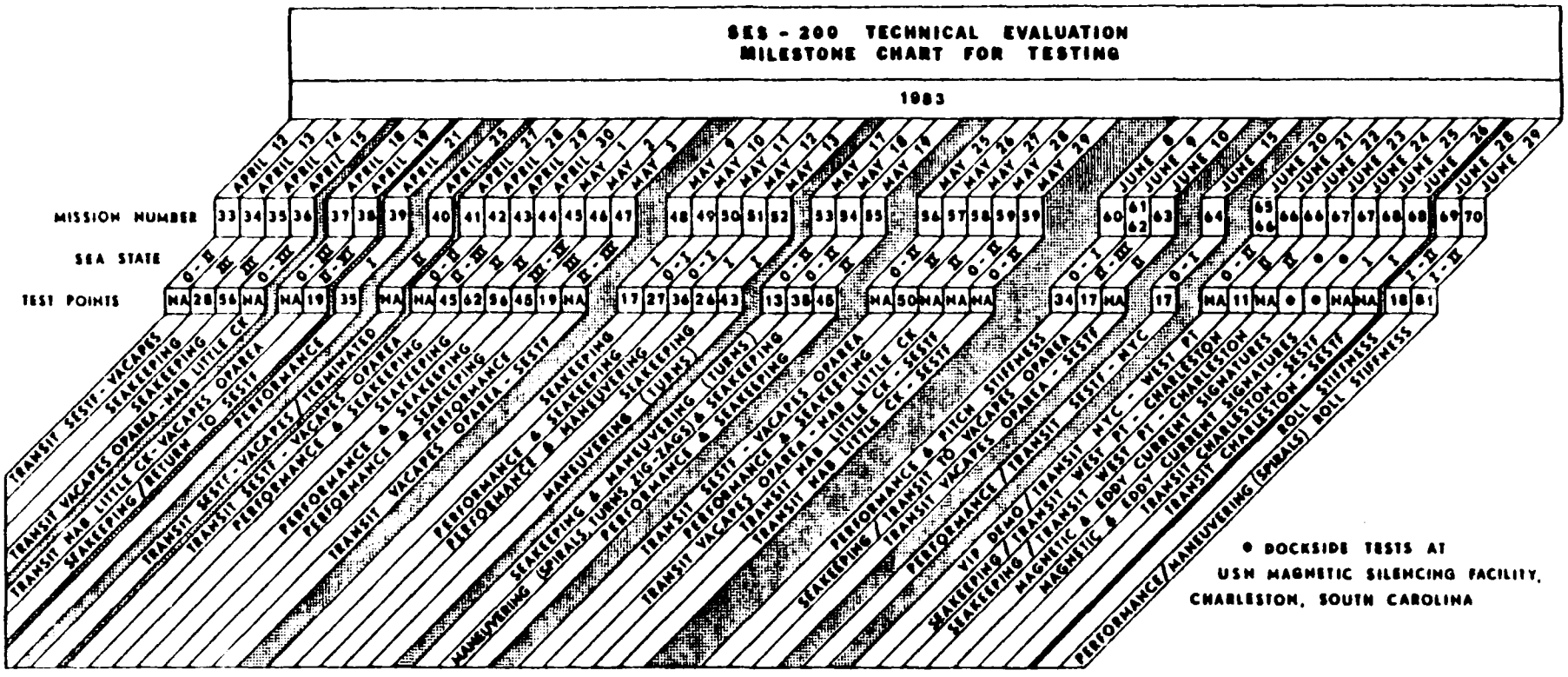
SES - 200 TECHNICAL EVALUATION
MILESTONE CHART FOR TESTING
1983
MISSION NUMBER
SEA STATE
TEST POINTS
TRANSIT SESTF - VACAPES
SEAKEEPING
TRANSIT VACAPES OPAREA - MAD LITTLE CK
SEAKEEPING/RETURN TO SESTF
TRANSIT SESTF - VACAPES/TERMINATED
PERFORMANCE
TRANSIT SESTF - VACAPES OPAREA
PERFORMANCE & SEAKEEPING
TRANSIT VACAPES OPAREA - SESTF
MANEUVERING (SPIRALS, TURNS, ZIG-ZAGS) & SEAKEEPING
TRANSIT MAD LITTLE CK - VACAPES OPAREA
PERFORMANCE & PITCH STIFFNESS
TRANSIT TO VACAPES OPAREA - SESTF
SEAKEEPING/TRANSIT SESTF - NYC
VIP DEMO/TRANSIT NYC - WEST PT
SEAKEEPING/TRANSIT WEST PT - CHARLESTON
MAGNETIC & EDDY CURRENT SIGNATURES
TRANSIT CHARLESTON - SESTF
ROLL STIFFNESS
PERFORMANCE/MANEUVERING (SPIRALS) ROLL STIFFNESS
• DOCKSIDE TESTS AT
USN MAGNETIC SILENCING FACILITY,
CHARLESTON, SOUTH CAROLINA

Back up wave height sensors were carried onboard the SES-200 and each day before starting and after completing testing, the crew deployed a small wave measuring buoy for approximately one hour. Additionally, a radar altimeter was mounted on the bow of the SES-200 to measure the vertical distance to the wave surface. Using special data processing techniques, the craft's motion was subtracted from this signal and a measurement of wave height was obtained.

During head sea tests, over 200 cycles of ship motion were recorded on each test point as this is an accepted standard for seakeeping tests. At off-head sea conditions, fewer cycles were recorded in order to cover the planned matrix of tests in the time available.

Recorded data were digitized and processed by SESTF personnel. Strip charts, mean values and standard deviations of each measurement were produced for all dedicated test conditions. Power spectra, histograms and other statistical data were computed for selected seakeeping tests.

Seakeeping data were subjected to special qualification tests known as stationarity checks. These tests assisted in identifying data segments in which unacceptable variations in the ship's operating condition or the sea state occurred. It is believed that this is the first application of these data qualification methods in full-scale ship trials.

A milestone chart for the test missions is shown in Figure 3-4. During the 79-day span covered by testing, the SES-200 was underway conducting tests or transiting to and from test areas a total of 41 days. The total underway time was 530 hours; 838 test points were recorded and 70 hours of test data have been processed. Five separate trips were made to the NOAA Buoy to obtain adequate sea state coverage. Seakeeping tests were conducted in Sea State II through high Sea State V. The longest at-sea period was seven days, and the longest non-stop transit covered 900 nautical miles.

Performance and Seakeeping Tests were conducted in both the Chesapeake Bay and in the Atlantic Ocean. The ocean operations were conducted approximately 200 miles due east of Cape Hatteras, NC within a 30-mile radius of NOAA Buoy 'RY41001' (Figure 3-2).

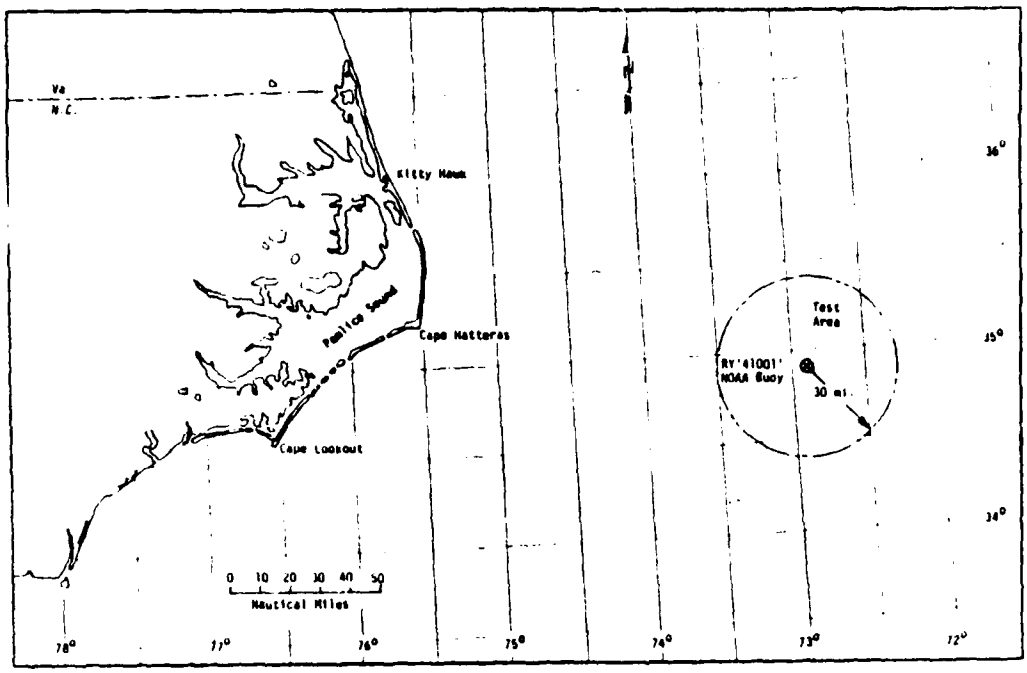

Figure 3-2 ATLANTIC OCEAN TEST AREA

This buoy (Figure 3-3) contains sensors which measure wave height, wind speed, wind direction, and the air and water temperatures. Every hour the buoy transmits this information to a satellite which relays it to a ground station.

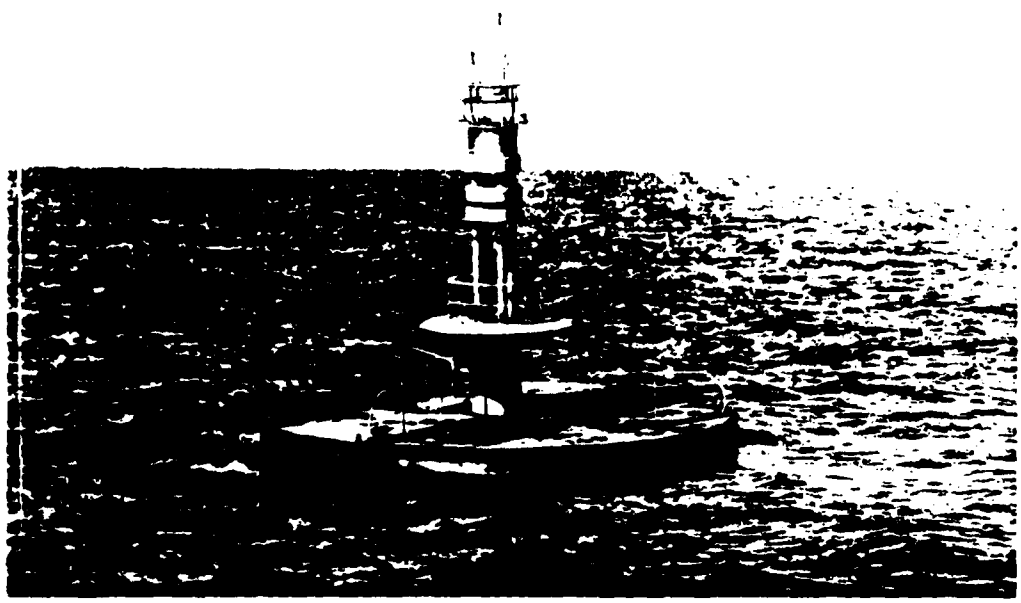

Figure 3-3 NOAA BUOY 'RY41001'

3. TECHNICAL EVALUATION PROGRAM

Prior to initiation of the Technical Evaluation, SESTF personnel assembled a Data Acquisition System and installed it on the SES-200. This system simultaneously recorded sixty ship and subsystem measurements during each test mission. Table 3-1 lists the primary measurements.

Table 3-1

PRINCIPAL DATA ACQUISITION SYSTEM MEASUREMENTS

Ship Condition:	Speed, Heading	Torques:	Propulsion Engines
Angular Motions:	Pitch, Roll	Fuel Flows:	Lift & Prop. Engines
Angular Rates:	Pitch, Roll, Yaw	RPMs:	Lift & Prop. Engines
Vertical Accelerations:	Bow, LCG, Stern	Rudder Position:	Port and Starboard
Lateral Accelerations:	Bow, LCG	Pressures:	Fan, Cushion, Seal
Long. Accelerations:	Bow, LCG	VV Positions:	Four Places

Tests were conducted in the following categories:

- Performance
- Seakeeping
- Maneuvering and Stability

Performance and Maneuvering Tests which required calm water were conducted in the Chesapeake Bay (Figure 3-1). The Maneuvering Tests were confined to the area covered by the NATC Chesapeake Test Range in order to obtain accurate tracking information.

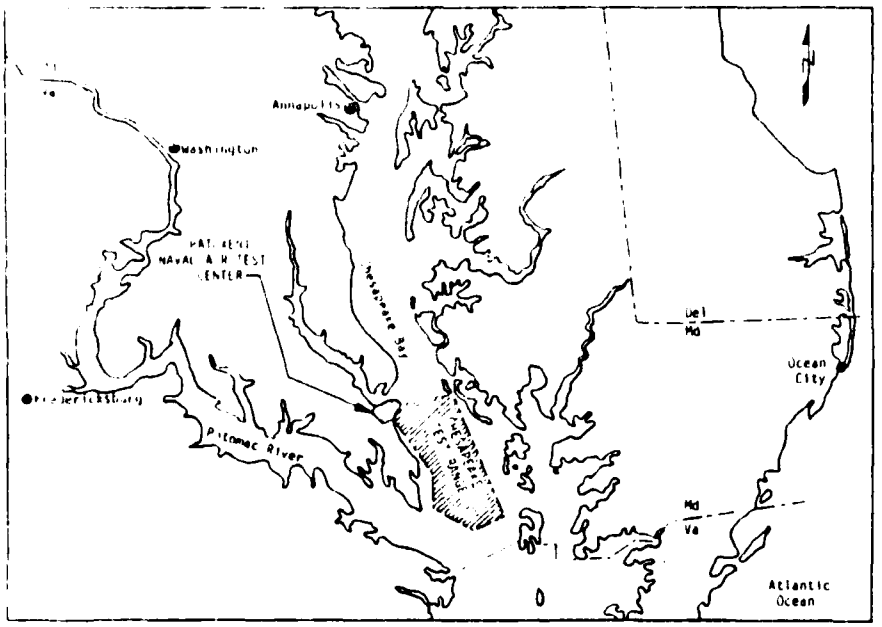

Figure 3-1 CHESAPEAKE BAY TEST AREA

Prior to initiation of the Technical Evaluation, the Surface Effect Ship Test Facility installed a Ride Control System (RCS) on the SES-200. RCS components include pressure sensors, a small electronic control unit, and a set of louver valves known as vent valves which are connected to the air cushion (Figure 2-1). In waves, the RCS minimizes pressure changes in the ship's air cushion by varying the vent valve air flow rate. This smooths out the ship's vertical motion.

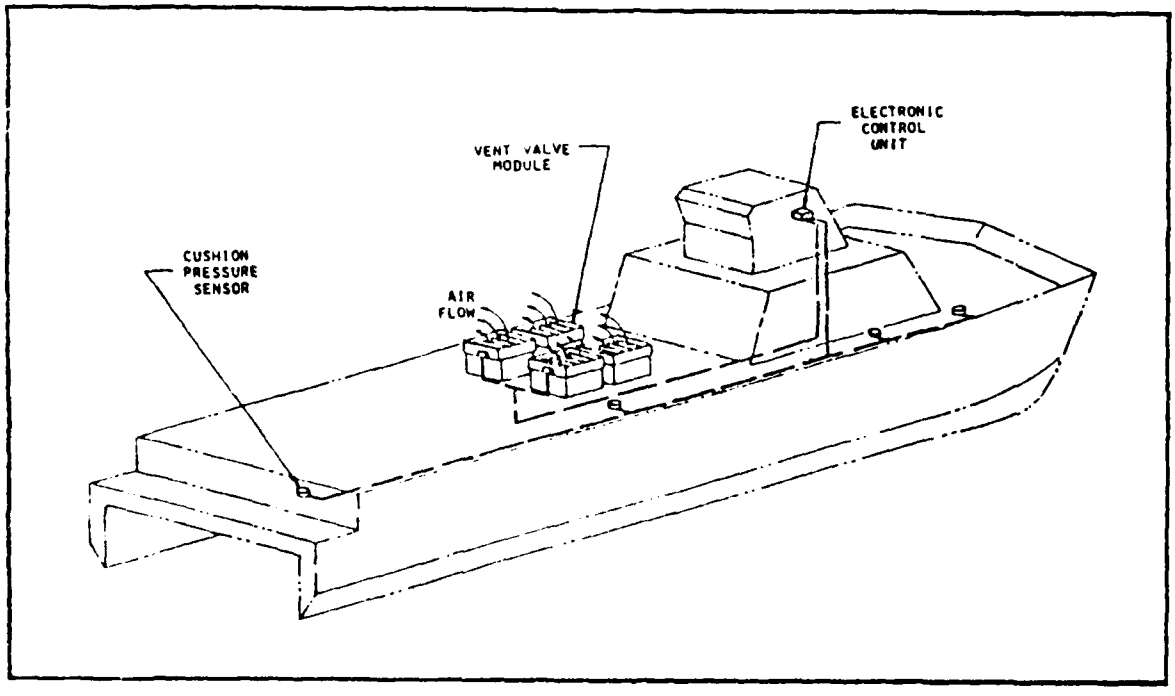

Figure 2-1 SES-200 RIDE CONTROL SYSTEM

The SES-200 RCS is a prototype unit built by Maritime Dynamics, Inc. Research and development for this system was initiated in December 1979 and completed in April 1981 using the XR-1D SES testcraft. The microprocessor-based control unit can be used on various size SES with only minor hardware and software modifications. Each vent valve module consists of three extruded aluminum louvers driven by a small hydraulic actuator. The SES-200's four vent valve modules were mounted on the main deck so that technical personnel could easily witness their operation during testing. In a production SES, the vent valves could exhaust out the sides to maximize use of deck space for other purposes.

The catamaran hull was commercially constructed of welded marine grade aluminum. Its structural arrangement is similar to that of a conventional longitudinally framed ship; tee extrusions stiffen and support the shell plating in the longitudinal direction while full depth bulkheads provide strength in the transverse direction. The catamaran hull provides excellent intact stablity and the full depth bulkheads provide compartmentalization for damage control. Other features of this hull form include a large internal volume and a spacious deck area.

The only SES-200 systems not found on conventional ships are the lift fans which provide the cushion airflow, the bow and stern seals which contain the air cushion, and the Ride Control System which smooths out wave induced pressure fluctuations in the air cushion. The propulsion, lift and electrical power plants are all standard marine diesels. Two fixed pitch three-bladed propellers are used for propulsion and two centrifugal fans are used for lift. The lift fans are similar to industrial units used in ventilation and material handling applications. Additional information on the vessel's structure, machinery and outfit is contained in Appendix A.

Power plants, propellers and lift fans used in the SES-200 are the original units installed in the BH-110. No significant machinery changes or modifications were made when the BH-110 was stretched. Table 2-2 compares the principal characteristics of the high length-to-beam SES-200 with those of the low length-to-beam BH-110. For the same installed horsepower, the SES-200 displacement is 65 tons (45%) greater than the BH-110, and it has nearly three times the fuel capacity. Less than 20% of the volume in the 50 ft hull extension was utilized to increase the fuel tankage. The remaining space has been left vacant for future Navy or Coast Guard additions.

Table 2-2

COMPARISON OF SES-200 AND BH-110
PRINCIPAL CHARACTERISTICS

	SES-200	BH-110
Displacement (100% Fuel & Supplies)(LT)	205	140
Fuel (LT)	59.6	21.7
Length Overall (ft)	159.1	109.1
Beam Overall (ft)	39.0	39.0
Depth Molded (ft)	15.2	15.2
Navigation Drafts (incl. rudder (ft):		
Hullborne FLD	9.1	8.3
Cushionborne FLD	5.1	5.5
Wet Deck Height (ft):		
Bow	7.5	7.5
Stern	5.1	5.0
Cushion Length/Beam Ratio	4.15	2.65

Table 2-1
SES-200
PRINCIPAL CHARACTERISTICS

WEIGHTS:		**SYSTEMS:**	
Displacement(100%Fuel&Supplies)(LT)	205	Propulsion Engines	Two GM 16V-149TI Diesels (1600 shp each)
Fuel (LT)	39.6	Propulsors	Two Three-bladed 40" Dia. by 48" Pitch
Light Ship (LT)	128	Lift Engines	Two GM 8V-92TI Diesels (435 shp each)
DIMENSIONS:		Lift Fans	Two Bell 42" Dia. OMDI Centrifugal
Length Overall (L_{OA})(ft)	150.1	Electrical:	
Beam Overall (B_{OA})(ft)	39.0	Primary	One GM 3-71 55-kW 60 Hz Diesel
Depth Molded (ft)	15.2	Back-Up	One KATO DAMAC 14 40-Kw 60 Hz
Mast Height Above Keel (ft)	41.5	Steering	Twin rudder, differential thrust and reverse
Navigation Drafts (incl. rudder(ft)):			with propellers
Hullborne FLD	9.3		
Cushionborne FLD	5.5	**CONSTRUCTION:**	
Wet Deck Height (ft):		Structure	Welded 5086-Aluminum
Bow	7.5	Bow Seal	Two-dimensional elastomer-coated fingers
Stern	5.0		(8 total)
Effective Cushion Length (L_C)(ft)	133.3	Stern Seal	Three-lobe elastomer-coated bag
Effective Cushion Beam (B_C)(ft)	31.6		
Cushion Length/Beam Ratio	4.25		
Nominal Cushion Pressure @ FLD (psf)	92		

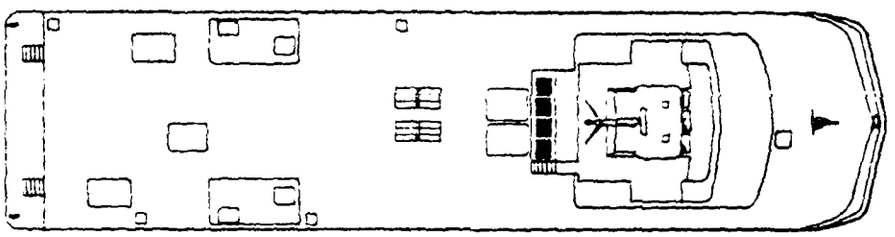

PLAN VIEW

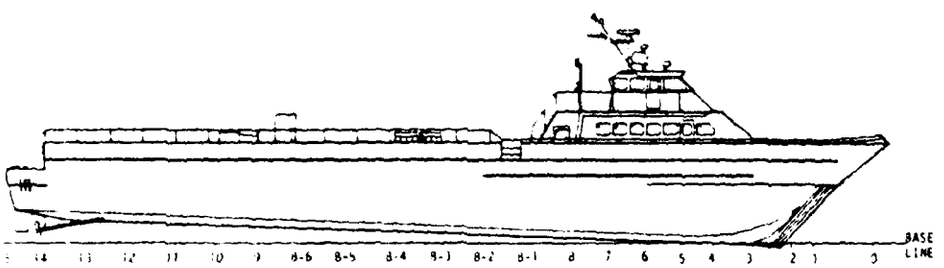

OUTBOARD PROFILE

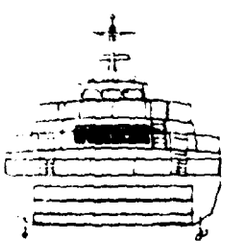

STERN VIEW

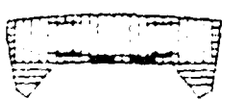

MID SHIP SECTION

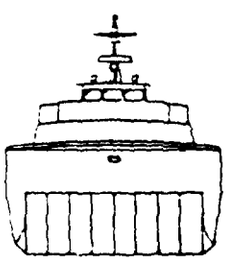

BOW VIEW

2. SES-200 BACKGROUND AND DESCRIPTION

In September 1980, the Navy procured a 110-ft low length-to-beam SES designated the BH-110 Mark I. This vessel was purchased under a Navy/Coast Guard program which had the following overall objectives:

- Evaluation of the 2.65 length-to-beam BH-110
- Modification of the BH-110 to a 4.25 length-to-beam
- Evaluation of the 4.25 length-to-beam platform

The BH-110 Mark I was built in New Orleans, LA in 1978 by a joint venture between Bell Aerospace Textron, Division of Textron, Inc., and Halter Marine, Inc. Prior to Navy acqusition, the vessel had been used by Bell-Halter to demonstrate and market the SES concept. During this demonstration period, the Coast Guard and the Urban Mass Transportation Administration leased the BH-110 and conducted a one-month test program in the lower Chesapeake Bay and coastal Atlantic waters off Norfolk, Virginia (Reference 2-1).

During these initial trials, the BH-110 demonstrated potential for being able to perform many Coast Guard missions. As a result, the Navy procurement included modifications to the BH-110 to make it function as a Coast Guard patrol boat. On 9 May 1981, the Navy accepted the vessel and designated it the SES-110. Eight weeks of Navy evaluation trials were conducted in the Gulf of Mexico (Reference 2-2), then the vessel was turned over to the Coast Guard Eighth District with headquarters in New Orleans, Louisiana.

The Coast Guard commissioned the vessel as the USCG Dorado (WSES-1). Six months of patrol boat type operations were performed with the Dorado throughout Eighth District waters (Reference 2-3), including law enforcement exercises as far south as the Yucatan Channel.

This operational evaluation confirmed the SES's ability to perform certain Coast Guard missions better than conventional vessels. Consequently, the Coast Guard has procured three (3) production versions of the BH-110 and placed them in law enforcement service operating out of Key West, Florida.

In January 1982, the Navy returned the BH-110 Mark I to Bell-Halter where its length-to-beam ratio was increased by adding a 50 ft hull extension amidships. The Navy accepted the stretched vessel on 24 September 1982 and designated it the SES-200. Table 2-1 lists the vessel's principal characteristics.

1. INTRODUCTION

Surface Effect Ships (SES) can operate hullborne like displacement ships or they can operate in a cushionborne mode by pressurizing the region between the catamaran hulls with air.

The air cushion exerts both a lift and a drag force on the hull as it moves over the water surface. The drag force, known as cushion wave making drag, represents a significant percentage of total SES resistance and hence, the required propeller thrust. Selection of cushion length-to-beam proportions is a fundamental part of SES design because the ratio of these dimensions determines the wave making resistance characteristics.

The Navy has been conducting research on the effect of length-to-beam proportions on SES performance, seakeeping and maneuvering since 1970. For ocean capable vessels, research showed that length-to-beam ratios of 4 to 1 or greater offer efficient operation at task force speeds without compromising the SES advantage of operating at significantly higher speeds. This balanced performance is attributable to shifting the peak of the high wave drag region known as "hump" outside the operating envelope. The name "High Length-to-Beam SES" has been given to these vessels to distinguish them from the previous generation of Navy SES which had lower length-to-beam ratios and had to be propelled through a high drag speed regime in order to attain efficient cruise speeds.

To validate high length-to-beam research, NAVSEA procured a 110 ft commercial SES and increased its length-to-beam ratio from 2.65 to 4.25 by installing a 50 ft hull extension amidships. This vessel is the SES-200 (Figure 1-1). It is the only large high length-to-beam surface effect ship in the world.

Under the direction of NAVSEA 05R47, an extensive Technical Evaluation of the SES-200 has been conducted for the Navy and the Coast Guard Office of Research and Development. Test planning, instrumentation, test operations and data processing have been performed by the Surface Effect Ship Test Facility located at the Naval Air Test Center, Patuxent River, Maryland. Under Contract N00167-83-C-0047, Maritime Dynamics, Inc. supported the test program, analyzed the test data and prepared this test report. The first five (5) sections present a synopsis of the entire program. Most of the material contained in these five (5) sections was previously presented in the SES-200 Technical Evaluation, Executive Summary Report (Reference 1-1). The remaining sections contain detailed discussions of the test program and the test results.

Figure 1-1 **SES - 200 HIGH LENGTH - TO - BEAM SURFACE EFFECT SHIP**

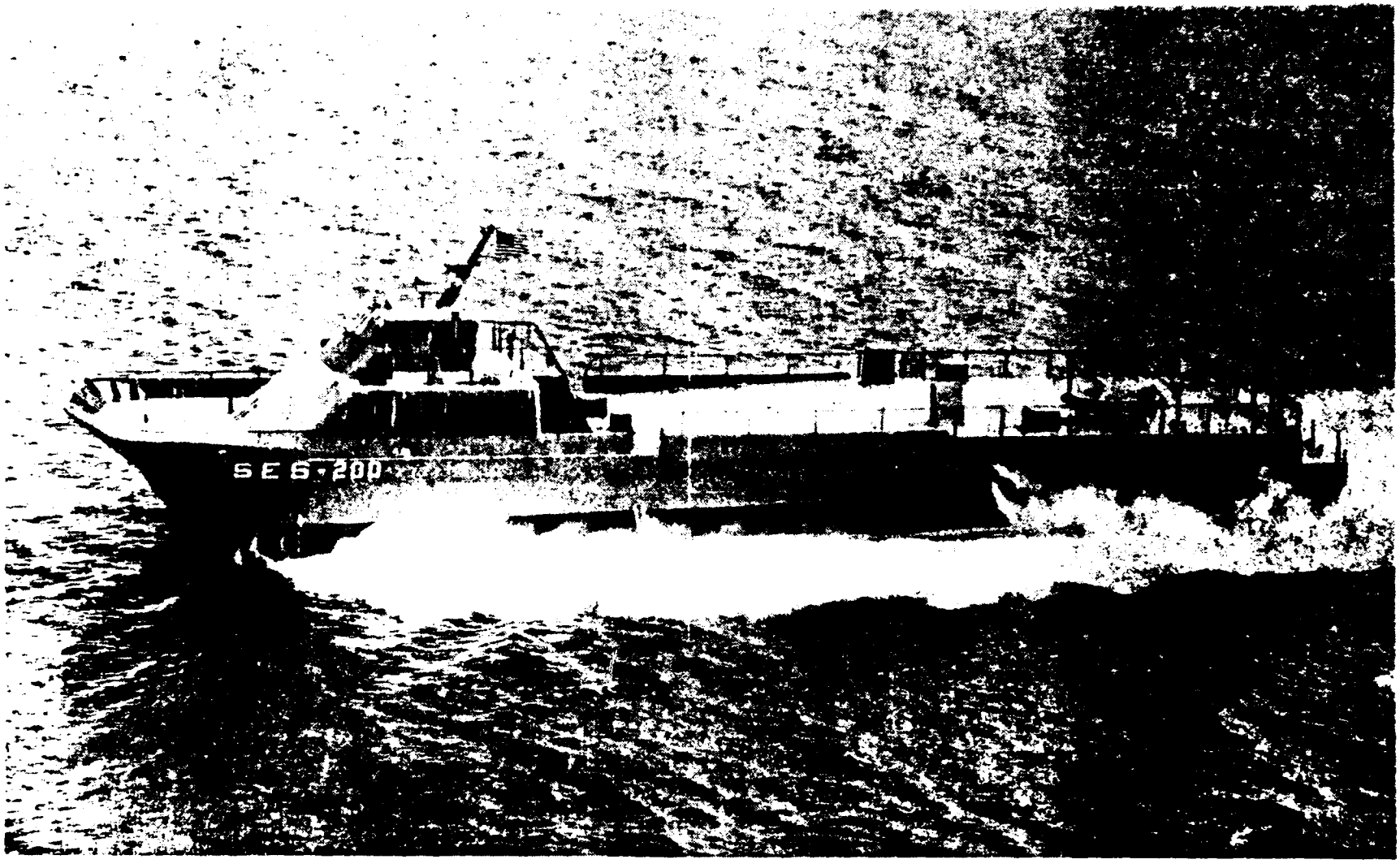

LIST OF TABLES

One method of presenting SES cushion wave making resistance is illustrated in Figure 4-6 (Reference 4-1). In this plot, the theoretical wave making resistance coefficient is plotted versus a speed parameter for SES length-to-beam ratios of 2.5, 3.5, 4.5 and 6.5. These curves are based on theoretical predictions (Reference 4-2) which have been found to closely match experimental data and therefore are often used to predict SES wave making drag for design purposes (Reference 4-3).

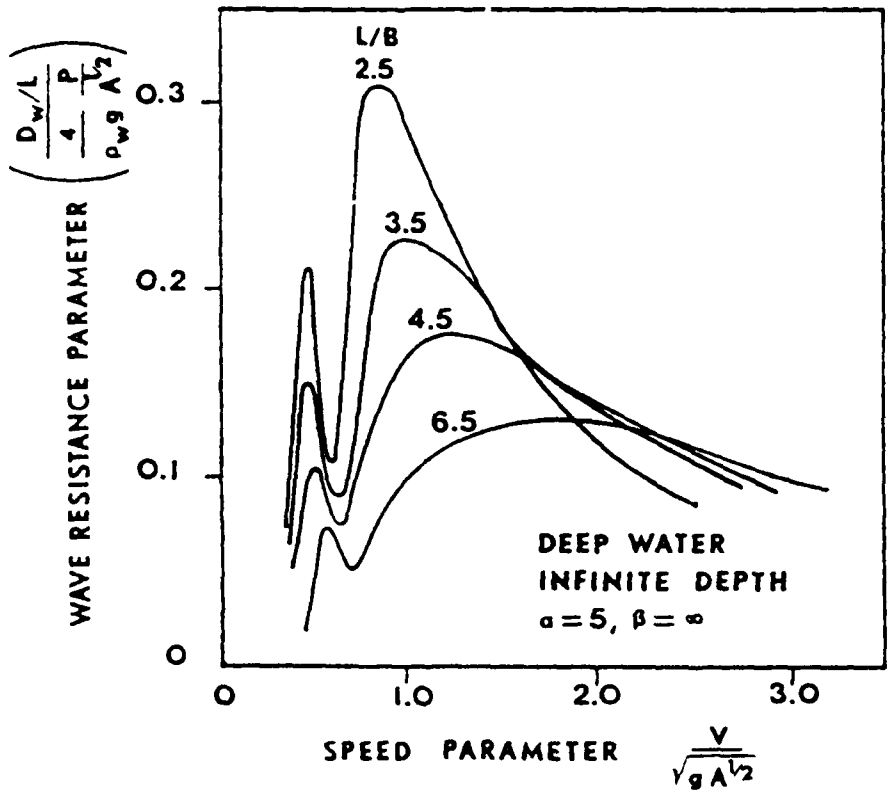

Figure 4-6 WAVE RESISTANCE PARAMETER VERSUS SPEED PARAMETER

The wave making resistance parameter plotted on the ordinate is expressed as a function of the wave drag (D_w), the cushion lift (L) and the cushion loading, i.e., the cushion pressure (P) divided by a square root of the cushion area (A). The speed parameter plotted on the abscissa is not the traditional Froude number as it is based on the square root of the cushion area rather than on cushion length.

Expressing both the wave resistance parameter and the speed parameter as functions of cushion area is useful in explaining the influence of length-to-beam proportions on wave drag. The case considered is that of vessels having different length-to-beam ratios but having equal displacement (cushion lift), cushion area, and cushion pressure (cushion lift ÷ area). As these vessel characteristics are equivalent, the effect of length-to-beam can be evaluated by simply comparing the magnitude of the curves shown in Figure 4-6.

As shown, increasing the cushion length-to-beam ratio decreases the wave drag in the secondary and primary hump regions at the expense of increasing the wave drag at speeds above the primary hump. Increasing the length-to-beam ratio also shifts the peak of the primary drag hump to higher speed. Although not shown in Figure 4-6, it is obvious that increasing the cushion length-to-beam ratio would also increase the sidehull drag. These characteristics make the selection of appropriate cushion length-to-beam proportions an important aspect of minimizing SES resistance.

The general influence of cushion length-to-beam proportions on total SES resistance is illustrated in Figure 4-7. In this example, the secondary drag hump has been omitted. SES are typically operated using reduced cushion pressure in this speed region as this significantly reduces or eliminates the secondary hump. Characteristics depicted in Figure 4-7 are typical of high and low length-to-beam SES having the same displacement, cushion area and installed power.

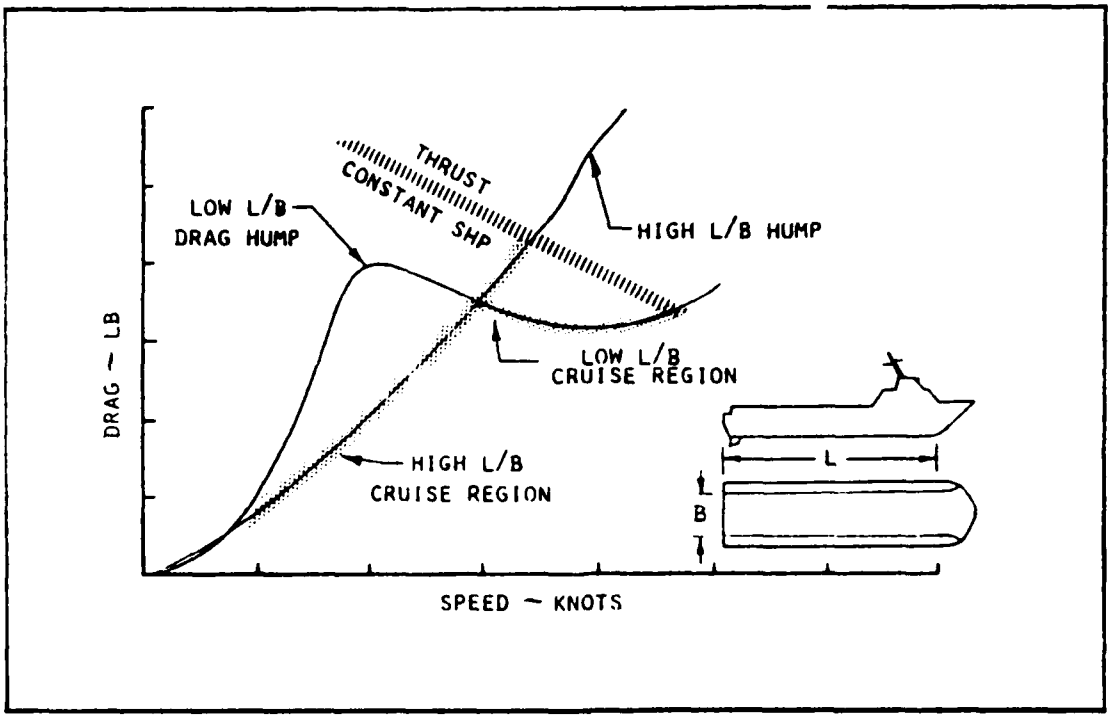

Figure 4-7 INFLUENCE OF LENGTH-TO-BEAM RATIO ON TOTAL DRAG

As shown, a low length-to-beam SES typically has a sizeable hump in its total resistance curve at the primary hump speed. Since this hump is within the operating envelope, the low length-to-beam SES must be powered through this region in order to attain efficient cruise speeds.

In contrast, vessels designated as "High Length-to-Beam SES" are purposely designed to have the peak of the primary drag hump outside the operating envelope. This is made possible by the fact that increasing the cushion length-to-beam ratio for a given displacement and cushion area shifts the primary drag hump to higher speed (refer to previous discussion of Figure 4-6). Additionally, increasing the length-to-beam ratio reduces the wave drag at the secondary and primary hump speeds and increases the sidehull drag. As illustrated in Figure 4-7 below a crossover speed, the high length-to-beam SES will typically have less total resistance as the reduction in wave making drag will be greater than the increase in sidehull drag up to this point.

Figure 4-7 illustrates that low length-to-beam SES are primarily suited to applications that require full time operation at high speed. The term high speed is used in a generic sense to indicate the upper end of the design envelope. Operation at reduced speed in the hump region requires a substantial amount of power and is relatively inefficient. A high length-to-beam SES operates at speeds below the peak of the primary hump where the drag characteristics gradually increase with speed like those of conventional ships. Therefore, a high length-to-beam design would be selected for applications that require sustained operation over a broad range of speed or for applications that would require a low length-to-beam SES to operate within its primary hump region. In both cases, a high length-to-beam would require substantially less power up to the crossover speed.

While it is anticipated that the trends discussed above will be reflected in future designs, it should be noted that the final length-to-beam ratio selected for a specific application will depend on other factors besides resistance and powering. Length-to-beam proportions also affect arrangements, structural loads, seakeeping, stability and maneuvering just to name a few. The designer uses this fundamental ratio along with other design parameters to optimize an SES to satisfy a set of operational requirements.

4.2 PERFORMANCE

Surface Effect Ship performance is measured in terms of the total propulsion and lift power required to achieve a given speed. Table 4-1 lists the matrix of test conditions for which performance was measured.

Table 4-1

SES-200 PERFORMANCE TEST MATRIX

Speeds (kts)	5, 10, 15, 20, 25, Max
Sea States	0, I*, II*, III, IV**
Headings	Head, Bow, Beam, Quartering, Following
Displacements	165 L.T.*** and 200 L.T.

* Head and Following seas only.
** Max. speed only.
*** Sea State Ø only.

At idle ahead conditions (5 to 8 knots), hullborne operation without lift consumes the least amount of power. The SES-200 rides with its wet deck clear of the water like any catamaran ship under these conditions. At higher speeds, lift power is applied to raise the ship out of the water as this consumes less total power than hullborne operation. The lift setting is gradually increased with speed to optimize performance, i.e., minimize the total power required. Figure 4-8 illustrates the total power variation with speed for the 200 ton load condition in calm water. Also shown are the individual propulsion and lift system horsepowers. Rough weather performance is discussed in the next section under Seakeeping.

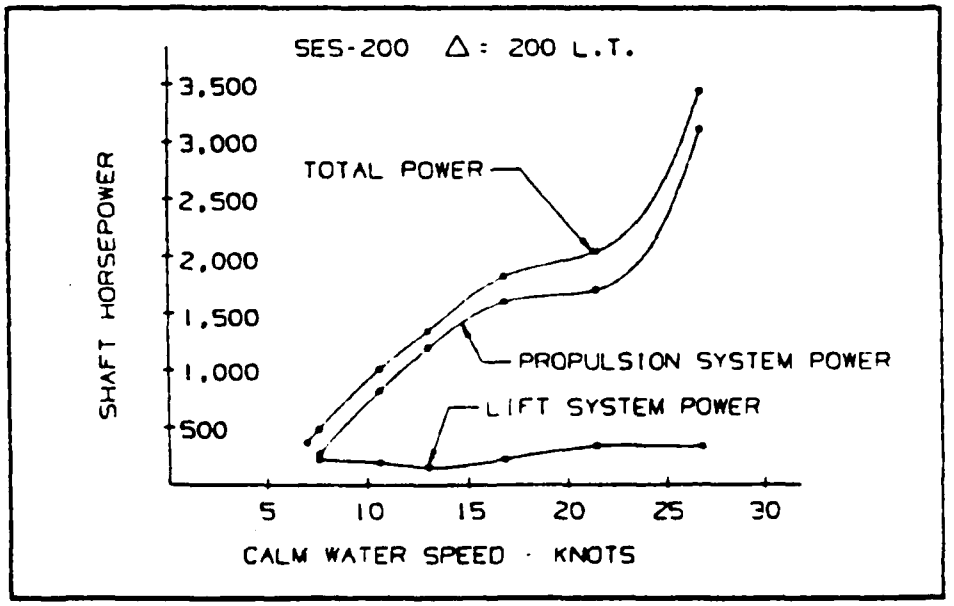

Figure 4-8 SES-200 PERFORMANCE AT 200 L.T.

Figure 4-9 compares the performance of the high length-to-beam SES-200 at 200 tons displacement with that of the 140-ton low length-to-beam BH-110.

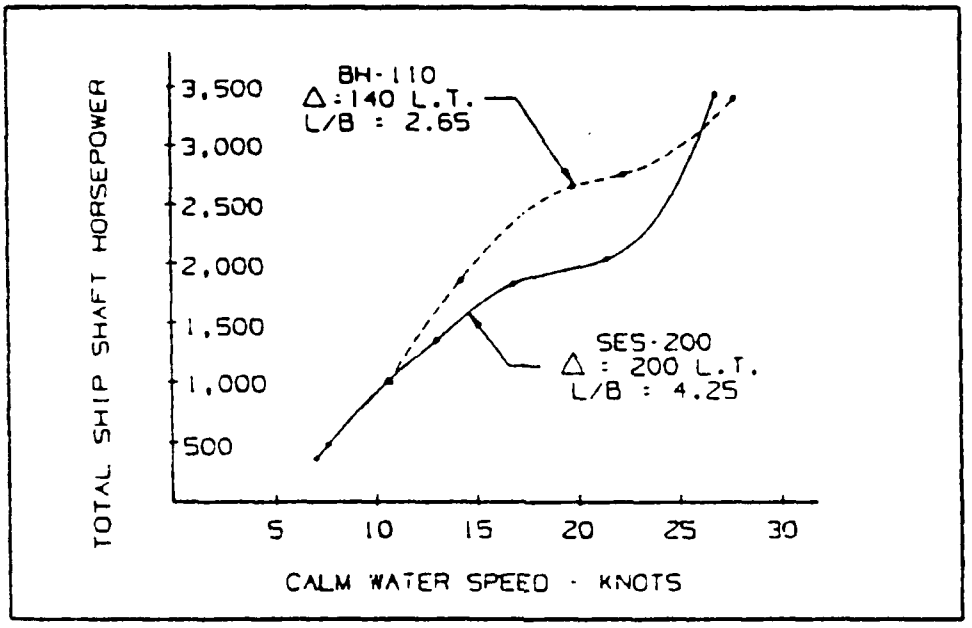

Figure 4-9 COMPARISON OF BH-110 AND SES-200 PERFORMANCE

Increasing the BH-110's length-to-beam ratio from 2.65 to 4.25 shifted the peak of the primary wave drag hump from 20 knots (which is inside the BH-110's operating envelope) to 33 knots (which is outside the operating envelope of both vessels). As shown, the low length-to-beam BH-110 has a 2-3 knot higher maximum speed; however, between 10 and 27 knots the SES-200 requires substantially less power. In this speed range, the reduction in wave making resistance achieved by increasing the length-to-beam ratio was greater than the increase in sidehull drag from the 50 ft hull extension. Therefore, in addition to being larger and carrying more fuel, the SES-200 also enjoys a powering advantage over a large portion of the operating envelope.

The SES-200's fuel consumption was measured and the vessel's range computed for various constant speed cruise conditions. Figure 4-10 illustrates the range in Sea State III heading directly into the seas.

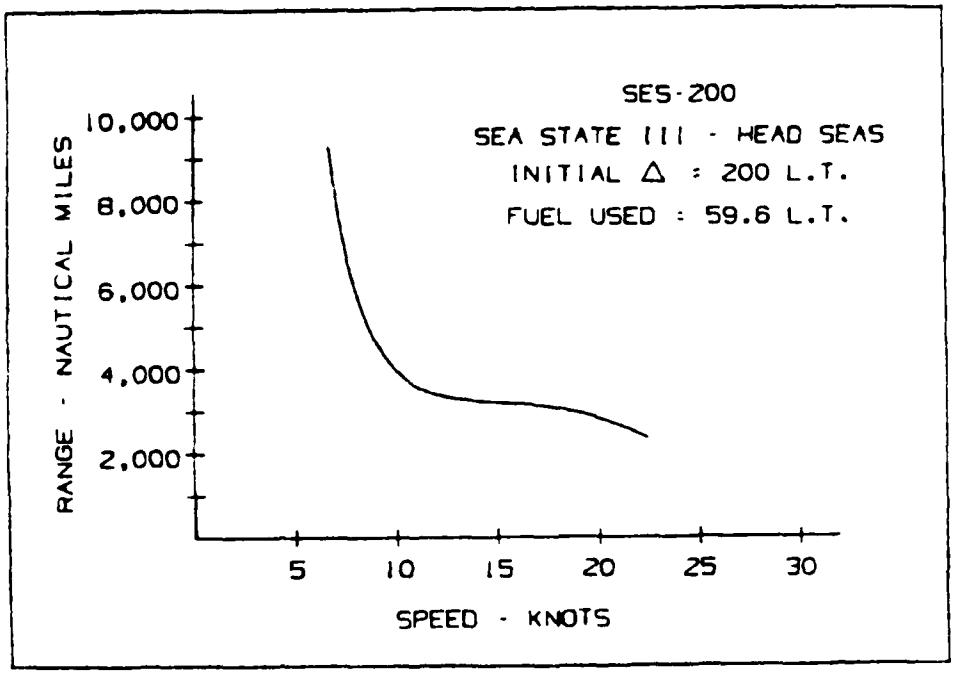

Figure 4-10 SES-200 RANGE VERSUS SPEED

At a sustained speed of 23 knots, the SES-200's projected range is over 2500 nautical miles. Range is substantially increased if mission requirements dictate that the SES-200 reduce speed and loiter for extended periods.

Prior to initiation of the Technical Evaluation, the SES-200 was transferred to SESTF upon completion of acceptance trials in New Orleans, LA. This 70-hour non-stop transit covered 1,660 miles at an average speed of 23.8 knots. A variety of sea conditions were encountered and 40 L.T. of fuel were consumed. Predictions made using the fuel flow measurements are in close agreement with the distance covered and fuel consumed during this extended cruise.

4.3 SEAKEEPING

Seakeeping is measured by the degree to which a ship can maintain speed and execute missions in heavy weather without excessive motion, slamming or deck wetness.

Table 4-2 lists the matrix of tests completed to measure and evaluate the SES-200's seakeeping characteristics. Tests were conducted in Sea States I-IV. These conditions encompass light, moderate and heavy weather operating conditions for small 200-ton vessels like the SES-200. For comparison, equivalent sea conditions for a 4000-ton, 400 ft Navy frigate are Sea States III, IV, V and VI.

Table 4-2

SES-200 SEAKEEPING TEST MATRIX

Speed (kts)	DTW, 5, 10, 15, 20, 25, Max.
Sea States	I*, II*, III, IV**
Headings	Head, Bow, Beam, Quartering, Following
Displacement	165 - 200 L.T.

* Head and Following seas only.
** Max. speed only.

Table 4-3 lists the range of wave heights that correspond to each sea state.

TABLE 4-3

SEA STATE CONDITIONS

	SIGNIFICANT WAVE HEIGHT (FT)	
SEA STATE	STANDARD DEFINITION (Ref. 4-4)	TEST CONDITION
I	0.3-1.2	1.0-1.2
II	1.2-3.0	1.7-2.8
III	3.0-5.7	3.3-5.4
IV	5.7-7.5	6.0-7.0

The SES-200's maximum speed in each sea state at various headings to the waves is presented in Figure 4-11.

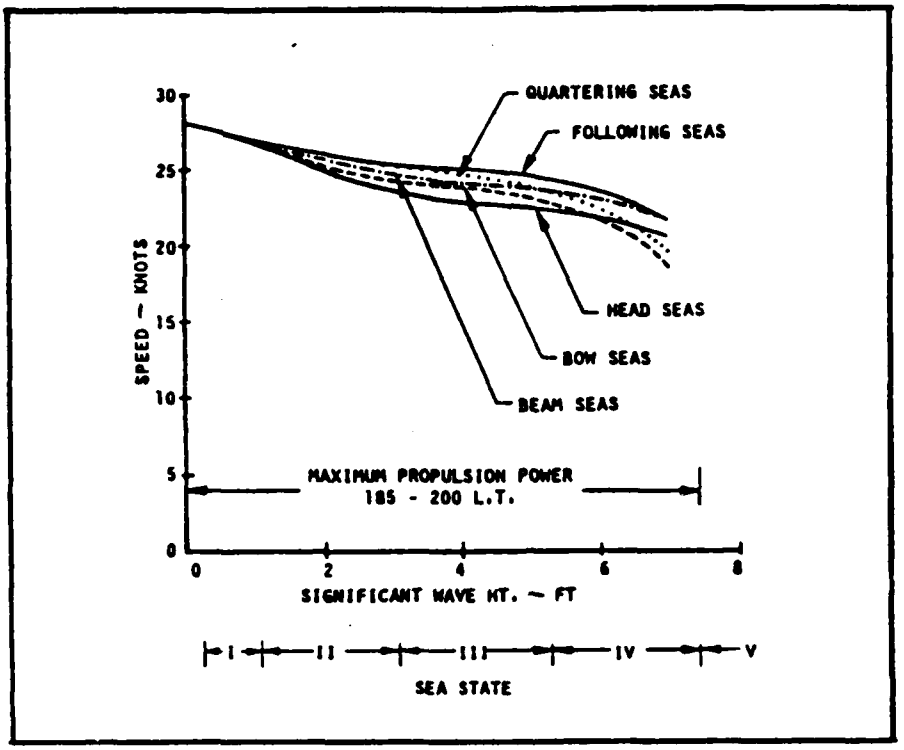

Figure 4-11 SES-200 SPEED VERSUS SEA STATE

As shown, the vessel's speed was not significantly degraded by wind and waves in Sea States I-IV. Speeds attained in these conditions were only 10-20% lower than in calm water and there was no need to reduce power or alter course to avoid excessive motions, slamming or deck wetness.

The Sea State III and IV tests conducted represent typical heavy weather operating conditions for conventional vessels in the SES-200's size range. Significantly higher sea conditions were encountered once during the Technical Evaluation and this was at night during a storm. The significant wave height measured 12 ft (High Sea State V) during the most severe conditions and the ship loitered at a speed of 10 knots throughout the storm while awaiting the next day of testing. As the seas subsided before morning, there was no opportunity to run controlled tests in these conditions.

During the Technical Evaluation, a substantial SES-200 motions data base was collected. The highest motions measured in Sea States I-IV are described and compared to Navy surface ship criteria (Reference 4-5) to give a general indication of the vessel's seakeeping ability.

Surface ship criteria used in this comparison are listed in Table 4-4.

Table 4-4

SURFACE SHIP MOTION CRITERIA

SUBSYSTEM	MOTION	LIMIT*	LOCATION
Personnel	Roll	8^{o}	CG
	Pitch	3^{o}	CG
	Vertical Accel.	0.4 g	Bridge
	Lateral Accel.	0.2 g	Bridge
Helo Operation	Roll	5^{o}	CG
	Pitch	3^{o}	CG

*Motion limits are significant single amplitudes.

Motion criteria for helicopter operation are used in the comparison as the SES-200's deck has sufficient space to launch and recover small military helicopters in a Coast Guard patrol boat application. This places a more severe restriction on the roll amplitudes than the other criterion listed in Table 4-4 which is for habitability. Note that helicopter operation is only considered from the standpoint of ship motions. Helicopter operating envelopes that are restricted by inappropriate relative wind velocity and direction are not identified as these are not unique to the SES-200. They should be the same for all vessels of a given speed/sea state capability.

The measured motion standard deviations were converted to significant single amplitude values for comparison with the criteria listed in Table 4-4. These conversions were made for a Rayleigh amplitude distribution which amounts to multiplying the standard deviations by a factor of two.

Figure 4-12 illustrates the pitch motion for head sea operation at full power in Sea States I-IV; the worst case for each seaway. Typical ship speeds for these conditions were illustrated in Figure 4-11. The measured pitch amplitudes increase with increases in wave height but do not exceed the 3 degree limit for helicopter operation. Less pitch motion was measured in each sea state at reduced power and off-head sea wave directions. Data points are shown in Figure 4-12 for operation with and without the Ride Control System (RCS) turned on. RCS operation does not significantly affect pitch motion; however, as will be discussed subsequently, it significantly reduces the vertical accelerations.

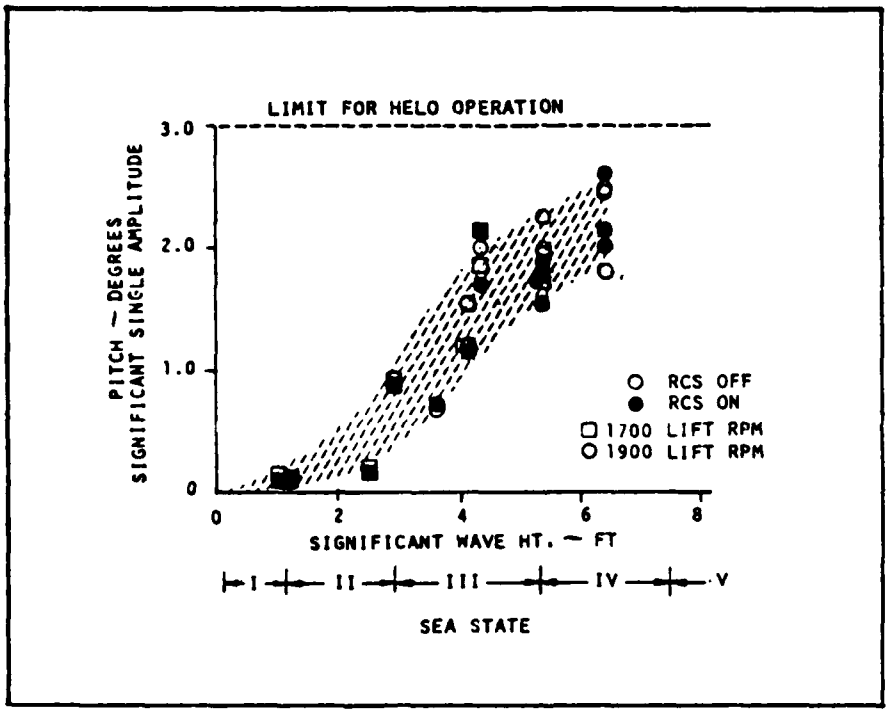

Figure 4-12 PITCH MOTION FOR FULL POWER OPERATION IN HEAD SEAS

Figure 4-13 illustrates the roll motion for beam sea operation at full power in Sea States III and IV. No beam sea data points were recorded in Sea States I and II as the roll amplitudes are much smaller and other testing had higher priority. The roll amplitudes are well below the 5 degree limit for helicopter operation in Sea State III. In Sea State IV, the measured data points are equal to the 5 degree limit with the RCS on and slightly above the limit with the RCS off. This modest reduction in roll due to RCS operation was somewhat surprising since the system primarily reduces heave motion. It is not simply a matter of scatter in the test data as similar reductions in roll were measured for other wave directions in Sea State IV.

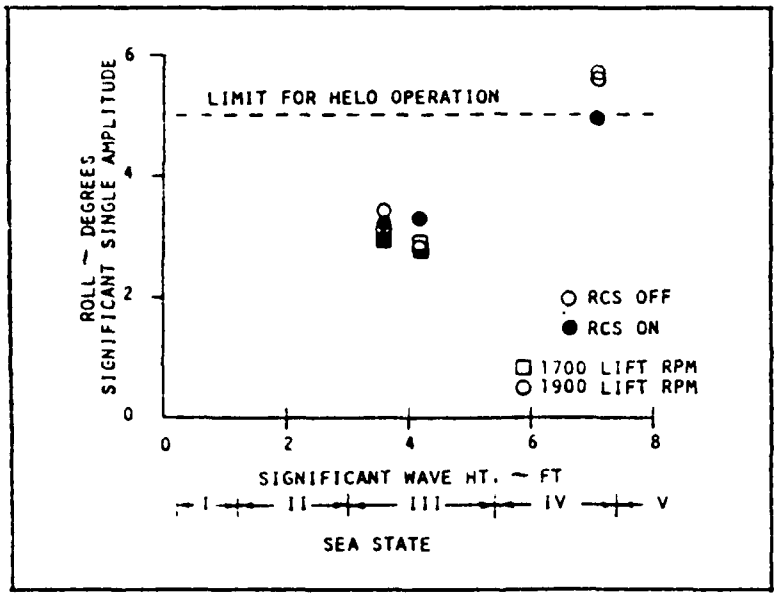

Figure 4-13 ROLL MOTION AT FULL POWER IN BEAM SEAS

Lower roll motions were measured at reduced power and at other headings. In general, Navy and Coast Guard operators have commented that the SES's catamaran hull form provides a very stable platform from a roll standpoint.

Bridge vertical accelerations were estimated by averaging the acceleration measurements made at the bow and at the ship's longitudinal center of gravity (i.e., the LCG). This simple technique should be adequate for computing the rigid body accelerations as the bridge is approximately halfway between the bow and the LCG and under most conditions the vessel tends to pitch about its LCG. Figure 4-14 compares the bridge accelerations at full power in head seas (worst case conditions) to the surface ship criterion. Data points are shown with and without the Ride Control System (RCS) turned on.

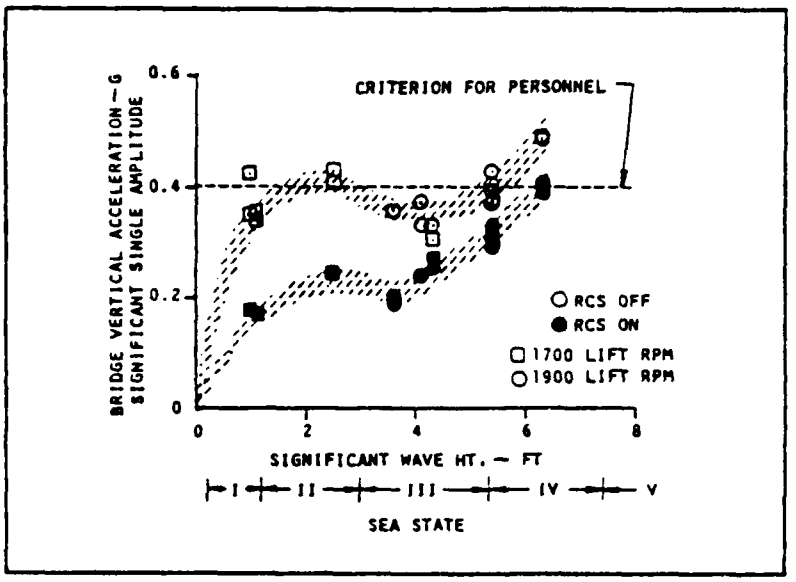

Figure 4-14 BRIDGE VERTICAL ACCELERATIONS AT FULL POWER IN HEAD SEAS

Cushionborne with the RCS off, the SES-200's heave motion is lightly damped and the bridge accelerations equal or exceed the criterion during full power operation in head seas. The accelerations do not increase rapidly with wave height because of the compensating effect of slightly reduced speed at full power in the higher sea states (refer to Figure 4-11).

With the RCS on, the cushion pressure fluctuations caused by wave action are reduced, and correspondingly the bridge accelerations are well below the surface ship criterion in Sea States I-III and equal to the criterion in Sea State IV. RCS effectiveness tends to decrease with increasing wave height as the system's ability to counter the rising wave induced pressure changes is limited by the available fan flow capacity. The RCS installed on the SES-200 is considered a minimal system as no additional lift fans were provided for ride control purposes when the vessel was stretched.

It should be noted that dumping pressurized air overboard through the vent valves during RCS operation can reduce the ship's speed. In the Technical Evaluation Program, the vent valve motions were limited such that these speed losses were restricted to 1 knot or less.

Vertical accelerations at the LCG (i.e., the heave accelerations) were also compared to the surface ship criterion for personnel as both crew quarters and occupied machinery spaces are located near this area of the ship. Figure 4-15 illustrates the results; the conditions are the same as for Figure 4-14 (i.e., head seas at full power in Sea States I-IV). The heave accelerations are lower than the vertical accelerations on the bridge as the bridge accelerations contain the vertical component of pitch motion.

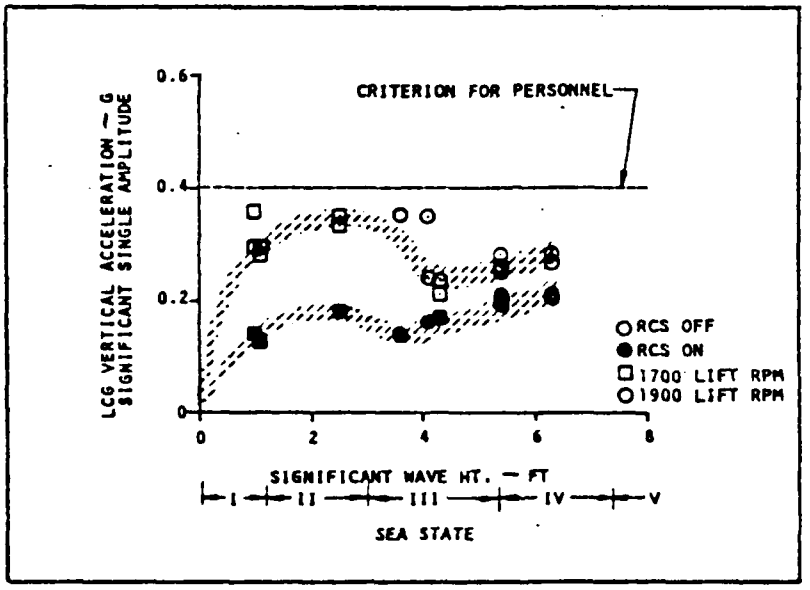

Figure 4-15 HEAVE ACCELERATION AT FULL POWER IN HEAD SEAS

With the RCS off, the heave accelerations are below the criterion for personnel in all sea states. RCS operation reduces the accelerations by about 50% in Sea States I and II, 30% in Sea State III and 25% in Sea State IV with the net effect that the amplitudes are reduced to less than half the 0.4g criterion in most cases. At reduced speed and off-head sea wave directions, the vertical accelerations in each seaway are substantially lower than the values shown in Figures 4-14 and 4-15.

Lateral accelerations were measured on the second deck at the CG and on the main deck at the bow. These measurements do not provide enough information to compute the lateral accelerations on the bridge. Therefore, a direct comparison with the surface ship criterion could not be made. During Sea State I-IV testing, the 0.2g limit was not exceeded at either lateral accelerometer location.

4.4 MANEUVERING AND STABILITY

The following maneuvering and stability tests were performed during the Technical Evaluation:

- Dieudonne Spiral Maneuvers
- Zig-Zag Maneuvers
- Turning Tests
- Pitch/Roll Stiffness Tests

Typical SES-200 operation utilizes differential propeller thrust for very low speed maneuvering such as docking. The twin rudders are used for maneuvering and turning over the remainder of the speed range. If required, differential thrust can be combined with rudder turning.

Dieudonne Spiral Maneuvers were performed to judge the ship's directional stability for both normal operation and impaired situations. These tests confirmed that the vessel is directionally stable for the following conditions:

- Normal operation with both engines and both rudders
- Impaired operation with a single engine and both rudders
- Impaired operation with a single engine and a single rudder

This covers all forseeable operating situations. The tests conducted to assess the directional stability for normal operation were conducted at 10 knots hullborne and at 10 knots, 20 knots and full power cushionborne. Tests in the impaired conditions were conducted at 10 knots cushionborne.

Zig-Zag maneuvers were conducted at speeds of 5 and 10 knots hullborne and at 20 knots and full power cushionborne. The heading overshoot angle obtained from zig-zag test data is a numerical measure of the ship's response to the helm; it is indicative of the amount of anticipation required by a helmsman when operating in restricted waters.

During the low speed hullborne tests, heading overshoot angles averaged 4 degrees. This is typically considered to be indicative of good turning response. At higher speeds cushionborne, the overshoot angles were 1-2 degrees lower indicating slightly better response. Figure 4-16 illustrates a segment from the cushionborne zig-zag maneuver conducted at full power.

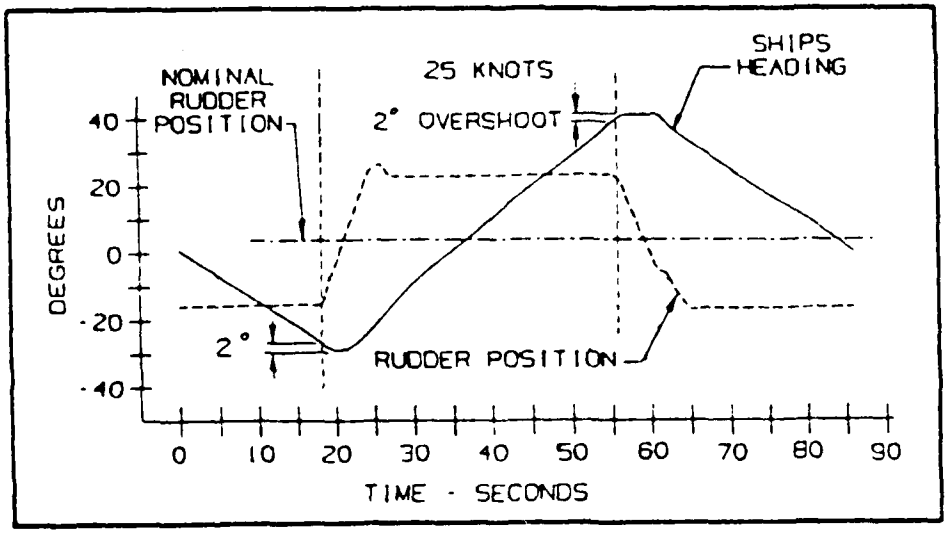

Figure 4-16 ZIG-ZAG MANEUVER AT FULL POWER

For this reason, it is best to take the time segments as long as possible while still maintaining a sufficient number of segment means to perform a significant test. This introduces a significant restriction on our capability to perform effective stationarity checks on the shorter duration test points. The SES-200 has some rather low frequency modes, so time segments of less than 30 seconds or so are not likely to yield sufficiently decoupled means. For a 3-minute data record, this allows only 6 segments which is rather low for any statistical test.

While the test is viewed primarily as a means of detecting mean value drifts, the results should also be viewed with some suspicion when the parameter becomes too large. High values indicate rapid (relative to the time segment lengths) oscillations in the means. This indicates an unexpected negative correlation in the deviations of adjacent segment means from the overall means, so the data again may be unstationary. As before, however, this may merely be due to a coupling of means through the craft dynamics and would again indicate that the time segments are too short. Generally, problems with drifts are considered more likely to corrupt the data than anything else. Therefore the appearance of high values is not considered to be as serious as low value occurrences.

The acceptance range for the test is shown on Table 6-5 at the 10% significance level, i.e., for samples drawn from a stationary ensemble of time series, we would expect to fail the test 10% of the time. Put another way, it would be expected that the test would reject perfectly good data one time in ten. (Of course, there is also a probability of bad data passing the test.) This is a relatively high significance level for use in this type of test, particularly in view of the possible coupling of segment means through the craft dynamics. The reason for choosing such a level is that, for a given test point, not one but a number of time histories will be subjected to the test. That is, one test for each measurement subjected to stationary time series processing. By examining the number of instrument outputs which fail the test, one can better judge whether the failure is due to random rejection or whether the overall group of time histories are suspect. This approach is further enhanced by the simultaneous availability of the test on variances to be discussed below.

The other stationarity test performed was on the variances of the time segments rather than on the means. The test used is the "run" test for random data (References 6-5, 6-7 and 6-8). This is a less powerful test than the s^2/s^2 test used on the means, but it is more widely applicable. The s^2/s^2 test requires the data used to be approximately normally distributed; this is generally expected of mean values but not of variances.

The next step is to run stationarity checks on the data with the trends removed. The tests which can be made in this regard are all of a statistical nature. They involve acceptance or rejection of the premise that a particular set of data is stationary on a probabilistic basis: Firm yes/no types of tests are not available. The failure of a data set to pass these stationarity tests indicates that either the test conditions were not of a suitably stationary character, or that the particular data set obtained by the luck of the draw does not happen to be a typical data set from the available ensemble. In the latter event, we are still justified in rejecting the data because the useages planned involve considering the results as representative of a typical test; we do not perform a multitude of duplicate tests (replication) to obtain results from ensemble averaging.

The tests performed are tests of wide-sense stationarity, i.e., the stationarity of means and standard deviations are checked. Tests of the more extensive strict-sense stationarity for the power spectra and distribution functions themselves are much more difficult and are generally considered unnecessary.

The means are tested using a δ^2/s^2 test described in References 6-4, 6-7 and 6-8. The overall data segment is first partitioned into a number of time segments of equal length and the mean values for each of these segments is obtained. The tests are made using the value of the parameter

$$\delta^2/s^2 = \left[\sum_{i=1}^{N-1} (X_{i+1} - X_i)^2\right] / \left[\sum_{i=1}^{N} (X_i - \bar{X})^2\right]$$

where the X's are mean values for the time segments employed and $\bar{X}$ is the average of the X's. It should be noted that these time segments are not necessarily the same ones employed for the Tab Data of Section 6.5. The denominator is proportional to the usual expression for computing the variance of the segment means. The numerator is proportional to another formula for calculating variances which is less sensitive to drifts in the means. If there are no drifts, etc., the value of the parameter is ideally equal to 2. A low value of this parameter indicates the presence of long term drifts or systematic low frequency variations. In our case, this might indicate that the linear trend removal is inadequate to render the data acceptably stationary. Unfortunately, it could also mean that our time segments are too short relative to the time constant of some low frequency craft dynamic mode. This allows such a mode to introduce a significant positive correlation between the segment means. This dynamic coupling of the segment means violates the assumptions of the test which assumes the segment means should be independently scattered about the overall mean in a truly stationary situation.

4. For each measurement processed, time segment averages are given, together with the start time of the segment employed in the averaging. The selection of the time segments used is discussed subsequently.

5. The overall mean value and standard deviation for the test point for each measurement processed.

6. The maximum and minimum values of each measurement encountered during the test point.

7. A summary of the craft weight and LCG, the fuel consumption for the individual lift fan engines, total lift engine fuel consumption, overall craft fuel consumption and the test point duration.

The segment time averages are used both to give a coarse version of time histories for the case of maneuvers and to allow stationarity checks to be made on the data for power spectra, histograms, etc. (see Section 6.3.3). The segment lengths to be used are specified on the Tab Data request forms. For the stationary time-series data, these segments are generally selected as multiples of 30-second intervals. Within this constraint, the segment lengths are generally selected to have not less than five (5) segments in a test point and not more than about ten (10).

6.3.3 Processing of Stationary Time-Series Data

6.3.3.1 Trend Removal and Stationarity Checks

The first steps taken in the processing and reduction of data for use in stationary time-series analyses are intended to enhance the stationarity of the data and to obtain some measure of the stationarity actually achieved. This is an important step and is discussed at length in Reference 6-4, as well as in standard texts such as Reference 6-5. Without assurances that the data may reasonably be considered stationary, very misleading results can be obtained from stationary processing techniques. The effects involved include overestimates of the low frequency end of power spectra, overestimates of standard deviations and distortion of histogram data (c.f.: Reference 6-4).

The first step is the removal of long time-constant trends from the data. This is done via techniques described in Reference 6-4 and amounts to least squares fitting a straight line to the test data and treating the values obtained from this fit as a "local" mean value for the data, i.e., this is the mean value removed from the data before computing standard deviations, power spectra and histograms (for the histograms, the overall mean is subsequently added back into the data). Intuitively, the idea behind this procedure is that the quantities of interest to the statistical processing are primarily deviations from the mean. If the data contain deviations from a "local" mean value which have the necessary stationarity characteristics, then they are generally considered suitable even though the "local mean" wanders somewhat.

6.3 DATA REDUCTION

This section describes the data reduction methods and techniques employed. The data reductions applied are generally of two types. First there are the kinds of data reduction that basically apply to any type of time-series data. These consist of strip charts which gave detailed time histories of selected channels and time-segment averaging giving average values over selected time intervals. The data reduced by these means were used in the analysis of performance and stability data involving time dependent maneuvers such as acceleration runs, turning tests, etc.

The second type of data reduction employed applies primarily to the processing of stationary time-series data. Data produced include overall mean values and standard deviations, power spectral density functions, and histograms in addition to the strip charts and time segment averaged data. These data are employed in the analysis of essentially steady (in a statistical sense) conditions such as performance runs for speed points at a given power setting and for motions data test points where stationary characteristics such as power spectra are to be employed in the analysis. Also included in the stationary techniques are the data involving wave measurements.

The data processed were all taken from the DAS PCM tapes except for the NOAA wave buoy data which are collected via a satellite link and processed by NOAA. Initial conversion of the PCM data tapes to formatted digital tapes was performed at the Naval Air Test Center's Real Time Processing System (RTPS) All subsequent processing was performed by SESTF civilian and military personnel on a PDP-11 computer.

6.3.1 Strip Charts

The strip charts are standard time histories of data channels selected as appropriate to a particular mission and test point sequence. All data are converted to engineering units prior to plotting the time-histories.

6.3.2 Tabulated Data

The tabulated data (Tab Data) are produced in a standard format for all test points. The data presented include the following:

1. A measurement deck list identifying all measurements present on the DAS tape including the mnemonics employed, interpretations of the mnemonics and the units used.

2. A calculation deck list giving mnemonics, definitions and units for the calculations processed for the Tab run.

3. For each test point, an identification of the test point (as specified on the Tab Data request form), together with the beginning and end times of the data segment processed.

TABLE 6-4
SES-200 TEST SUMMARY
LIGHT SHIP TEST CONDITION

TEST OBJECTIVE	MISSION NUMBER (LIGHT SHIP) 26	48	49	50	51	52	53	54	55	69	70
PERFORMANCE ACCELERATION & DECEL. S.S. 0 S.S. II S.S. III S.S. IV				▽							
SPEED/POWER S.S. 0 S.S. II S.S. III S.S. IV			▽	▽					▽		▽
SEAKEEPING S.S. I (RCS ONLY) S.S. II S.S. III S.S. IV S.S. V (RCS ONLY)		▽			▽	▽		▽			
MANEUVERING & STABILITY PITCH STIFFNESS ROLL STIFFNESS ZIG-ZAG & SPIRALS	▽							▽		▽	▽ ▽
DIFF. THRUST TURNS S.S. 0 S.S. II-III							▽				
RUDDER TURNS S.S. 0 S.S. II-III						▽		▽			▽
COMBINED TURNS S.S. 0 S.S. II-III S.S. IV-V											
COURSEKEEPING S.S. IV-V S.S. 0 (FIXED RUDDER)				▽							

▽ - APPLICABLE DATA RECORDED

TABLE 6-3
SES-200 TEST SUMMARY
HEAVY SHIP TEST CONDITION

TEST OBJECTIVE	MISSION NUMBER (HEAVY SHIP) 34	35	38	39	42	43	44	45	48	60	62	64
PERFORMANCE												
ACCELERATION & DECEL.				▽								
S.S. 0								▽	▽			
S.S. II												
S.S. III												
S.S. IV												
SPEED/POWER												
S.S. 0	▽	▽	▽	▽	▽	▽	▽		▽	▽		▽
S.S. II												
S.S. III												
S.S. IV												
SEAKEEPING												
S.S. I (RCS ONLY)	▽	▽	▽		▽	▽	▽	▽	▽		▽	
S.S. II												
S.S. III												
S.S. IV			▽									
S.S. V (RCS ONLY)			▽									
MANEUVERING & STABILITY												
PITCH STIFFNESS										▽		
ROLL STIFFNESS												
ZIG-ZAG & SPIRALS												
DIFF. THRUST TURNS												
S.S. 0												
S.S. II-III												
RUDDER TURNS												
S.S. 0												
S.S. II-III												
COMBINED TURNS												
S.S. 0												
S.S. II-III												
S.S. IV-V												
COURSEKEEPING												
S.S. IV-V												
S.S. 0 (FIXED RUDDER)												

▽ - APPLICABLE DATA RECORDED

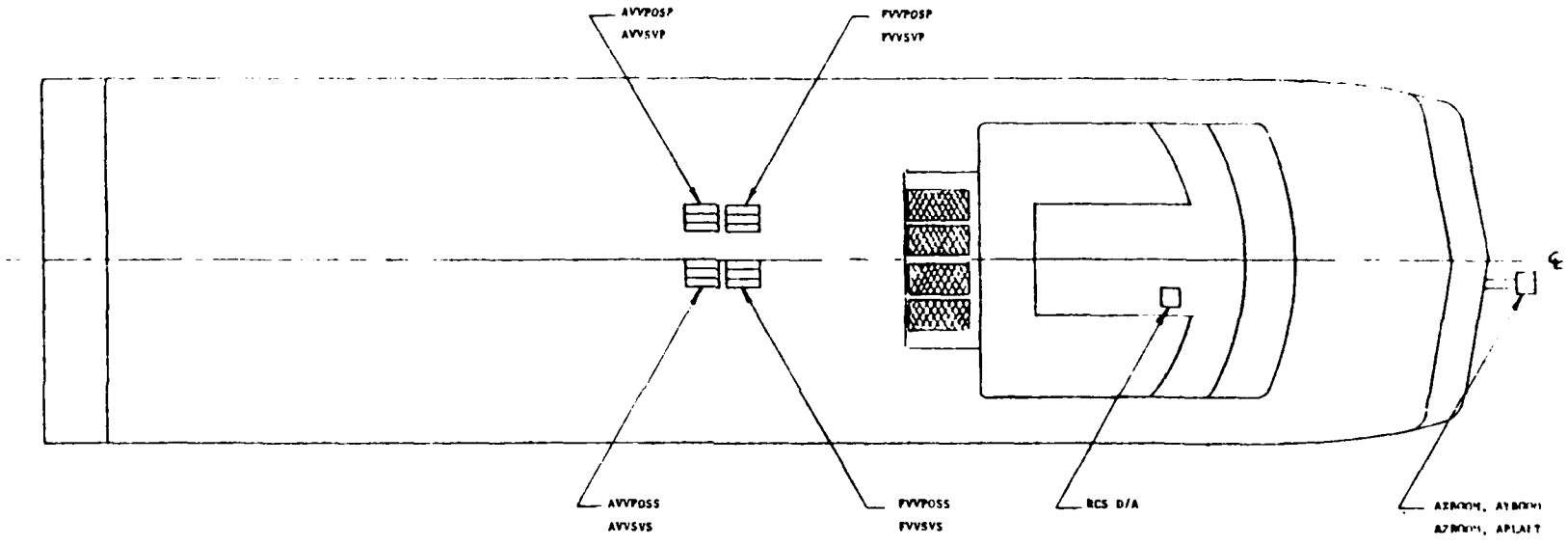

Figure 6-2 SES-200 TRANSDUCER LOCATIONS - MAIN DECK AND BRIDGE

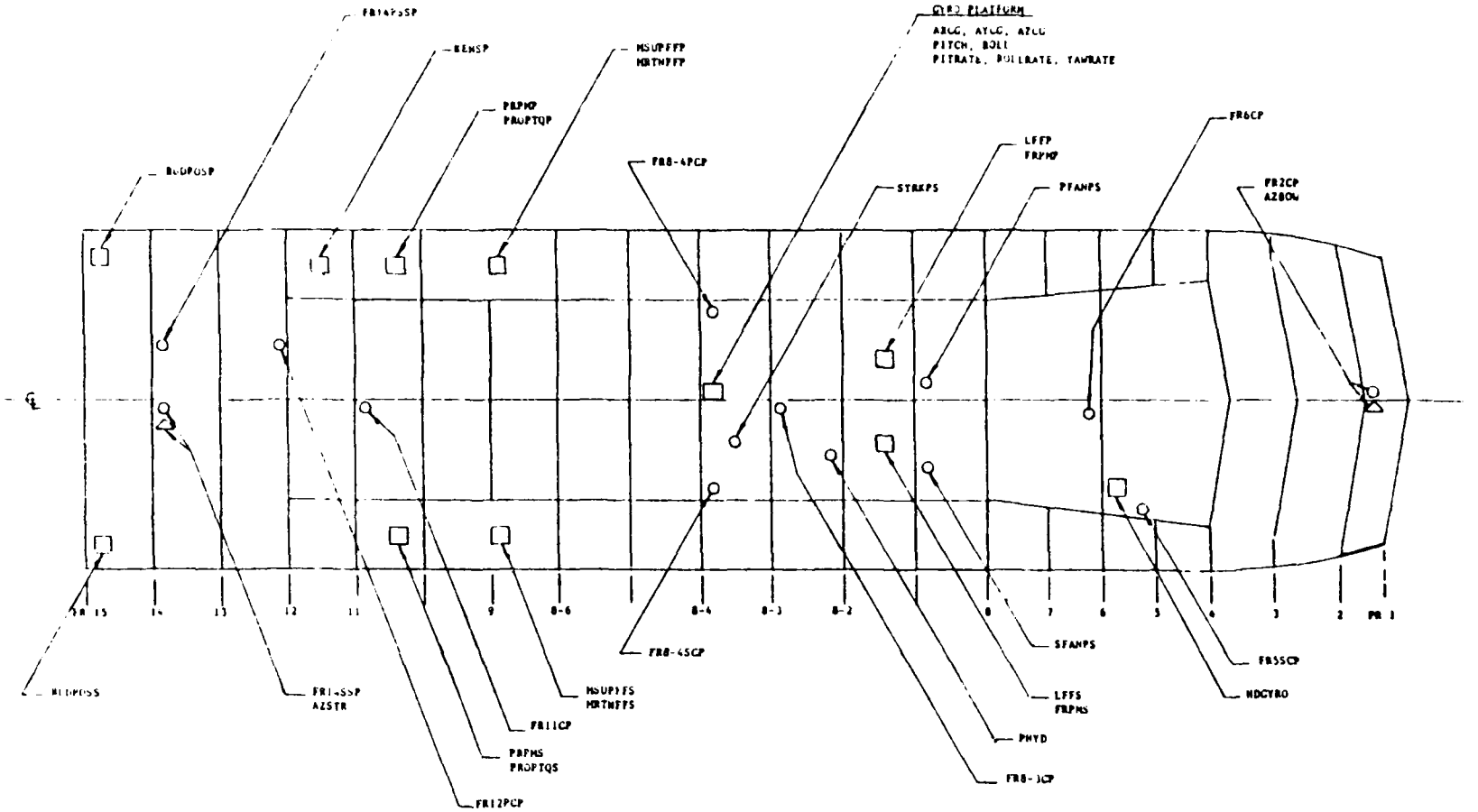

Figure 6-1 SES-200 TRANSDUCER LOCATIONS - SECOND DECK

TABLE 6-2 (Continued)

SES-200 MEASUREMENT LIST

MEASUREMENT	MNEMONIC	RANGE	DAS RESOLUTION	LOW PASS FILTER FREQUENCY
Port Main Supply Fuel Flow	MSUPFFP	.5-6 GPM	.006 GPM	20 Hz
Port Main Return Fuel Flow	MRTNFFP	.5-6 GPM	.006 GPM	20 Hz
STBD Main Supply Fuel Flow	MSUPFFS	.5-6 GPM	.006 GPM	40 Hz
STBD Main Return Fuel Flow	MRTNFFS	.5-6 GPM	.006 GPM	40 Hz
Kenyon Speed	KENSP	0-36 Kn	.04 Kn	40 Hz
Port Rudder Position	RUDPOSP	-32 to +30 Deg.	.06 Deg.	40 Hz
STBD Rudder Position	RUDPOSS	-32 to +30.5 Deg.	.06 Deg.	40 Hz
Port Lift Fan RPM	FRPMP	0-2500 RPM	2.5 RPM	40 Hz
STBD Lift Fan RPM	FRPMS	0-2500 RPM	2.5 RPM	40 Hz
Port Lift Fuel Flow Hundreds	LFFP .01	0-.09	.01 GPM	40 Hz
Port Lift Fuel Flow Tenths	LFFP 0.1	0-.9		40 Hz
Port Lift Fan Fuel Flow Units	LFFP 1.0	0-9		40 Hz
Port Lift Fuel Flow Tens	LFFP 10	0-90		40 Hz
STBD Lift Fuel Flow Hundreds	LFFS .01	0-.09	.01 GPM	40 Hz
STBD Lift Fuel Flow Tenths	LFFS 0.1	0-.9		40 Hz
STBD Lift Fuel Flow Units	LFFS 1.0	0-9		40 Hz
STBD Lift Fuel Flow Tens	LFFS 10	0-90		40 Hz
RCS Fwd. VV Position, Port	FVVPOSP	0-100%	.1%	40 Hz
RCS Aft VV Position, Port	AVVPOSP	0-100%	.1%	40 Hz
RCS Fwd. VV Position, STBD	FVVPOSS	0-100%	.1%	40 Hz
RCS Aft VV Position, STBD	AVVPOSS	0-100%	.1%	40 Hz
RCS Fwd. VV Servovalve, Port	FVVSVP	±10 v.	.02 v.	40 Hz
RCS Aft VV Servovalve, Port	AVVSVP	±10 v.	.02 v.	40 Hz
RCS Fwd. VV Servovalve, STBD	FVVSVS	±10 v.	.02 v.	40 Hz
RCS Aft VV Servovalve, STBD	AVVSVS	±10 v.	.02 v.	40 Hz
RCS D/A Output	D/A	0-100%	.1%	40 Hz
Buoy Wave Height Filtered	BUOYWHF	±5 meters	.005 m	10 Hz
Buoy Wave Height Unfiltered	BUOYWHUF	±5 meters	.005 m	-

TABLE 6-2

SES-200 MEASUREMENT LIST

MEASUREMENT	MNEMONIC	RANGE	DAS RESOLUTION	LOW PASS FILTER FREQUENCY
Frame 2 Cushion Press.	FR2CP	0-200 PSFD	.2 PSFD	40 Hz
Frame 5 STBD Cushion Press.	FR5SCP	0-300 PSFD	.3 PSFD	40 Hz
RCS Frame 6 Cushion Press.	FR6CP	0-200 PSFD	.2 PSFD	40 Hz
RCS Frame 8-3 Cushion Press.	FR8-3CP	0-200 PSFD	.2 PSFD	40 Hz
Frame 8-4 Port Cushion Press.	FR8-4PCP	0-200 PSFD	.2 PSFD	40 Hz
Frame 8-4 STBD Cushion Press.	FR8-4SCP	0-200 PSFD	.2 PSFD	40 Hz
Port Fan Static Press.	PFANPS	0-200 PSFD	.2 PSFD	40 Hz
STBD Fan Static Press.	SFANPS	0-200 PSFD	.2 PSFD	40 Hz
STBD Trunk Static Press.	STRKPS	0-200 PSFD	.2 PSFD	40 Hz
RCS Frame 11 Cushion Press.	FR11CP	0-200 PSFD	.2 PSFD	40 Hz
RCS Frame 14 Stern Seal Press.	FR14SSP	0-200 PSFD	.2 PSFD	40 Hz
Frame 14 Port Stern Seal Press.	FR14PSSP	0-300 PSFD	.2 PSFD	40 Hz
Hydraulic System Press.	PHYD	0-4000 PSI	4 PSI	20 Hz
APL Boom Longitudinal Accel.	AXBOOM	±1 G	.002 G	20 Hz
APL Boom Lateral Accel.	AYBOOM	±1 G	.002 G	20 Hz
APL Boom Vertical Accel.	AZBOOM	±4 G	.008 G	20 Hz
APL Altimeter	APLALT	1-30 ft	.029 ft	20 Hz
Vertical Accel. at Bow	AZBOW	-1 to +3 G	.004 G	40 Hz
Longitudinal Accel. at CG	AXCG	±1 G	.002 G	40 Hz
Lateral Accel. at CG	AYCG	±1 G	.002 G	40 Hz
RCS Vertical Accel. at CG	AZCG	-1 to +3 G	.004 G	5 Hz
Vertical Accel. at Stern	AZSTR	-1 to +3 G	.004 G	40 Hz
Pitch Rate	PITRATE	±20 Deg/Sec	.04 Deg/Sec	40 Hz
Roll Rate	ROLLRATE	±20 Deg/Sec	.04 Deg/Sec	20 Hz
Yaw Rate	YAWRATE	±20 Deg/Sec	.04 Deg/Sec	20 Hz
Pitch Attitude	PITCH	±10 Deg.	.02 Deg.	40 Hz
Roll Attitude	ROLL	±10 Deg.	.02 Deg.	20 Hz
Heading Gyro	HDGYRO	0-360 Deg.	.36 Deg.	40 Hz
Port Propeller RPM	PRPMP	0-1000 RPM	1 RPM	40 Hz
STBD Propeller RPM	PRPMS	0-1000 RPM	1 RPM	40 Hz
Port Propeller Torque	PROPTQP	0-10K ft-lb	10 ft-lb	20 Hz
STBD Propeller Torque	PROPTQS	0-10K ft-lb	10 ft-lb	20 Hz

The PCM encoder is a 10-bit device which provides 1024 counts for a full scale input of 0-5 volts. This results in a resolution of 0.005 v or 0.1% of full scale when a channel is multiplexed. The PCM encoder's digital output is recorded on magnetic tape along with an IRIG-B time code for reference during data reduction.

The SES-200 transducers are listed in Table 6-2. The full-scale resolution that results from PCM multiplexing is listed for each transducer. Locations of these transducers are shown in Figures 6-1 and 6-2 for sensors located on the second and main decks, respectively.

Any eight (8) of the PCM channels can also be decommutated, converted from digital to analog and displayed on an eight-channel strip chart recorder for real time or playback monitoring. Sampled output voltages from all channels can also be examined on a Data Logger equipped with a digital voltmeter and paper tape.

6.2 TEST MISSIONS

References 6-1 and 6-2 describe the test program that was jointly established by the Navy and Coast Guard offices which sponsored the SES-200 Technical Evaluation. The Surface Effect Ship Test Facility converted these documents to a set of prioritized test matrices (Reference 6-3). Tests were selected from these matrices based on weather and ship's loading condition and incorporated in daily test plans.

Tests were conducted in the following categories:

1. Performance
2. Seakeeping
3. Maneuvering and Stability

Tables 6-3 and 6-4 summarize the tests completed in each of the above categories for the heavy and light ship test conditions, respectively. The heavy ship tests encompass displacements between 190 and 206.5 L.T. and the light ship tests encompass displacements between 160 and 170 L.T. SES-200 missions conducted to satisfy each test category are also shown in these tables. Sections 7, 8 and 9 discuss the performance, seakeeping and maneuvering test results, respectively.

6. TEST PROGRAM DESCRIPTION

6.1 DATA ACQUISITION SYSTEM

The Data Acquisition System (DAS) installed on the SES-200 measures and records data to satisfy test program objectives. The system provides excitation power to the various transducers, conditions the transducer output signals and records all of the outputs on magnetic tape. The major DAS components are listed in Table 6-1.

TABLE 6-1

SES-200 Data Acquisition System Components

DESCRIPTION	MANUFACTURER	SPECIFICATIONS
PCM Encoder	EMR 372	120 Channels
D/A Converter	EMR 656-01	8 Channels
PCM Decommutator	EMR 2746	
PCM Bit Sync	EMR 746	
Strip Chart Recorder	Gould 481	8 Channels
Data Logger	Fluke 2240A	60 Channels
Tape Recorder	Bell & Howell M14E	14 Track
Time Code Generator	Systron Donner 8154	IRIG B
Time Code Remote Display	Systron Donner 8781	
Power Supply Package:		
115 VAC 400 Hz	Unitron Static Inverter	
28 VDC	Technipower PM 28.0-12.0A	12 Amps
5 VDC	Technipower PM 5.1-3.0A	3 Amps
±15 VDC	Technipower PM 14.5-6.0A	6 Amps
Patch Panel		24 x 32
Junction Boxes (6)		30 Channels ea.
FM Multiplex		56 Channels

The DAS has both PCM and FM multiplex capability. During the Technical Evaluation, only the PCM channels were utilized. The various analog transducer outputs are filtered at 5, 10, 20 or 40 Hz using 4-pole low pass Butterworth filters. These filters prevent aliasing any high frequency noise into the data band during PCM multiplexing or subsequent digital processing of the data. After filtering, the PCM encoder samples each transducer at 200 samples per second. This high sample rate is used so that acceleration, cushion pressure and vent valve command and position signals up to 40 Hz can be resolved for RCS design and analysis purposes.

5. OPERATIONAL SUMMARY

The assigned crew for open ocean testing consisted of the officers and enlisted personnel listed in Table 5-1 plus 2-3 technical observers. No special training was provided for the 14-man Navy crew.

Table 5-1

SES-200 CREW FOR OCEAN OPERATIONS

DUTY ASSIGNED	RANK/RATE	PRIOR SEA DUTY (YRS.)
OIC	LT	4.5
AOIC	LT	4.0
Chief Engineer	GSM1	5.5
Asst. Engineer	GSM1	5.5
Engineer	EM2	4.0
Engineer	MM2	3.0
Engineer	EMFN	0.0
Engineer	FN	0.0
Electrician/IC	EM1	4.0
Electronic Tech.	ET2	3.0
Data System Tech.	DS2	2.0
Deck Supervisor	BM2	3.0
Deck Hand	SN	3.0
Cook	MS2	2.0

A total of 28 days of open ocean operations were conducted with the longest underway period being seven days. Enlisted crew members were in a three-section watch rotation and actively participated in all aspects of the testing and data collection.

All machinery and systems were operated, maintained and repaired both underway and in port by assigned crew members. SESTF personnel developed and implemented a Planned Maintenance System (PMS) for each ship system. During refueling for open ocean testing, routine repair work was performed by the Ship Intermediate Maintenance Activity at Little Creek Naval Amphibious Base. This expedited the continuation of testing. The repairs were such that they could have been performed by the crew during normal maintenance periods at SESTF.

The only systems on the SES-200 which are not found on conventional ships are the lift fans and the seals. SESTF personnel replaced both fan bearings and bow seal fingers without training, special tools or outside assistance.

The systems on the SES-200 utilize commercial, off-the-shelf components with the exception of the seals. No support problems were encountered during the Technical Evaluation. A Consolidated Ships Allowance List (COSAL) was developed and refined as operating experience was gained. During open ocean testing, the SES-200 carried all spare parts and back-up equipment required.

SES-200 tactical turning diameters were measured for initial speeds of 5 and 10 knots hullborne and 20 knots and maximum speed cushionborne. Figure 4-17 illustrates the measured diameter for a full power turn using 30 degrees of rudder deflection. The tactical diameter is 1264 ft (8 ship lengths) and the initial steady turning diameter is 860 ft (6 ship lengths).

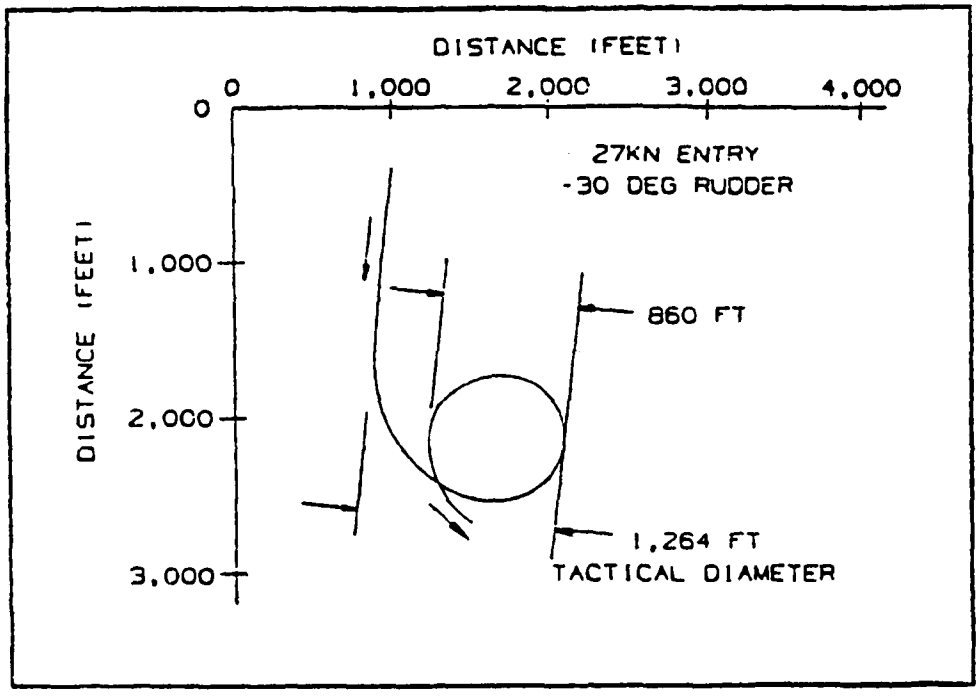

Figure 4-17 TURNING DIAMETER AT FULL POWER

The pitch and roll stiffness showed that the ship's large sidehulls provide excellent on-cushion stability. Hullborne, the catamaran form provides large roll restoring moments for intact stability under severe wind, wave and icing conditions. The vessel has a transverse metacentric height (GM_T) in excess of 50 ft at the 200-ton displacement.

TABLE 6- 5

CRITICAL RANGE FOR
δ^2/s^2 - TEST AT THE 10% SIGNIFICANCE LEVEL

K	$(\delta^2/s^2)_{min}$	$(\delta^2/s^2)_{max}$
8	0.9825	3.0175
9	1.0244	2.9756
10	1.0623	2.9378
11	1.0965	2.9035
12	1.1276	2.8724
13	1.1558	2.8442
14	1.1816	2.8184
15	1.2053	2.7947
16	1.2272	2.7728
17	1.2473	2.7527
18	1.2660	2.7340
19	1.2834	2.7166
20	1.2996	2.7004

The number of "runs" in a time series is determined by first finding the median value of the segment variances. A run is then a sequence of segment standard deviations which is either above or below this median value. The distribution function for the number of runs occurring in a given total number of time segments is known and can be used to check that the data are typical of stationary situations. For reasonable numbers of segments, the distribution is approximately normal (c.f.: Reference 6-6), so the acceptance band for the test at the 10% significance level is the expected number of runs plus or minus 1.65 times the standard deviation of the number of runs. The mean is given by

$$\mu = 2*N1*N2/N + 1$$

and the standard deviation is given by

$$\sigma = \text{SQRT } (2*N1*N2* [2*N1*N2 - N]/(N**2)*[N - 1])$$

where N1 is the number of standard deviations above the median and N2 is the number below. Details of the test are given in Reference 6-4.

For the SES-200 test data, the results of the δ^2/s^2 tests and the run tests were not used as a hard and fast means of accepting or rejecting data, particularly in marginal cases but, rather, as a means of raising a caution flag with regard to a particular data set. Poor marks on these tests indicated the data should be regarded as suspect and assigned less credibility in drawing conclusions from the data.

6.3.3.2 Power Spectral Density Functions

For the motions data, power spectra are obtained for parameters of primary interest to the motions and ride environment for selected test conditions. These are obtained by means of standard FFT methods as described in detail in Reference 6-6. The digitized DAS tape data are first decimated to a sample rate appropriate to the frequency bandwidth of interest for the data being processed. For the on-cushion test conditions of the SES-200, most data were decimated from the 200 pps rate of the DAS to 100 pps giving a Nyquist (or folding) frequency of 50 Hz. Since the SES-200 exhibits significant responses at rather high frequencies, this is about as far as the decimation could be carried without risking significant aliasing effects into the range below 20 Hz, the bandwidth felt to be of most significance for analysis purposes. With a Nyquist frequency of 50 Hz, spectral peaks beyond 50+ (50 - 20) = 80 Hz can erroneously be mapped into the region below 20 Hz. If the data were further decimated to, say, 50 pps giving a Nyquist frequency of 25 Hz, anything beyond 25+ (25 - 20) = 30 Hz would be aliased; since significant responses have been observed in RCS tests of the SES-200 well beyond 30 Hz, this is not acceptable.

For off-cushion conditions, however, these high frequency responses are not as significant. Therefore, the data for the off-cushion test points were decimated to 50 pps. This effectively halves the computational effort required for spectral analysis in these cases.

After decimating the data, removing the means and correcting for trends in the data (see Section 6.3.3.1), the resultant time series is modified by applying a (1 - cosine) taper to the first and last 10% of the data. This provides a so-called window function smoother than the 'boxcar' window (see References 6-5 and 6-9) associated with a simple truncation of a time series to obtain a finite length data segment. This minimizes the tendency for the spectral estimates to contain effects from frequency intervals other than intended for that estimate due to side lobes in the window transform. Since this tapering lowers the rms values of the data, the spectra must subsequently be corrected by dividing all spectral estimates by 0.875 (Reference 6-5).

The computed raw power spectra are smoothed to reduce the sampling variability inherent in these data by averaging together raw spectral estimates at contiguous frequencies as is standard practice (c.f.: References 6-5 and 6-9). The selection of the number of such raw estimates to be averaged together is included as part of the data reduction request form. This selection is made on the basis of a tradeoff between frequency resolution in the final spectra and the sampling variability. The coding of the FFT algorithm employed imposes constraints on the selection of the smoothing interval with the end result that all data were smoothed to yield a resolution bandwidth of 0.2 Hz. This results in somewhat higher variability in the estimates than might be desired, particularly for the shorter data runs, but the next broader resolution bandwidth available within the FFT program constraints would be unacceptably coarse for the data analysis purposes at hand. This selection results in a standard deviation of the spectral estimates of 16.9% for a three-minute test point. For the longest test points of 15 minutes, this is reduced to 7.5%.

The power spectra are produced in plotted form by the SESTF data reduction staff suitable for direct use in the report.

The SESTF FFT program can also produce cross-spectra and the associated statistics such as coherence functions, etc., together with estimates of the associated transfer functions. In most applications, such data processing is performed primarily to obtain transfer functions between the measured variables. While no pursuit of internal transfer functions was undertaken in this program, there is one area where the cross-spectral techniques were employed. This is in the reduction of the on-board radar altimeter data to obtain wave height data. The techniques for accomplishing this are given in Reference 6-12. They involve the cross-spectra between the vertical acceleration measurements made at the altimeter location and the altimeter readings. These cross-spectra are used to correct the altimeter data for craft motion effects and allow the estimation of the wave height power spectra.

6.3.3.3 1/3-Octave Band Data

The 1/3-octave band data are merely an alternate means of displaying power spectra. The spectra are numerically integrated over the 1/3-octave bands to obtain the variance of the data in these passbands. They are required for the present test program because the habitability criteria by which the ride is judged are usually stated in these terms. The method of obtaining these data is described in Reference 6-6.

6.3.3.4 Histograms

The methods of obtaining histograms are described in Reference 6-10. Only a small amount of histogram data were processed for the SES-200 program.

7. PERFORMANCE

7.1 PERFORMANCE TESTS

Performance data were collected during most missions as the required measurements were recorded at all times during test operations. Tables 6-3 and 6-4 identify the types of tests completed.

Propulsion horsepower was calculated for each engine using the measured propeller shaft RPM and torque. The torque strain gauges were calibrated using the shunt resistance method and there is some evidence that the torque measurements may be 5-10% high. If this is the case, the horsepowers presented are high by a similar amount.

Lift horsepower was calculated for each fan from the Bell fan curves using the measured fan exit static pressure and measured RPM. No corrections were made for operation at non-standard atmospheric conditions. On a few occasions, the fan exit static pressures for the starboard fan appeared too high. In these instances, starboard fan horsepower was set equal to that of the port fan as the fan RPMs were reasonably matched.

Lift and propulsion engine fuel flows were measured directly at each engine and all range calculations are based on these measurements. Engine performance curves were not used except to verify that the measured fuel flow rates were comparable to the manufacturer's predictions.

Displacements and longitudinal center of gravity (LCG) positions were calculated using draft readings and the Bell-Halter draft tables reported in Reference 7-2.

LCG positions are defined relative to amidships which is located 11-7/16 in. forward of Frame 8-4. LCG values are denoted (+) if forward and (-) if aft of amidships.

Water depth during calm water performance tests conducted in the Chesapeake Bay was typically on the order of 60-100 ft. As these depths are approximately equal to or greater than one-half (1/2) the nominal cushion length (133 ft), the test results should not be affected by shallow water effects.

There were no model drag data available to do a model/ship powering correlation. Therefore, no attempt was made to measure the ambient air temperature and humidity and the water temperature and specific gravity during testing.

7.2 HORSEPOWER VERSUS SPEED

7.2.1 Sea State 0/I Horsepower Versus Speed

Four missions were conducted to measure the SES-200's performance in calm water and Sea State I conditions. These missions and the test conditions are summarized below in Table 7-1.

TABLE 7-1

Sea State 0/I Performance Tests

Mission Number	Displacement (L.T.)	LCG Position (ft)	Sea State
39	199.7 - 203.9	-1.51 to -1.98	Low I
49	161.9 - 163.9	-1.96 to -2.12	0
50	161.9 - 163.9	-1.72 to -1.98	0
64	200.0 - 206.5	-1.49 to -1.77	0

The displacements during Missions 39 and 64 are referred to as the heavy ship test condition as these missions were conducted with the vessel fully loaded with fuel. Also, sufficient supplies and spare parts were onboard to conduct extended ocean operations. The nominal displacement for the heavy ship test condition is 200 L.T.

Displacements during Missions 49 and 50 are referred to as the light ship test condition. These missions were conducted with a 35-40% fuel load. 165 L.T. is the nominal displacement for this test condition.

All performance tests were conducted using LCG locations between 1.5 and 2.1 ft aft of amidships. As will be discussed subsequently, LCG positions in this range optimize performance, i.e., minimize the total lift and propulsion horsepower required to achieve a given speed.

Figure 7-1 illustrates the measured variation in total lift and propulsion horsepower with speed at the heavy and light ship test conditions in calm water and Sea State I test conditions. Data points plotted are for the lift setting which resulted in minimum total power. At idle ahead conditions (6-8 knots), hullborne operation without lift consumed the least amount of power. At higher speeds, lift power is applied to raise the ship out of the water as this consumes less total power than hullborne operation. As will be discussed subsequently, the lift setting is gradually increased with speed to minimize the total power required.

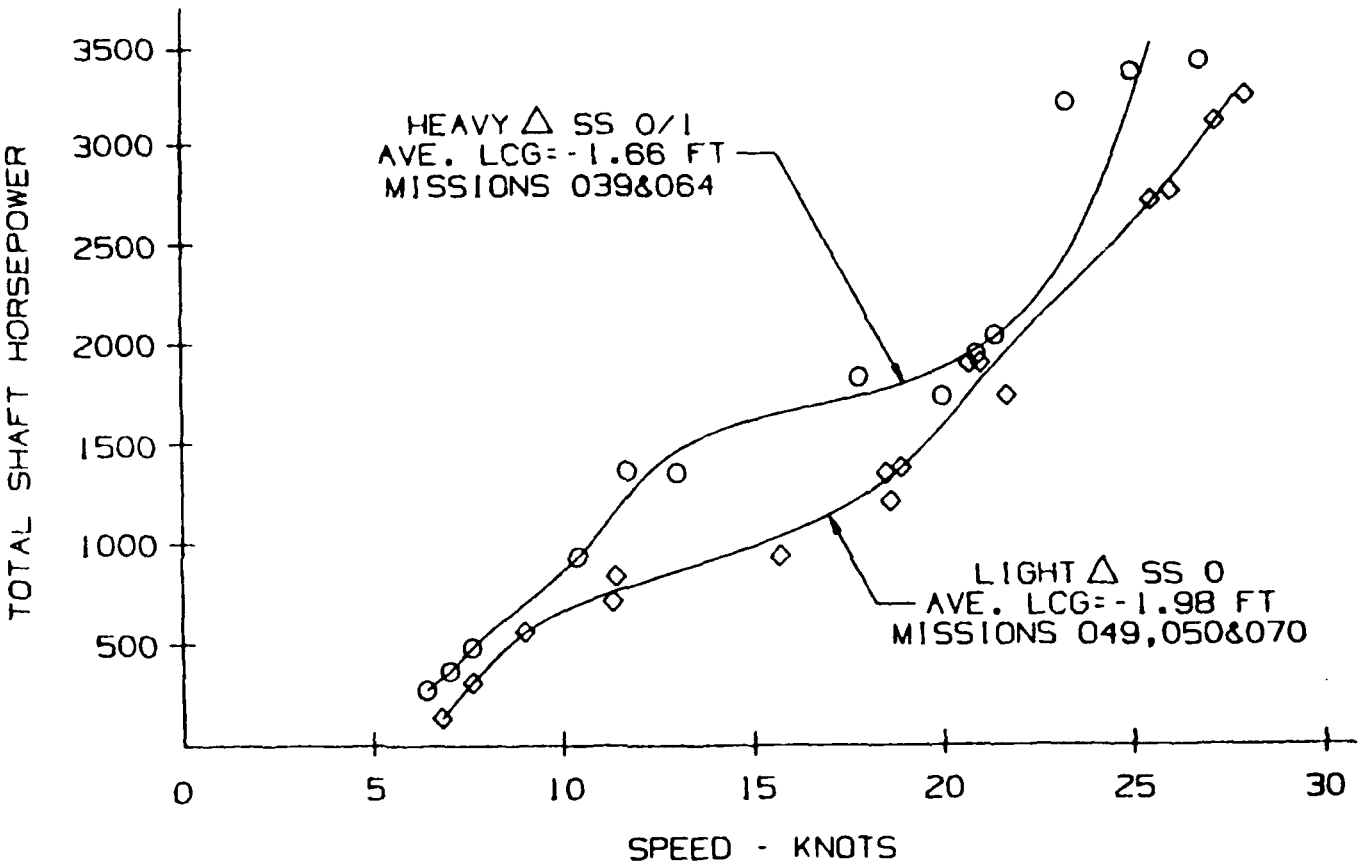

FIGURE 7-1 : SES-200 TOTAL SHIP HORSEPOWER VERSUS SPEED, HEAVY AND LIGHT SHIP TEST CONDITIONS, BEST LIFT FAN RPM

Several aspects of the SES-200's sensitivity to loading are illustrated in Figure 7-1. In the vicinity of the secondary wave making drag hump (14 knots), the power requirements increase with displacement as would be expected. However, at cruise speeds in the vicinity of 20 knots, the power required is relatively insensitive to displacement. This corresponds to the operating region between the secondary and primary wave making drag humps where the wave making resistance component is very low. Trends shown in Figure 7-1 illustrate that the SES-200's displacement could be significantly increased and the vessel could still obtain calm water speeds well over 20 knots without increasing the installed power.

Figures 7-2 and 7-3 illustrate the division of power between lift and propulsion versus speed for the heavy and light ship test conditions, respectively. These data are also for the lift setting which minimized total power. At maximum speed, lift power represents less than 12% of the total power. The amount of scatter in the data plotted in Figures 7-1 through 7-3 is considered quite reasonable for a full scale test program.

7.2.1.1 Sea State 0/I - Hullborne Versus Cushionborne Operation

Figure 7-4 illustrates the SES-200's low speed power requirements. Curves are shown for hullborne and cushionborne operation at the light (165 L.T.) and heavy (200 L.T.) ship test conditions. Hullborne, the SES-200 rides with its wet deck clear of the water like any catamaran ship. The data with air cushion lift are for 1300 fan RPM as this was judged best for low speed cushionborne operation. However, as no cushionborne tests were conducted using less than 1300 RPM, this lift setting may not represent the minimum power required for low speed cushionborne operation.

At 165 L.T., hullborne operation requires slightly less power up to 10 knots; above this speed, use of air cushion lift is considerably more efficient. At 200 L.T., hullborne operation only requires less power at the idle ahead condition.

7.2.1.2 Sea State 0/I - Effect of Lift Fan Flow Rate

Figures 7-5 and 7-6 illustrate the horsepower requirements for cushionborne operation at the heavy and light ship test conditions, respectively. The data are plotted on the basis of horsepower per knot versus speed for five (5) different lift settings, i.e., 1300, 1500, 1700 and 1900 and 2000 RPM. The horsepower per knot presentation is used as it provided a good illustration of the effect of lift setting on the total horsepower required at each speed.

Lift settings which minimize total power at each speed were identified from these figures and the corresponding data points were plotted in Figures 7-1 through 7-3 to illustrate the vessel's best performance. At the heavy ship test condition, either 1300 or 1500 lift fan RPM is best up to 12 knots, 1500 RPM is most efficient between 12 and 18 knots and 1700 RPM is best above 18 knots. At the light ship test condition: 1300 RPM is best up to 15 knots; 1500 RPM is most efficient between 15 and 22 knots;

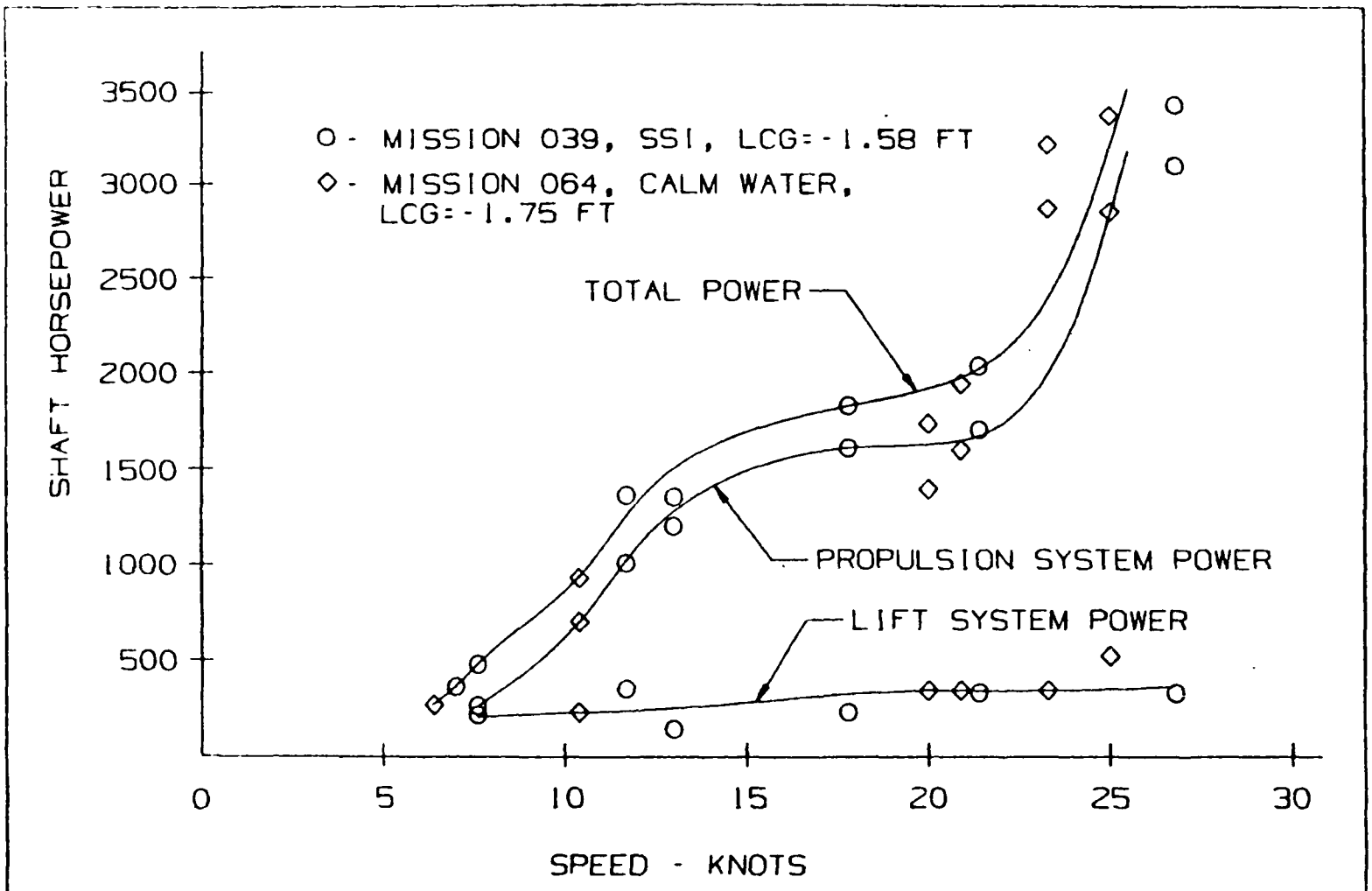

FIGURE 7-2 : SES-200 DIVISION OF POWER VERSUS SPEED, HEAVY SHIP TEST CONDITION, BEST FAN RPM

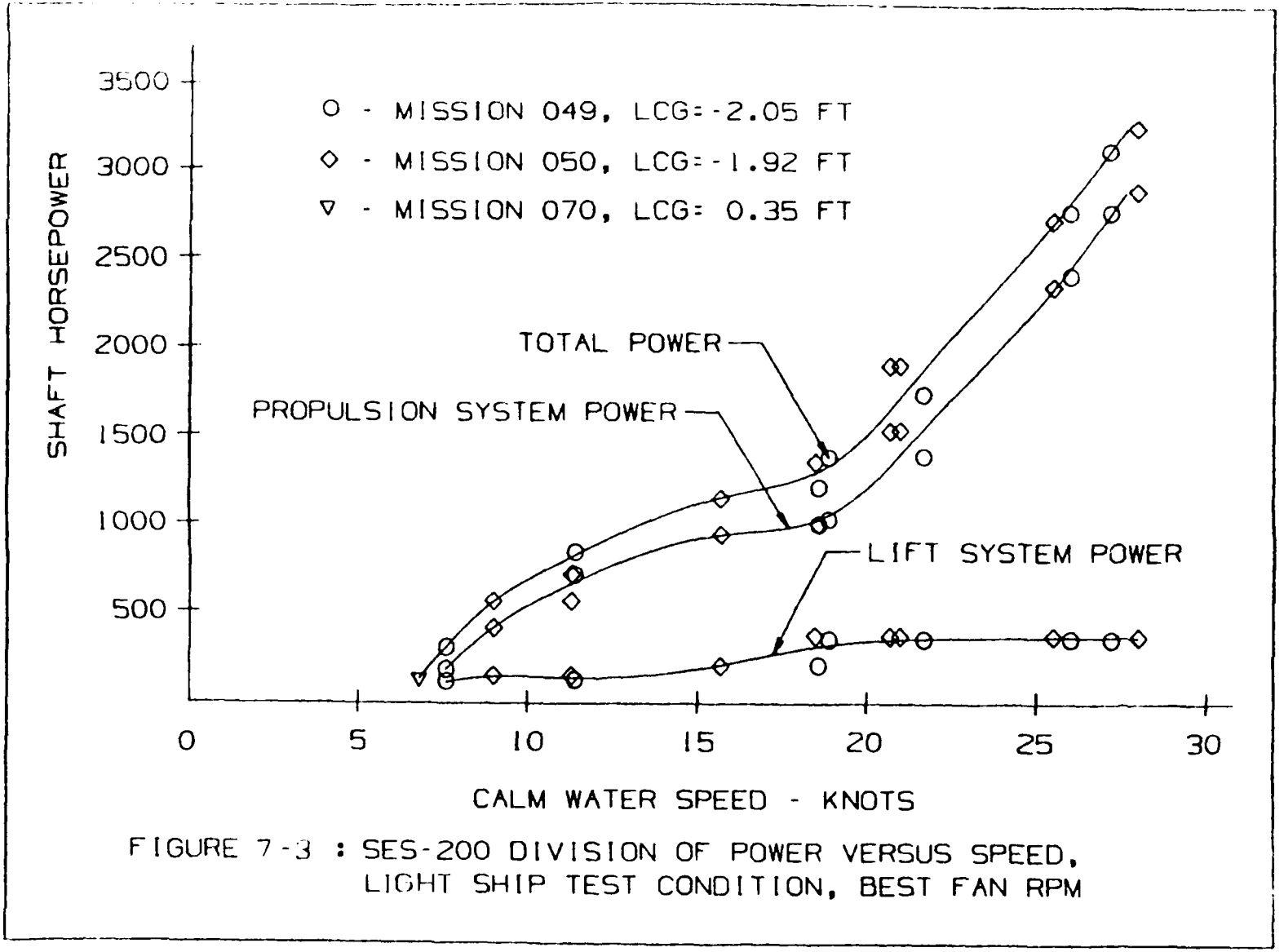

FIGURE 7-3 : SES-200 DIVISION OF POWER VERSUS SPEED, LIGHT SHIP TEST CONDITION, BEST FAN RPM

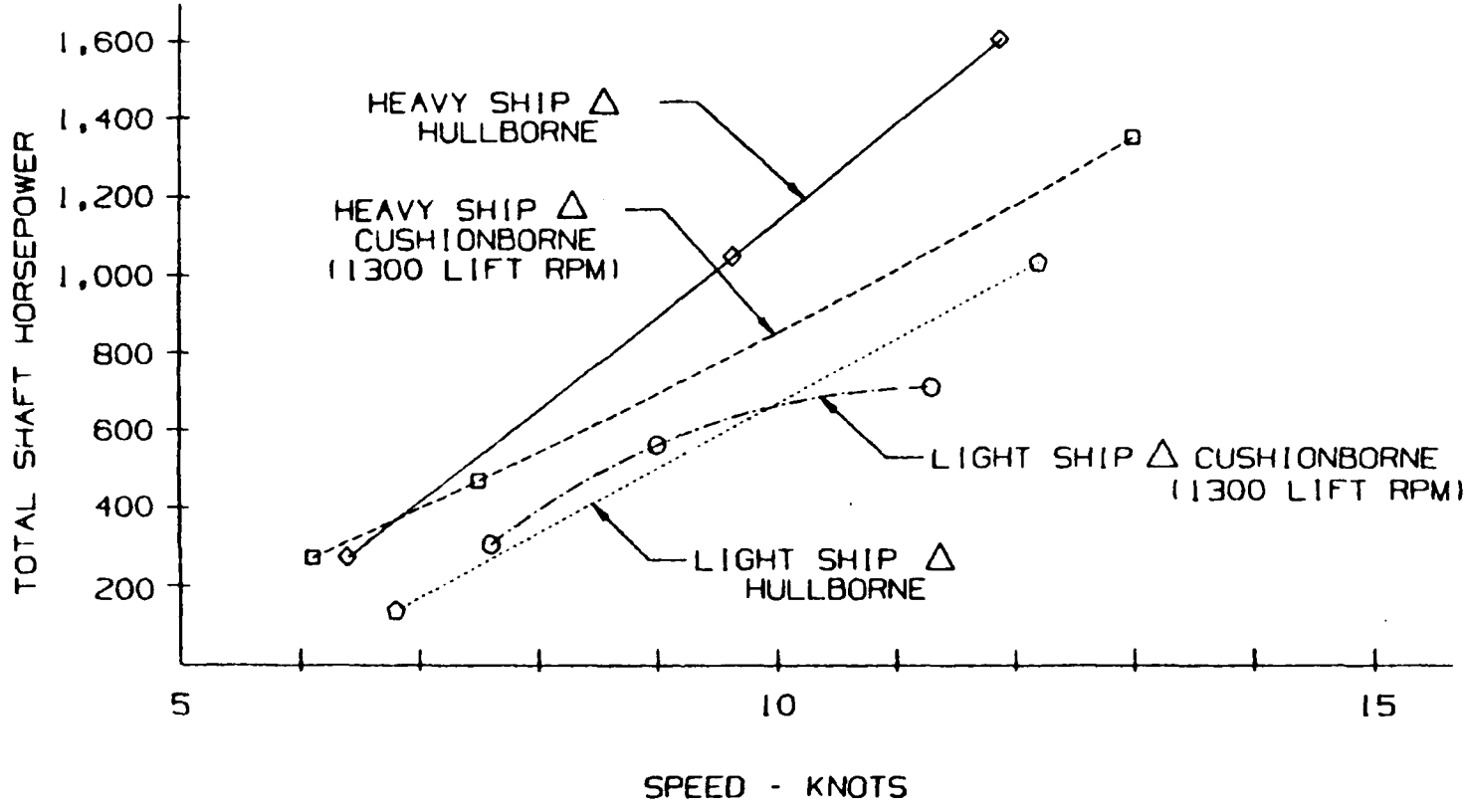

FIGURE 7-4 : SES-200 TOTAL POWER REQUIRED AT LOW SPEED, HEAVY AND LIGHT SHIP TEST CONDITION, HULLBORNE AND CUSHIONBORNE WITH BEST LIFT FAN RPM

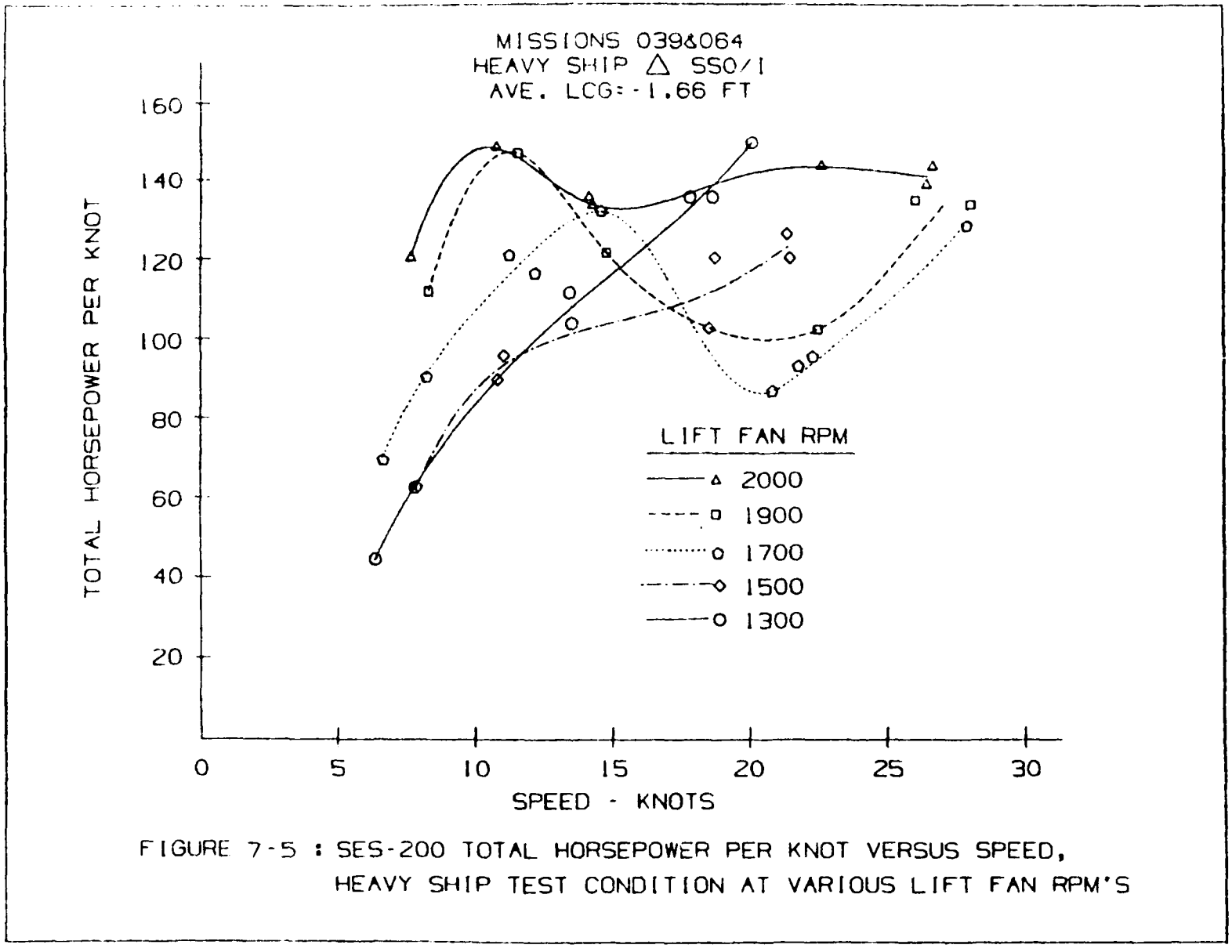

FIGURE 7-5 : SES-200 TOTAL HORSEPOWER PER KNOT VERSUS SPEED, HEAVY SHIP TEST CONDITION AT VARIOUS LIFT FAN RPM'S

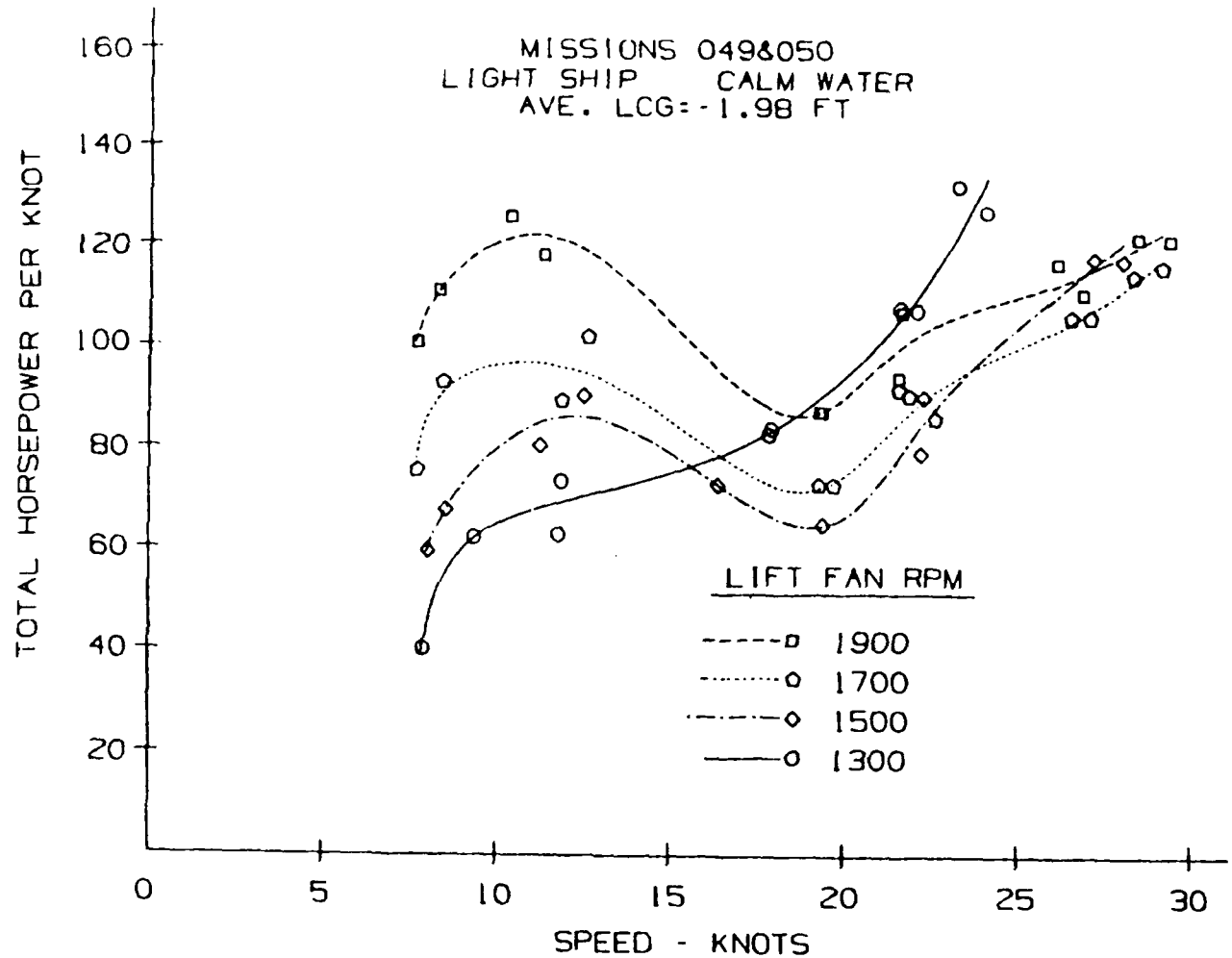

FIGURE 7- 6 : SES-200 TOTAL HORSEPOWER PER KNOT VERSUS SPEED, LIGHT SHIP TEST CONDITION AT VARIOUS FAN RPM'S

and 1700 RPM is best above 22 knots. Lift fan RPM's between 1700 RPM and 2100 RPM (the maximum) are not as efficient for calm water operation as the lower fan speeds. However, at maximum propulsion power, increasing the fan speed from 1700 to 1900 RPM will produce another 0.5 - 1 knot of speed.

The reason that maximum lift power does not automatically minimize the total power is that SES resistance is made up of components that depend on the cushion pressure and sidehull immersion. Wave drag varies as the square of cushion pressure, while the sidehull and seal drag components depend on immersion. As increasing the fan speed increases the cushion pressure (wave drag) and reduces the immersion (sidehull and seal drag), it is important to select a fan speed (flow rate) which minimizes the combined resistance of these components.

Figures 7-7 and 7-8 illustrate the cushion pressure and fan flow, respectively, at each combination of fan speed and ship speed for which heavy ship tests were conducted. Figures 7-9 and 7-10 illustrate the same data for the light ship test condition. For the heavy ship test condition (Figure 7-7), fan speeds of 1700 RPM and up are nominally referred to as "full cushion operation", as increasing the fan speed above this value does not significantly increase the cushion pressure. That is, the air cushion lift reaches a maximum under these conditions. As operation at fan speeds below 1700 RPM significantly reduces the cushion pressure (cushion lift) and increases the immersion (sidehull lift), it is referred to as "partial cushion operation". For the light ship test condition (Figure 7-9), 1500 fan RPM represents "full cushion operation". Applying these terms to the heavy ship test condition (Figures 7-4 and 7-5) indicates that hullborne operation is best up to 7 knots, partial cushion is most efficient between 7 and 18 knots and above 18 knots, full cushion operation is best. For the light ship (Figures 7-4 and 7-6), the comparable transition speeds are 10 and 15 knots, respectively.

Mission 060 was conducted to evaluate the SES-200's pitch stiffness and to evaluate the effect of longitudinal center of gravity (LCG) position on performance. The tests were conducted by shifting ballast water to vary the LCG from 1 ft forward to 4 ft aft of amidships. At each LCG position, data were recorded for three speeds (15, 20 and 25 knots) and two fan RPMs (1700 and 1900).

Figure 7-11 shows the total horsepower required per knot at each LCG position for speeds of 17 to 18 knots and 23 to 24 knots using 1700 fan RPM. Most of the test data fell in these two speed ranges. As 1900 fan RPM is less efficient than 1700, the data for 1900 RPM are not presented.

The curves shown in Figure 7-11 demonstrate that the LCG position of 2 ft aft of amidships recommended by Bell-Halter (Reference 7-2) is close to optimum. Also, the curves show that an LCG variation of ± 2 ft from this nominal position has only a small effect on the power required. In general, it has been found that a high L/B SES is less sensitive to LCG position than a low L/B SES as it does not have to be powered through the primary drag hump and therefore maintaining proper trim angle is not as critical.

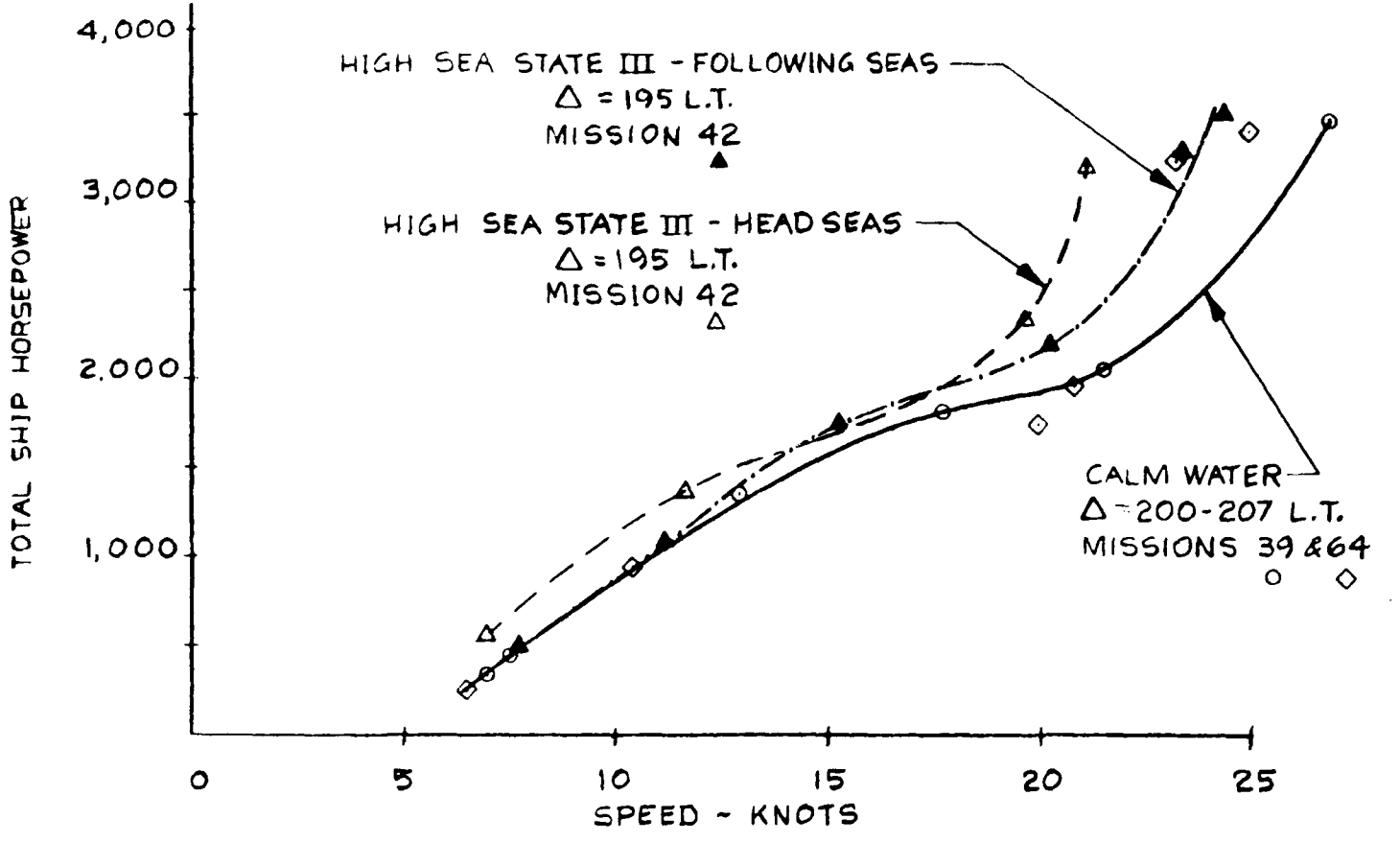

FIGURE 7-16 SES-200 TOTAL SHIP HORSEPOWER VERSUS SPEED, HEAVY SHIP TEST CONDITION, BEST LIFT FAN RPM, CALM WATER AND HIGH SEA STATE III

At first glance the data do not appear to be entirely consistent, as between 10 and 15 knots the vessel requires slightly more power in calm water than it does in Low Sea State III conditions. This is the region of the secondary wave making drag hump which peaks at 14 knots. As previously explained, the ship is sensitive to displacement in this region (see Figure 7-1) and the vessel was approximately 10 tons (5%) heavier during the calm water tests. This is the only explanation offered as to why calm water operation required more power in this speed regime.

Above 15 knots, the data appear entirely consistent, as there is a modest increase in power required to achieve a given speed due to operation in low Sea State III. Additionally, as would be expected, head sea operation requires more power than following seas.

Figure 7-16 compares the horsepower required to achieve a given speed in high Sea State III with the calm water horsepower for the heavy ship test condition. Curves are plotted for both the head and following sea wave directions. In this higher sea condition, there is an increase in horsepower required at all speeds except for the following sea case below 10 knots which is identical to the calm water performance line.

One significant aspect of Figures 7-15 and 7-16 that should be noted is that, up to 20 knots, Sea State III operation requires very little additional power to achieve a given speed over that required in calm water. Above 20 knots, the additional power required in Sea State III shows a strong dependence on speed and heading as would be expected.

Wave spectra measured during the low and high Sea State III performance tests are presented in Figure 7-17. The significant wave height measured was between 3.5 and 3.9 ft during the low Sea State III tests and between 4.8 and 6.1 ft during the high Sea State III tests.

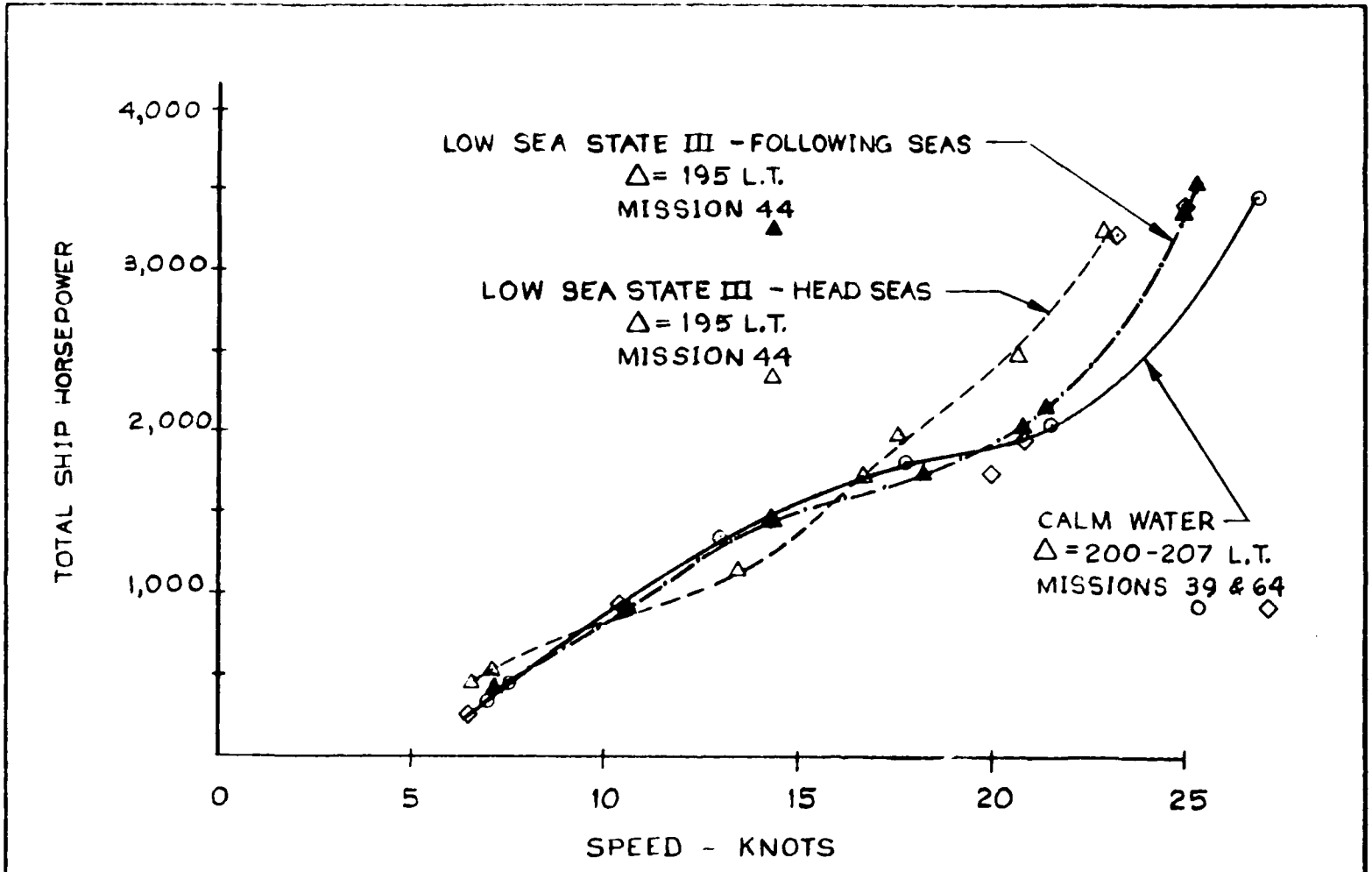

FIGURE 7-15 SES-200 TOTAL SHIP HORSEPOWER VERSUS SPEED, HEAVY SHIP TEST CONDITION, BEST LIFT FAN RPM, CALM WATER AND LOW SEA STATE III

FIGURE 7-14 WAVE SPECTRA FOR SEA STATE II PERFORMANCE TESTS

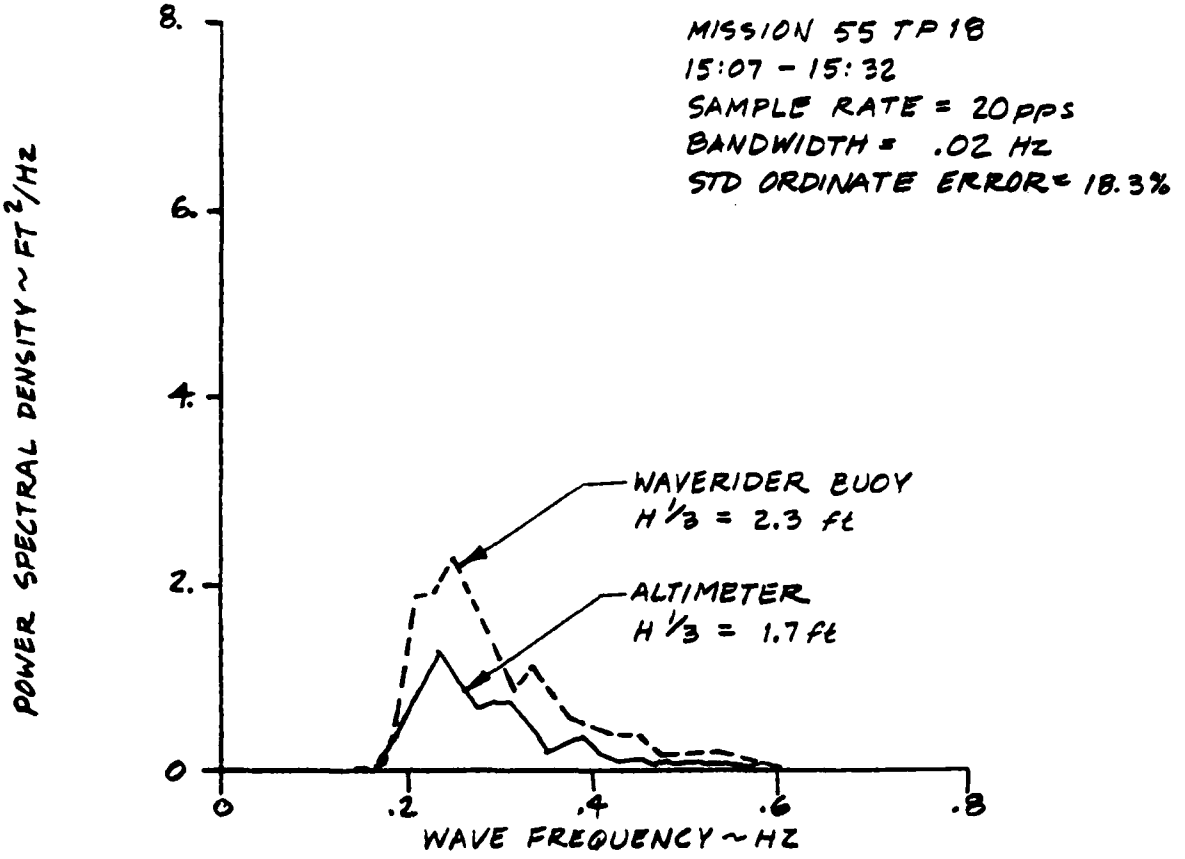

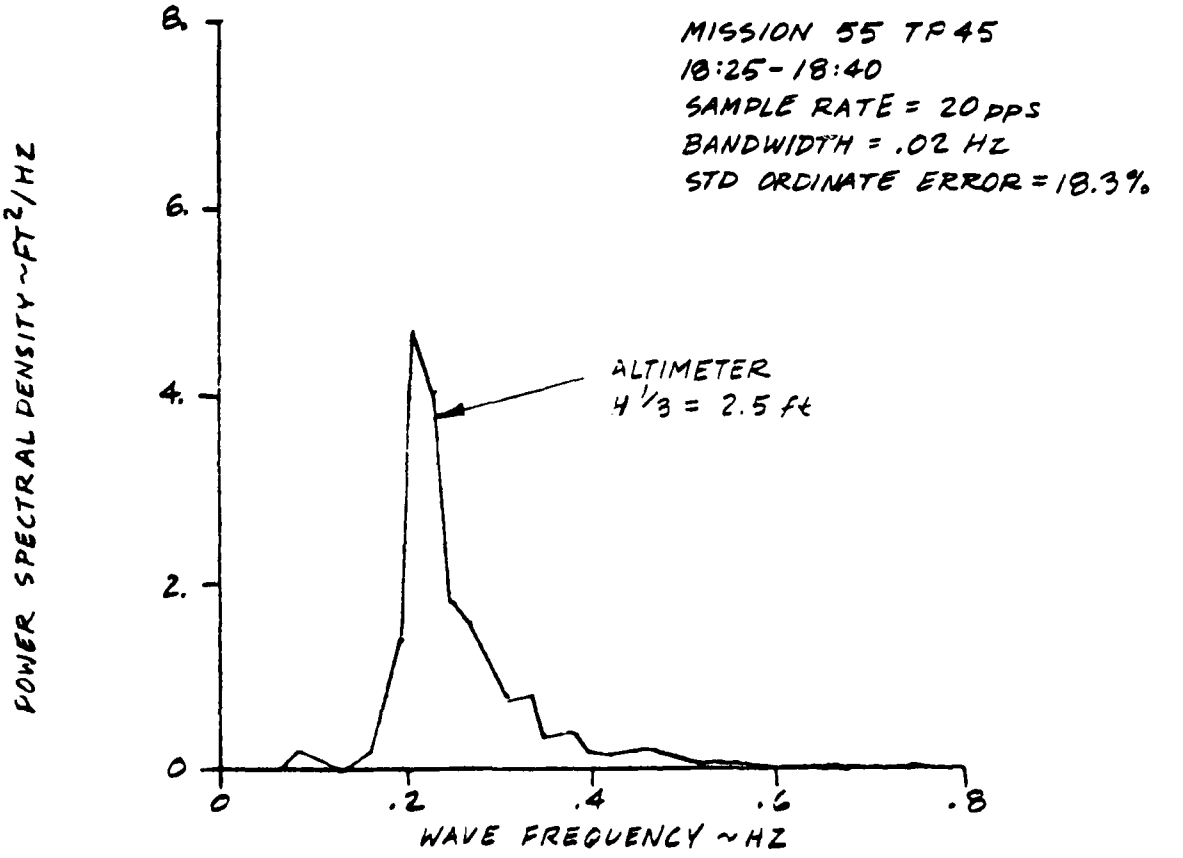

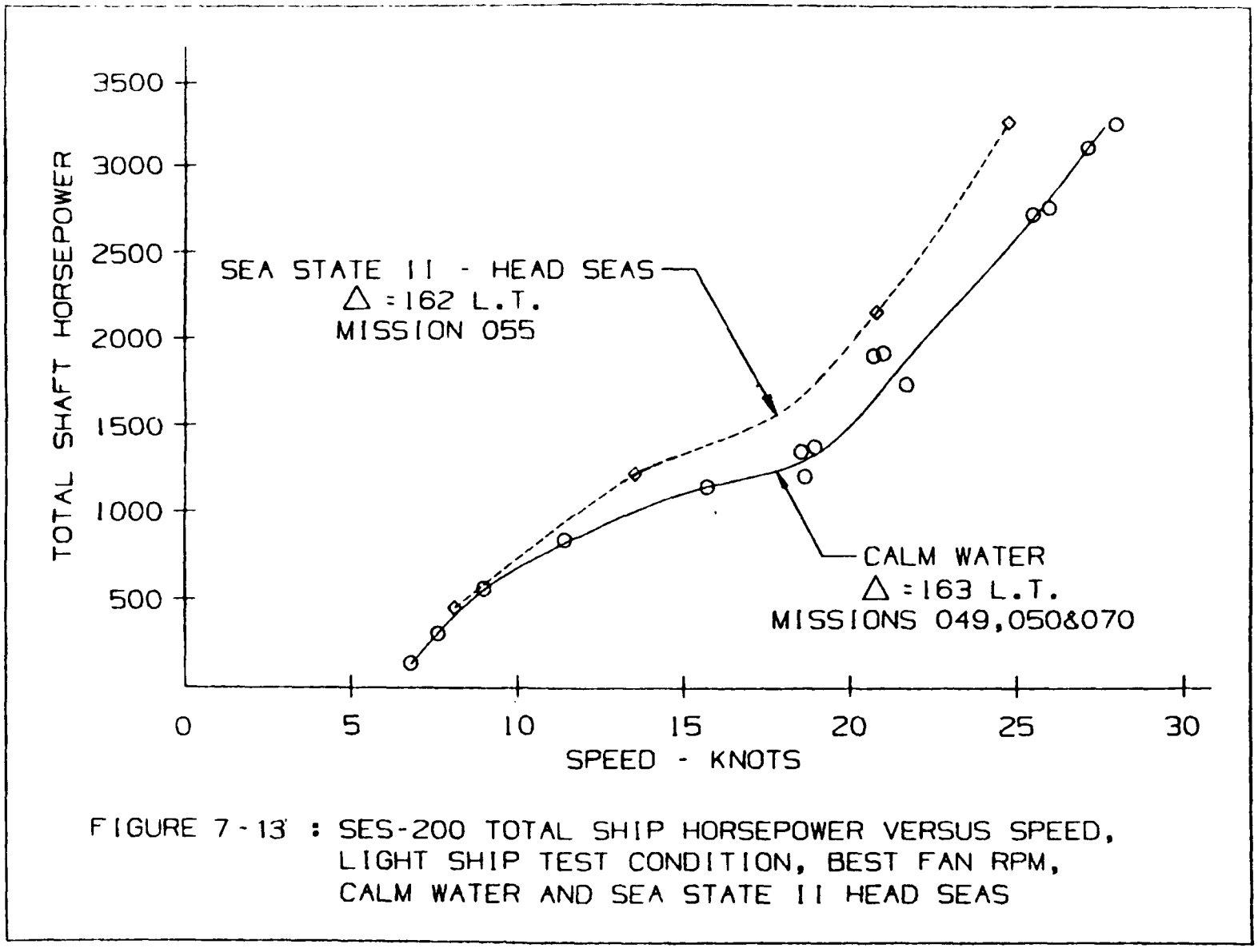

FIGURE 7-13 : SES-200 TOTAL SHIP HORSEPOWER VERSUS SPEED, LIGHT SHIP TEST CONDITION, BEST FAN RPM, CALM WATER AND SEA STATE II HEAD SEAS

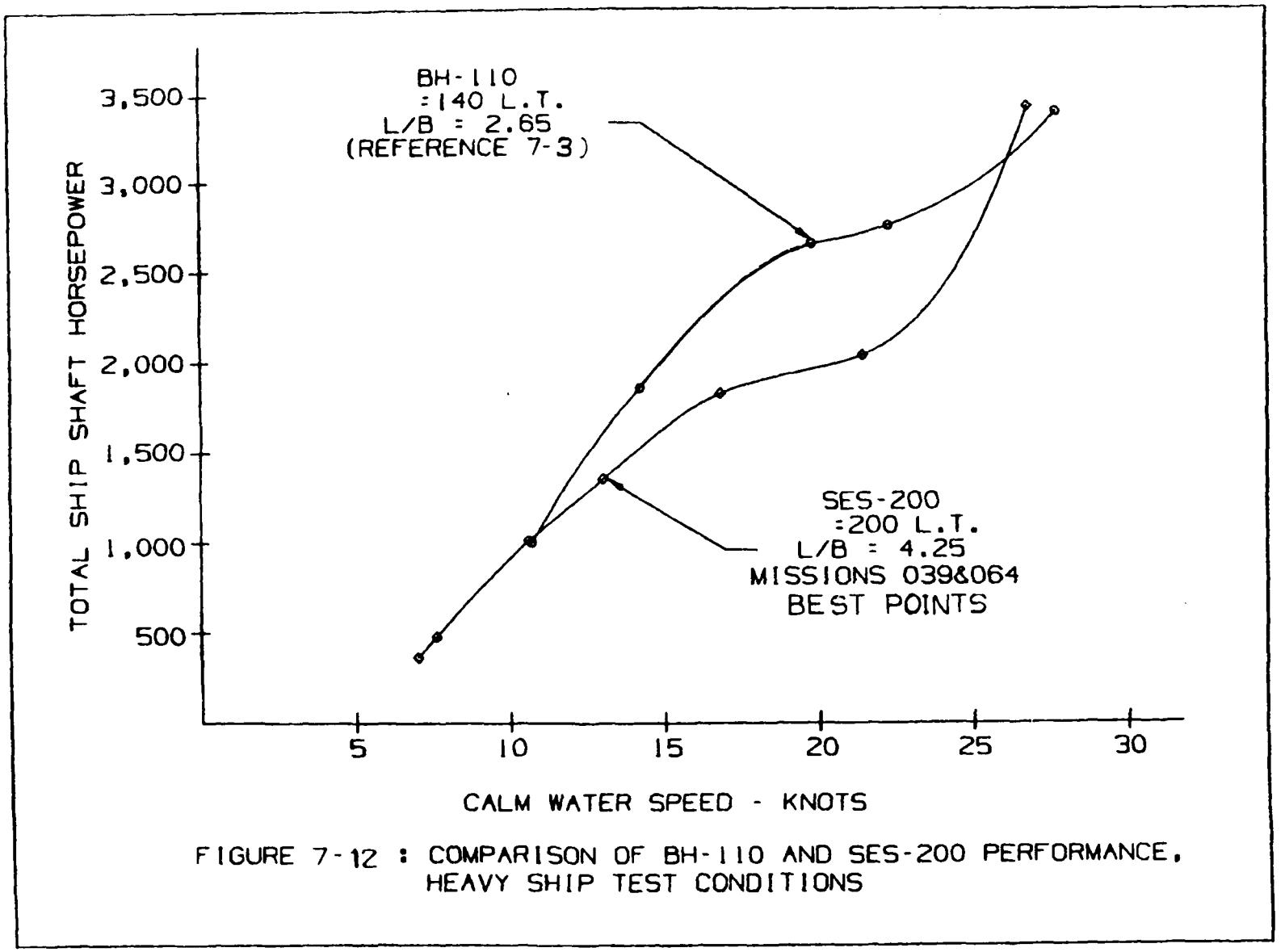

FIGURE 7-12 : COMPARISON OF BH-110 AND SES-200 PERFORMANCE, HEAVY SHIP TEST CONDITIONS

7.2.1.5 Sea State 0/I - Comparison of SES-200 and BH-110 Performance

Figure 7-12 compares the SES-200's performance at 200 L.T. displacement with data from tests of the BH-110 at 140 L.T. reported in Reference 7-3. These displacements represent heavy ship test conditions for both vessels.

Increasing the BH-110's length-to-beam ratio from 2.65 to 4.25 shifted the peak of the primary wave drag hump from 20 knots (which is inside the BH-110's operating envelope) to 33 knots (which is outside the operating envelope of both vessels. As shown, the low length-to-beam BH-110 has a 2-3 knot higher maximum speed; however, between 10 and 27 knots, the SES-200 requires substantially less power. In this speed range, the reduction in wave making resistance achieved by increasing the length-to-beam ratio was greater than the increase in sidehull drag from the 50 ft hull extension. Therefore, in addition to being larger and carrying more fuel, the SES-200 also enjoys a powering advantage over most of the operating envelope.

7.2.2 Sea State II Horsepower Versus Speed

The ship's performance in Sea State II was measured on Mission 055 at the light ship test condition. Figure 7-13 compares the horsepower required to achieve a given speed in head seas with the calm water horsepower requirements. Both sets of data are plotted for the lift settings which resulted in minimum total power. As shown, there is a modest increase in the power requirements for Sea State II operation. Wave spectra measured during the Sea State II tests are shown in Figure 7-14. Significant wave height measured between 1.7 and 2.5 ft, which corresponds to mid Sea State II. As no Sea State II performance tests were conducted at the heavy ship test condition, the effect of displacement cannot be assessed.

7.2.3 Sea State III Horsepower Versus Speed

The SES-200's performance in low and high Sea State III at the heavy ship test condition was measured on Missions 44 and 42, respectively. During the Mission 44 tests, the displacement was 195 L.T. and the LCG was located between 1.8 and 2.2 ft aft of amidships. In Mission 42, the displacement was 193 L.T. and the LCG was 1.4 to 1.6 ft aft of amidships.

Figure 7-15 compares the horsepower required to achieve a given speed in low Sea State III with the calm water horsepower for the heavy ship test condition. Low Sea State III curves are plotted for both head and following sea wave directions. All curves are plotted for the lift setting which resulted in minimum total power at each speed.

TABLE 7-2
ACCELERATION - DECELERATION TEST RESULTS

Test Conditions	Craft Speed—Kn Initial	Craft Speed—Kn Final	Elapsed Time — Sec.	Wave Direction
SES-200				
Heavy Ship Test Condition, Acceleration at rest with aft seal cleared of water (fan RPM=1000) to max. speed SSO/I	0	23.6	57	-
Heavy Ship Test Condition, Acceleration at rest with aft seal cleared of water (fan RPM=1300) to max. speed SSIII	0 0 0 0 0	24.2 24.2 23.5 29.6 25.7	96 70 66 75 69	Head Bow Beam Quartering Following
Heavy Ship Test Condition, Deceleration from max. speed to DIW with fan RPM 1900 to 0, SSO/I	26.2	0	39	-
Heavy Ship Test Condition, Deceleration from max. speed to DIW with fan RPM 1900 to 0, SSIII	22.1 23.1 24.2 26.9 25.1	0 0 0 0 0	48 50 52 67 72	Head Bow Beam Quartering Following
BH-110 (REFERENCE 7-3)				
Acceleration at rest with aft seal cleared of water (fan RPM=1280), to high speed, ave. of 4 events	0	29.3	79	Unknown
Decelerate from high speed to rest by cutting power to both propulsion and fan engines, ave. of 2 events	27.0	0	18	Unknown

7.2.1.3 Sea State 0/I Acceleration/Deceleration

Acceleration and deceleration times in calm water were measured on Missions 039 and 050. The acceleration tests were conducted with the stern seal initially drained of water as this is the normal method of operation. Damage to the stern seal may occur if acceleration begins before the bag has a chance to drain. Table 7-2 presents results of all SES-200 acceleration and deceleration tests. Sea State III data from Missions 45 and 46 is included with the Sea State 0/I results. Also, two BH-110 tests from Table 8 of Reference 7-3 are included for comparison. All of the SES-200 data tabulated are at the heavy ship test condition. The BH-110's displacement was not reported.

It should be noted that tests of this type are difficult to conduct in a controlled fashion as the operator inputs required (e.g., setting the engine throttles and maintaining constant heading) are not usually accomplished in a precise manner. Additionally in waves, the results are of limited value as they are only indicative of the time required to accelerate to maximum speed (or decelerate from maximum speed) through a specific train of waves. Numerous tests would have to be performed to get an average acceleration or deceleration time in a given seaway.

The results indicate that the SES-200 can accelerate from rest to a speed in the neighborhood of 25 knots in 60 to 90 seconds and it can decelerate from 25 knots to DIW in 40 to 70 seconds. These times appear to be sea state and heading dependent, as would be expected; however, the data are too limited to draw any definite conclusions.

BH-110 acceleration time to 29 knots is comparable to that of the 200's time to accelerate to 25 knots. However, the deceleration time reported for the BH-110 is half that reported for the SES-200. This is probably more a matter of data interpretation (e.g., marking when the vessel actually went DIW) than a difference in vessel characteristics.

7.2.1.4 Sea State 0/I Single Engine Performance

Single engine performance data were collected during Mission 050 at the light ship test condition. Both hullborne and partial cushion tests were conducted using a single propulsion engine. The test procedure used was to declutch one propulsion engine and apply idle, 1/2 ahead, or full ahead power to the other propulsion engine. Under the 1/2 ahead condition, similar speeds were attained with either propulsion engine. During full power tests, only the port engine was tested but, based on the 1/2 ahead results, the starboard engine results are expected to be the same.

For the 1/2 ahead setting, the hullborne speeds recorded were 6.0 kn (port engine) and 6.3 kn (starboard engine). At the full ahead setting, a speed of 8.4 kn was achieved with the port engine. In the partial cushion mode (1500 RPM lift fans) and at 1/2 maximum power, the speeds recorded were 9.5 kn (port engine) and 9.3 kn (starboard engine). At the maximum power setting with the port engine, a speed of 14.1 knots was achieved.

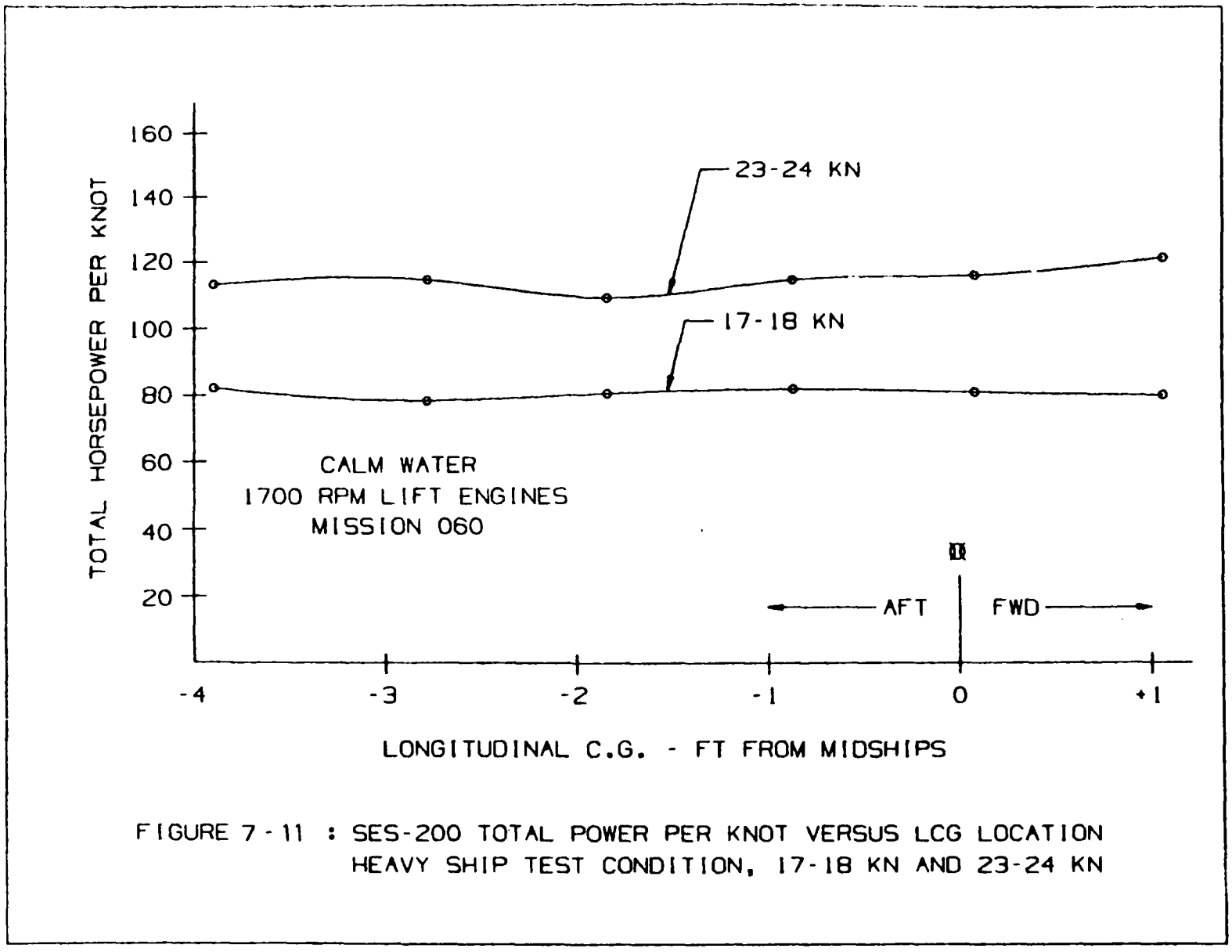

FIGURE 7-11 : SES-200 TOTAL POWER PER KNOT VERSUS LCG LOCATION
HEAVY SHIP TEST CONDITION, 17-18 KN AND 23-24 KN

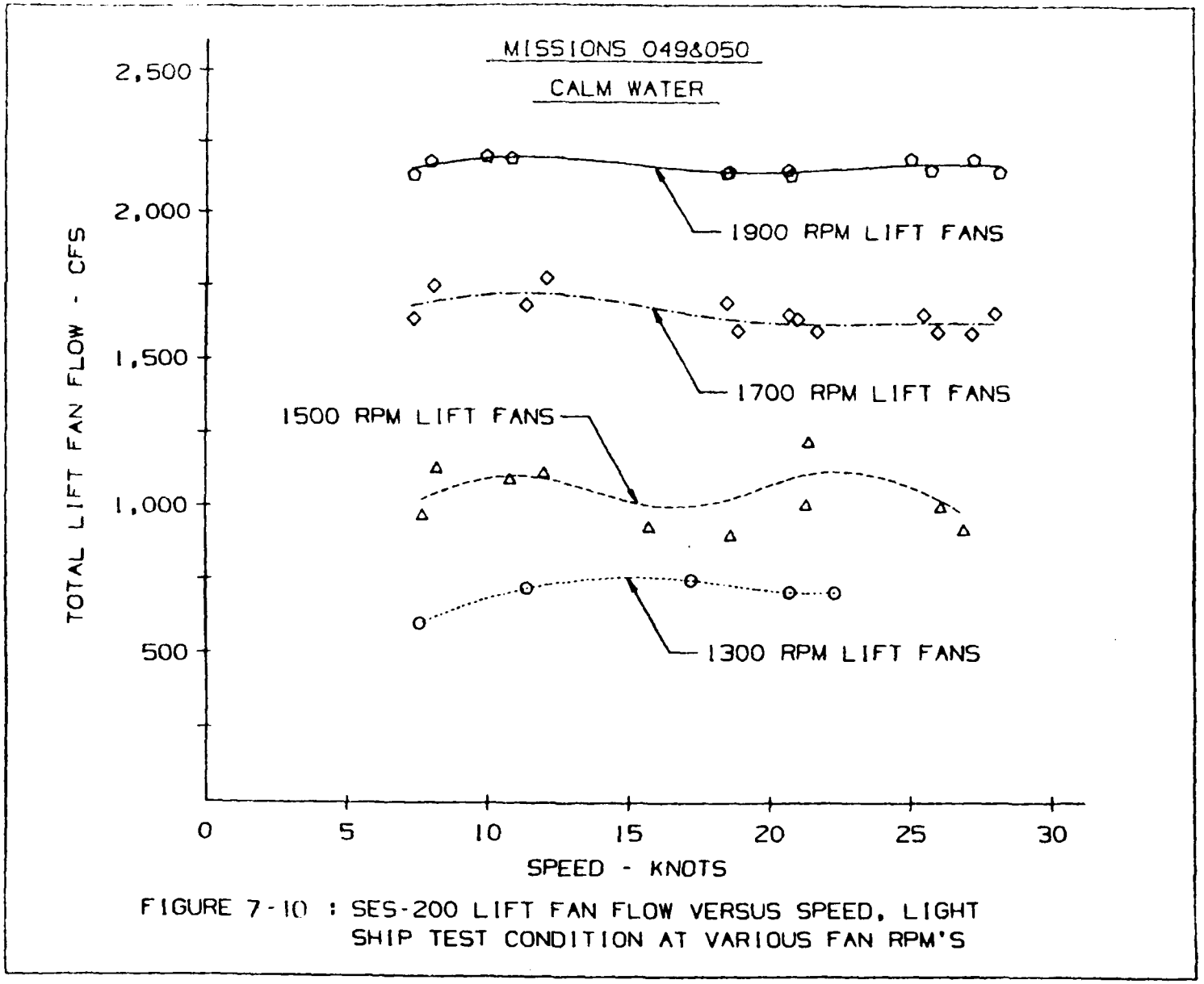

FIGURE 7-10 : SES-200 LIFT FAN FLOW VERSUS SPEED, LIGHT SHIP TEST CONDITION AT VARIOUS FAN RPM'S

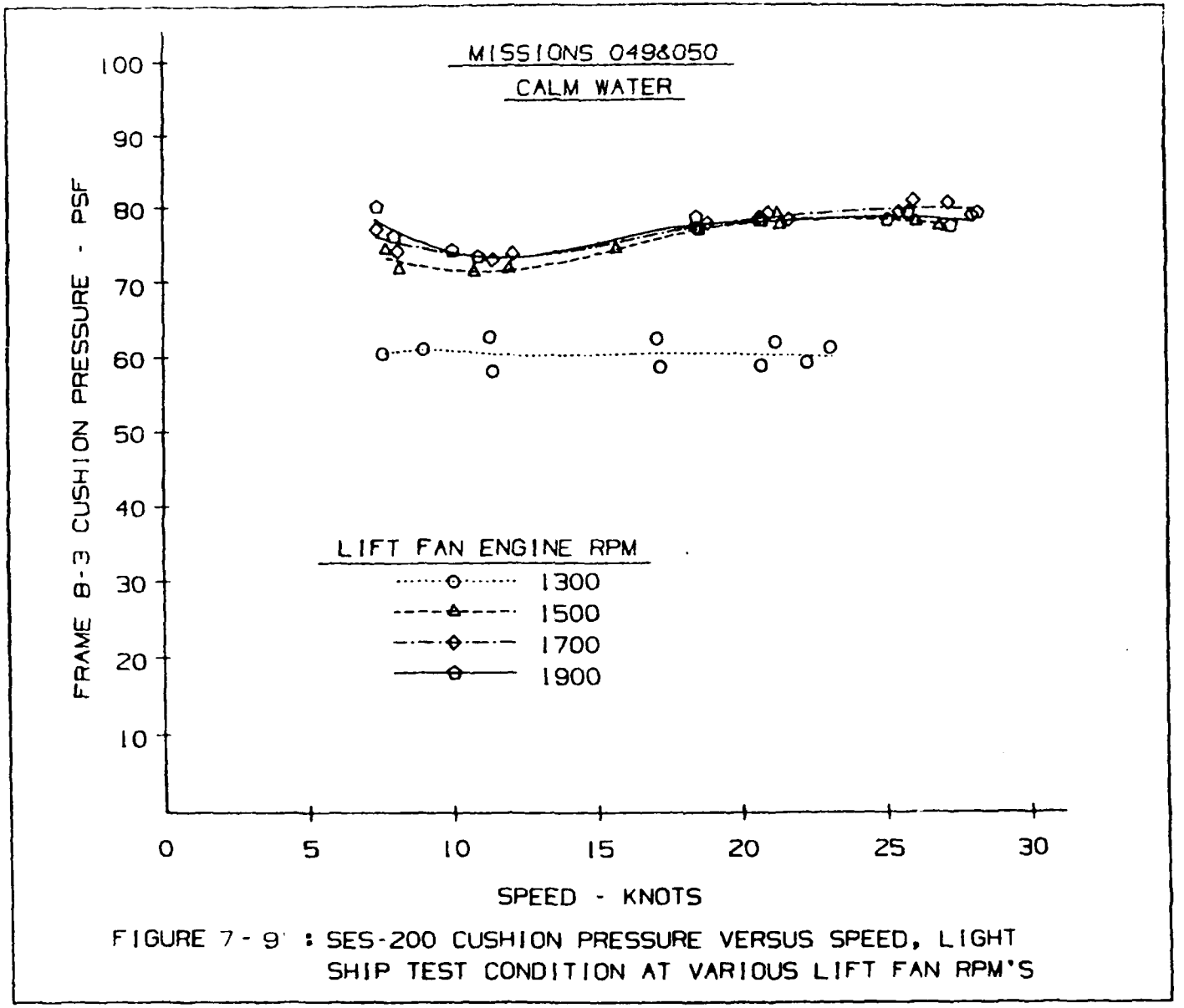

FIGURE 7 - 9 : SES-200 CUSHION PRESSURE VERSUS SPEED, LIGHT SHIP TEST CONDITION AT VARIOUS LIFT FAN RPM'S

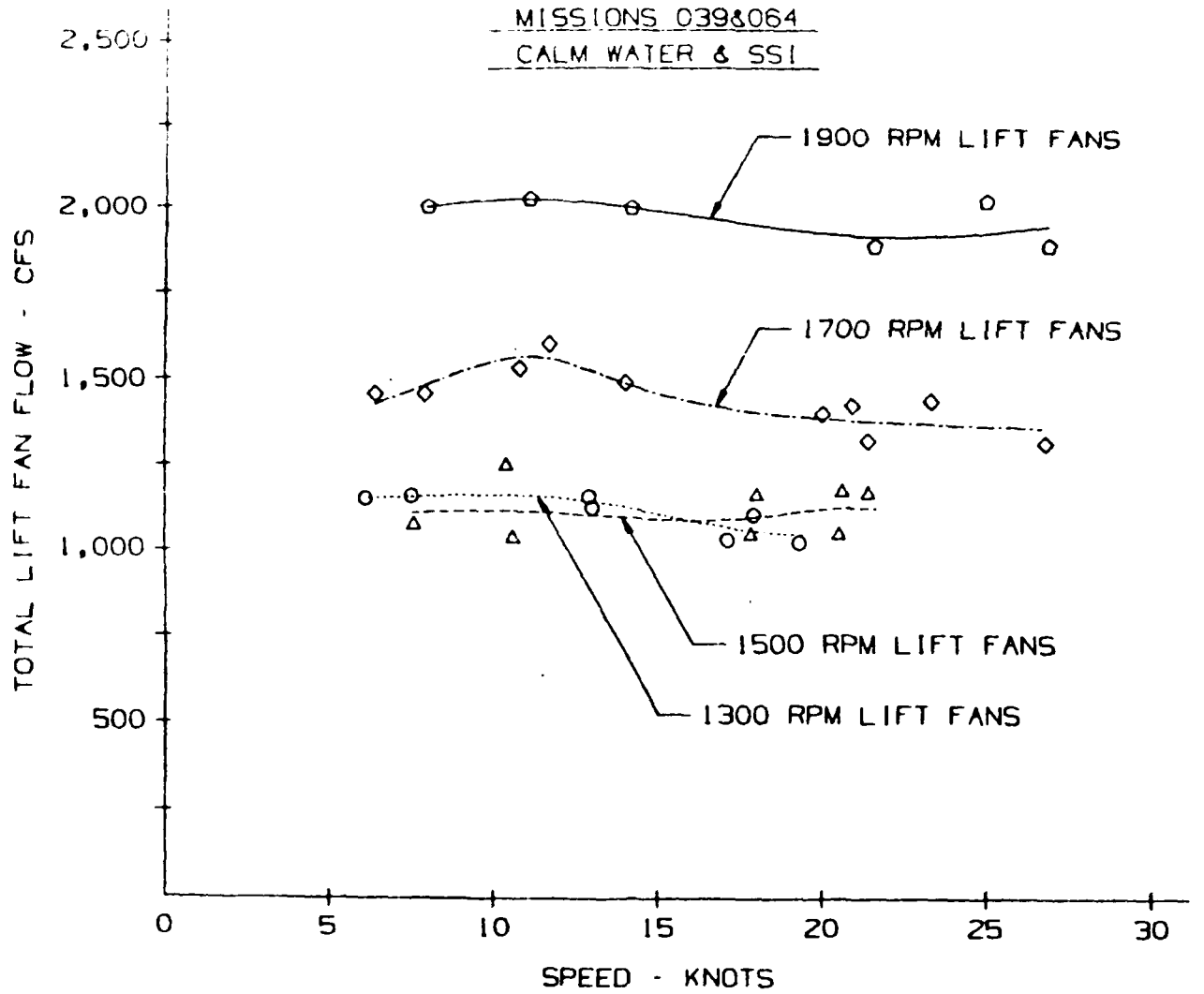

FIGURE 7-8 : SES-200 LIFT FAN FLOW VERSUS SPEED, HEAVY SHIP TEST CONDITION AT VARIOUS FAN RPM'S

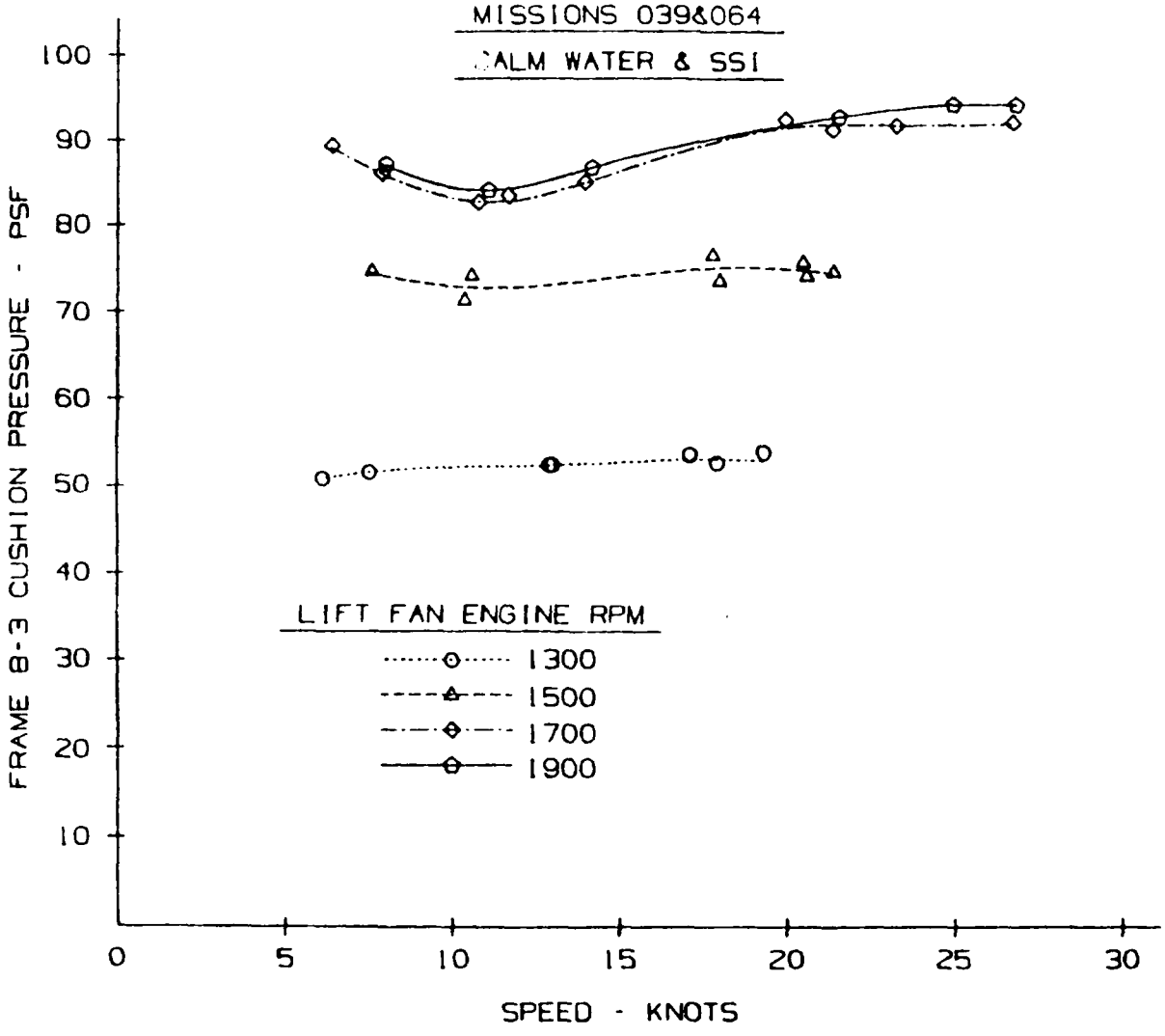

FIGURE 7-7 : SES-200 CUSHION PRESSURE VERSUS SPEED, HEAVY SHIP TEST CONDITION AT VARIOUS LIFT FAN RPM'S

FIGURE 7-17 WAVE SPECTRA FOR SEA STATE III PERFORMANCE TESTS

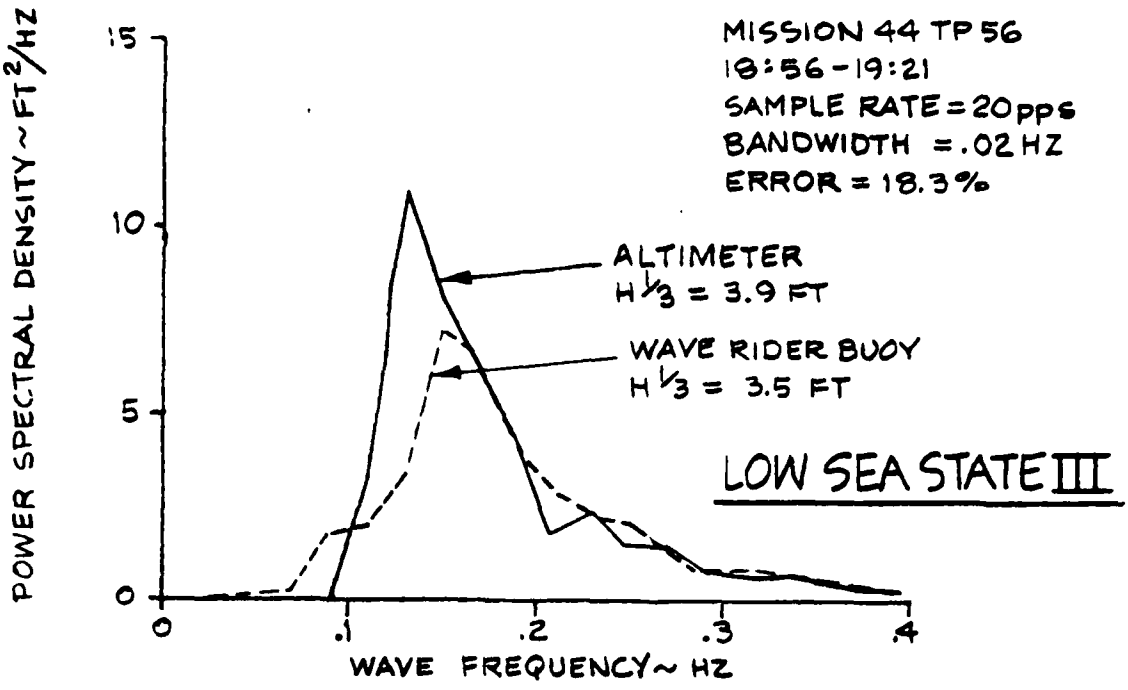

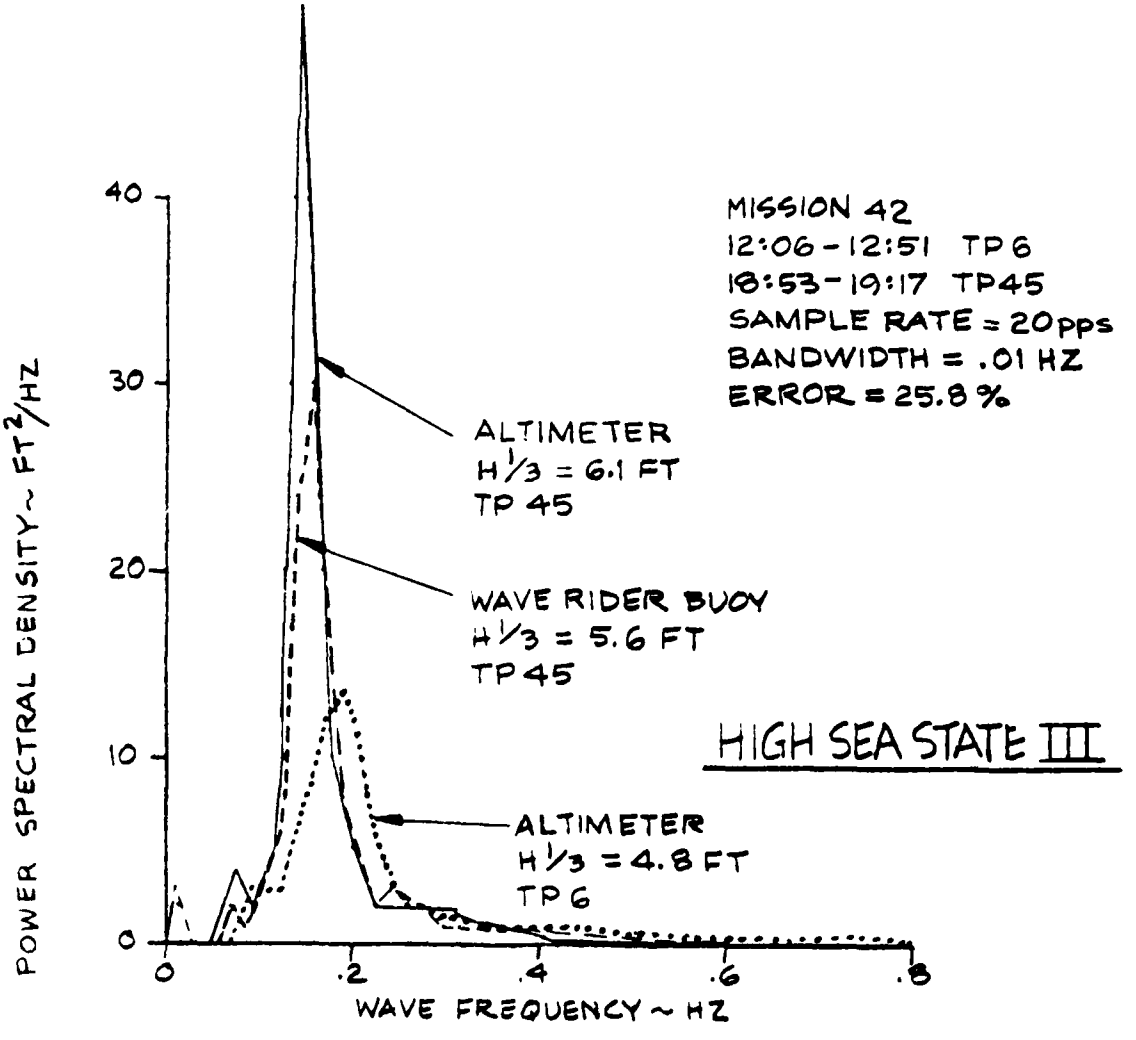

7.3 RANGE VERSUS SPEED

The SES-200's range was calculated using the engine fuel flow rates measured under various constant speed cruise conditions. At each speed, range computations were made for the lift setting which minimized total lift and propulsion horsepower. This method does not automatically optimize the vessel's range at each speed. Changes in the lift and propulsion engine's specific fuel consumption with power setting and RPM could make it desirable to absorb more power at a given speed for purposes of optimizing range. This effect has been examined on a cursory basis and all indications are that it is not significant.

Two methods of calculating the vessel's range were employed. The first method accounts for the improvement in SES performance that occurs as fuel is consumed and the vessel's gross weight is reduced. This performance improvement primarily results from the fact that both cushion pressure and wave making resistance decrease as the vessel gets lighter due to fuel burnoff. Also, for hullborne operation, there is less draft and hence less wetted surface as the vessel gets lighter. The second method uses the fuel flow rates measured at the heavy ship test condition and makes no allowance for the effects of fuel burnoff.

For calm water operation, the SES-200's range was calculated using the first method. The variation in fuel flow rate with ship displacement was assumed to have the following form:

$$m = k_o + k_1 W \tag{7-1}$$

where:

m = total lift and propulsion fuel flow rate (lb/hr)

W = ship displacement (lb)

The constants k_o and k_1 were computed for ship speeds of 7.5, 10, 15, 20 and 25 knots from fuel flow measurements made at the heavy and light ship test conditions. This was accomplished by solving two simultaneous equations of the form given by Equation 7-1.

The vessel's range is given by:

$$R(nm) = VT \tag{7-2}$$

where:

V = ship speed (kt)

$T = \int_{W_f}^{W_o} \frac{dW}{k_o + k_1 W}$ = ship operating time in hours for a given change in ship displacement due to fuel useage.

W_o = initial displacement (lb)

W_f = final displacement (lb)

Substituting this expression for T into Equation (7-2) and integrating gives the following formula for range:

$$R(nm) = \frac{V}{k_1} \ln\left(\frac{k_o + k_1 W_o}{k_o + k_1 W_f}\right) \qquad (7\text{-}3)$$

This equation was solved for various constant speed cruise conditions as a function of fuel useage. The results are presented in Figure 7-18 for calm water operation. At sustained speeds of 7.5, 10, 15, 20 and 25 knots, the vessel's maximum range is 10300, 8500, 5000, 4300 and 3600 nautical miles, respectively.

In higher sea states, fuel flow measurements were only available for the heavy ship test condition. As the range formula given above requires fuel flow measurements at two displacements, it could not be utilized. Therefore, the range in higher sea states was computed using the heavy ship fuel flow rates measured for each sea state and no allowance was made for performance improvement due to fuel burnoff. This ensures a conservative range prediction.

Figure 7-19 compares the maximum range computed for head sea operation in Sea State III without any allowance for fuel burnoff with the maximum calm water range computed using Equation 7-1. These two curves set reasonable lower and upper bounds, respectively, on the vessel's maximum range for operation in Sea States 0-III. There were insufficient data to make range predictions for operation in higher sea states.

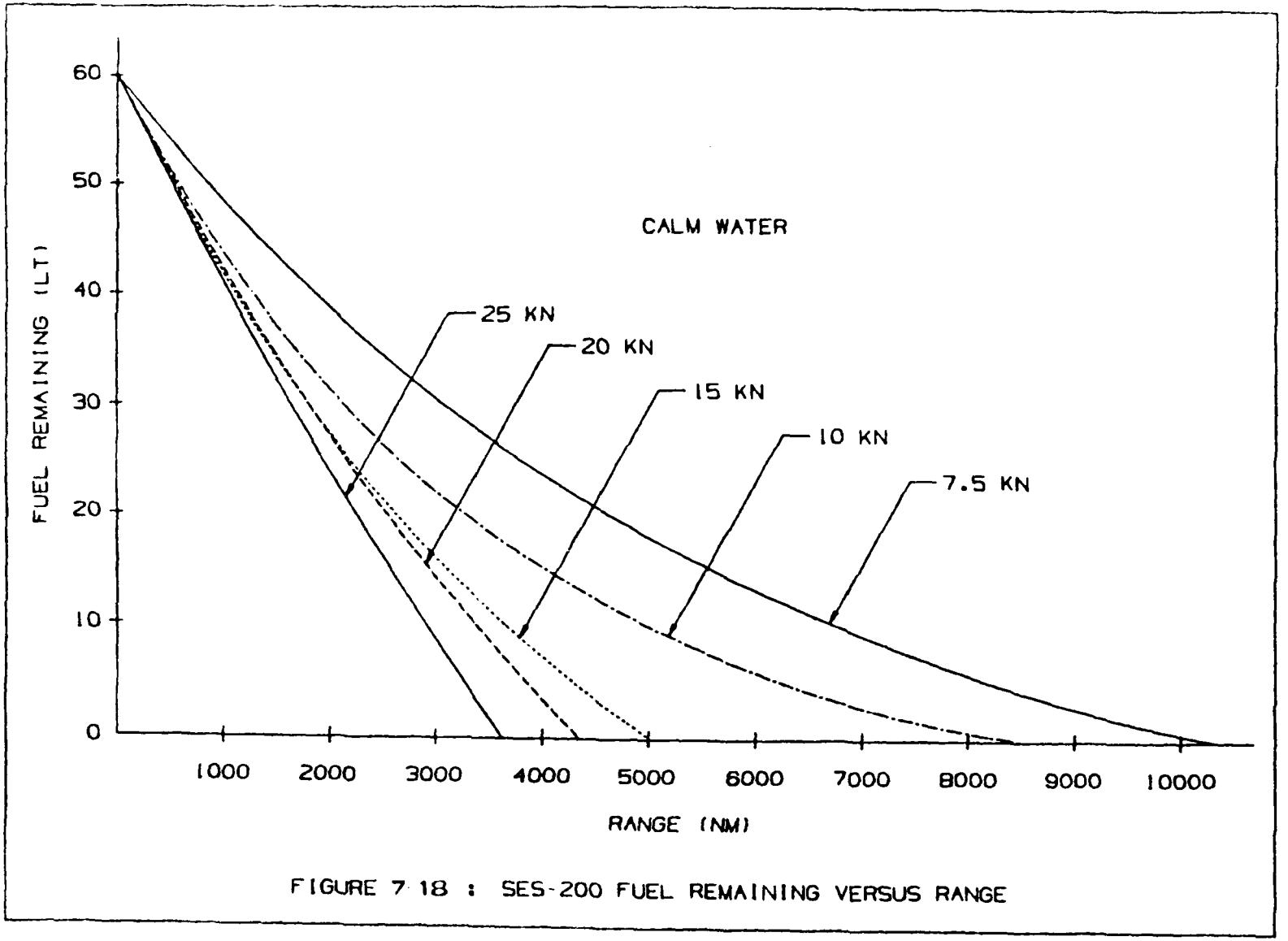

FIGURE 7-18 : SES-200 FUEL REMAINING VERSUS RANGE

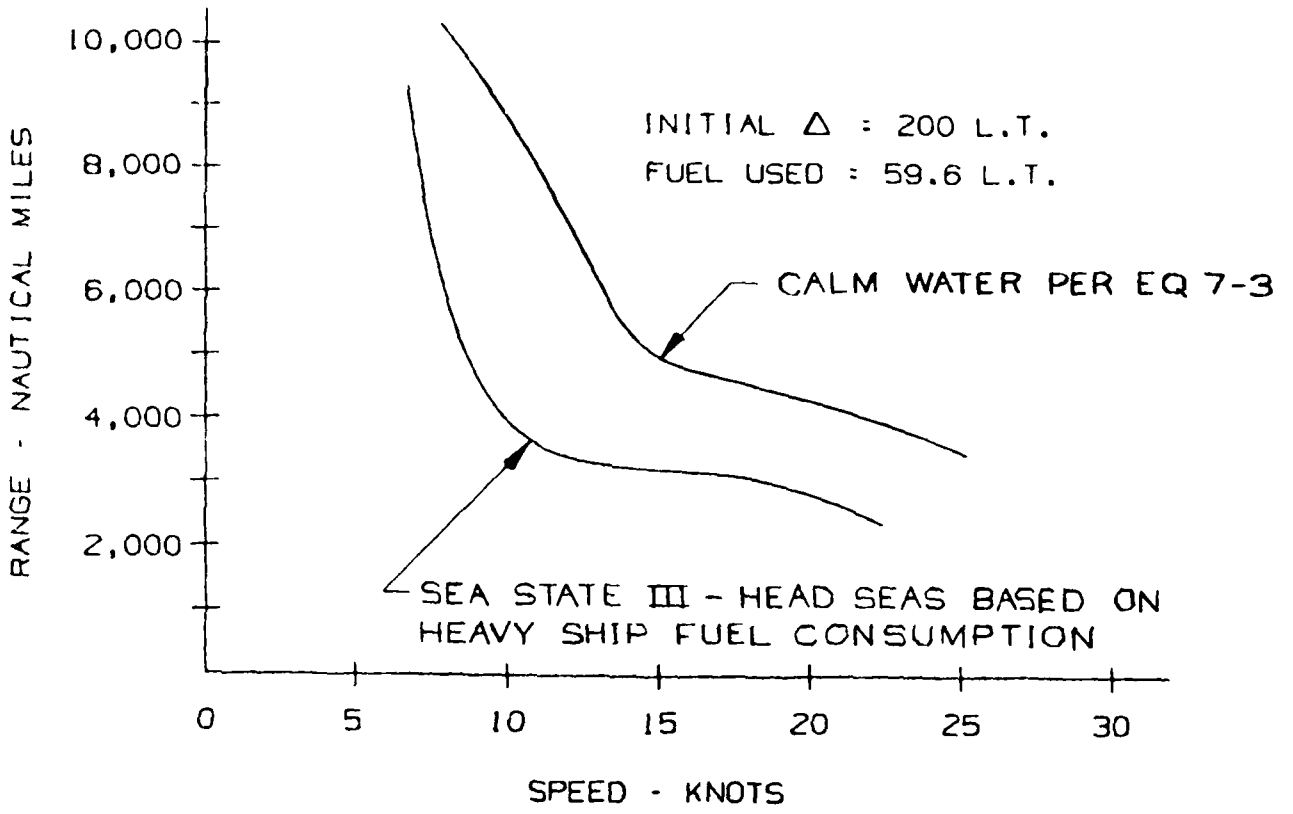

FIGURE 7-19 : SES-200 RANGE VERSUS SPEED, IN CALM WATER AND SEA STATE III HEAD SEAS

8. SEAKEEPING

This section discusses results of underway tests in waves conducted for the purpose of determining the vessel's seakeeping characteristics. The data of interest here are those relating to the various aspects of craft motion responses in waves, particularly with respect to the ride quality and habitability characteristics. The test conditions covered include both hullborne and cushionborne operation. The cushionborne conditions encompass both RCS-on and RCS-off operation; the effectiveness of the RCS in improving the ride quality is evaluated.

The range of operating conditions covered is summarized in Tables 6-3 and 6-4. Data were acquired in Sea States I to V. The on-cushion (cushion-borne) data were generally acquired for craft speeds of 20 kn and for maximum speed in each sea state. Most data were taken with fan speeds of 1700 and 1900 rpm. Headings relative to the waves were varied from head seas to following seas in 45 degree increments.

The off-cushion (hullborne) tests covered speeds from zero to 10 kn at all headings.

In the following subsections, a discussion of the types of data employed and their general useage is first given (Section 8.1). Then the data are presented and discussed separately for each sea state (Sections 8.2 through 8.6).

Before reviewing this section, it should be noted that the accelerometer and cushion pressure data presented were processed out to frequencies well past the bandwidth of rigid body motions. As this is not typical in ship motions work, some explanation is provided. The SES-200's rigid body responses are confined to frequencies below 3 Hz; however, there are higher frequency responses at structural bending modes and air supply system acoustic modes. The lowest of these modes is an acoustic mode at 4 Hz. The accelerometer and pressure data were processed out to 50 Hz to ensure that the responses at these high frequency modes due to wave excitation or to operation of the RCS are not detrimental to the vessel's seakeeping ability. Responses that were observed at these high frequency modes are therefore discussed in this section. In general, these responses were lower than the low frequency rigid body responses and are of no concern from the standpoint of seakeeping. They are within the ride control system's bandwidth, however, and it is important that the RCS not amplify the responses at these frequencies. This subject is also discussed in this section.

8.1 GENERAL DISCUSSION OF THE TYPES OF DATA EMPLOYED

Several different types of data processing were employed for each set of test data. The outputs of these individual processes are each directed at satisfying particular needs in the data analyses. Discussions of the general purpose of each type of data reduction and the data processing methods employed are given in Section 6. Here we briefly summarize the useage from the data analysis standpoint.

8.1.1 Standard Deviations

Standard deviations are the rms variations from the mean value. They provide basic data for characterization of the motions. Data of this type offer the significant advantage of reducing each measurement history for a given test point to a single number. This allows concise presentation of the effects on the outputs as one or more input quantities are varied. It also allows the investigation of correlations between the various measured quantities.

The standard deviations are, in a sense, the grossest form of the motions data characterizations. They comprise a measure of the overall amplitude characteristics and may be regarded as providing an overview at the highest level. If more detailed representations are required, power spectra, 1/3-octave band data, etc. must be employed. The difficulty with the latter types of data is that they represent too much detail. Concise summaries of the effects of variations in operating conditions are no longer possible.

8.1.2 Power Spectra

The most detailed level of data representations employed is that of the power spectral density functions (referred to hereafter as power spectra or simply as spectra). The power spectra contain essentially all data of direct interest except for the distribution functions. They provide detailed motion reponses on a frequency-by-frequency basis. These data are affected by both the input (wave) power spectra and the craft transfer function amplitudes including the responses in all dynamic modes (including rigid body motions, acoustic model responses, structural modes, etc.). They characterize the motions in considerable detail and, if the input (wave) spectra are known, provide a measure of the transfer function amplitudes frequency by frequency. They are used to examine the detailed characteristics of the motions. They are particularly useful in determining the manner in which the RCS affects the overall craft dynamics; details of the RCS effects are obtained by comparison of spectra for RCS-on and RCS-off conditions.

8.1.3 1/3-Octave Band Data

The 1/3-octave band data represent integrals of the power spectra over 1/3-octave bands. They may be interpreted as the variance of the data which would be obtained at the output of ideal 1/3-octave band-pass filters.

1/3-octave band data are used primarily because ride quality criteria are generally given in terms of these data. They are equivalent to the power spectra except in the frequency resolution employed. By lumping the spectral data into 1/3-octave bands, the finer details of the spectra are suppressed, particularly at the higher frequencies.

8.1.4 Histograms

Histograms are used to examine the distribution functions (also known as the frequency distribution functions) of the data. These data are not generally regarded as primary characterizations of the motions data except where extremes of the excursions are of predominant interest (as in loads studies, for instance). Therefore only limited use is made of histograms in this report.

8.1.5 Stationarity and Quality Checks

Some data items other than those presented in this section are discussed in Section 6. Specifically we will not present the results of the data reductions performed to provide stationarity checks on the test data. Such checks are important and were utilized in the data analysis task, but they are specifically referenced only where pertinent and necessary to the discussion of the test data.

8.1.6 Wave Data

Since the motions of interest to seakeeping are the responses to wave inputs, the characteristics of the waves in which the tests are conducted are of considerable direct interest. The basic wave measurements for these tests were obtained from two sources. The primary data were taken from the Waverider buoy. It provides wave measurements in the immediate vicinity of the test course just before and just after the tests are conducted. Some supporting wave data were obtained from the NOAA buoy when the test course was in the vicinity of this buoy. However, the amplitude resolution of these data are considerably coarser than desired for our purposes. Both types of buoy data were processed to yield both standard deviations and power spectra.

In addition to the buoy measurements, there was an on-board radar altimeter which provided a measurement of the distance from the boom-mounted sensor to the water surface as the tests were in progress. In order to produce wave displacement time-histories, it is necessary to remove the effects of craft motions from these data using accelerometer outputs. If this can be properly accomplished, then this clearly provides the best type of wave data. It is taken where the craft is rather than just nearby and can be time-correlated with the craft motions data. This measurement was incorporated on an experimental basis to provide some verification of the data processing technique proposed to remove the craft motion effects. The verification is obtained by comparing the results with buoy data. Since such verification had not been previously obtained, the altimeter data were not regarded as primary. Where the processed data were available, they are presented.

In presenting data on the effects of the RCS, one method of presentation used removes the dependence on wave measurements altogether. In these cases, the standard deviations for the RCS-on condition were plotted versus those for the RCS-off condition for the advantage of removing any uncertainties due to the lack of temporal and/or spatial proximity of the wave buoy data and of providing a very direct evaluation of the effects of the RCS operation.

8.2 SEA STATE I MOTIONS

8.2.1 Test Conditions

Two missions (M-48 and M-51) were conducted in high Sea State I. The coverage of this sea state is minimal since the motions in such small waves are of less interest than those in higher sea states. Both missions were conducted in Chesapeake Bay.

Both missions were at light ship conditions. For M-48, the gross weight ranged from 166.5 to 168 L.T. and the LCG was in the range of -1.3 to -2.0 ft. For M-51, the gross weight varied from 161.9 to 163.9 L.T. and the LCG ranged from -2.0 to -2.1 ft.

Tests were conducted in head seas and following seas only. Craft speeds were a nominal 20 kn and maximum speed at each heading. No tests were performed below 20 kn because the low speed motions are negligible in Sea State I. Lift fan speeds of 1700 and 1900 rpm were employed at each speed and heading.

Test points of 5 minutes duration were used in all cases. This is sufficient to provide 200 or more wave encounters in the head sea cases. For the following sea cases, a lesser number of wave encounters was considered acceptable because of the test time available and the low priority of the test condition.

To permit proper evaluation of the effects of the RCS, the test sequence employed was generally RCS-off, RCS-on, RCS-off. Thus the RCS-off runs available for comparison were made immediately before and after the RCS-on run so that operating conditions as nearly alike as possible were employed.

8.2.2 Wave Measurements

Wave data were acquired from both the Datawell Waverider buoy and the boom-mounted TRT radar altimeter. The altimeter data were acquired at zero craft speed to allow direct comparison with the Waverider data. Also, the data were recorded simultaneously to facilitate the comparisons. Wave data test points were obtained at the beginning and end of each mission.

Each wave data test point was of 25 minutes duration to assure that power spectra of adequate resolution and sampling error could be produced. The data were taken at a sample rate of 20 pps. The wave spectra were processed to give 0.02 Hz resolution bandwidth. This yields spectra with a sampling error having an 18.3% standard deviation, i.e., the standard deviation of each estimate in the power spectrum (each frequency) is 18.3% of the amplitude estimate.

The resulting wave spectra are shown on Figures 8-1 and 8-2. Considering the magnitude of the expected sampling errors, the comparisons between the altimeter and Waverider buoy data must be regarded as excellent in all cases. The significant (1/3-highest) wave height is also shown on the figure. These, too, are in reasonable agreement showing that the overall level of the spectra are consistent. The comparisons of the spectra provide verification of the technique (Reference 8-1) for correcting the altimeter data for the effects of craft motions using the accelerometer data. The consistency between the data from the two sources, together with the lack of "raggedness" of the spectra obtained, confirms that the test duration and sampling rate are commensurate with the frequency resolution employed.

It may be noted that the power spectral shapes exhibit little variation over the two missions. This helps to assure a self-consistent data set over the two missions. The significant wave heights are around 1 ft in all cases. The greatest deviation is for M-51, TP-26, which indicates the waves were decreasing slightly over the duration of M-51.

It is worth noting that both missions were conducted in Chesapeake Bay and that the wave spectra in the bay generally differ from those prevalent in the open sea. Wind and fetch limitations in the bay prohibit full development of the sea. This manifests itself in the form of higher frequency waves for a given wave height and, consequently, greater wave steepness. Additionally, bay spectra do not show the presence of long period swells that are typical of the ocean.

8.2.3 Standard Deviations

The most important standard deviations from M-48 and M-51 are presented in summary form as functions of craft speed on Figures 8-3 and 8-4. Note that standard deviations are denoted as 1σ values in the figures. The data presented are the results for three vertical accelerometers (AZBOW at the bow, AZSTR at the stern and AZCG at the nominal LCG), longitudinal (AXCG) and lateral (AYCG) accelerometers (both at the LCG), and pitch and roll angles from the vertical gyro.

Figure 8-3 summarizes the motions in head seas. Note that the vertical acceleration levels depend strongly on forward speed. There is some indication that the lateral and longitudinal accelerations depend slightly on speed (as would seem reasonable), but this is not conclusively demonstrated by these data. The roll and pitch angle amplitudes exhibit no distinct speed dependence.

It is worth noting that, throughout the data presented in this report, the (nominally) laterally symmetric test conditions of head and following seas generally produced lateral accelerations and roll amplitudes of levels which cannot be regarded simply as noise; non-negligible responses in these lateral motions is definitely indicated. This may, at least in part, be attributed to the impossibility of exactly achieving the desired head or following sea condition and to the departure of the seaway from one-dimensionality.

FIGURE 8-1 SEA STATE I WAVE SPECTRA - MISSION 48

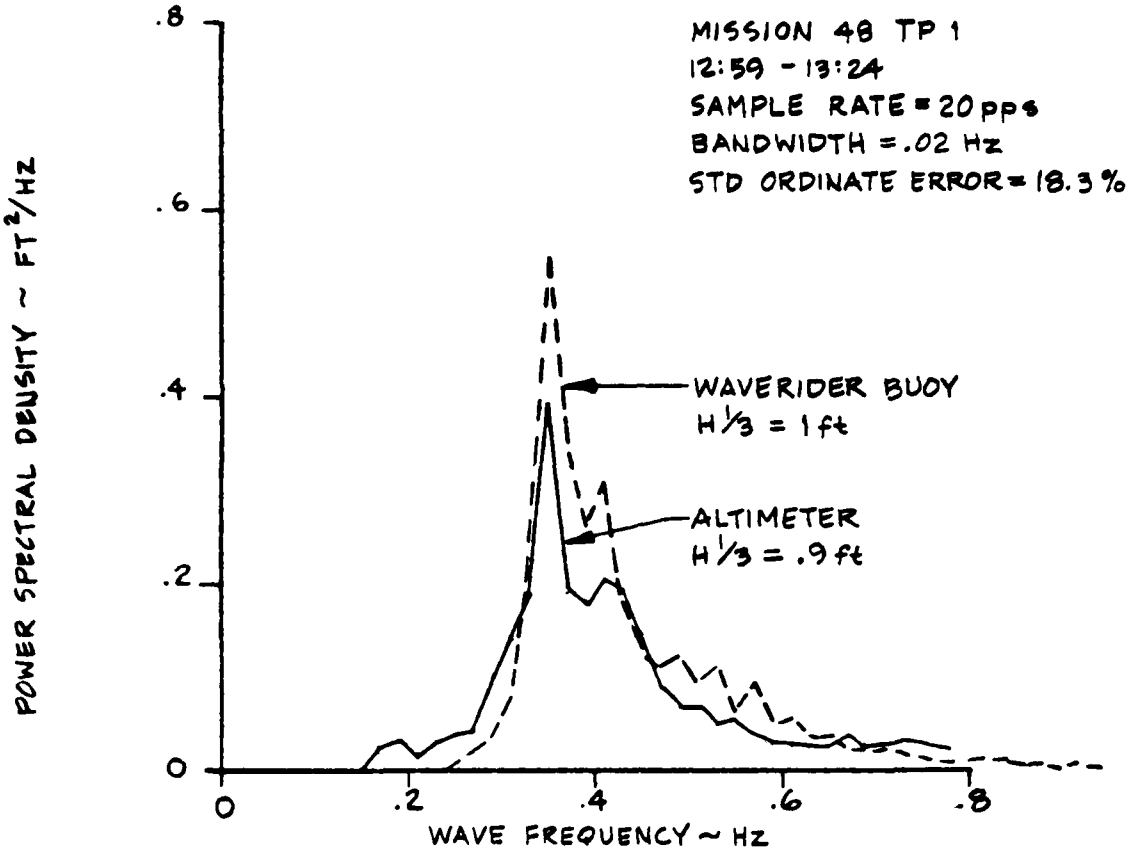

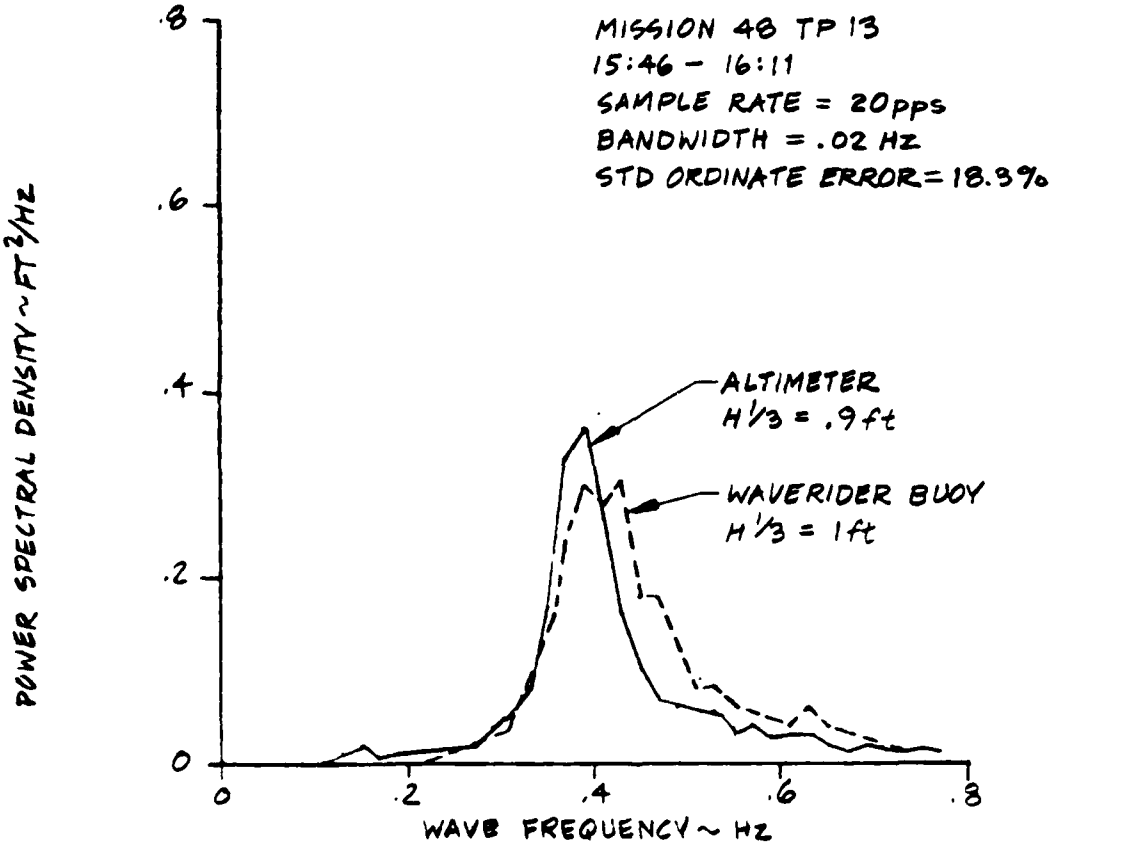

FIGURE 8-2 SEA STATE I WAVE SPECTRA-MISSION 51

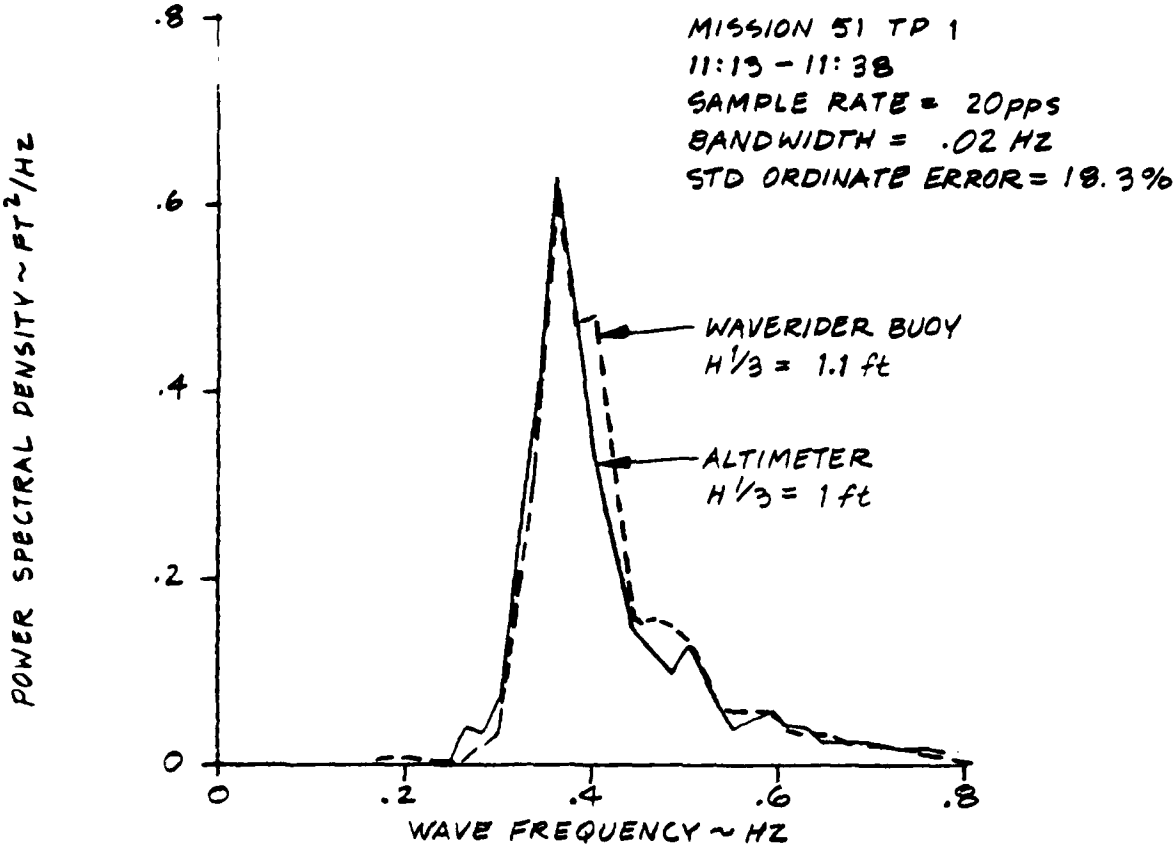

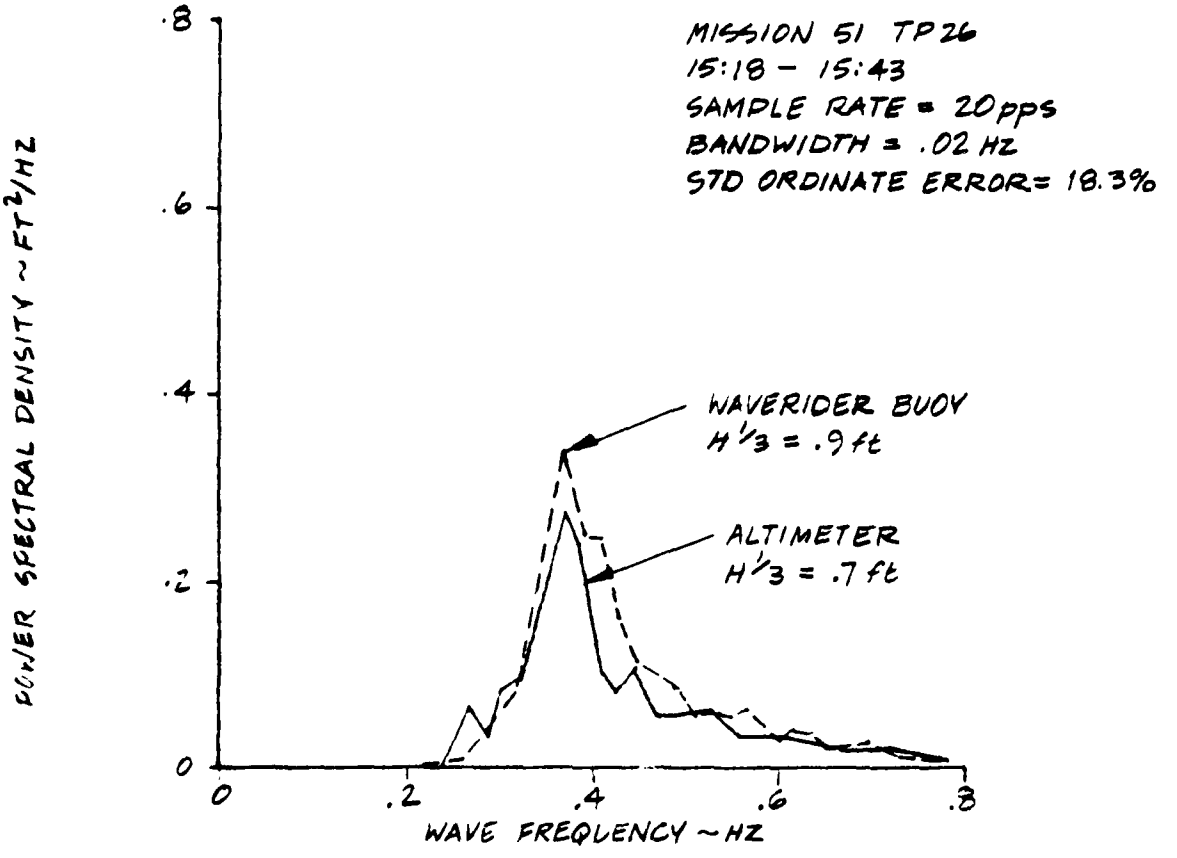

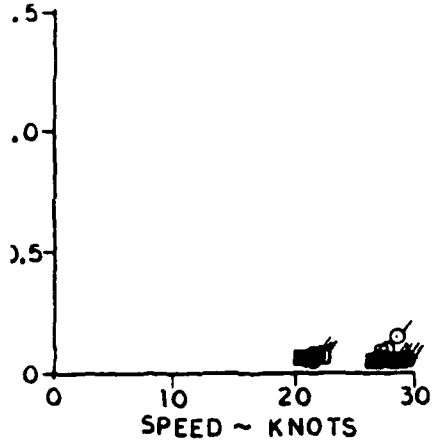

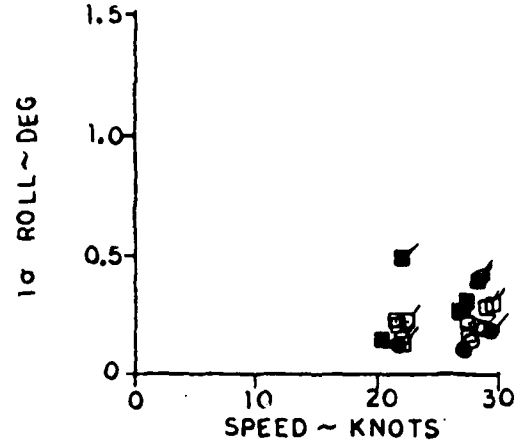

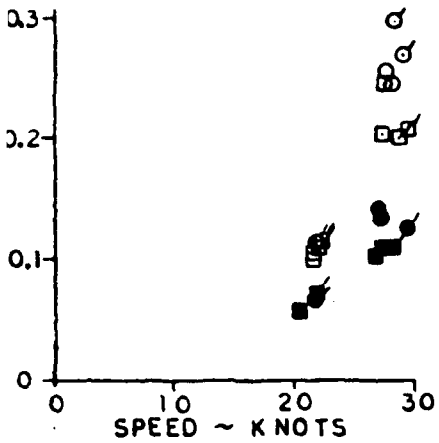

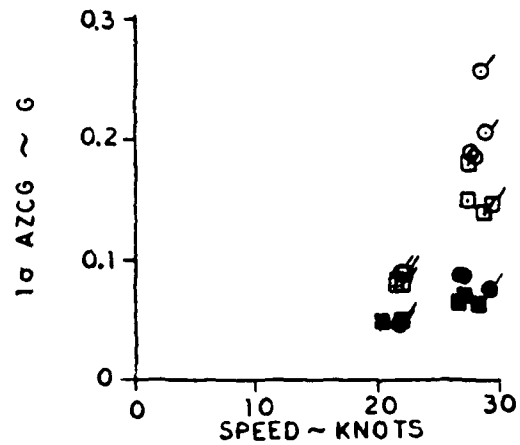

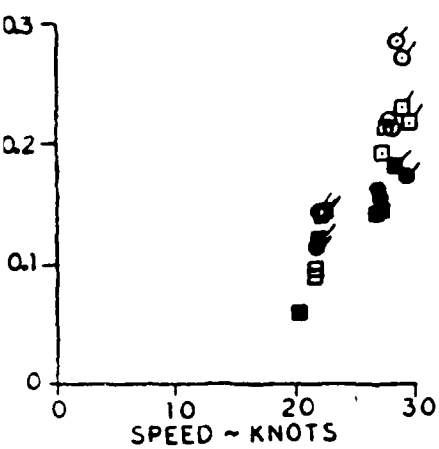

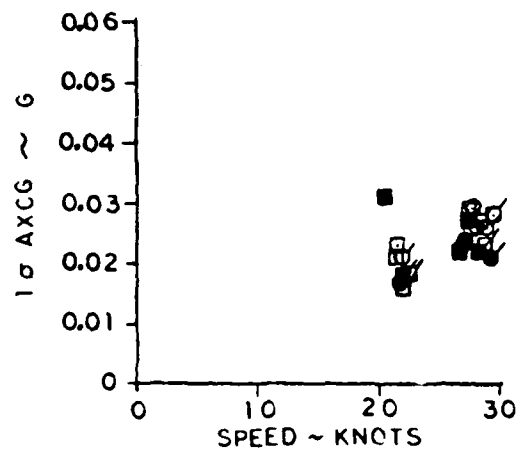

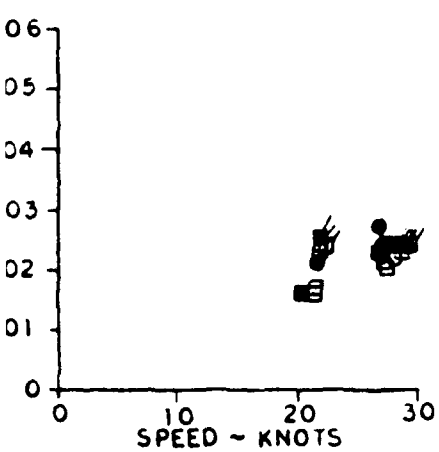

FIGURE 8-3
SEA STATE I MOTIONS
HEAD SEAS

LIFT RPM SYMBOL RCS
1900 ○ ● ON
1700 □ ○ OFF

MISSION 48 ○
MISSION 51 ♂

AD-A152 344 SES-200 (SURFACE EFFECT SHIP) TECHNICAL EVALUATION TEST REPORT(U) MARITIME DYNAMICS INC TACOMA WA J D ADAMS ET AL. JAN 84 MD-R-1199-2 USCG-D-1-85 2/3

UNCLASSIFIED N00167-83-C-0047 F/G 13/10 NL

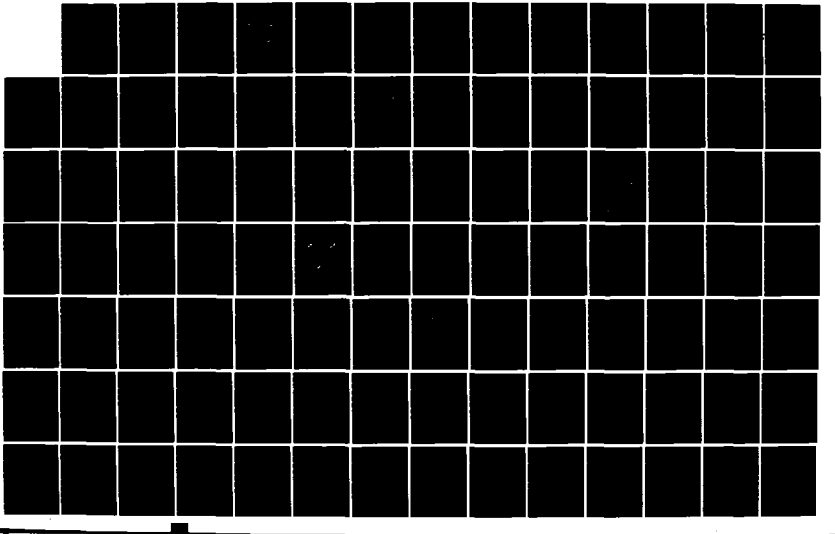

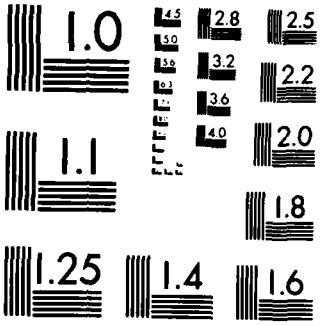

MICROCOPY RESOLUTION TEST CHART
NATIONAL BUREAU OF STANDARDS-1963-A

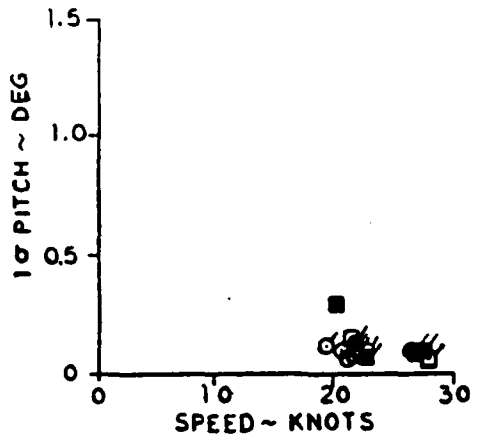

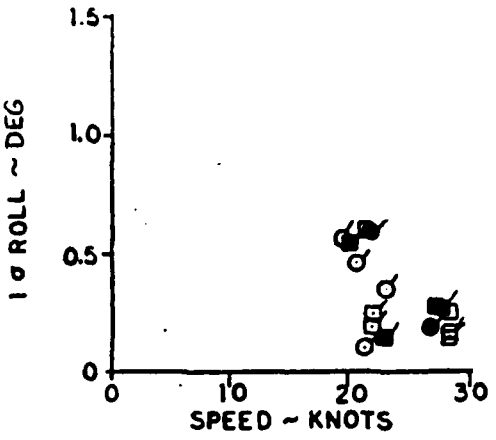

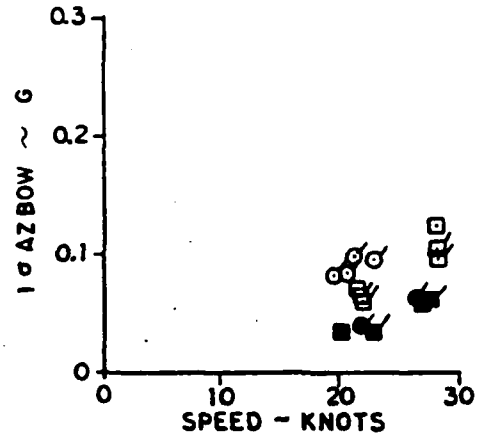

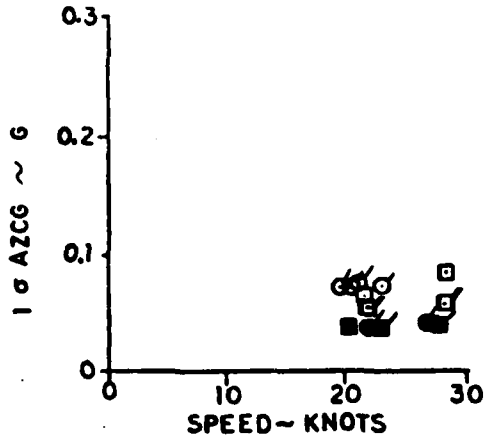

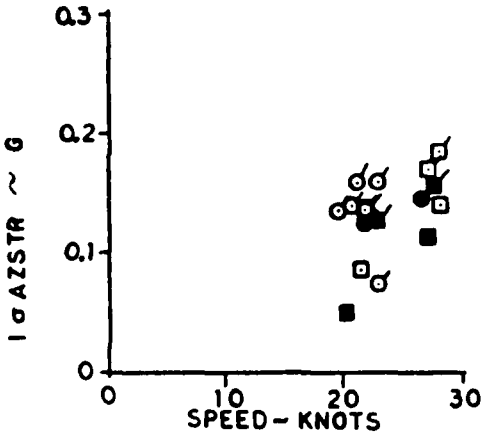

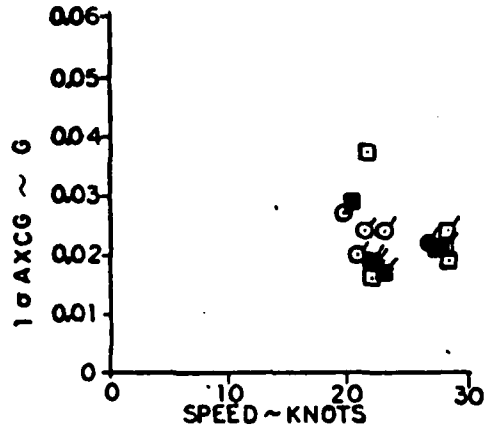

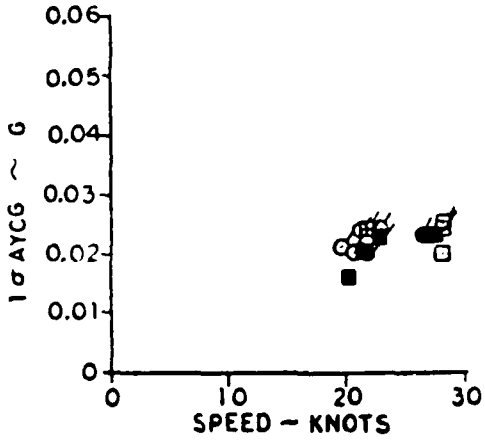

FIGURE 8-4
SEA STATE I MOTIONS
FOLLOWING SEAS

LIFT RPM	SYMBOL	RCS
1900	○	● ON
1700	□	○ OFF

MISSION 48 ○
MISSION 51 σ

Figure 8-4 shows the result for following seas. The comments on the dependence of the data on speed in the head sea case are applicable here also. In the following seas, however, the vertical accelerations vary much less with speed and, in fact, there is no clear indication of any speed dependence of the vertical accelerations at the LCG.

The low levels of the pitch standard deviations shown in both figures indicates that the motions due to waves in Sea State I are predominantly heave. It will be shown subsequently (Sections 8.2.4 and 8.2.5) that the greatest part of the heave motions are in the normal heave mode.

The effects of the RCS on the vertical accelerations are clearly evident on Figure 8-3. The bow and stern accelerations are roughly halved by the RCS while the LCG accelerations are reduced to about 1/3 at the maximum speed condition (around 28 kn) and about 1/2 at 20 kn. It is important to note that the vertical acceleration levels shown for the maximum speed RCS-off case in head seas represent a rather rough ride, even in this low sea state. These levels of rms g's are certainly enough to considerably impair crew effectiveness through fatigue for missions of any appreciable duration. The action of the RCS in this condition is very beneficial.

In following seas, the bow and LCG vertical accelerations are roughly halved by the action of the RCS. There are reductions in the stern accelerations but no clearly defined percentage.

In all cases (particularly in head seas at maximum speed), the RCS-off data for 1900 fan rpm show distinctly higher vertical acceleration levels than do the RCS-off data for 1700 rpm. This is due to the increase in the fan characteristic slope associated with the higher rpm on this particular fan map. With the RCS on, there is no clear effect of fan rpm. Since the higher rpm represents an added power requirement with no benefits, 1700 is the preferred operating rpm in Sea State I.

The effects of RCS operation are more clearly shown on Figure 8-5. Here we have plotted parameters for the RCS-on condition versus the same parameter for the corresponding RCS-off condition. The RCS-off test points were obtained immediately before and immediately after the RCS-on test point. Where the two RCS-off data points differ appreciably, we have plotted the average value and have indicated the data spread by a horizontal bar. Also shown on each plot is the line of perfect correlation (in this case, the line of no effect).

The SES-200 RCS is a cushion pressure feedback system rather than an acceleration feedback system, so the effect of the RCS in reducing cushion pressure excursions is relevant. Were it not for the effects of structural and acoustic modes, the cushion pressure and the vertical accelerations would be virtually interchangeable for this purpose. The cushion pressure plotted here as FR8-3CP which is located at Frame 8-3, about 8 ft forward of amidships. As may be seen, the RCS quite consistently reduces the cushion pressure standard deviations to about 30% of the RCS-off values over the range of test conditions employed.

FIGURE 8-5

SEA STATE I EFFECT OF RCS ON HEAVE ACCELERATION, CUSHION PRESSURE AND SHIP SPEED

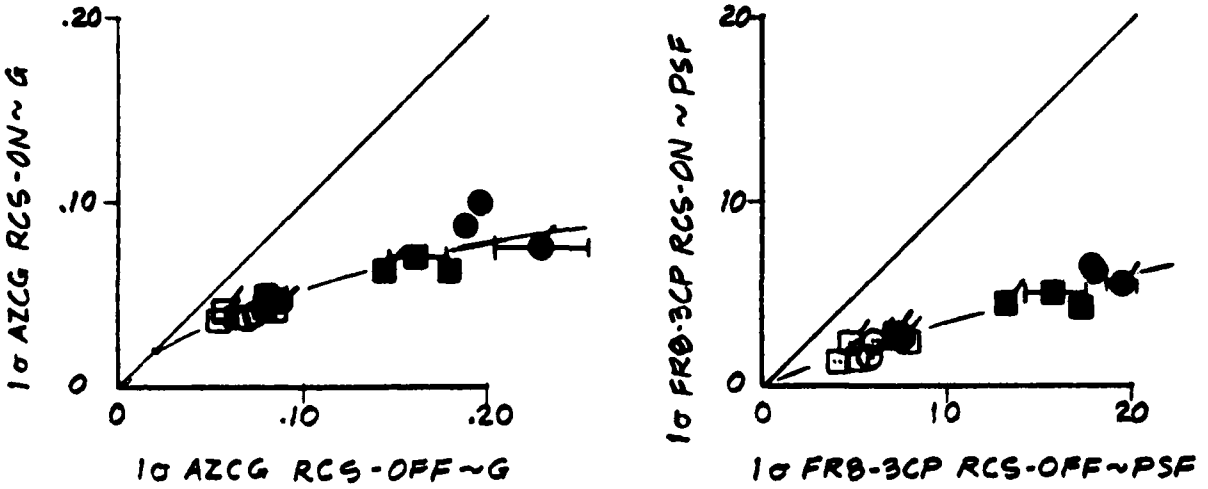

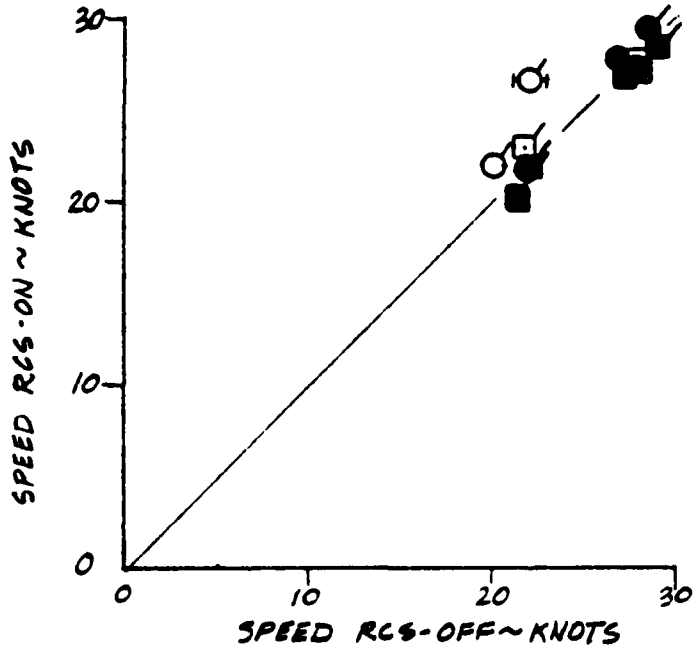

□ 1700 RPM
○ 1900 RPM
○□ FOLLOWING SEAS
●■ HEAD SEAS
ᑕ□ MISSION 51

The accelerometer data shown were low-pass filtered to 5 Hz in order to reduce the effects of machinery-induced noise in the signals. Nonetheless, there is evidence of some residual machinery noise contributing about 0.02 g's to the measured accelerations. This is the reason for fairing the curve through the acceleration data of Figure 8-5 to intercept the no-effect line at 0.02 g's. This level of residual is present independent of wave effects or RCS operation. Note that the higher RCS-off acceleration levels are attenuated to about 40% by the RCS action, i.e., somewhat less attenuation than is apparent in the cushion pressure. Adjusting this for the 0.02 g machinery noise level brings the data into better agreement with the cushion pressure data.

The correlation plot of maximum speed RCS-on and -off indicates little or no effect of the RCS on speed in head seas. In following seas, there appears to be some increase in top speed when the RCS is on. Since the RCS definitely dissipates power by discharging pressurized air overboard, one would expect the mean cushion pressure to decrease, thus increasing the sidehull wetted cushion area; therefore this apparent drag reduction requires some explanation. A possible explanation is that, by suppressing the heave motions, the mean change in sidehull immersion due to wave action is decreased somewhat by the RCS operation, thus decreasing the sidehull frictional drag. The validity of this explanation depends partly on the phase relationship between the heave motions and the wave displacements; this relationship has not been examined. However, part of the explanation lies in the asymmetry of the sidehull wetting in waves. If the sidehulls broach, the wetted area cannot go negative as required for symmetry; reduction of the immersion amplitude may decrease this asymmetry and therefore reduce the drag.

8.2.4 1/3-Octave Band Acceleration Data

Figures 8-6 through 8-8 represent the 1/3-octave band vertical accelerations for operation in Sea State I. The data are shown for 1700 fan rpm with and without RCS. Where available, the RCS-off cases obtained immediately before and after the RCS-on cases are both plotted in each figure. The accelerations at the bow, stern and LCG are shown. In comparing the results for the three accelerometer locations, it is important to note that the LCG accelerometer outputs were low-pass filtered to 5 Hz, whereas the bow and stern accelerometer data were filtered to 40 Hz. Therefore, the LCG accelerometer data exhibit less effect of machinery noise and of the higher frequency structural and acoustic mode contributions.

Figure 8-6 shows the results at maximum speed in head seas. Note the pronounced peaks near 2 Hz in all cases. This is the heave mode response and represents the most significant contribution to the vertical acceleration environment. It is particularly prominent at the LCG. The bow and stern accelerations are more affected by responses in the first bending mode (around 5 Hz) both because of the filtering of the LCG data and because the modal displacements are less at the LCG. They therefore exhibit larger peaks at that frequency relative to the heave peak. This is particularly

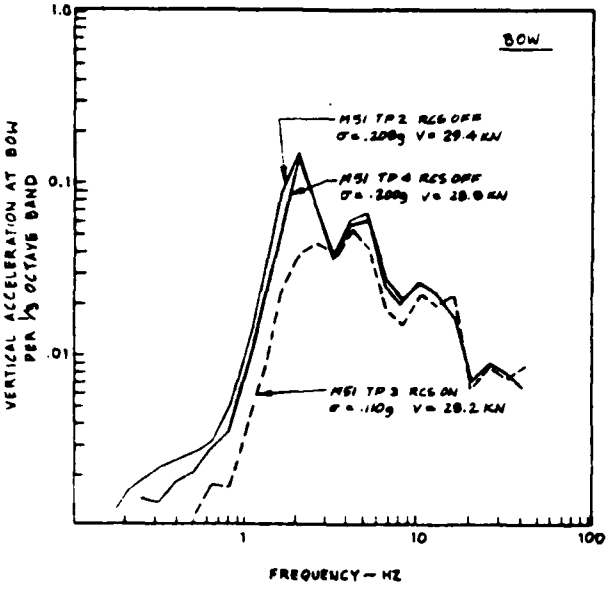

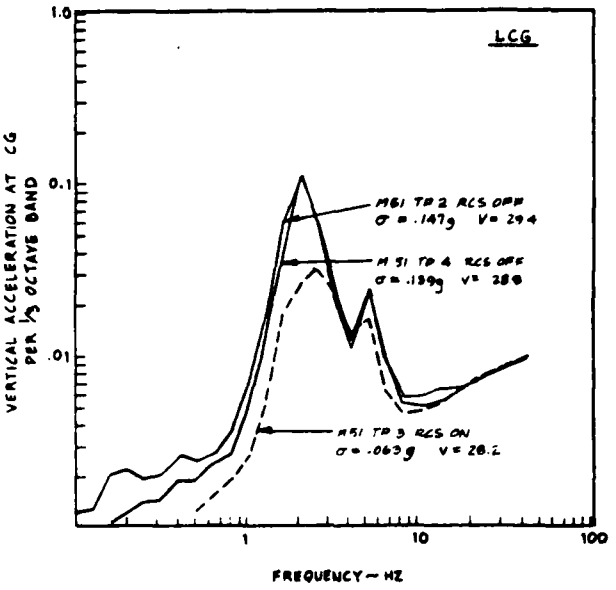

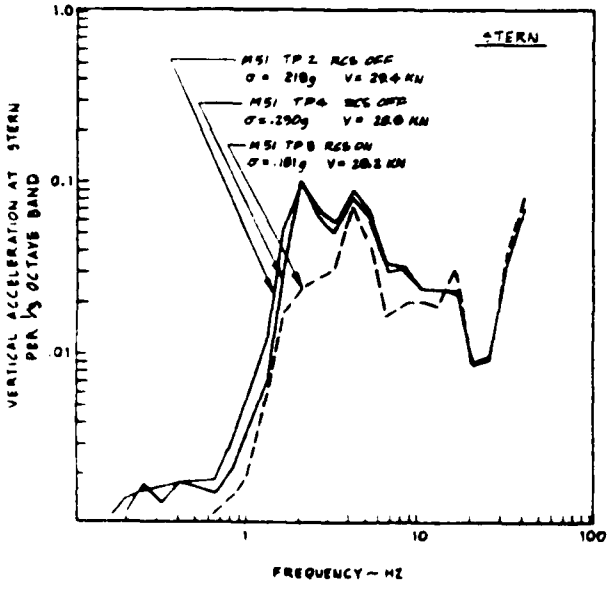

FIGURE 8-6

SEA STATE I VERTICAL ACCELERATION PER 1/3 OCTAVE BAND HEAD SEAS — MAXIMUM SPEED — 1700 LIFT FAN RPM

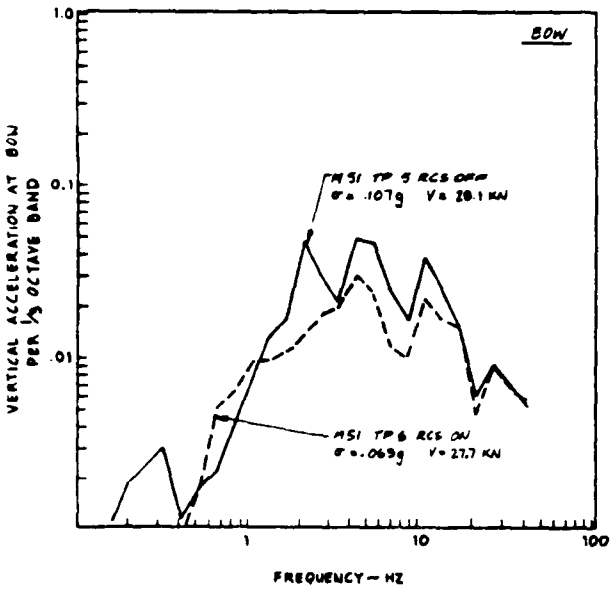

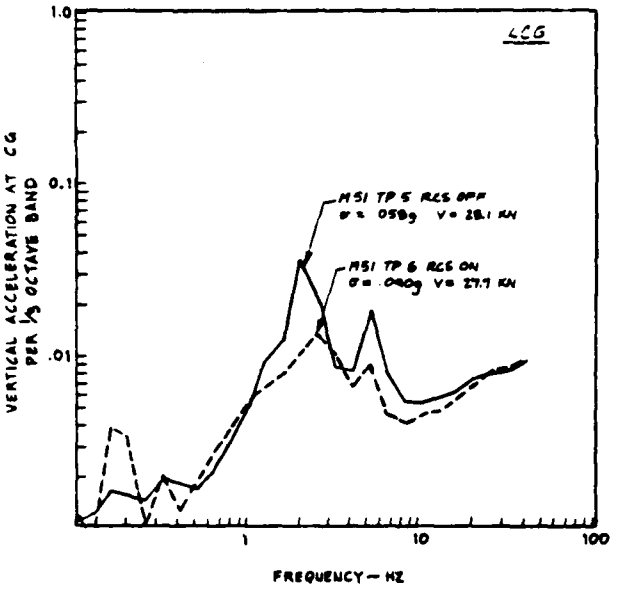

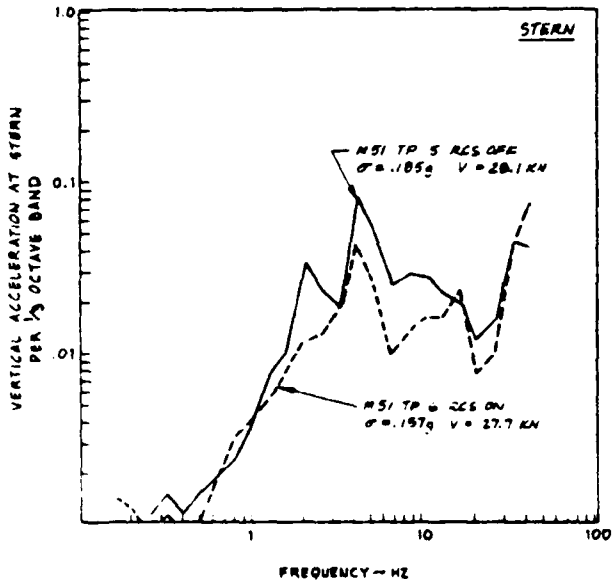

FIGURE 8-7
SEA STATE I VERTICAL ACCELERATION
PER 1/3 OCTAVE BAND - FOLLOWING SEAS
MAXIMUM SPEED - 1700 LIFT FAN RPM

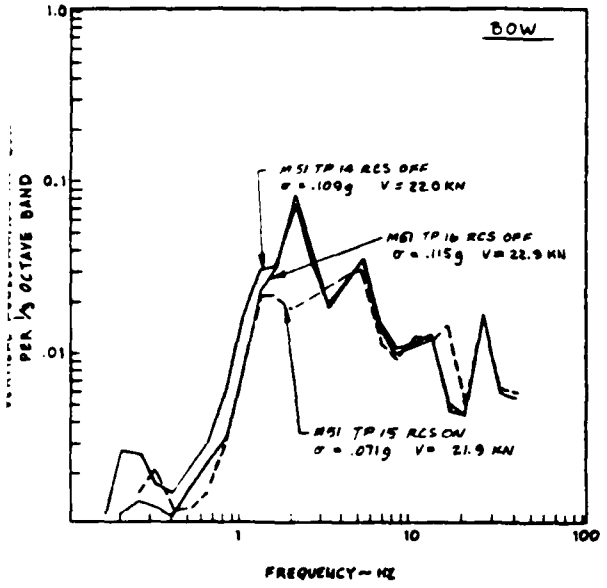

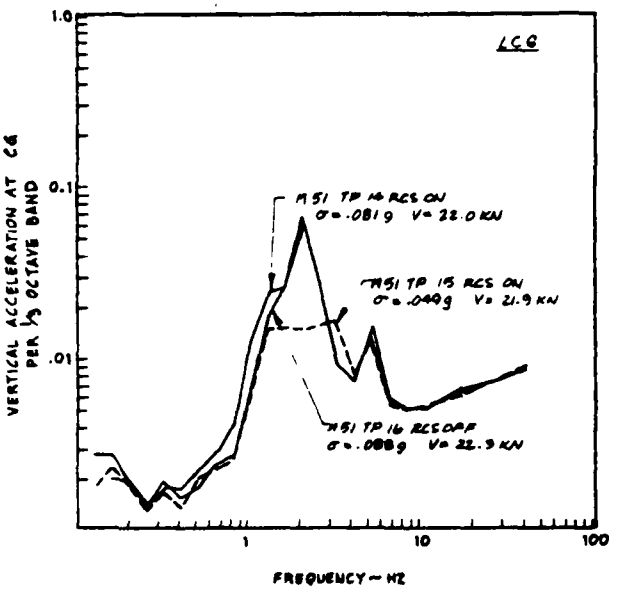

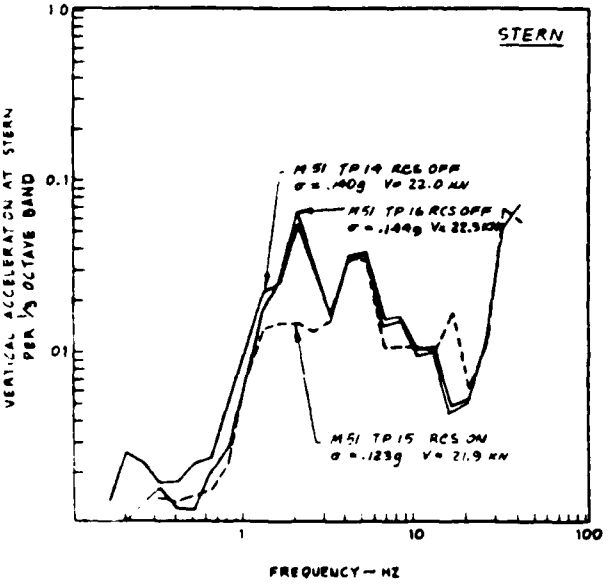

FIGURE 8-8
SEA STATE I VERTICAL ACCELERATION PER 1/3 OCTAVE BAND HEAD SEAS - 20 KNOTS 1700 LIFT FAN RPM

true for the stern accelerometer where there may also be some effect of the phase relationship between the (small) pitch motions and heave tending to decrease the rigid body responses. The less pronounced peaks beyond 5 Hz arise primarily from acoustic mode responses.

The sharp rise at high frequency end of the curves for the stern accelerations may be due to machinery noise arising from the proximity of the stern accelerometer to the main engines and the generator. The integration of the spectra over the 1/3-octave bands transforms wide-band noise into a rather steep curve versus frequency.

The close agreement of the data for the two RCS-off cases (in all three figures) speaks well for the quality and consistency of the data.

Figure 8-6 clearly shows the effect of the RCS on the accelerations. It greatly attenuates the motions in the heave mode as was the intent of the RCS design. It also significantly reduces the amplitudes at lower frequencies. This is desirable since these low frequency motion components are the primary contributors to seasickness. Some attenuation at and beyond the 5 Hz bending mode frequency is also evident.

At higher frequencies, the RCS is not intended to produce much attenuation of the motions; the primary contributions to ride discomfort are at lower frequencies. It is important, however, that the RCS not produce unreasonable amplification of any of the higher frequency accelerations. Such amplification would deteriorate the ride somewhat. More importantly, it would indicate the presence of significant high frequency power in the RCS actuators and linkages which would be detrimental to the life of the hardware. High frequency amplifications would also degrade the closed-loop stability of the system which would, in turn, unnecessarily restrict the useable RCS gain and, therefore, effectiveness. Figure 8-6 indicates no significant amplifications at higher frequencies.

Figure 8-7 presents the 1/3-octave band data for maximum speed in following seas. These data are very similar to those of Figure 8-6 except that the responses in the heave mode are significantly smaller. The lower amplitudes in the heave mode would be expected since the lower encounter frequencies associated with following sea operation concentrate the input spectral power at frequencies further from the heave natural frequency.

The RCS again primarily attenuates the heave mode responses. However, the attenuation at and beyond the bending mode frequency appears to be somewhat greater than was obtained in the head sea case. No explanation for this is presently available.

Figure 8-8 shows the results for head seas at 20 kn. Comparison with Figure 8-6 shows the RCS-off data to be very similar to the maximum speed data. The response levels are somewhat lower at 20 kn as would be expected. The RCS effects on the heave mode responses are also similar to those for the maximum speed case. However, the 20 kn results do not support the data of Figure 8-6 insofar as the attenuations at frequencies well removed from the heave frequency. In fact, the bow and stern data indicate slight amplification in the 15 to 20 Hz region. The difference between the two cases has not been explained. However, it is pointed out that the discrepancy could simply be sampling errors, i.e., due to normal scatter in the data.

8.2.5 Power Spectra of Heave Acceleration and Cushion Pressure

Figure 8-9 presents the power spectral data for operation in Sea State I at 1700 fan rpm for both RCS-off and RCS-on operations. These spectra were all obtained from testpoints of five minutes duration. The data were recorded at 200 pps and subsequently filtered and decimated to 100 pps before use to produce spectral estimates. The decimated data were processed to a resolution bandwidth of 0.2 Hz. This yields a sampling error on the individual spectral estimates having a standard deviation of 12.9% of the amplitude of the estimate. The close correspondence between the two RCS-off spectra for the same conditions indicates the data to be quite consistent. Spectra for the vertical accelerations at the LCG and the FR8-3CP cushion pressure are given for each condition.

Power spectra contain essentially the same data as the 1/3-octave band data of Section 8.2.4. However, the integration over 1/3-octave bands results in loss of detail (particularly at the higher frequencies) and greatly accentuates the high frequency data. Therefore the power spectral format presents a quite different view of the data.

The very pronounced peak around 2 Hz in all the spectra is the response of the heave mode. It is clearly the dominant contributor to the acceleration environment. The acceleration spectra also display well defined peak responses in the first longitudinal bending mode which has a natural frequency of about 5 Hz. The cushion pressure spectra tend to show little response to the bending mode activity because the free-free bending mode shape involves very little change in cushion volume.

While there is little evidence of cushion pressure response in the first bending mode, the data for following seas at maximum speed show a great deal of power in the 3.5 to 5.5 and 6 to 10 Hz ranges. These responses are primarily associated with acoustic modes in the air supply system. Acoustic modes have been tentatively identified at 4, 8, 14.5 and 18 Hz with two or three more modes lying between 18 and 20 Hz; some of the higher frequency modes may be structural modes or coupled structural-acoustic modes.

FIGURE 8-9 SEA STATE 5 HEAVE ACCELERATION AND CUSHION PRESSURE POWER SPECTRA - HEAD & FOLLOWING SEAS - 1700 LIFT FAN RPM

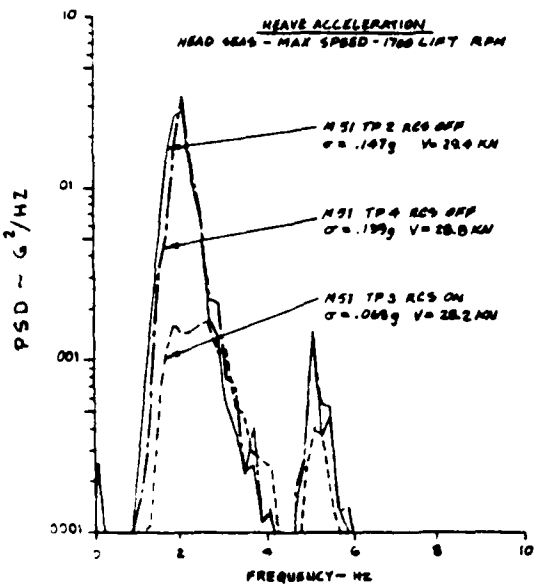

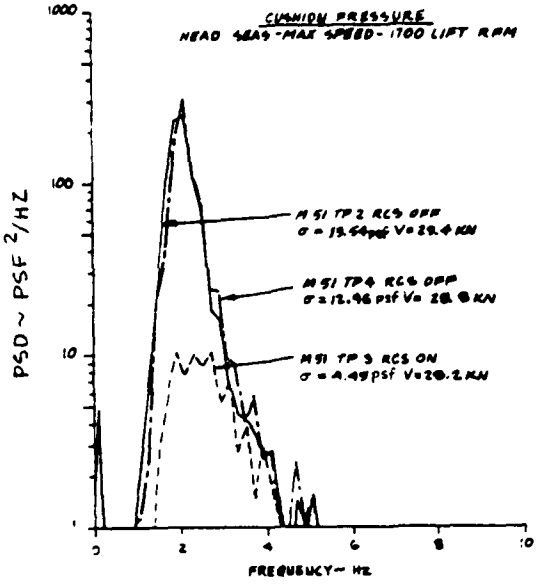

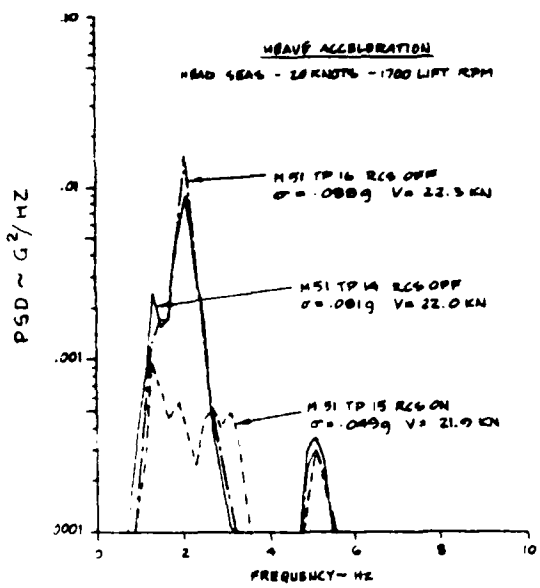

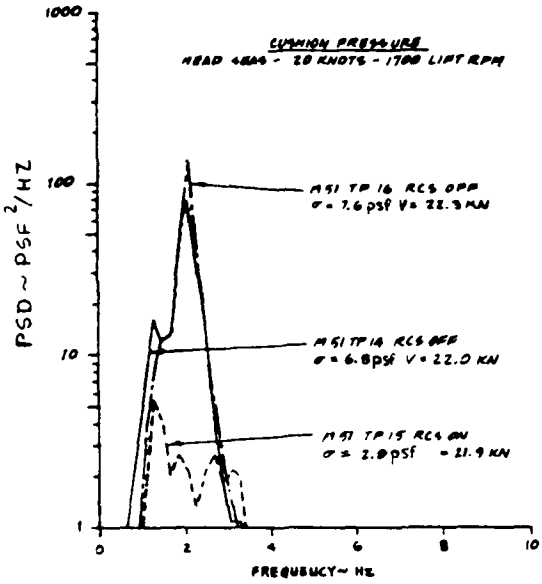

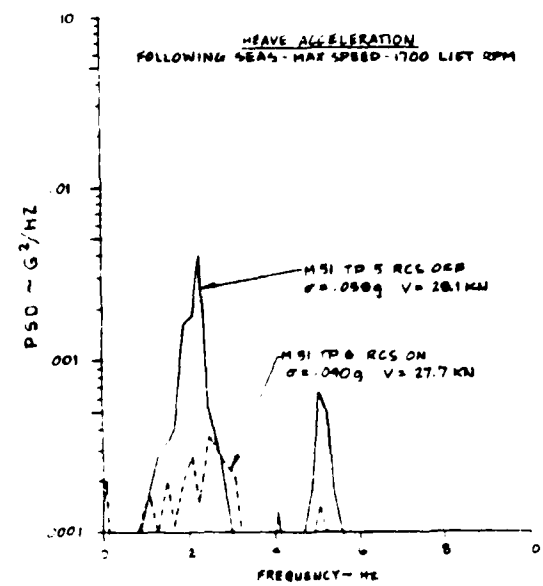

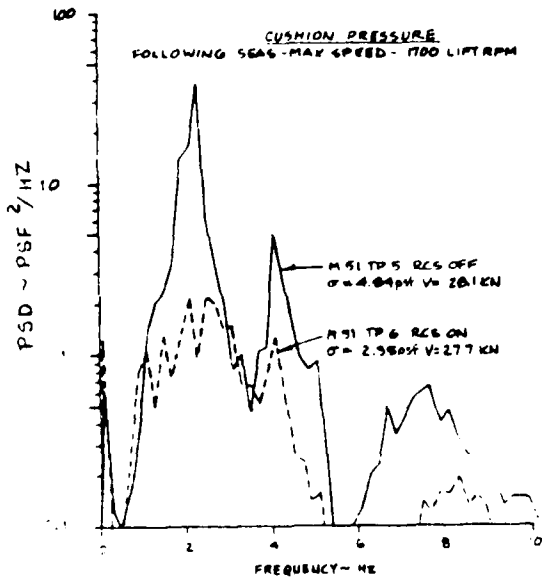

The apparent presence of these modes in the following sea case and not in the head sea cases is due mostly to the choice of scales to fit the data onto the plot. Since the maximum cushion pressure spectral level is smaller in the following sea case, the plot was extended to lower values. If the head sea cases had been plotted down one more decade, they would probably also show these modes.

The apparent narrowness of the 20 kn head sea spectra compared to the maximum speed case is also due to the scale cut-off level. Since the spectra for 20 kn are lower, the lowest levels of the spectra are shifted off the bottom of the plots.

The effect of the RCS in attenuating the heave mode responses is clearly evident in these plots. There is also some attenuation of the bending mode response. The considerable attenuation of the cushion pressures out to 10 Hz in the following sea case is somewhat surprising, since the RCS was not expected to be that effective at such high frequencies. It is possible that some of the high frequency power arises from non-linearities in the sidehull broaching phenomenon. Occurrences of brief local broaches could excite acoustic modes. The effect of the RCS in reducing the broaching occurrences would then result in a reduction of the energy in the acoustic modes.

8.3 SEA STATE II MOTIONS

8.3.1 Test Conditions

Two missions (M-54 and M-55) were conducted in high Sea State II. As in Sea State I, the coverage of this sea state is less complete than in higher sea states since the motions in Sea State III and above are of more interest. Both missions were conducted in Chesapeake Bay.

Both missions were at light ship conditions. For M-54, the gross weight varied from 163.4 to 164.5 L.T. and the LCG was between -1.8 to -2.2 ft. For M-55, the gross weight ranged from 161.6 to 163.4 L.T. and the LCG was in the range of -2.1 to -2.7 ft.

Tests were conducted in head and following seas only. Craft speeds were a nominal 20 kn and maximum speed at each heading. Fan speeds of 1700 and 1900 rpm were employed at each speed and heading. In addition, for the RCS-off condition, tests were conducted at 10 kn with 1600 rpm and at 15 kn with 1700 rpm.

As in Sea State I, 5-minute test durations were employed to give at least 200 wave encounters in head seas with fewer encounters accepted in following seas to conserve test time.

To facilitate proper evaluation of the RCS effects, the test sequence employed was RCS-off, RCS-on, RCS-off to permit comparisons at operating conditions as nearly alike as possible.

8.3.2 Wave Measurements

The wave data were again obtained both from the Waverider buoy and from the boom-mounted TRT radar altimeter. The processing parameters were the same as for Sea State I, i.e., 25-minute sample durations at 20 pps sample rate, and 0.02 Hz frequency resolution giving sampling errors with standard deviations of 18.3% of the amplitude estimate. The resulting wave spectra are shown on Figures 8-10 and 8-11. The Waverider data for M-55 TP-45 were omitted due to dropout problems on the data channel.

The altimeter and buoy data are in close agreement for M-55 TP-1. Similar agreement was found in Section 8.2.2 for the Sea State I data. However, while the spectral shapes seem consistent, the amplitude data for M-54 TP-31 and for M-55 TP-18 do not agree. The reason for this is not presently known. In Chesapeake Bay, it is possible for the wave heights to vary significantly between locations separated by a relatively modest distance. However, the craft and the buoy were in reasonable proximity during the wave data test points so that the disagreements shown seem unreasonably large to attribute to this cause alone. It is also possible that the craft heading was not correct for the test point; a following sea condition could result in the craft interfering with the wave profile. Lacking a satisfactory explanation for the discrepancy, the wave height data for these test points must be considered suspect.

FIGURE 8-19

SEA STATE II HEAVE ACCELERATION & CUSHION PRESSURE
POWER SPECTRA - HEAD SEAS - 1700 LIFT FAN RPM

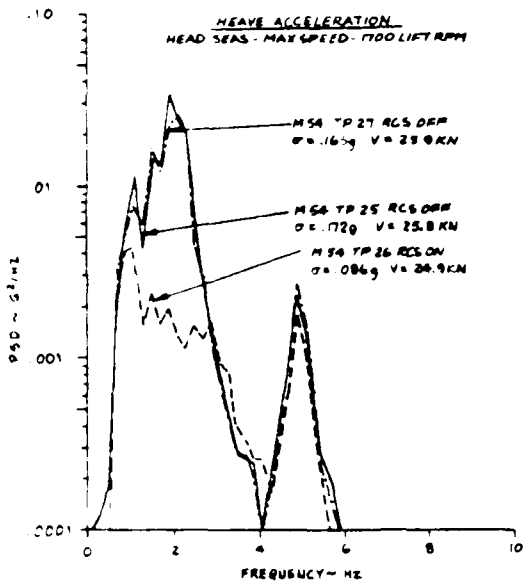

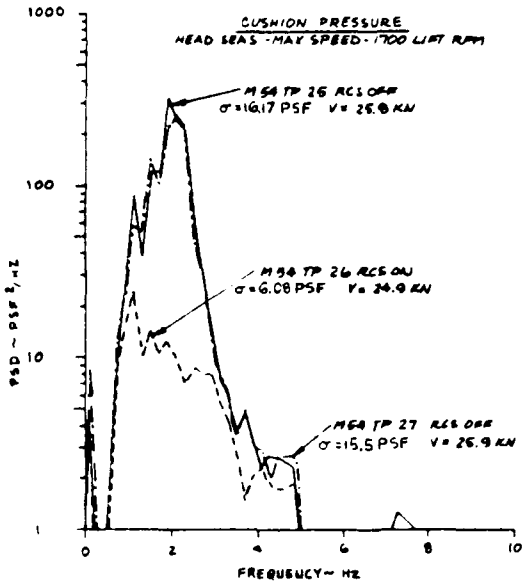

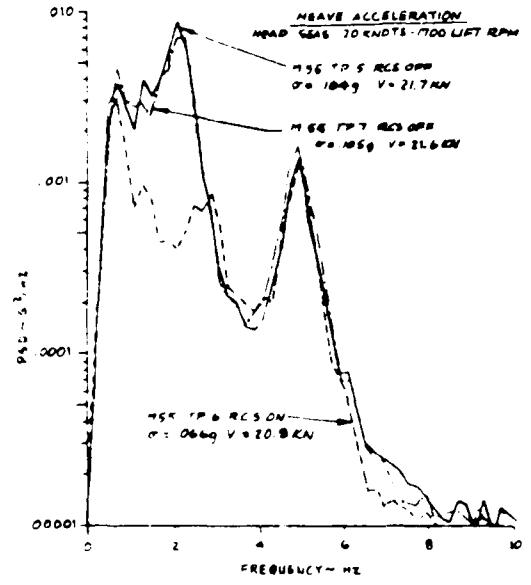

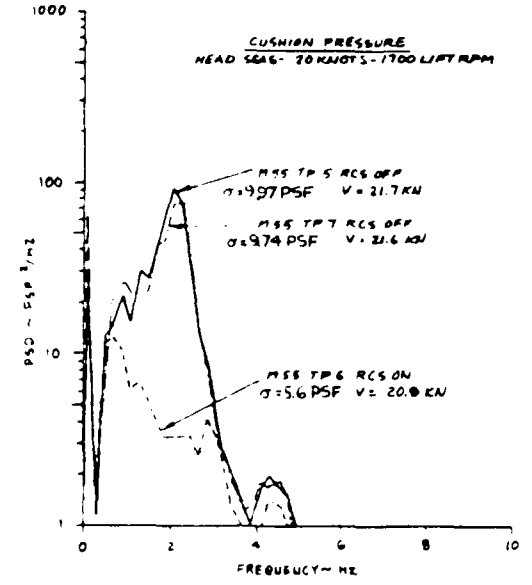

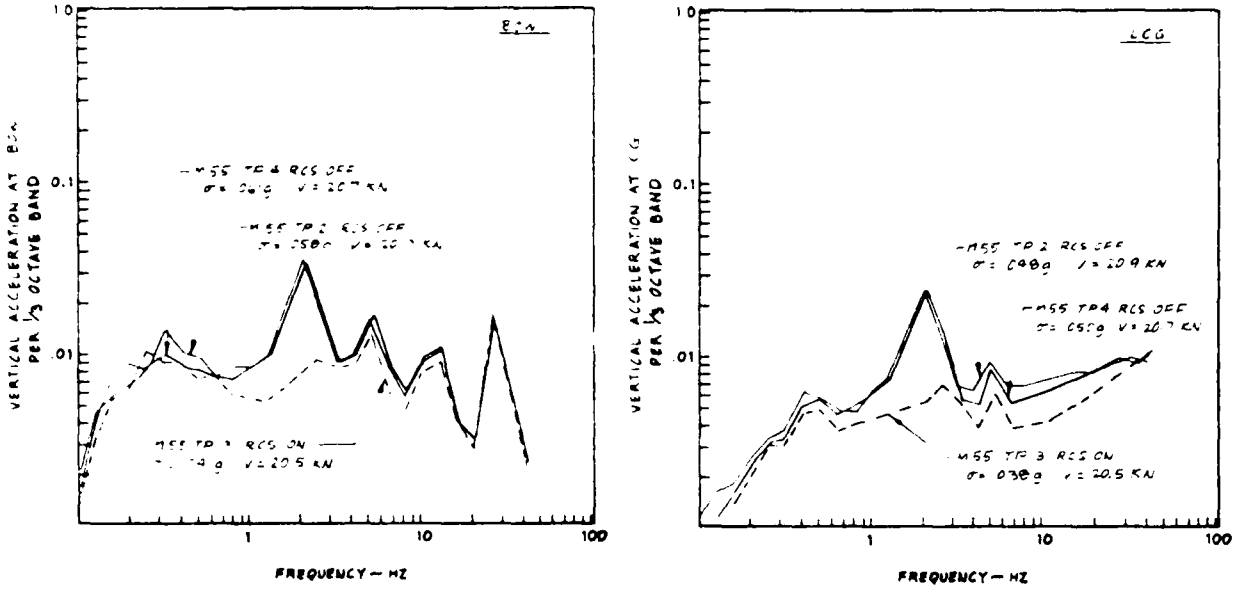

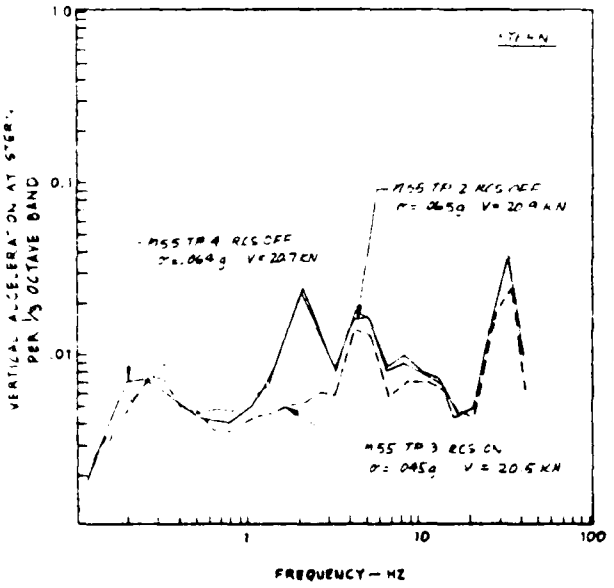

FIGURE 8-18
SEA STATE II VERTICAL ACCELERATION
PER 1/3 OCTAVE BAND - FOLLOWING SEAS
20 KNOTS -1700 LIFT FAN RPM

Figure 8-18 shows the data for 20 kn in following seas. The general trends shown for maximum speed in following seas are again displayed here, but the increased contributions of low frequency responses is even more pronounced because of the lower encounter frequencies at 20 kn. Pitch mode contributions are quite evident. The RCS attenuates substantially around the heave mode and achieves some reductions at higher frequencies.

8.3.5 Power Spectra of Heave Acceleration and Cushion Pressure

Figures 8-19 and 8-20 present the power spectra for the vertical accelerations at the LCG and the cushion pressure at Frame 8-3. The data are shown for 1700 fan RPM. The processing parameters (5-minute data segments, 100 pps, 0.2 Hz resolution bandwidth with sampling errors of 12.9% of the amplitude estimates) are the same as used for Sea State I.

The general characteristics observed in Sea State I are apparent here also. As noted in the previous section, there is considerably more energy at frequencies around and below 1 Hz in the higher sea state.

The tendency of the cushion spectra to display pronounced peaks at very low frequencies deserves some comment. It is probably due to the presence of strong spectral components having periods which are not insignificant relative to the data segment length processed. The processing used for the power spectra embodies a trend removal procedure to correct the data for long term drifts in mean values, since these are known to corrupt the spectra (power spectral density functions are entities defined in relation to statistially steady data, i.e., for stationary time series). However, the techniques employed only remove linear trends from the data. A cyclic "drift" component having a period comparable to the data segment length cannot be properly suppressed in this manner. The end result is incorrectly high spectral levels at very low frequencies. Note that the spectra do go to zero at zero frequency. This is forced by removal of the data mean value.

A lesser tendency of the same type is apparent for the Sea State I data.

The accelerometer data are less subject to this effect since they cannot have significant drifts over a long data segment if the craft is to maintain a reasonable range of heave positions.

Figure 8-19 shows the head sea results. For the maximum speed case, comparison with Figure 8-9 shows the primary difference from the Sea State I results is the presence of more low frequency power, i.e., at and below 1 Hz. The greatest contributor to the spectra is still the 2 Hz heave mode and there is significant acceleration spectral power in the first bending mode at 5 Hz. The cushion pressure spectra again exhibit little response to first bending mode activity because the mode shape involves little cushion volume variation.

The RCS is quite effective in reducing the heave mode responses and has little effect at frequencies well outside the 1-3 Hz bandwidth.

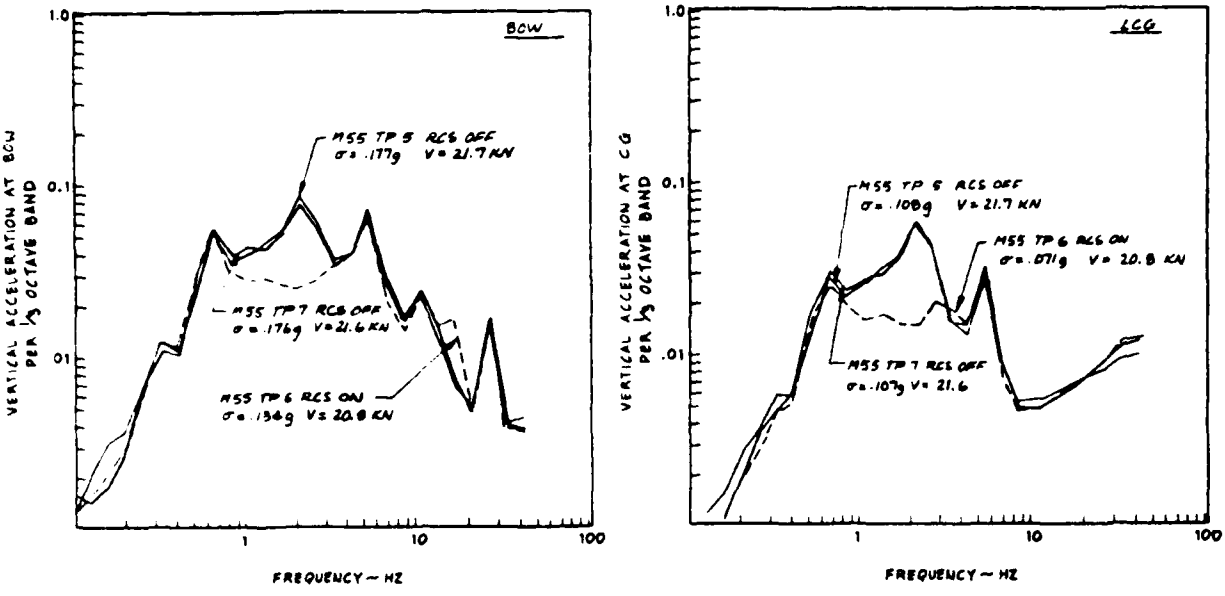

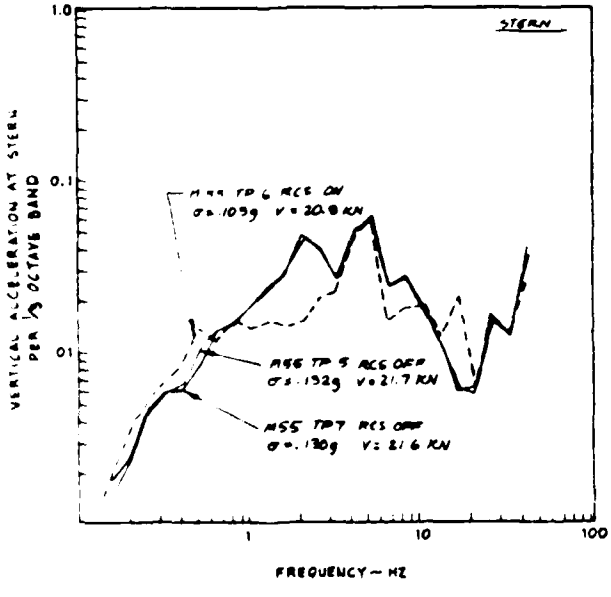

FIGURE 8-17
SEA STATE II VERTICAL ACCELERATION
PER 1/3 OCTAVE BAND - HEAD SEAS
20 KNOTS - 1700 LIFT FAN RPM

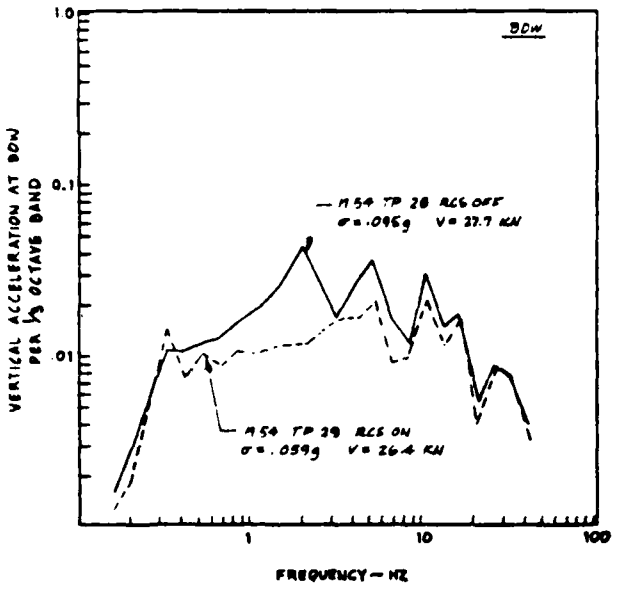

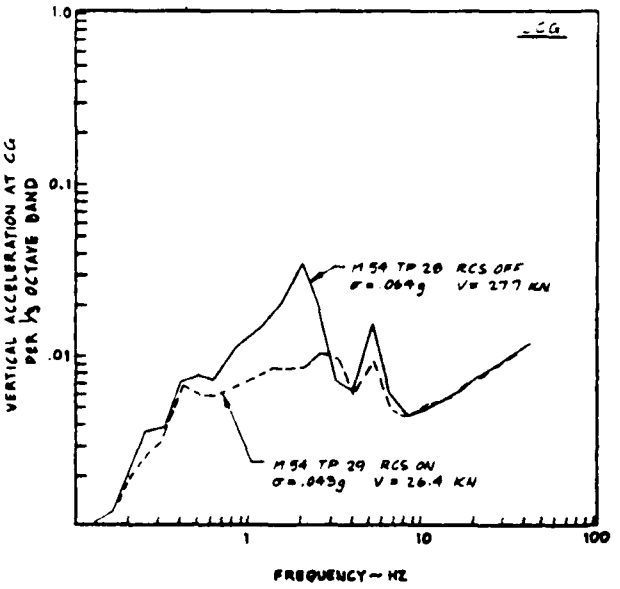

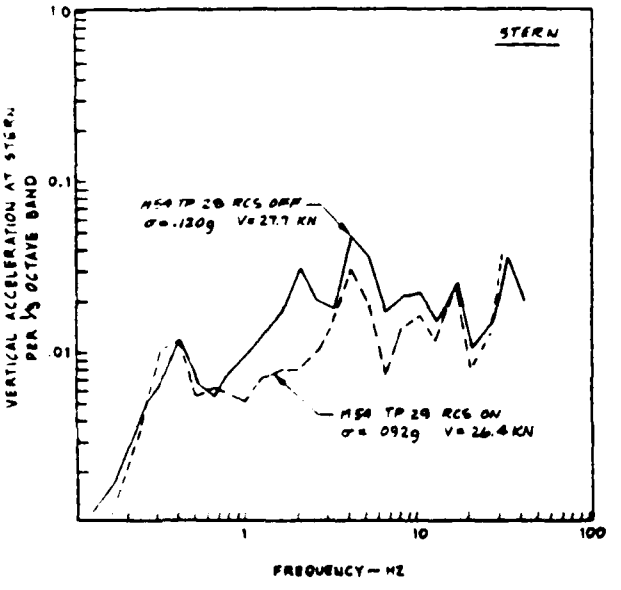

FIGURE 8-16
SEA STATE II VERTICAL ACCELERATION PER 1/3 OCTAVE BAND - FOLLOWING SEAS MAXIMUM SPEED - 1700 LIFT FAN RPM

that the levels beyond the peak frequency are essentially independent of wave height; the spectra simply extend to higher peaks at lower frequencies. For a linear system, the motions responses would have the same characteristic. In the present case, the decrease in maximum speed in the larger waves should have caused some shift of the high frequency spectrum toward lower encounter frequencies; since this is not observed, it is suspected that the high frequency acceleration spectrum for the same speed is actually somewhat higher in the Sea State II case. This is confirmed in the 20 kn data to be discussed subsequently.

The RCS clearly acts to attenuate the responses in the heave mode with little effect at other frequencies, i.e., the greatest effect is confined to a 1-3 Hz band around the heave frequency. There is also a tendency to reduce the low frequency responses somewhat. These data do not support the larger reductions at other frequencies shown on Figure 8-6, but they are in agreement with the 20 kn Sea State I head sea case of Figure 8-8 and with the 20 kn data of Figure 8-17.

Figure 8-16 shows the maximum speed results in following seas. Comparison with Figure 8-7 again shows that the results are quite close to the Sea State I results at and beyond 2 Hz, but the Sea State II data have more energy at lower frequencies. The tendency to peak in the neighborhood of 0.3 Hz indicates the presence of significant pitch interaction since this is about the pitch natural frequency; the more pronounced pitch influence at the bow and stern accelerometers is as would be expected. As desired (see the discussion of Section 8.2.4), the RCS causes no significant amplifications of the responses at higher frequencies.

In the following seas, the RCS again primarily affects the heave mode response. However, the RCS influence appears to extend over a wider frequency band than for the head sea case. In particular, there is a greater attenuation of the 5 Hz first bending mode. This could be due to the non-linear effects of sidehull broaching as discussed in Section 8.2.5 in connection with the Sea State I following sea results.

Figure 8-17 shows the data for 20 kn in head seas. Comparison with the corresponding Sea State I data (Figure 8-8) again shows the tendency for the spectra to be very similar at frequencies beyond 2 Hz. Now, however, the Sea State II data are somewhat higher. This supports the contention that the maximum speed data showed no increase because of the compensating effect of the reduced speed in the higher seas.

Except for the higher levels at low frequencies, the data are very similar to the Sea State I data both RCS-on and RCS-off. The RCS again primarily attenuates the heave mode responses (around 2 Hz). Note that the tendency for the RCS to somewhat amplify the responses around 15 to 20 Hz at the bow and stern is in agreement with the data of Figure 8-8. Therefore this effect must be assumed to be real rather than due to sampling variability. The effect is less pronounced at maximum speeds and is not present at all in following seas.

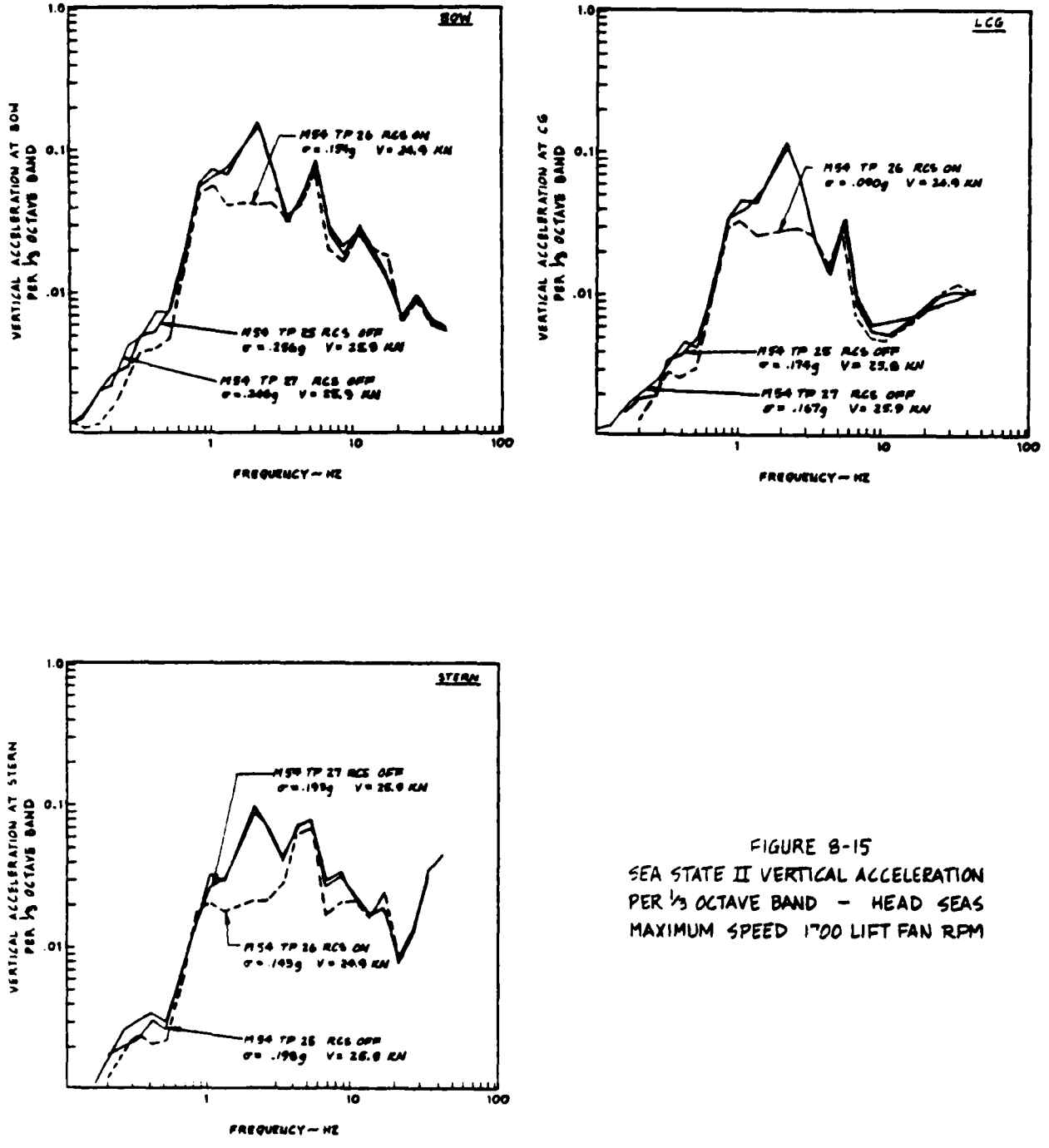

FIGURE 8-15
SEA STATE II VERTICAL ACCELERATION PER 1/3 OCTAVE BAND - HEAD SEAS MAXIMUM SPEED 1700 LIFT FAN RPM

FIGURE 8-14

SEA STATE II EFFECT OF RCS ON HEAVE ACCELERATION CUSHION PRESSURE AND SHIP SPEED

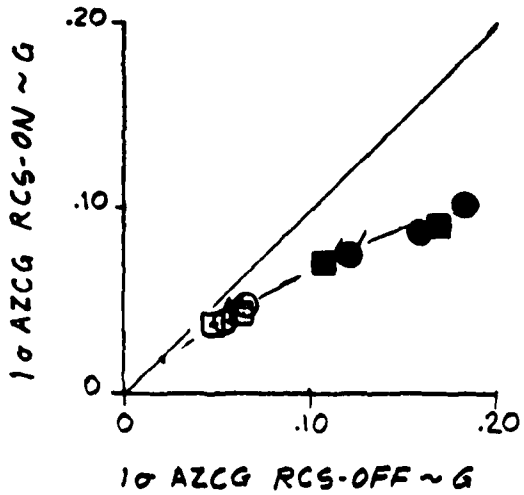

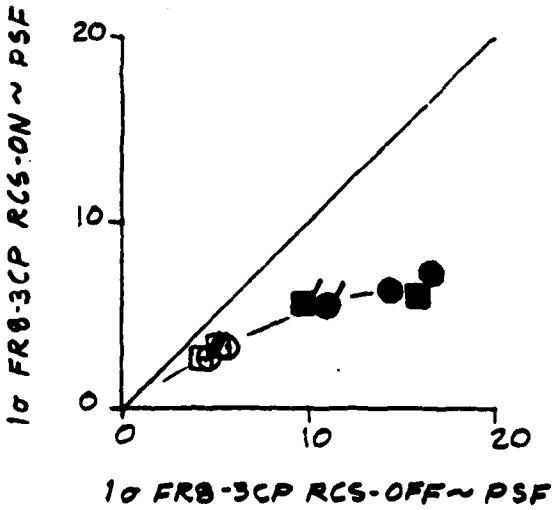

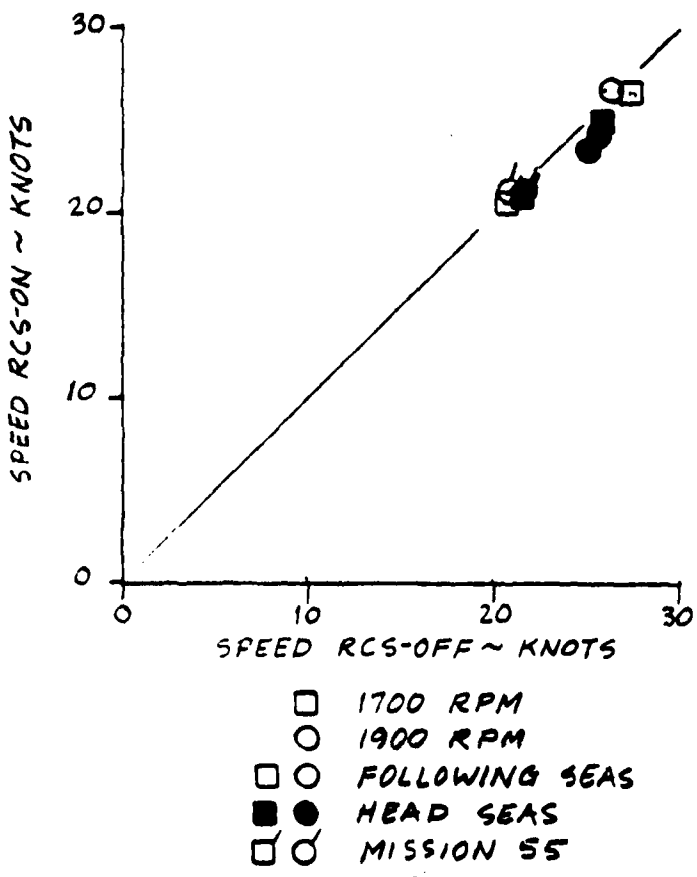

In head seas with the RCS off, increasing the fan speed from 1700 to 1900 rpm again appears to increase the vertical accelerations, although this trend is less distinctly displayed than for the Sea State I data. As explained in Section 8.2, this is associated with the change in the fan characteristic slope. An even less pronounced similar trend is shown in following seas. For both headings, the RCS-on data indicate little effect of fan speed. As was found in Sea State I, the higher fan RPM costs power with no benefits derived, so 1700 rpm is the preferred fan speed for operation in Sea State II at 20 kn or more.

The effects of RCS operation on the vertical acceleration levels may readily be seen in Figures 8-12 and 8-13. However, they are more clearly defined in the plots of Figure 8-14 where the RCS-on results are plotted against the RCS-off data. For the conditions giving the roughest ride (the M-54 head sea cases), the cushion pressure deviations are reduced to 40-45% of the RCS-off results and the LCG vertical accelerations are reduced to about 55% of RCS-off. Correcting for the 0.02 g machinery noise residuals would decrease the latter percentage slightly. Again, even in these relatively small waves, the ride at top speed in head seas is rather rough so the RCS contribution is quite beneficial.

The correlation plot of speeds at constant throttle settings indicates no effect of RCS operation in following seas and a slight speed reduction due to RCS operation in head seas. These results appear to be independent of fan speed.

8.3.4 1/3-Octave Band Acceleration Data

Figures 8-15 through 8-18 present the 1/3-octave band vertical acceleration data at the bow, stern and LCG. Data are shown for 1700 fan rpm at maximum speed and at a nominal 20 kn.

Figure 8-15 shows the results for maximum speed in head seas. The pronounced peaks near 2 Hz again indicate the dominance of the heave mode contributions to the acceleration environment. These data are very similar to those obtained for Sea State I except that there is more energy at frequencies below the heave mode, particularly near 1 Hz. This is due to the lower encounter frequencies associated with the longer Sea State II wavelengths and with the lower maximum speeds achieved here. In fact, careful comparison with Figure 8-6 shows that the data at and beyond 2 Hz are virtually identical to those shown here; the differences lie entirely at lower frequencies. It is characteristic of wave frequency spectra such as the Pierson-Moskowitz spectra

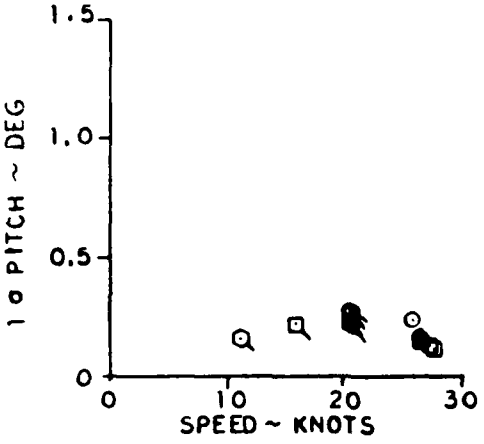

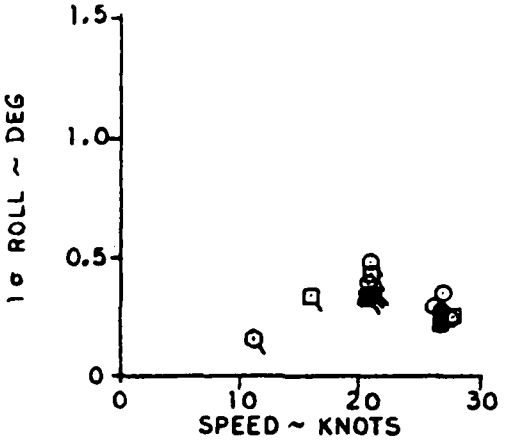

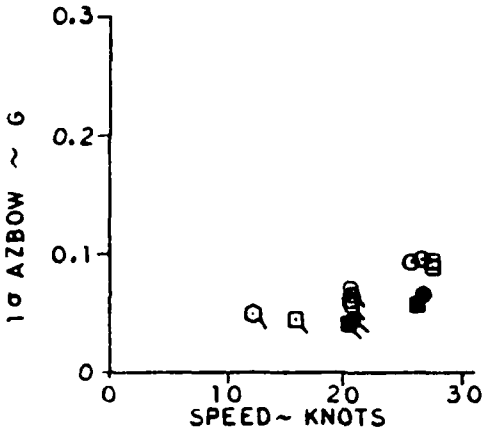

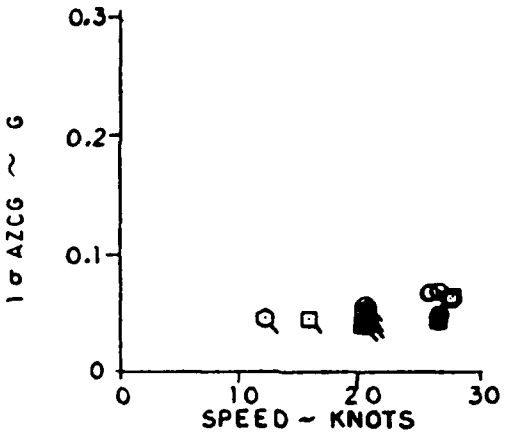

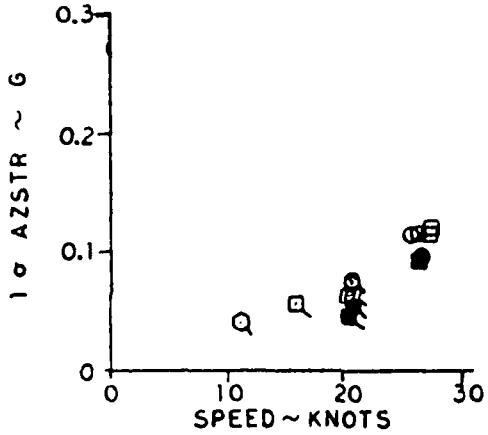

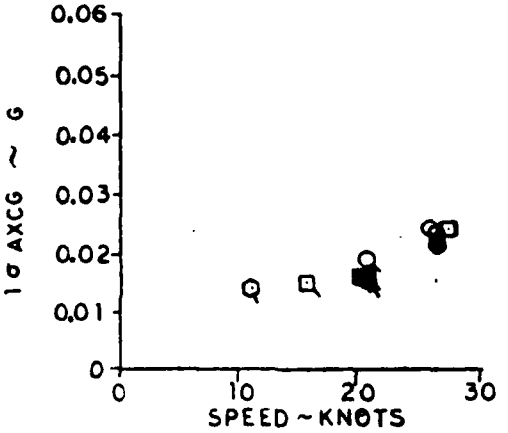

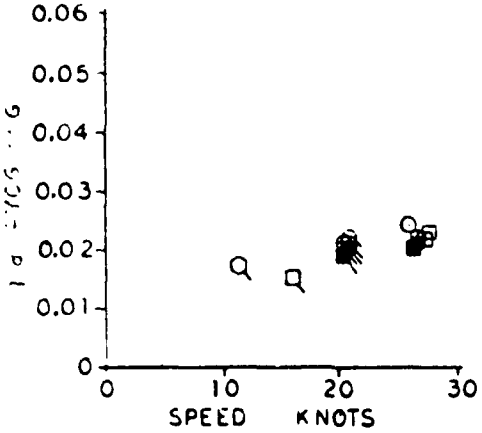

SEA STATE II MOTIONS
FOLLOWING SEAS

LIFT RPM	SYMBOL	RCS
1900	○	● ON
1700	□	○ OFF
1600	○	

MISSION 54 ○
MISSION 55 Q

FIGURE 8 - 13

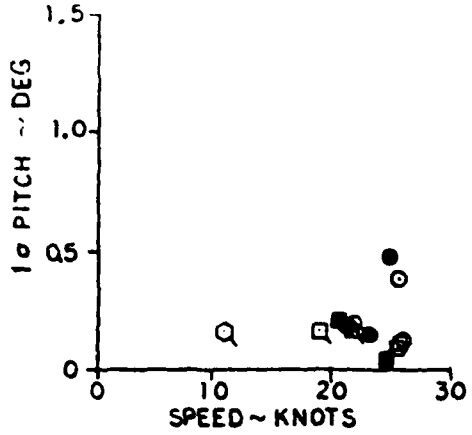

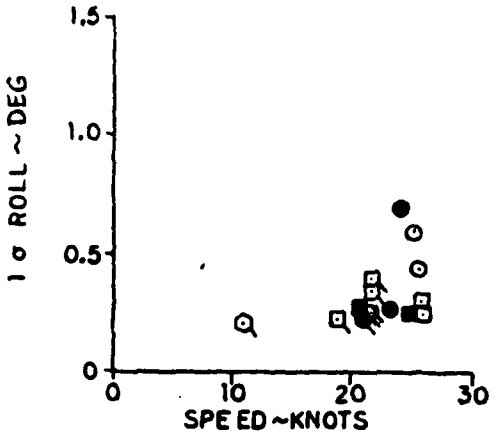

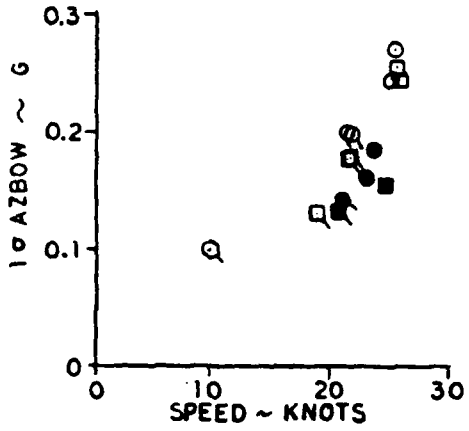

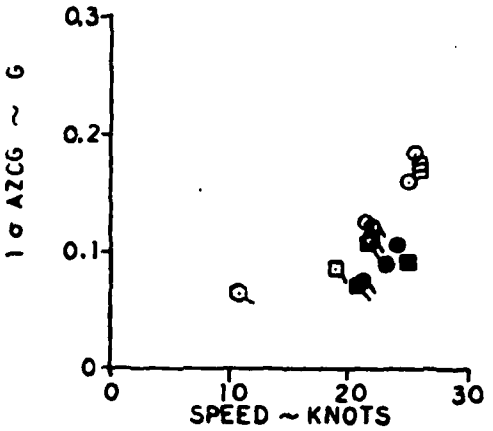

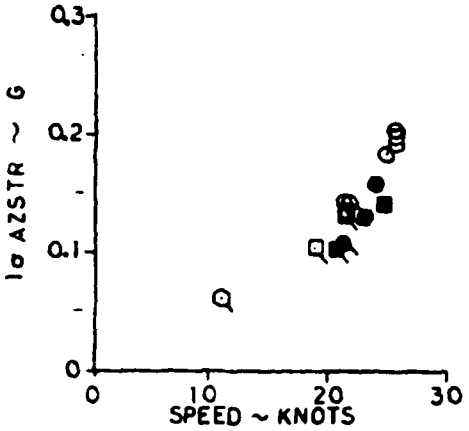

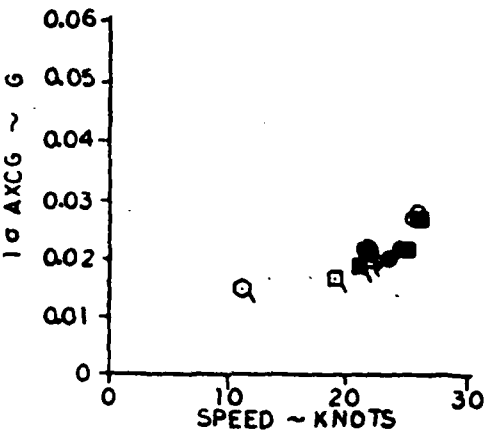

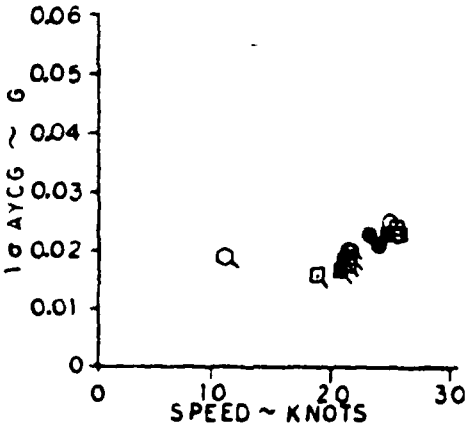

SEA STATE II MOTIONS
HEAD SEAS

LIFT RPM	SYMBOL	RCS
1900	○	● ON
1700	□	○ OFF
1600	○	
MISSION 54	○	
MISSION 55	Q	

FIGURE 8-12

Except for M-55 TP-45, the Waverider data were used for the correlations against wave heights for Sea State II.

The comments of Section 8.2.2 regarding differences between wave spectra in the open ocean and in Chesapeake Bay apply here also.

8.3.3 Standard Deviations

The principal standard deviations from M-54 and M-55 are shown as functions of craft speed on Figures 8-12 and 8-13. Standard deviations are denoted as 1σ values. Data are presented for three vertical accelerometers located at the bow (AZBOW), the stern (AZSTR) and the LCG (AZCG), together with LCG axial (AXCG) and transverse (AYCG) accelerations and the pitch and roll angles from the vertical gyro.

For head seas (Figure 8-12), the strong dependence of the vertical accelerations on craft speed observed for Sea State I are again evident. Also, there are now clear trends of the lateral and longitudinal accelerations increasing with speed. This is as would be expected, but the Sea State I data did not clearly display this characteristic.

Figure 8-12 also indicates a dependence of roll amplitudes on speed. However, there is even more tendency to show increased scatter in the data with increasing speed for both roll and pitch. In line with the comments on roll in head and following seas given in Section 8-2, we interpret this as indicating an increased sensitivity to errors in achieving the desired relative wave heading and to deviations of the seaway from one-dimensionality. This speed dependence is as expected.

The small pitch amplitudes again show that heave is the dominant wave-induced motion in Sea State II.

The following sea data (Figure 8-13) again show less dependence of vertical accelerations on speed, particularly at the LCG.

The following sea longitudinal and lateral accelerations appear to be about the same as in head seas and display the same speed dependence.

For the following sea case, the pitch and roll angle standard deviations now display a distinct speed dependence. Both show maxima at around 20 kn. Sea State I data did not display a similar effect. However, as speeds lower than 20 kn were not run in Sea State I, the trend would not be so apparent.

FIGURE 8-11 SEA STATE II WAVE POWER SPECTRA - MISSION 55

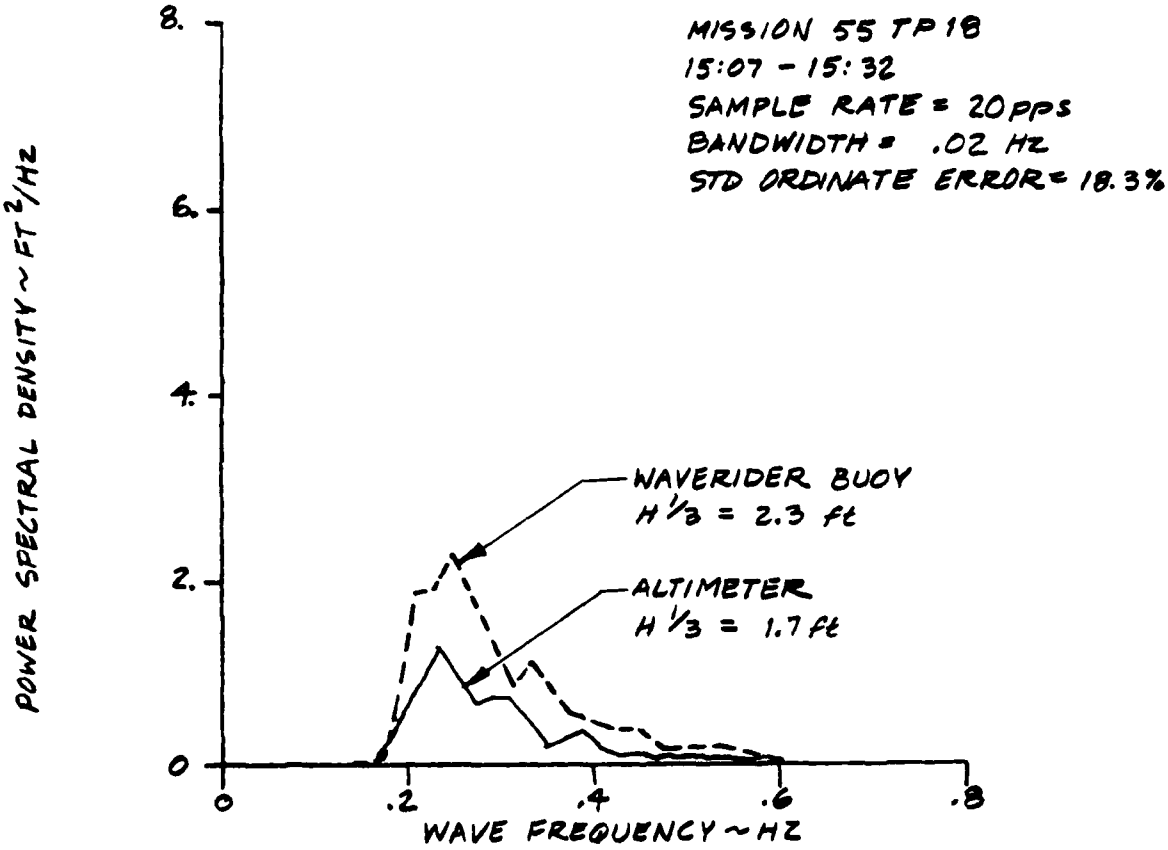

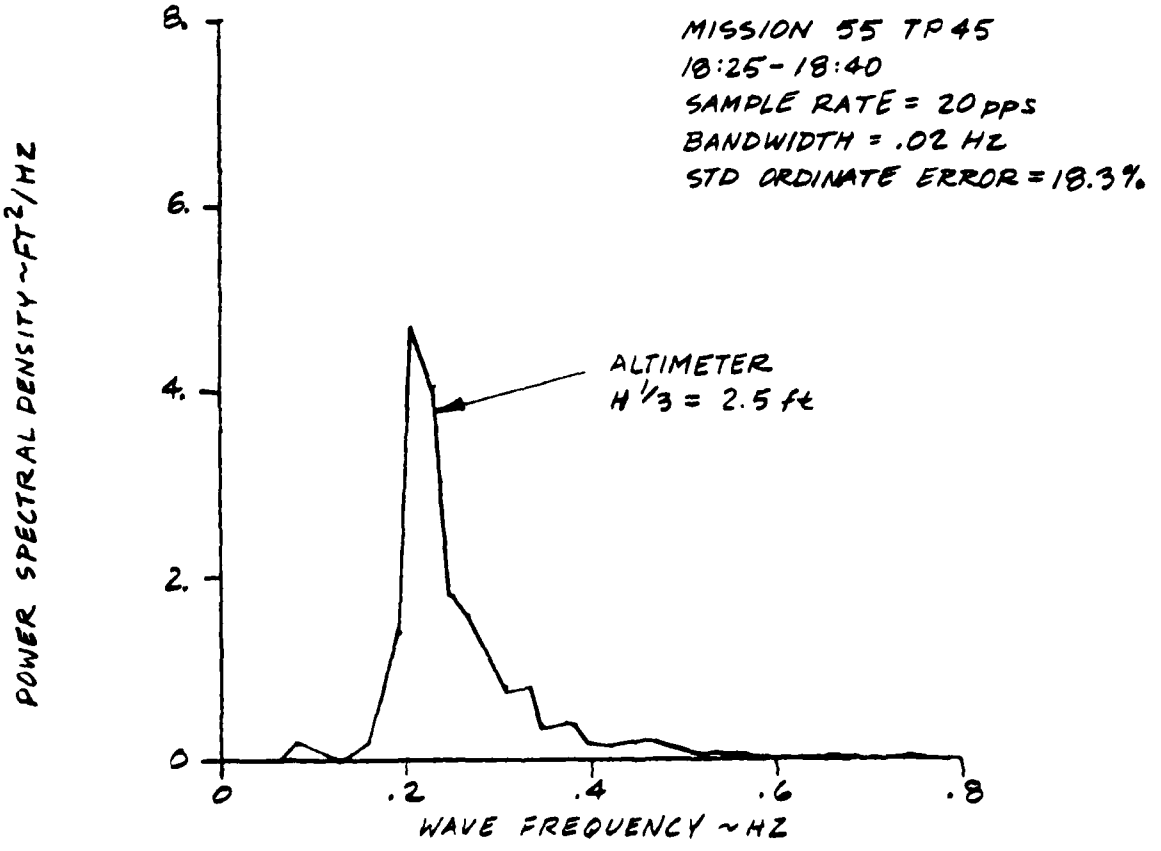

FIGURE 8-10 SEA STATE II WAVE POWER SPECTRA - MISSION 54 & 55

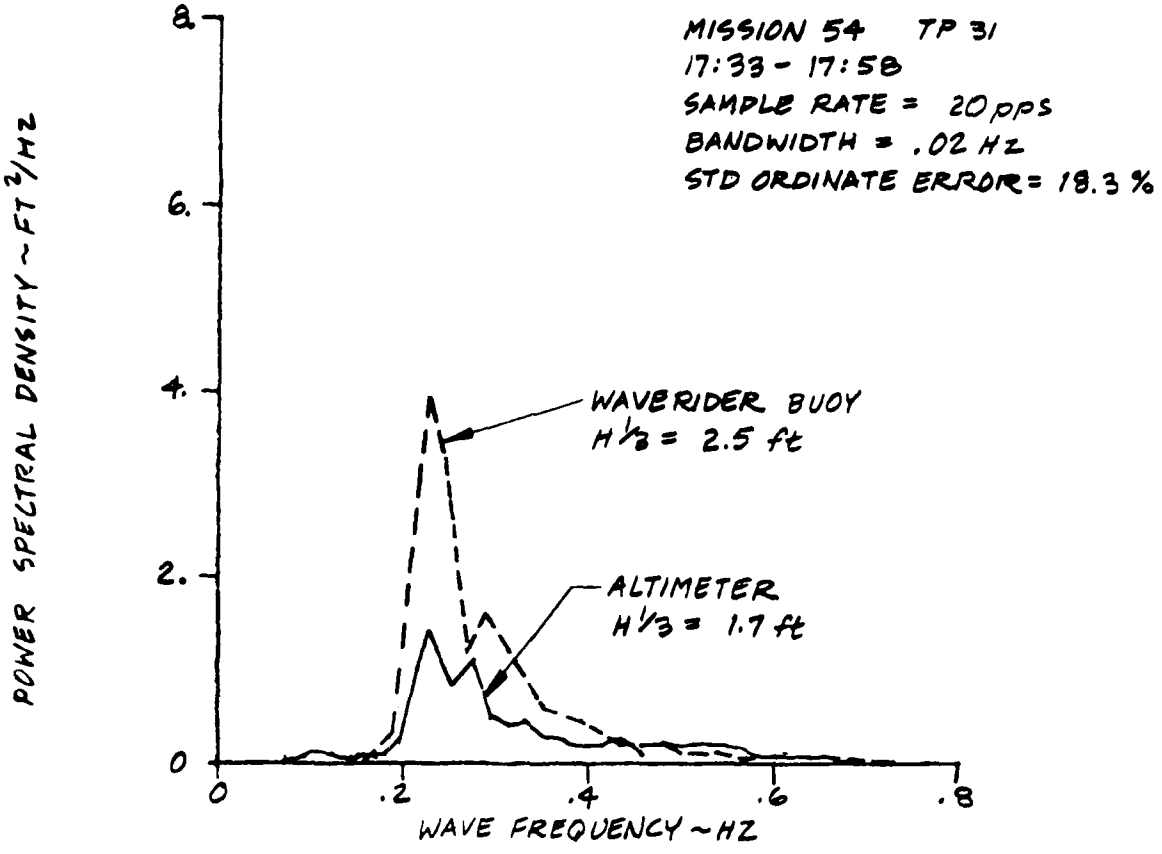

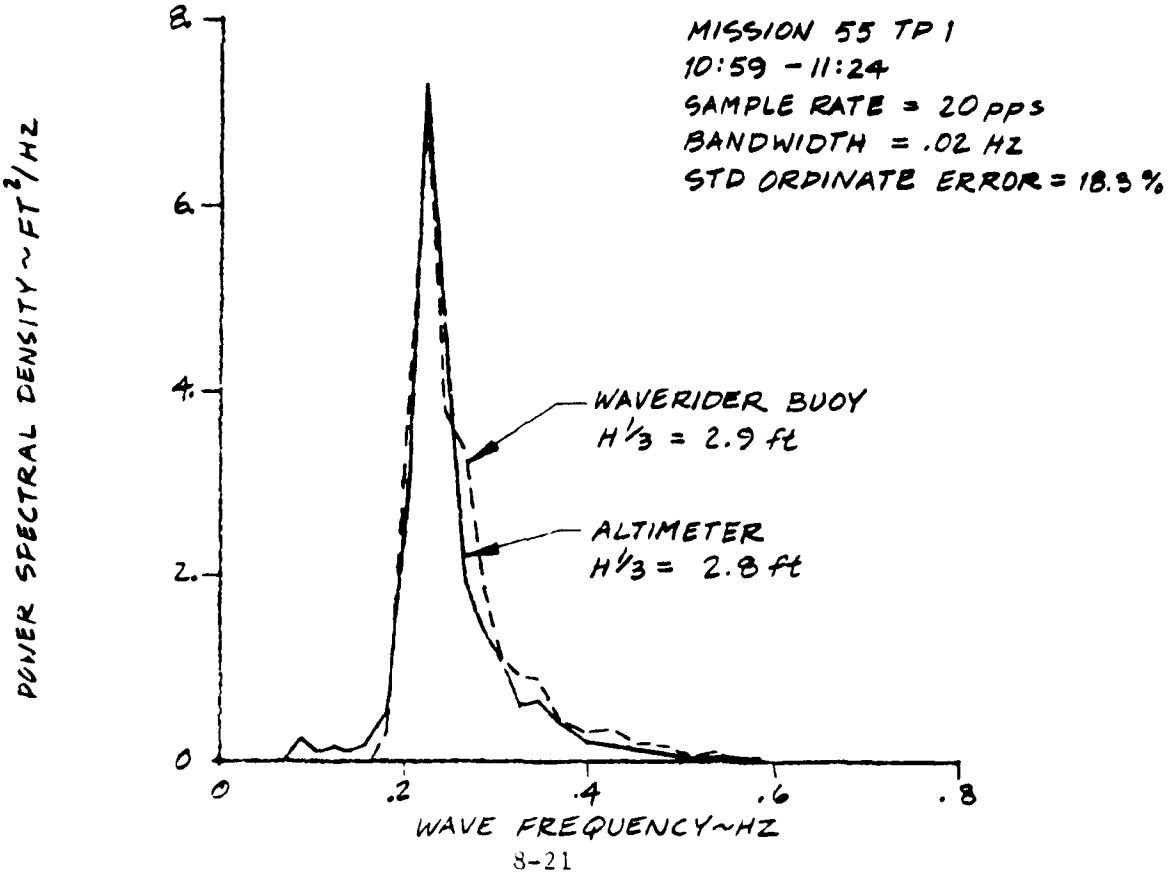

FIGURE 8-20

SEA STATE II HEAVE ACCELERATION & CUSHION PRESSURE

POWER SPECTRA - FOLLOWING SEAS-1700 LIFT FAN RPM

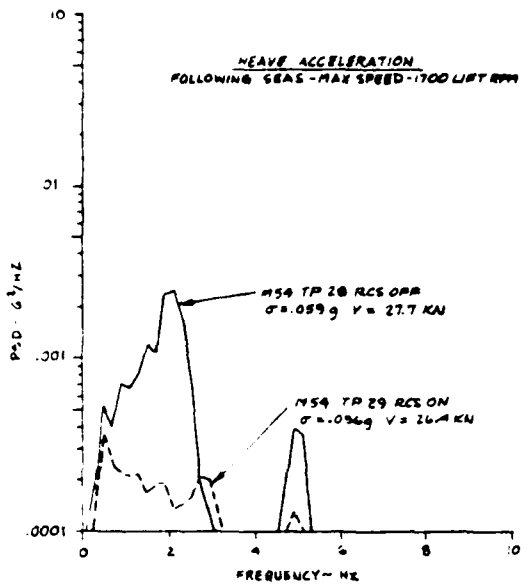

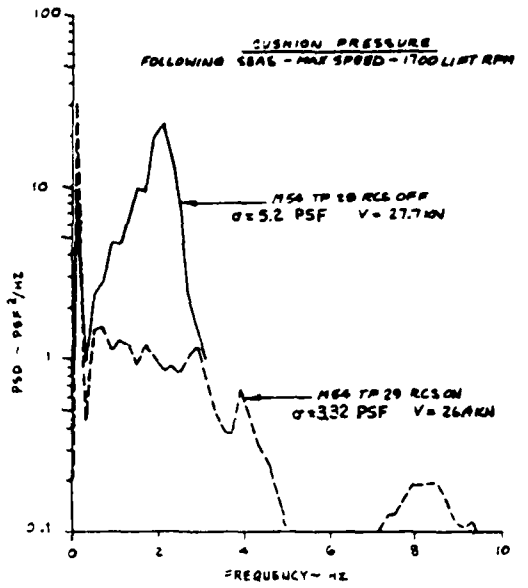

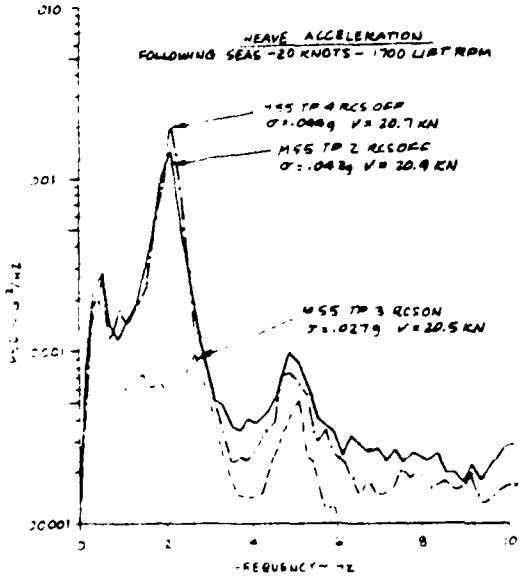

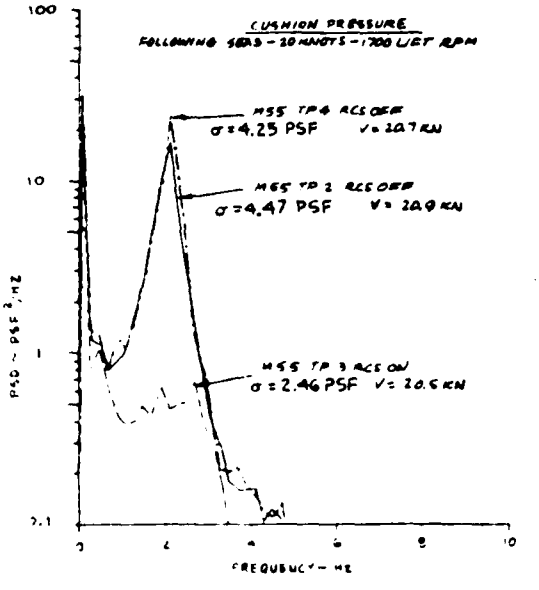

The acceleration spectrum for the 20 kn case appears much broader than for the corresponding Sea State I case because the scaling happened to fit the plot format better. The data here are plotted one decade further down than in Figure 8-9.

The following sea data are shown on Figure 8-20. The 20 kn acceleration spectrum is notable in that it displays a well defined peak at the 0.3 Hz pitch natural frequency and the RCS action yields a considerable attenuation of the spectrum at high frequencies. As was discussed in Section 8.2.5, this probably indicates that much of the energy at higher frequencies is non-linear in origin and results from local broaching of the sidehulls pulsing the cushion. The RCS action reduces the occurrences of broaching and therefore results in less excitation of the higher modes.

8.4 SEA STATE III MOTIONS

The Sea State III condition received by far the most extensive test coverage for the SES-200 Technical Evaluation Program. Such complete coverage of all sea states would have resulted in an unreasonably massive test program. However, it is necessary to have rather complete coverage of at least one condition. Sea State III was selected because it is representative of moderate-to-heavy weather operating conditions for a 200-ton vessel. This sea state has waves of sufficient magnitude that essentially all phenomena of interest are exhibited.

The data analysis effort is, of course, also emphasized for this sea state, so the fullest range of data presentation is given in this section.

It might be mentioned at this point that the tests conducted in bow and quartering seas presented considerable difficulty in terms of holding a constant heading approximating the desired relative wave heading. Under these conditions in this sea state, there is some difficulty in accurately judging whether the heading attained is really at 45 degrees to the wave crests, particularly in the quartering sea case where craft speeds of 20 knots are near the wave propagation velocity.

8.4.1 Test Conditions

A number of missions were conducted in Sea State III; however, only results from Missions 34, 35 and 44 are presented as the seas were most consistent during these missions. All three missions were conducted at sea rather than in Chesapeake Bay, as were the Sea States I and II missions. The test sites were all about 200 nm. east of Cape Hatteras near the location of the NOAA Wave Buoy 'RY41001'.

All three missions were at heavy ship conditions. For M-34, the gross weight varied from 192.7 to 195.1 L.T. and the LCG varied from -1.2 to -1.3 ft. For M-35, the gross weight was from 188.8 to 192.1 L.T. and the LCG was -1.9 ft. For M-44, the gross weight was in the range of 191.8 to 195.0 L.T. and the LCG varied from -1.8 to -2.2 ft.

Tests were conducted using headings from following to head seas in 45 degree increments. On-cushion test points used fan speeds from 1700 to 1900 rpm. Off-cushion test points were also run. Most of the data were obtained on-cushion at maximum speed and (nominally) 20 kn. The off-cushion data were obtained dead-in-the-water (DIW) and at 5 and 10 kn.

For all head sea test points, data were recorded for approximately 200 wave encounters. For other headings, lower numbers of encounters were accepted in the interest of completing the sizeable volume of testing required within time constraints and while the requisite sea state prevailed. Longer test points would also have created difficulties remaining in the general neighborhood of the NOAA wave buoy.

For the DIW and 5 kn cases, 15 minute durations were used. For the 10 kn cases, 10 minute duration test points were used and for the 20 kn and maximum speed cases, 3 or 5 minute test points were used.

To permit proper evaluation of the RCS effects, the test sequence of RCS-off, RCS-on, RCS-off was used to provide reference data immediately before and after the RCS-on test point.

8.4.2 Wave Measurements

The wave spectra are shown on Figures 8-21 through 8-23. The data presented are for the Datawell Waverider Buoy (when available) and comparable data obtained from the boom-mounted TRT radar altimeter in the DIW condition. These latter data were corrected for craft motion effects using the boom-mounted vertical accelerometer. The NOAA wave buoy data were abandoned due, primarily, to the coarse resolution of the data from this source. Wave data test points were obtained at the beginning and end of each mission except for M-35 where the onset of darkness prevented this.

The wave data test points, except for M-44 TP-1, were of 25 minute duration. Sample rates of 20 pps were used and the data were processed to a 0.02 Hz bandwidth yielding a standard deviation of the estimation error of 18.3% of the amplitude. For M-44 TP-1, a 50 minute duration was used giving a standard error of 12.9%; the Waverider Buoy data for this test point were abandoned due to data drop-out problems.

The significant wave heights from the buoy and the altimeter are in reasonable agreement with the buoy data consistently indicating somewhat smaller waves. The greatest disagreement is for M-34 TP-28 where the buoy data shows 4.5 ft against 5.3 ft for the altimeter (a 15% discrepancy). The power spectra are in rough agreement with the buoy data generally indicating less power in the low (less than 0.2 Hz) frequency range. Some of this disagreement may be associated with the use of standard accelerometer data at rather low frequencies coupled with the effects of discretization imposed by the DAS PCM arrangement.

Some insight into the level of agreement which might be expected between spectra from the two data sources is obtained from Figure 8-22. Here, the wave test point was actually run with a 50 minute duration, but the data were processed as two 25-minute contiguous time segments. As may be seen, the variation between the spectra for the two time segments with either the altimeter or the buoy is of the same order as the variation between the spectra from the two sources for a single time segment. This would indicate that the apparent discrepancy between data from the two instruments is perhaps no greater than should be expected.

FIGURE 8-21 WAVE SPECTRA FOR SEA STATE III

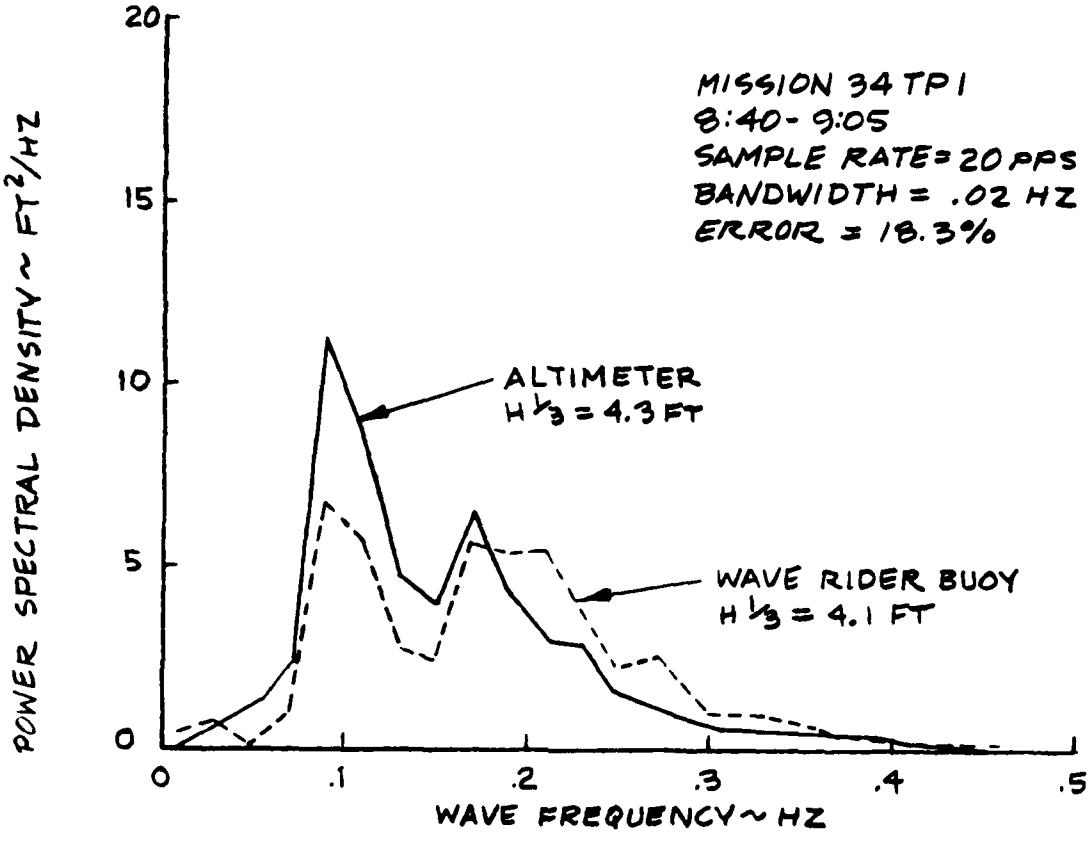

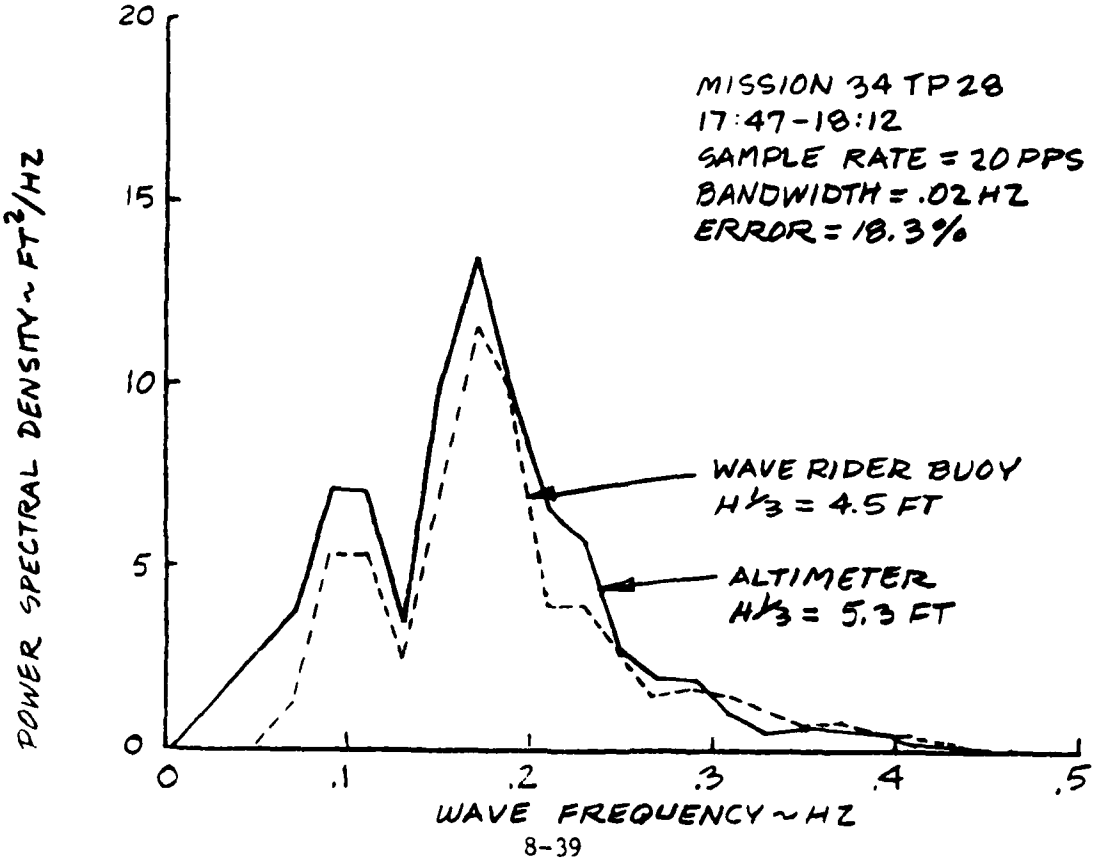

FIGURE 8-22 WAVE SPECTRA FOR SEA STATE III

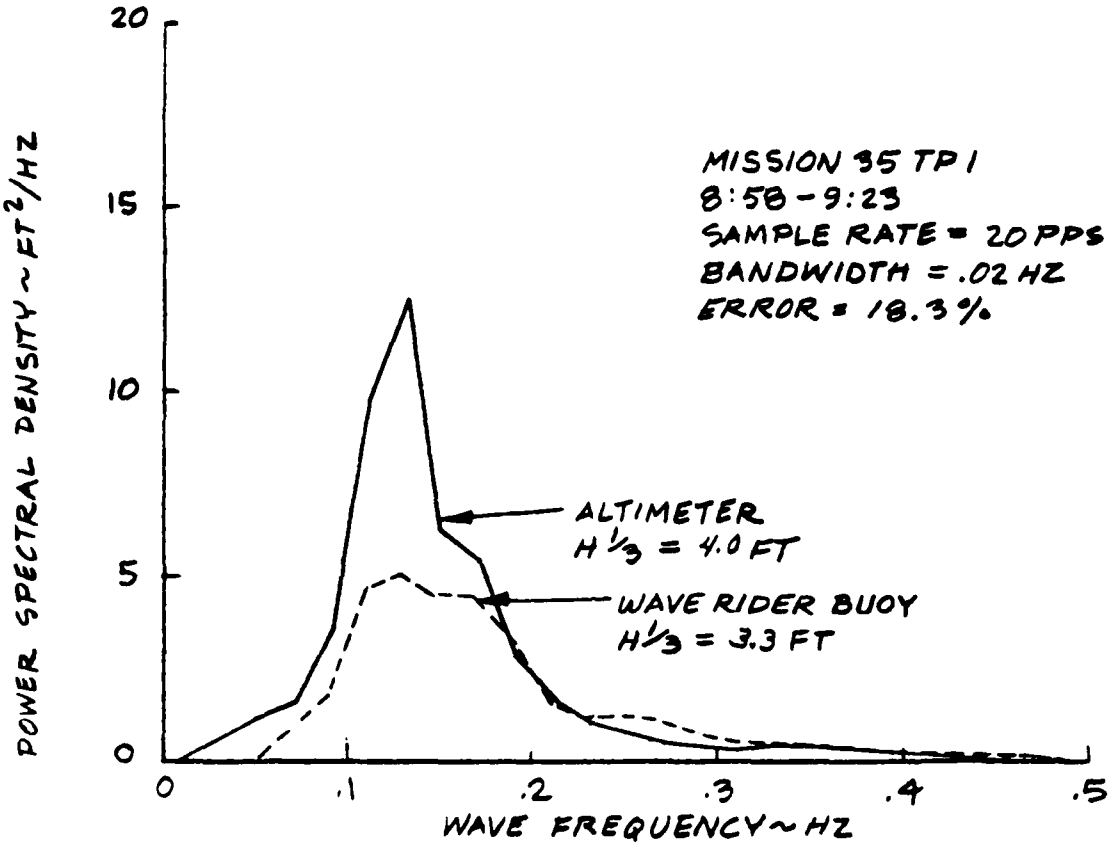

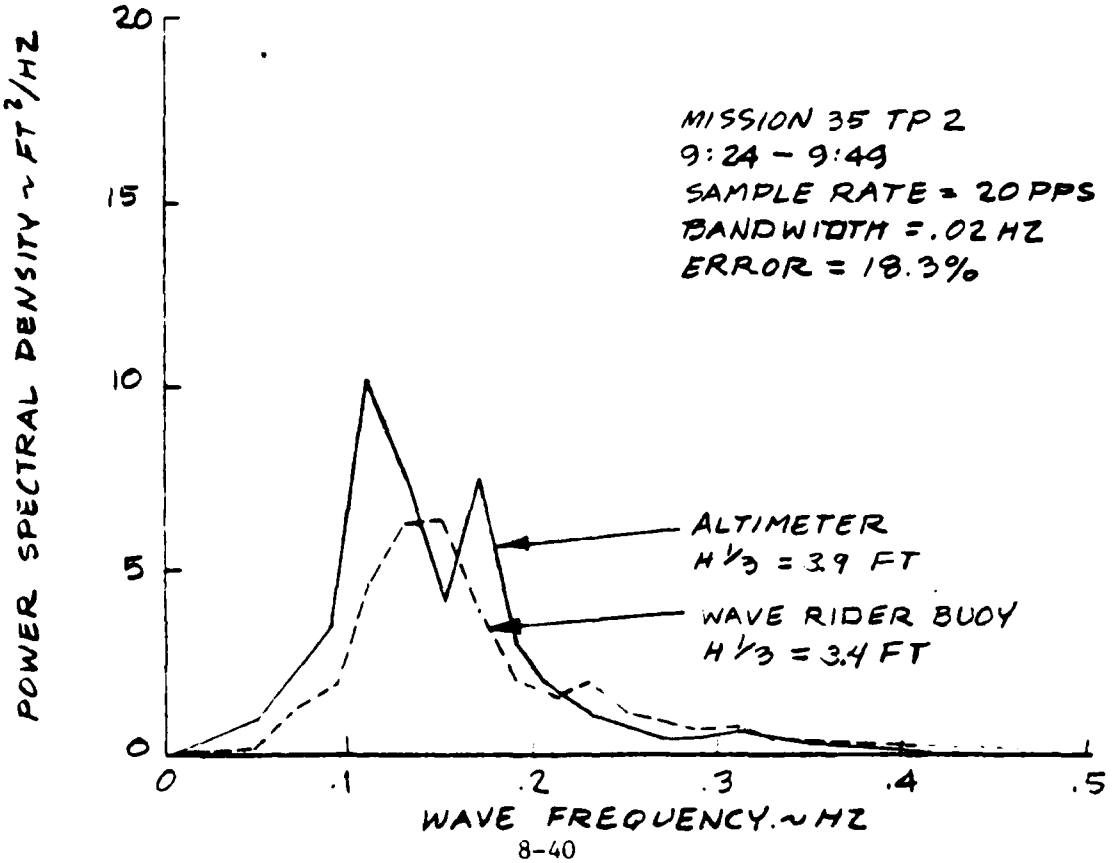

FIGURE 8-23 WAVE SPECTRA FOR SEA STATE III

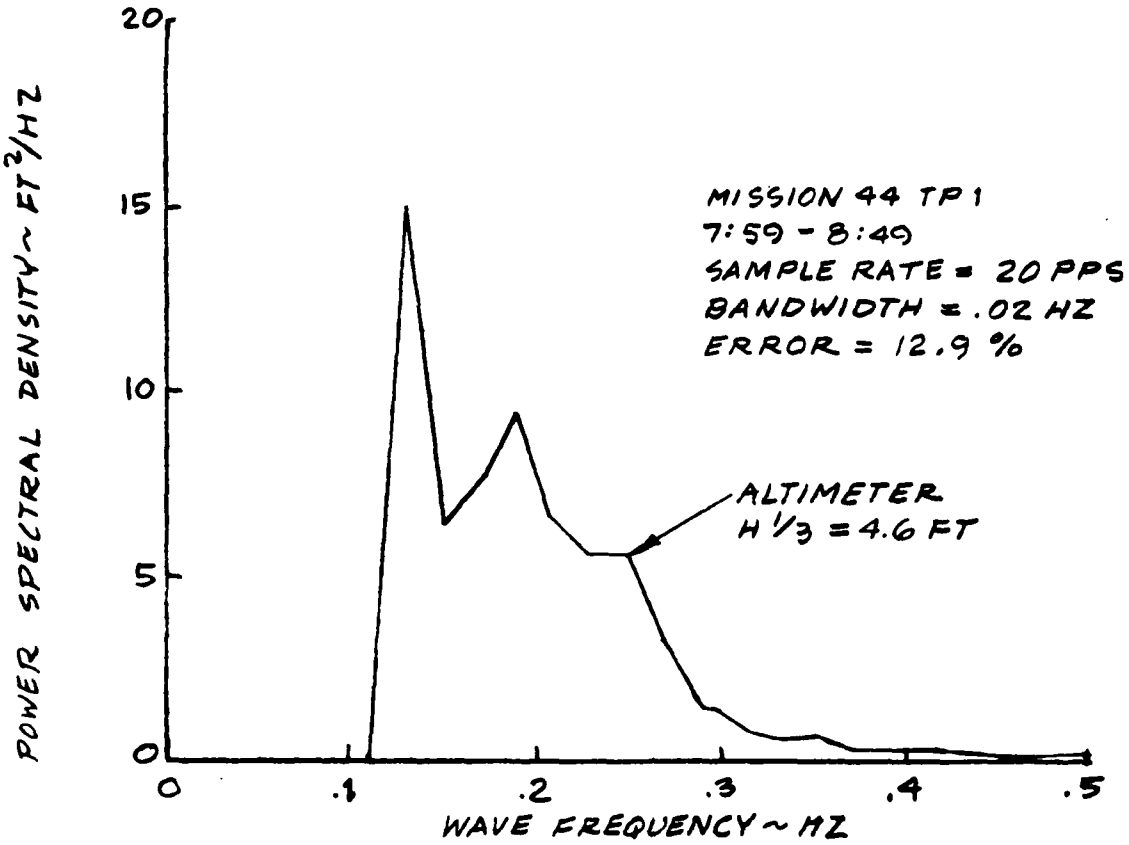

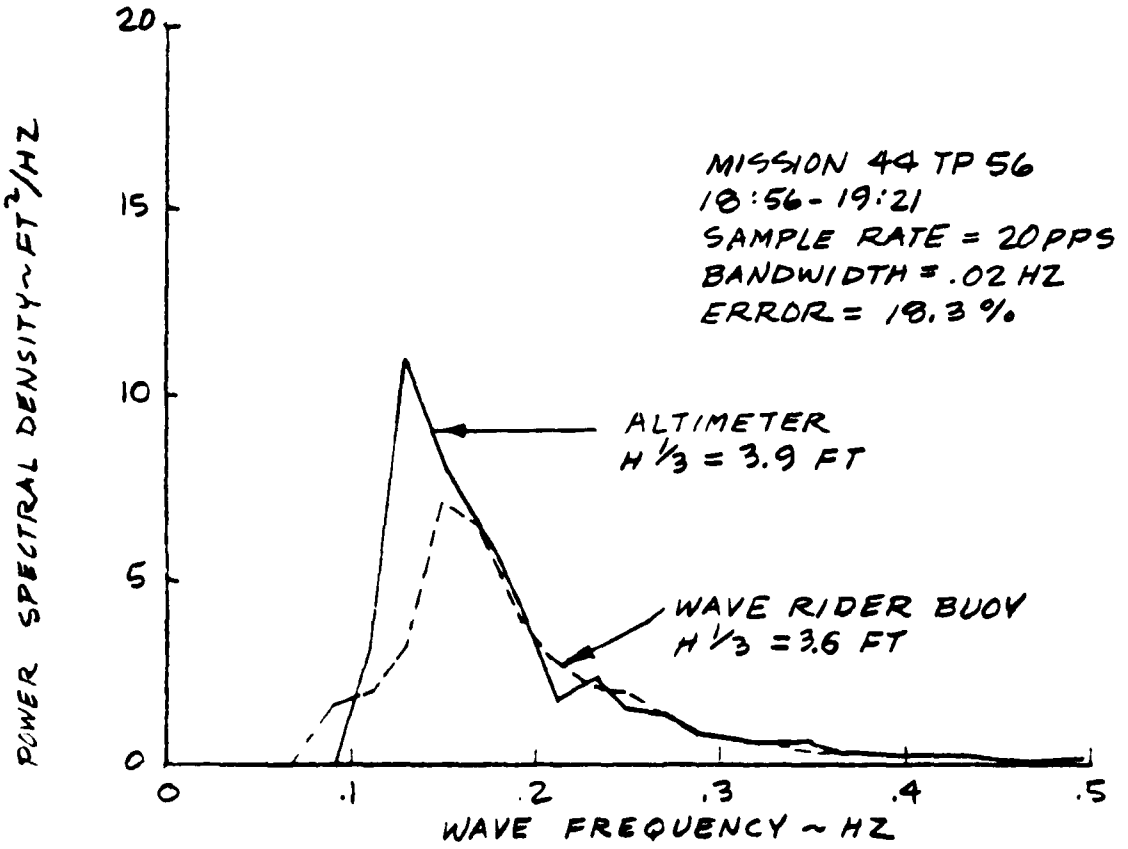

8.4.3 Standard Deviations

The standard deviation data are presented in three different formats which will be discussed separately below. The first form is that of plotting the standard deviations versus craft speed for various headings and is discussed in Section 8.4.3.1. Then (Section 8.4.3.2) the data are presented as functions of heading at different speeds. Finally, Section 8.4.3.3 presents correlations between RCS-on and -off conditions.

8.4.3.1 Standard Deviations as Functions of Craft Speed

The standard deviations are presented as functions of speed on Figures 8-24 through 8-28. Note that, for all these plots, the data below 20 kn are for the off-cushion condition. The plots show the standard deviations of vertical accelerations at the bow (AZBOW), LCG (AZCG) and stern (AZSTR), longitudinal (AXCG) and lateral (AYCG) accelerations at the LCG, and pitch and roll angles from the vertical gyro. Standard deviations are denoted as 1σ values on the figures.

8.4.3.1.1 Head Seas

Figure 8-24 summarizes the motions in head seas. As was the case in the lower sea states, the vertical accelerometer data show a strong speed dependence. On-cushion, this is somewhat more difficult to distinguish accurately than in the smaller waves because the maximum speed and the nominal 20 kn speed are not much different here. The effect of the RCS is discernible here, but will be shown more clearly on Figure 8-31.

For the RCS-off, the vertical accelerations with 1900 fan rpm are slightly higher than with 1700 rpm; the RCS-on data show little difference. In spite of the higher rms acceleration levels indicated, it was generally felt that the 1900 rpm condition gave a more acceptable ride in Sea State III as higher mean cushion pressures were maintained. This reduced the tendency to occasionally completely vent the cushion.

As in the lower sea states, the accelerations at the bow and stern are distinctly higher than at the LCG. This is again due in part to the activity of the first longitudinal bending mode. However, unlike the situation in Sea States I and II, the pitch motion in Sea State III is large enough to also have a significant influence on the bow and stern accelerations.

Comparison with Figure 8-12 reveals that the highest values of the vertical acceleration standard deviations are comparable to or lower than those in Sea State II. This appears to be primarily due to the reduction in maximum speed for this higher sea state reducing the accelerations sufficiently to compensate for the larger wave disturbances.

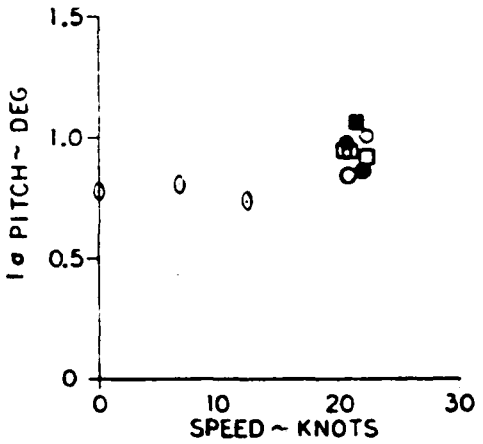

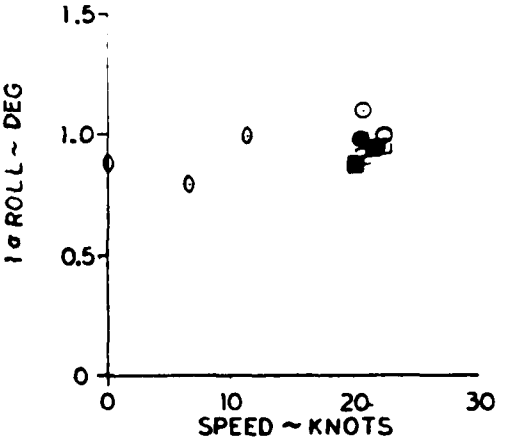

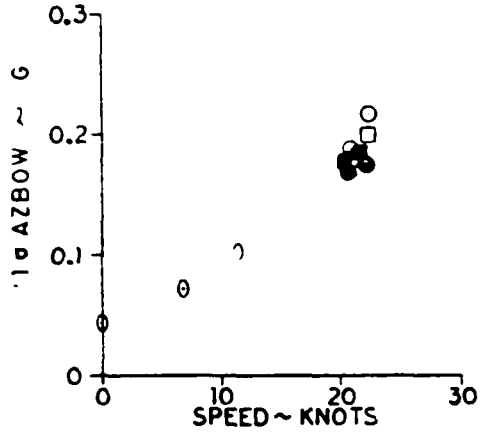

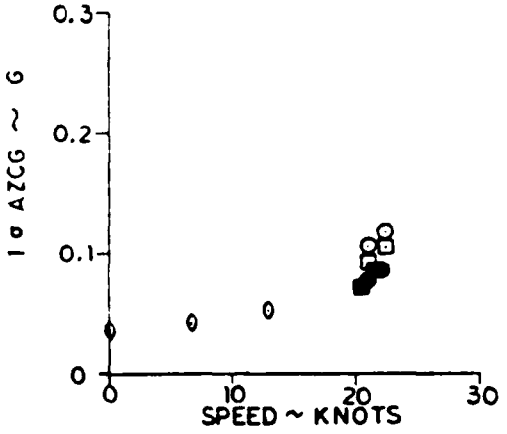

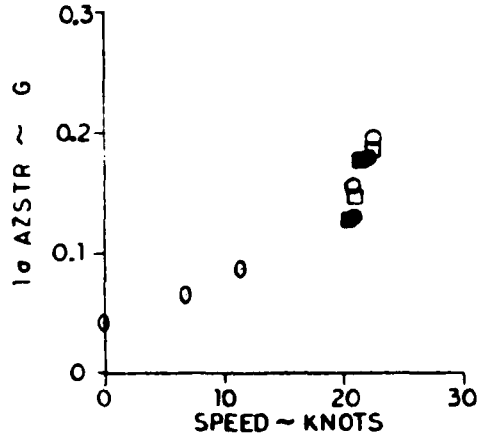

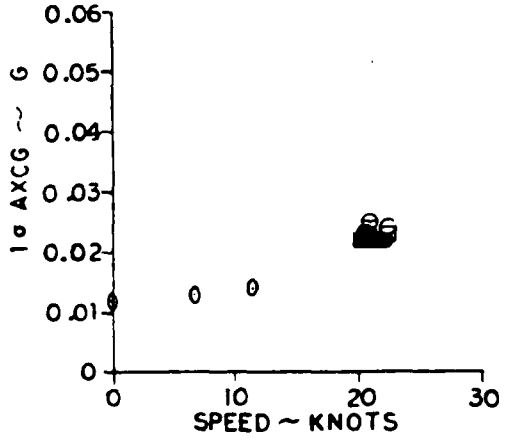

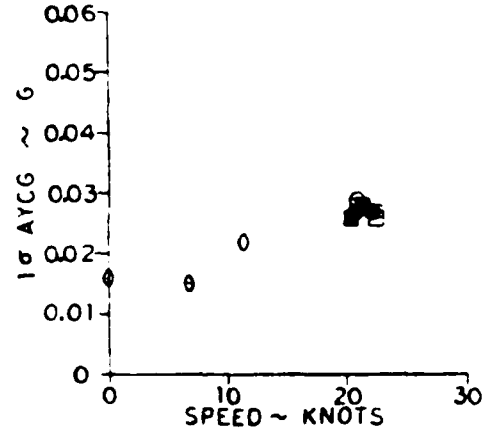

SEA STATE III MOTIONS
HEAD SEAS

LIFT RPM	SYMBOL	RCS
1900	○	● ON
1700	□	○ OFF
1500	△	
1300	◇	
000	0	

MISSION 35
FIGURE 8-24

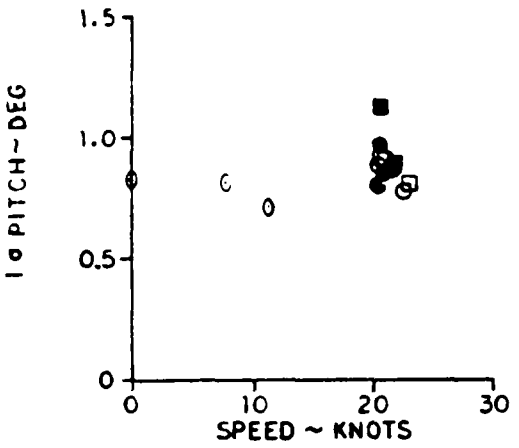

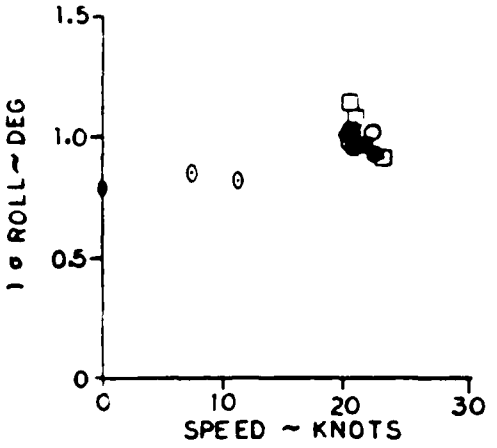

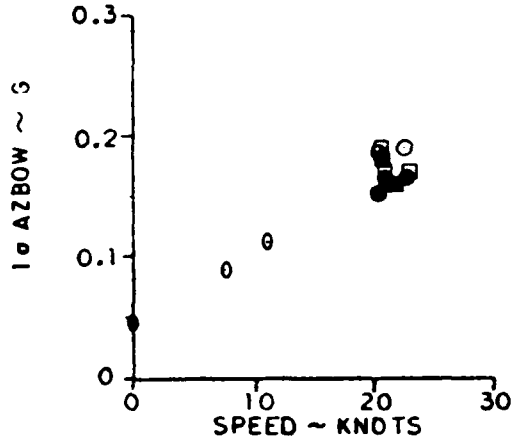

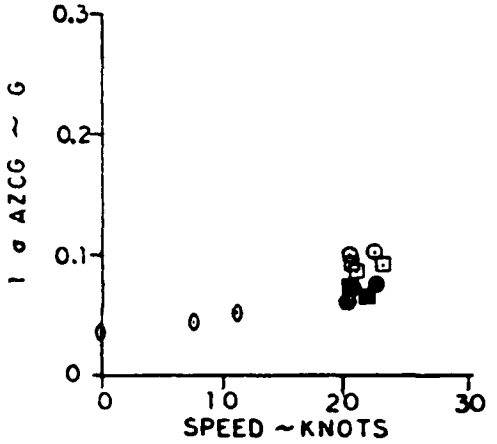

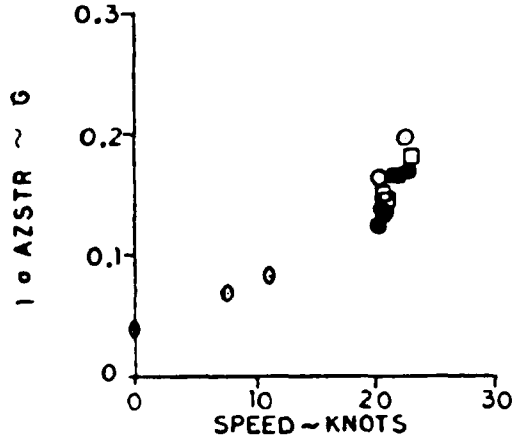

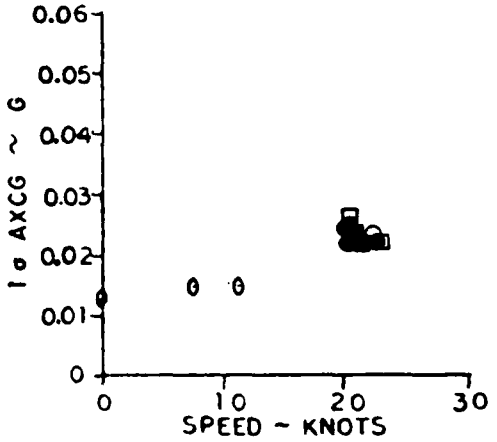

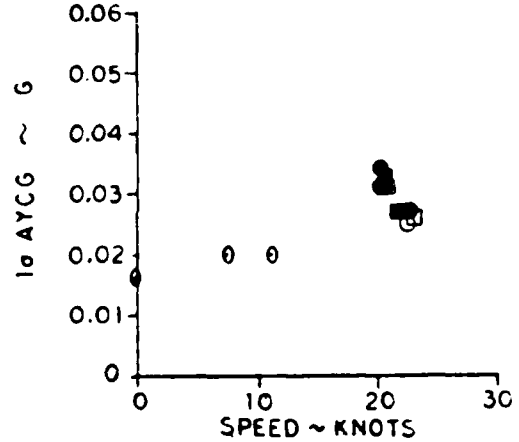

SEA STATE III MOTIONS
BOW SEAS

LIFT RPM	SYMBOL	RCS
1900	○	ON
1700	□	OFF
1500	△	
1300	◇	
000	0	

MISSION 35

FIGURE 8-25

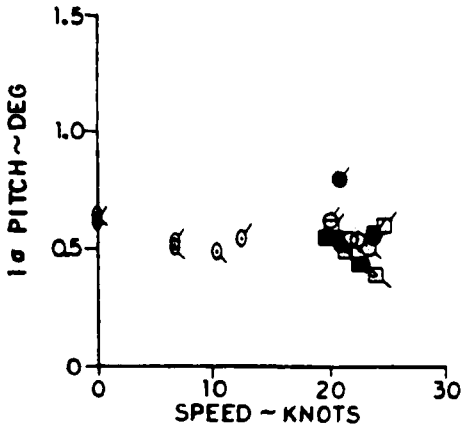

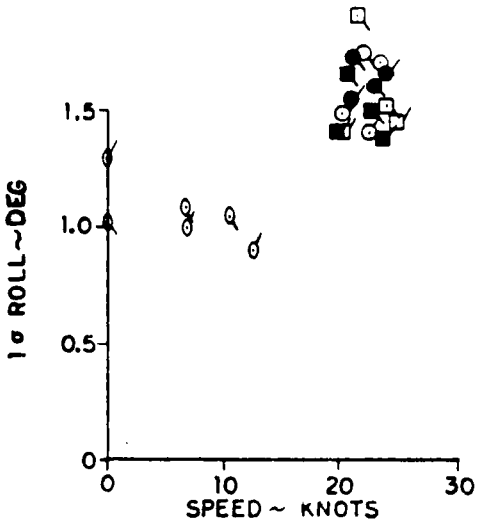

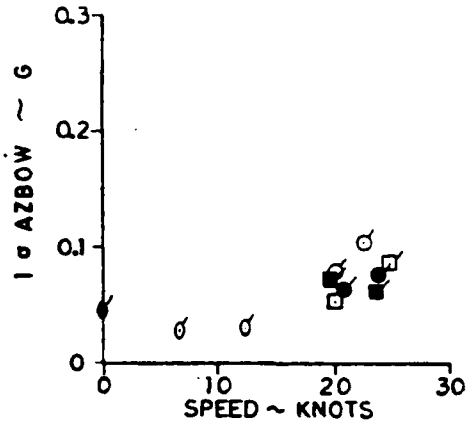

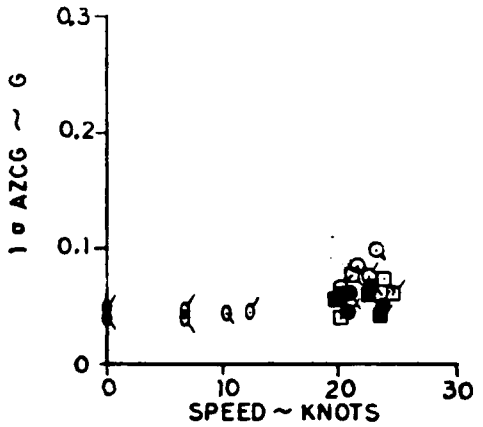

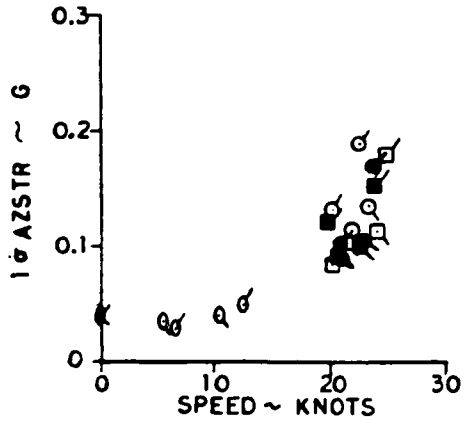

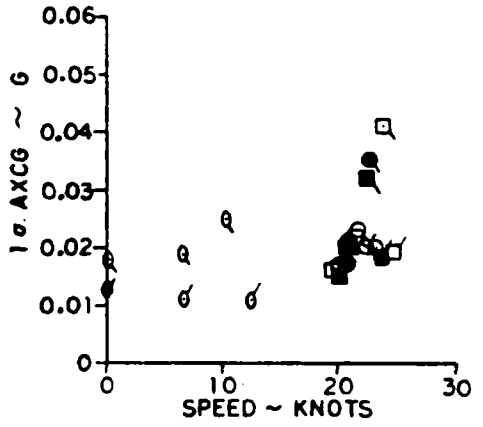

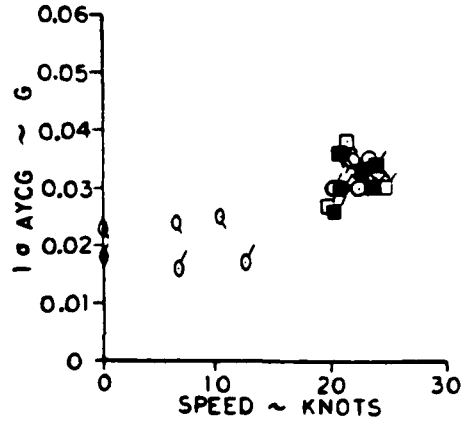

SEA STATE III MOTIONS

BEAM SEAS

LIFT RPM	SYMBOL	BCS
1900	○	● ON
1700	□	○ OFF
1500	△	
1300	◇	
000	0	

MISSION 35 ♂

MISSION 44 ♀

FIGURE 8-26

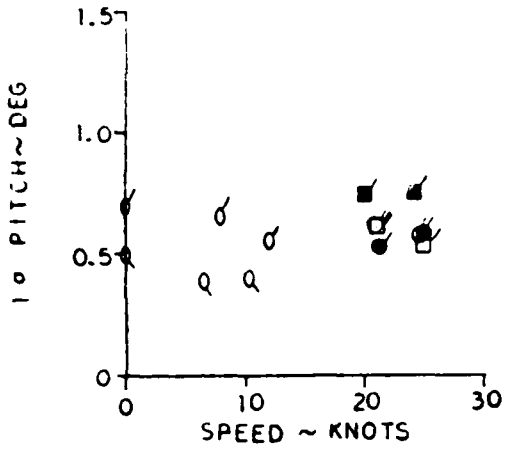

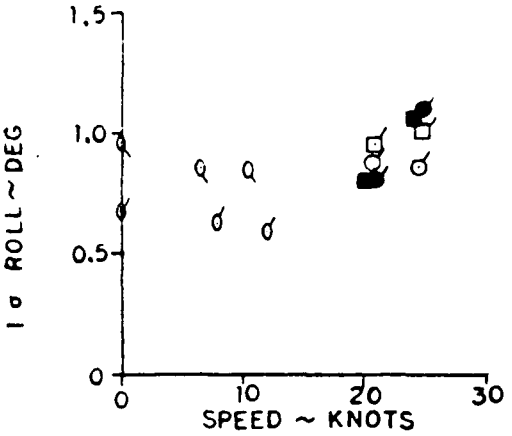

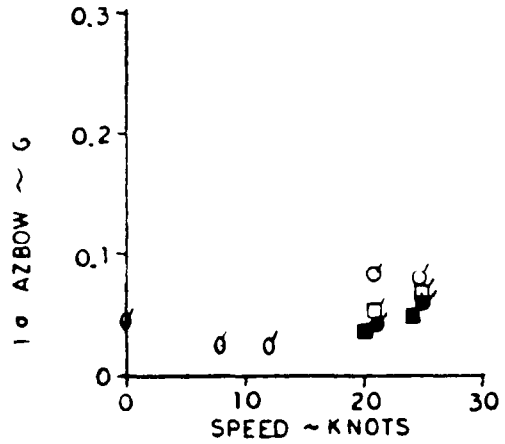

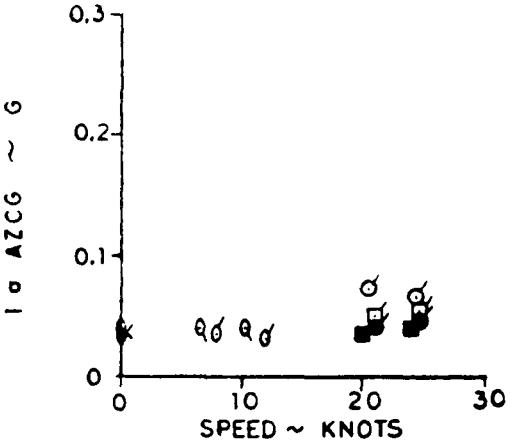

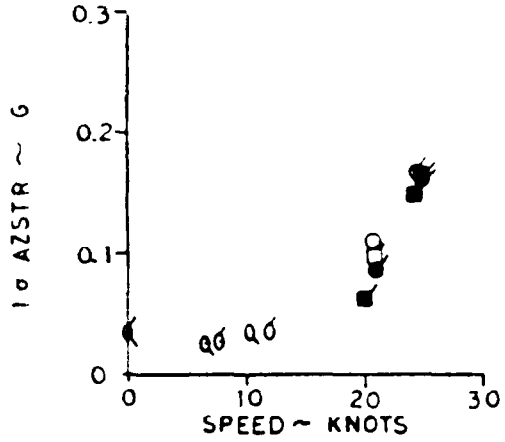

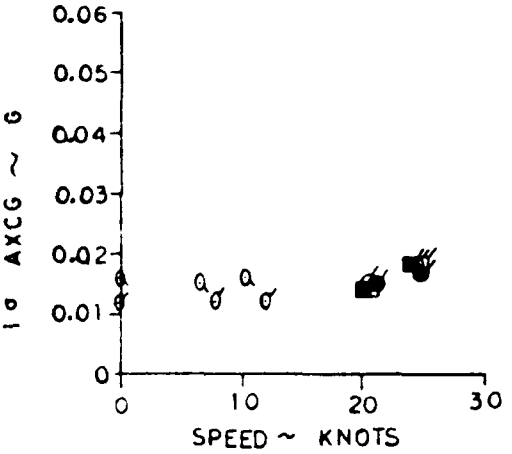

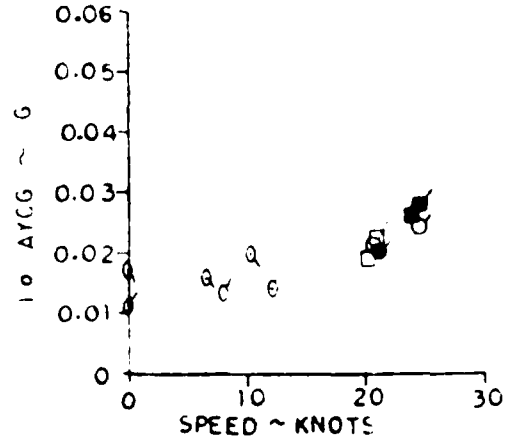

SEA STATE III MOTIONS
QUARTERING SEAS

LIFT RPM	SYMBOL	RCS
1900	○	● ON
1700	□	○ OFF
1500	△	
1300	◇	
000	0	

MISSION 35 ♂
MISSION 44 ♀

FIGURE 8-27

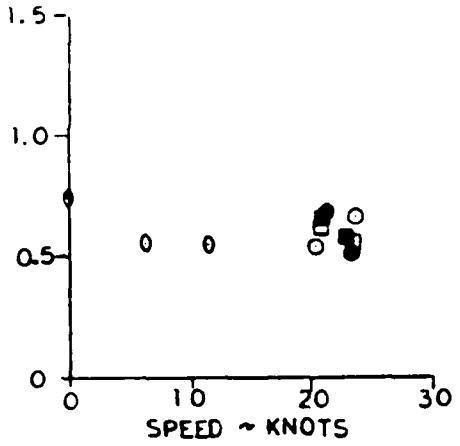

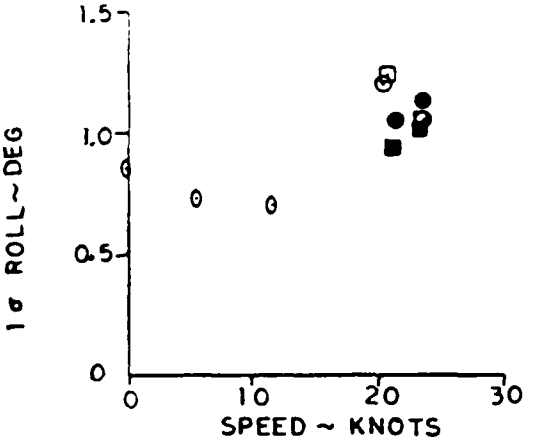

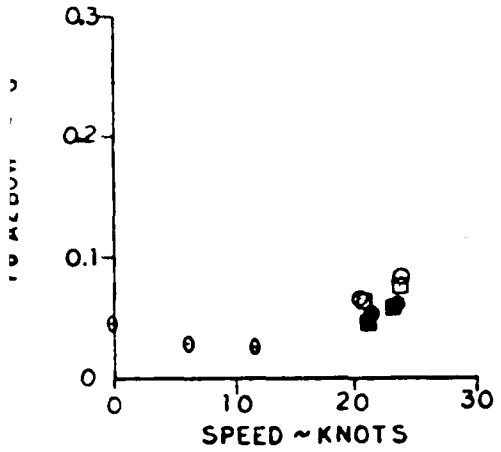

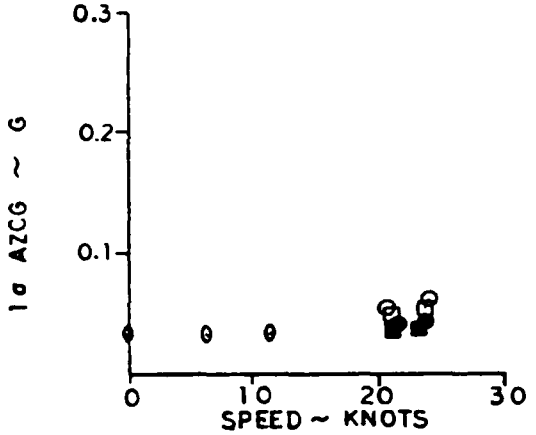

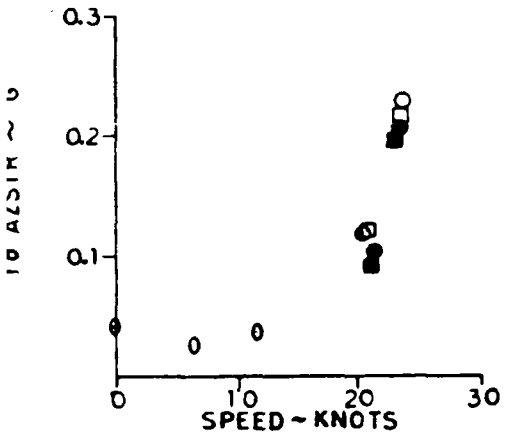

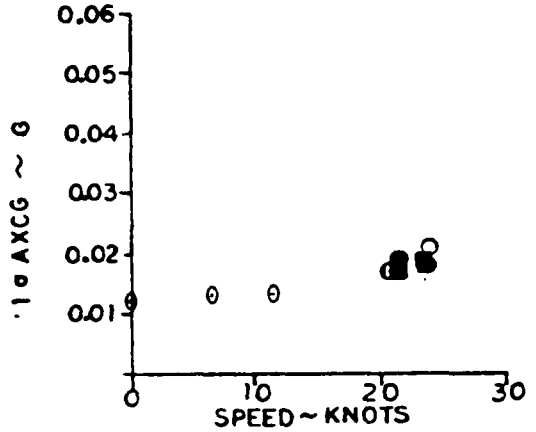

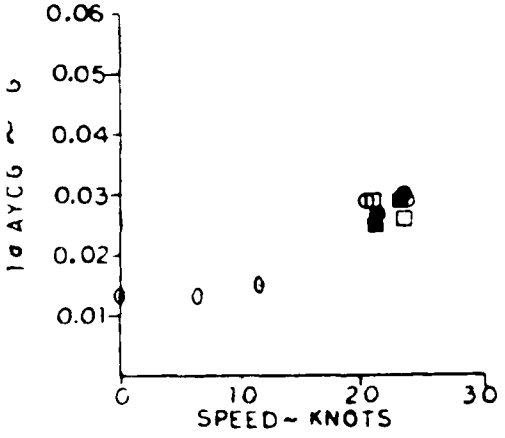

SEA STATE III MOTIONS
FOLLOWING SEAS

LIFT RPM	SYMBOL	RCS
1900	○	● ON
1700	□	○ OFF
1500	△	
1300	◇	
000	0	

MISSION 34

FIGURE 8-28

The off-cushion vertical accelerations also exhibit the expected speed dependency and are again higher at the bow and stern than at the LCG. The off-cushion data as functions of speed appear to form consistent curves with the on-cushion data. This is coincidental.

The longitudinal and lateral accelerations are also comparable to the Sea State II data.

The pitch and roll angles are now of considerably larger amplitude than for Sea State II. The standard deviations are around one degree on-cushion and slightly less off-cushion. No consistent trend with either fan speed or craft speed (remembering the small range of speeds represented on-cushion) is apparent. Part of the increase from the Sea State II conditions is probably due to the lower encounter frequencies in the larger waves yielding larger excitations near the pitch and roll natural frequencies (both near 0.3 Hz). The significant roll amplitude in this (ideally) symmetrical condition is again notable.

The comparable magnitudes of the on- and off-cushion angular excursions is not surprising since these motions are dominated by sidehull buoyancy effects.

8.4.3.1.2 Bow Seas

Figure 8-25 shows the standard deviations for the bow sea condition. The results are very comparable to the head sea case with the vertical accelerations now being slightly less except at the stern.

8.4.3.1.3 Beam Seas

Figure 8-26 presents the standard deviations for the beam sea condition. Vertical acceleration levels at the bow and at the LCG are markedly lower than for the head sea case, particularly the bow accelerations. The stern vertical accelerations are not reduced nearly so much. The heave and pitch motions in beam seas appear to be phased such that the combined motion is greatest at the stern.

The axial acceleration data for M-35 are comparable to and slightly lower than the head sea data (which was all for M-35). However, the data for M-44 indicate higher values. The reason for the difference between the two missions is not known.

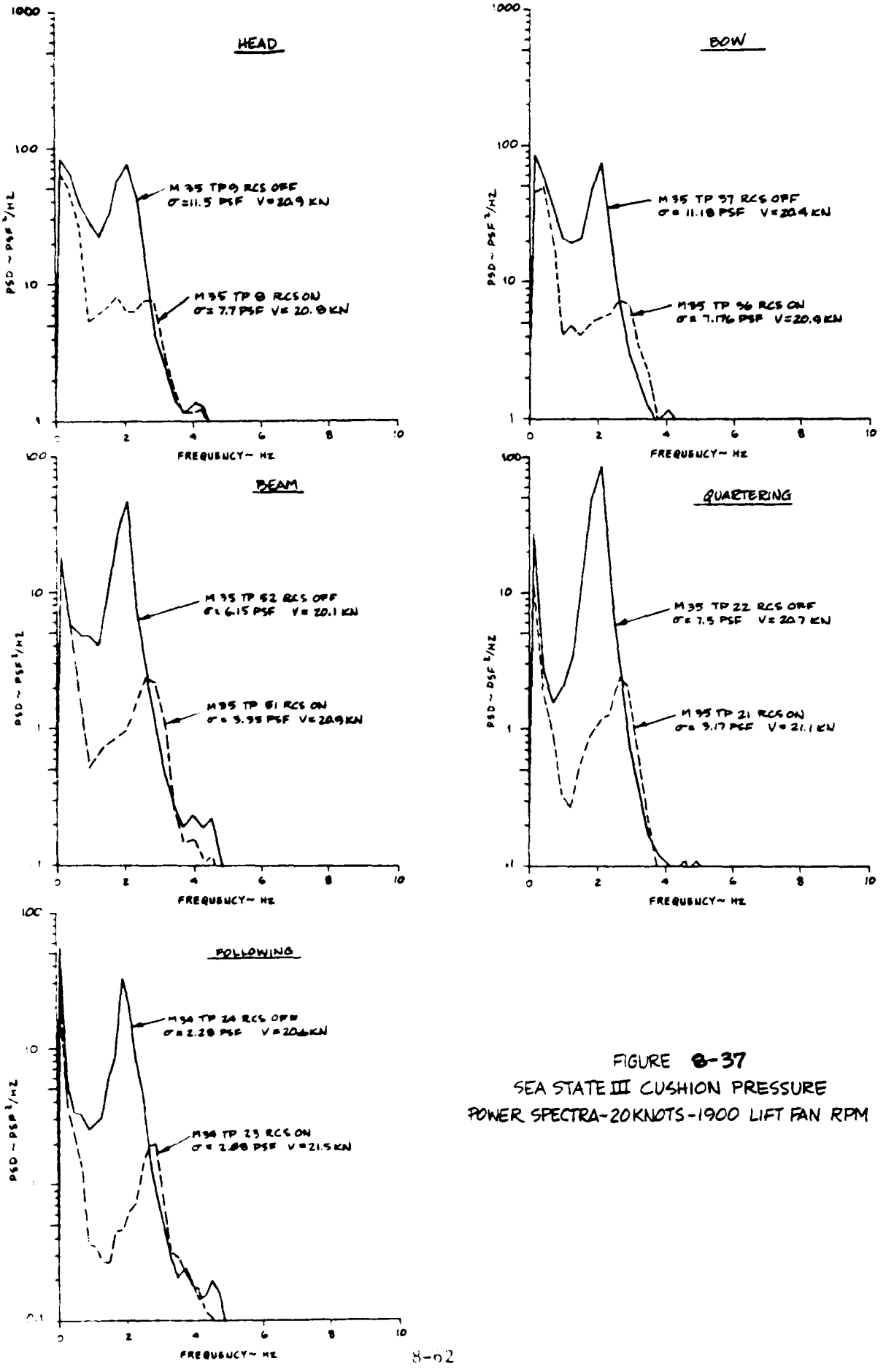

FIGURE 8-37
SEA STATE III CUSHION PRESSURE
POWER SPECTRA-20 KNOTS-1900 LIFT FAN RPM

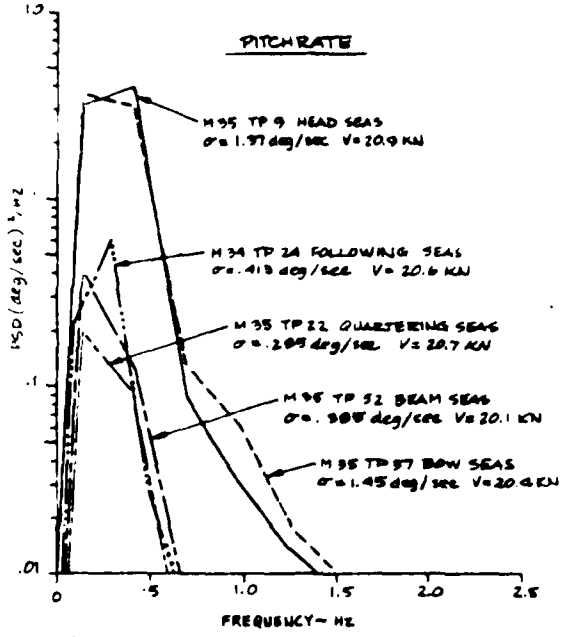

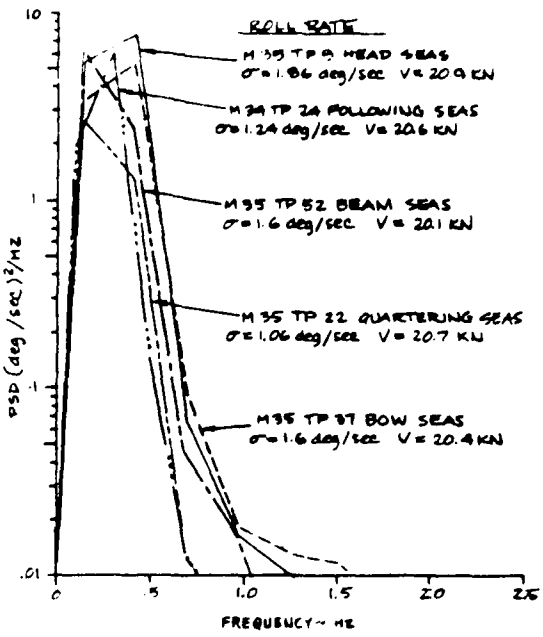

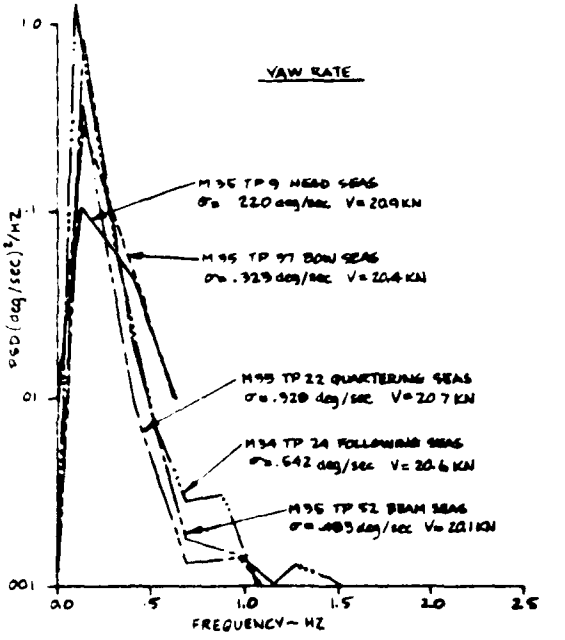

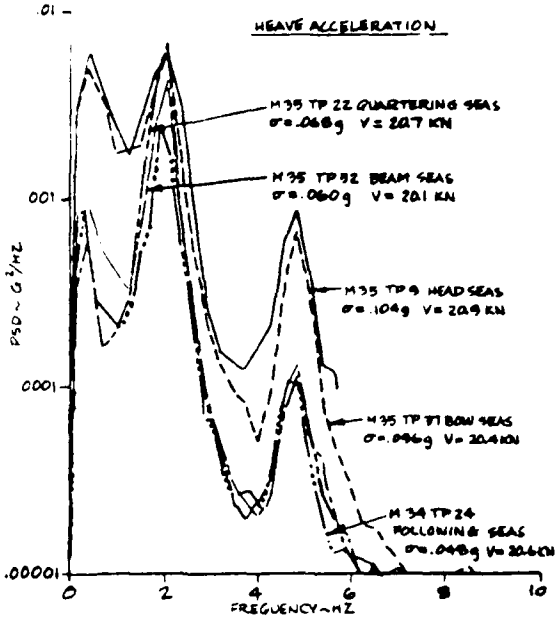

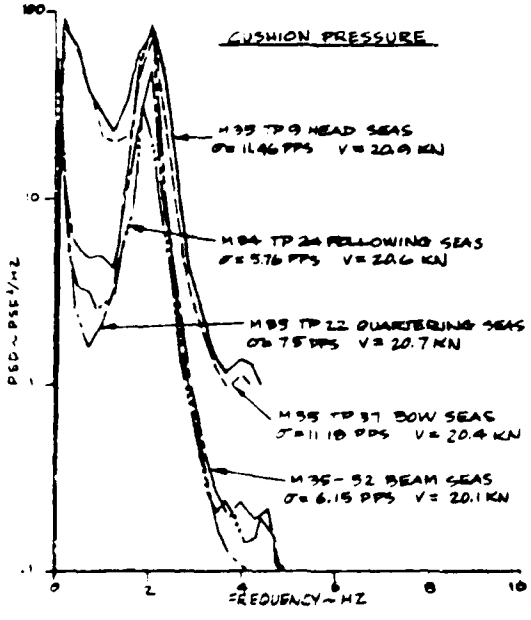

FIGURE 8-36
SEA STATE III POWER SPECTRA
20 KNOTS - 1900 LIFT FAN RPM
RCS-OFF

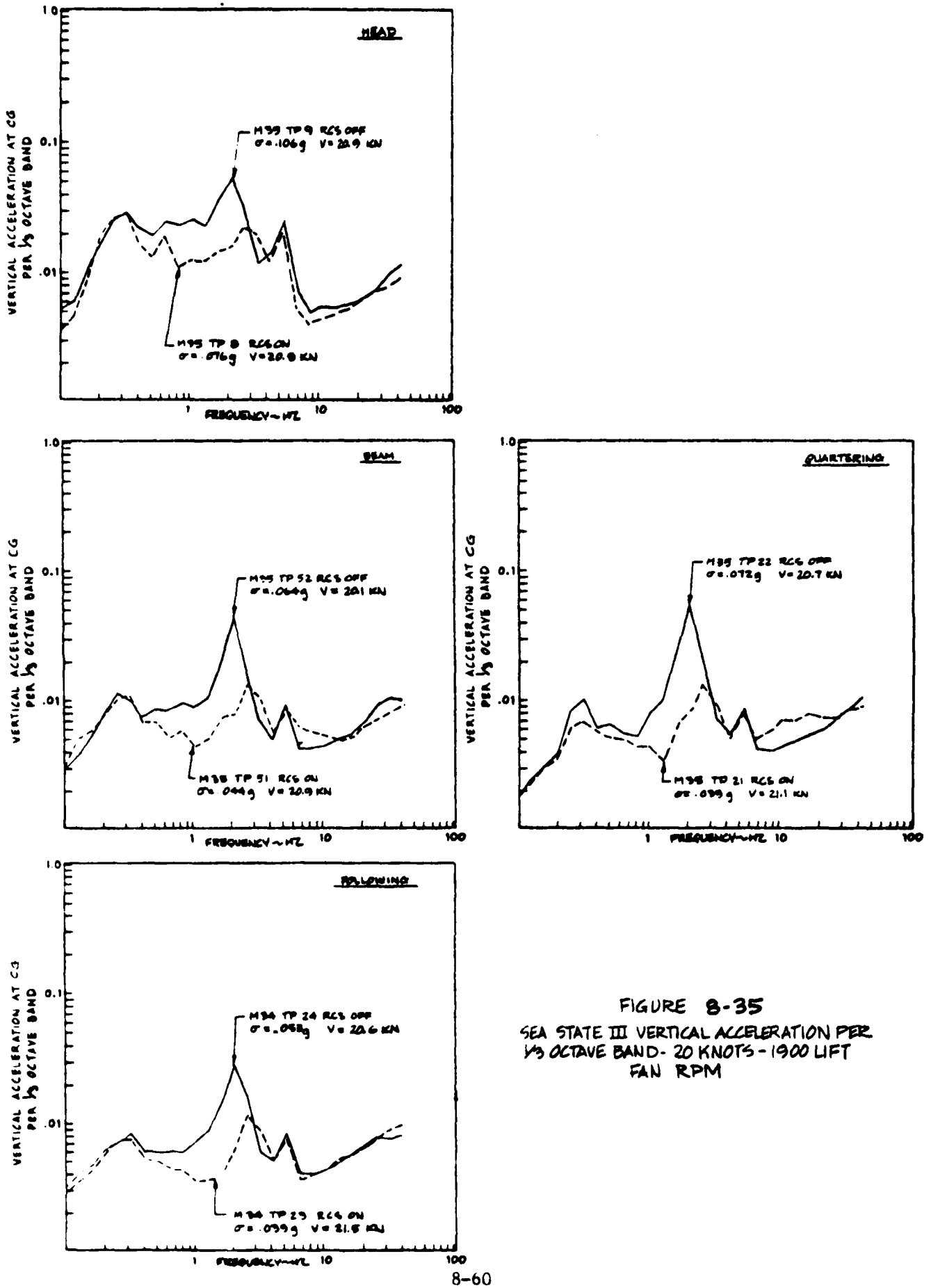

FIGURE 8-35

SEA STATE III VERTICAL ACCELERATION PER 1/3 OCTAVE BAND - 20 KNOTS - 1900 LIFT FAN RPM

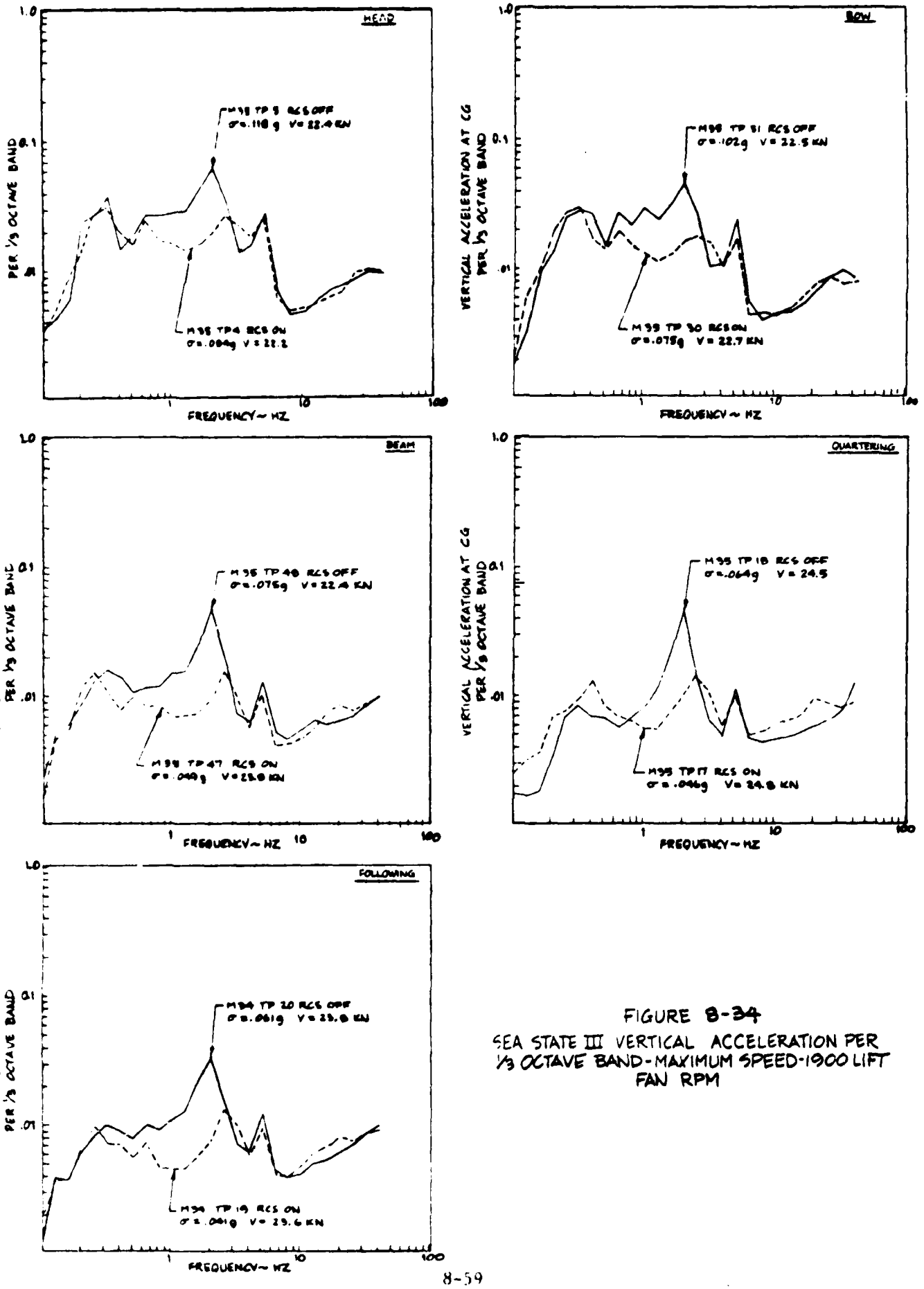

FIGURE 8-34

SEA STATE III VERTICAL ACCELERATION PER 1/3 OCTAVE BAND-MAXIMUM SPEED-1900 LIFT FAN RPM

Figure 8-33 presents the corresponding data for the nominal 20 kn speed. Note that the bow sea data are absent from these plots. The tendency for the beam to following sea cases to group together is still apparent here, but now they tend to spread out near the heave frequency and also below the pitch frequency with little spreading between 0.3 and 1 Hz. At the heave frequency, the responses for quartering seas are as large as for head seas with following and beam seas giving progressively lower values. Below the pitch frequency, the order in lessening effects is the same as for the maximum speed case.

For the head sea case, the 1/3-octave band data differ but little between 20 kn and maximum speed. Of course, maximum speed is not much greater than 20 kn for this case. For the beam to following sea cases, the levels in the 20 kn case are distinctly lower than for maximum speed. The differences here are more apparent than for the head seas, at least in part, because the speed changes from maximum speed are somewhat larger.

The benefits gained in terms of ride improvement by avoiding the head and bow sea conditions are quite apparent in Figures 8-32 and 8-33. The quite large reduction around and below 1 Hz is particularly helpful.

8.4.4.2 RCS Effects

Figures 8-34 and 8-35 show the effects of the RCS on the 1/3-octave band vertical accelerations. The data are for the 1900 fan rpm case. RCS-on and -off conditions are compared for each heading.

For the maximum speed case (Figure 8-34), it is clear that the RCS acts primarily to reduce the acceleration levels around the heave natural frequency. The reductions are mostly in the 0.8 to 2.5 or 3 Hz range. The resultant RCS-on curves are relatively flat from 0.3 to 5 Hz. There is little effect on the 5 Hz bending mode peak.

As shown on Figure 8-35, the results at 20 kn are similar. At this speed, however, the attenuation of the accelerations is greater at and below 1 Hz and the effects extend to lower frequencies (down to the 0.3 Hz pitch mode).

Overall, a considerable improvement in the ride is indicated for use of the RCS.

8.4.5 Power Spectra

The power spectra for Sea State III are presented in Figures 8-36 through 8-38. The data shown are all for the nominal 20 kn speed and 1900 fan rpm. The spectra are obtained from test points of 3 minute duration and are processed to a resolution bandwidth of 0.27 Hz giving a sampling error standard deviation of 14.1% of the estimated spectral amplitude.

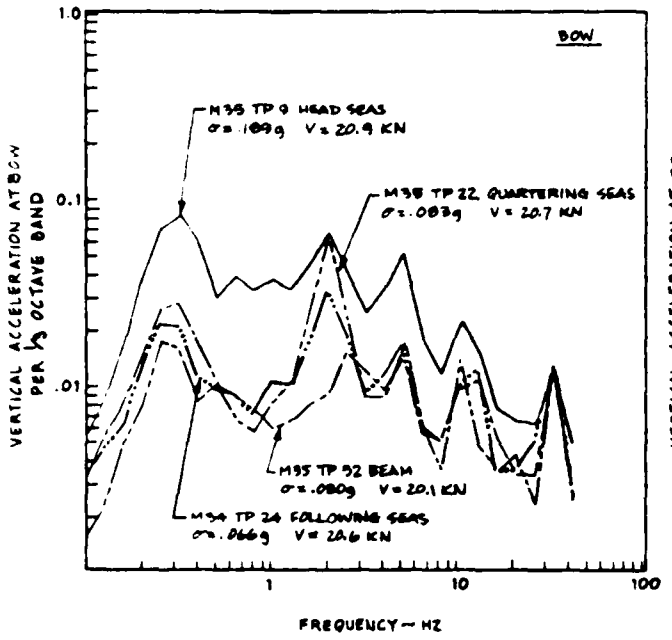

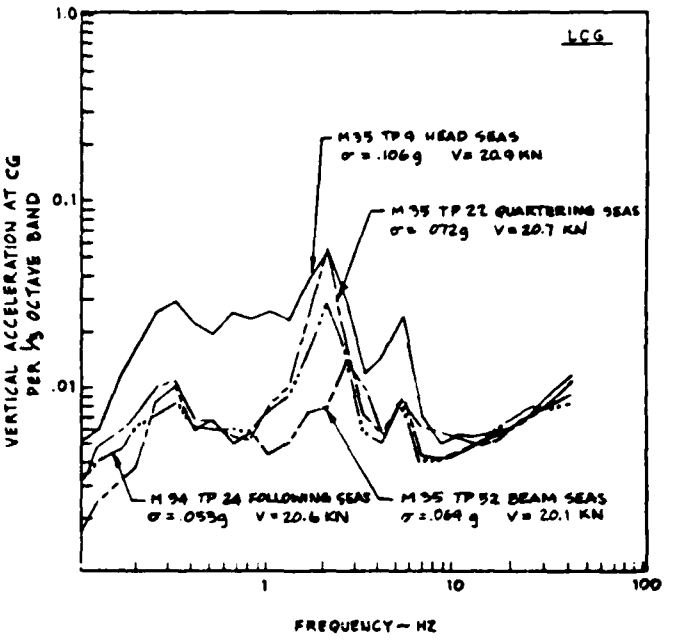

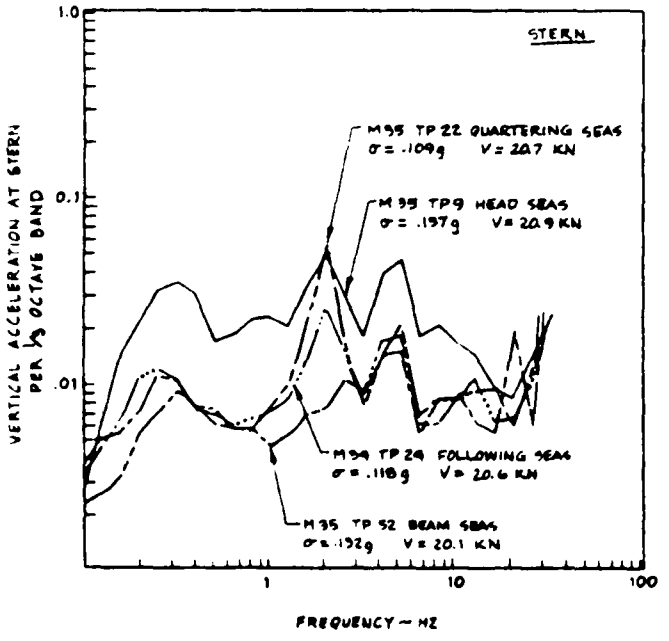

FIGURE 8-33
SEA STATE III VERTICAL ACCELERATION
PER 1/3 OCTAVE BAND- 20 KNOTS
1900 LIFT FAN RPM- RCS OFF

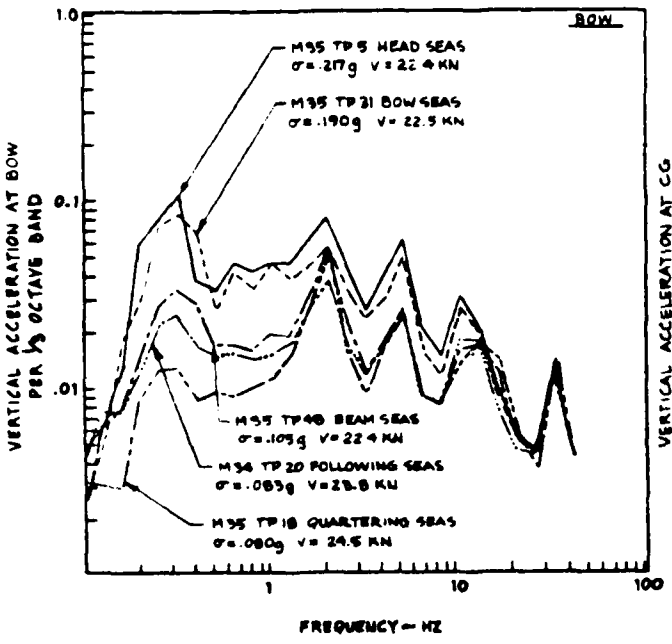

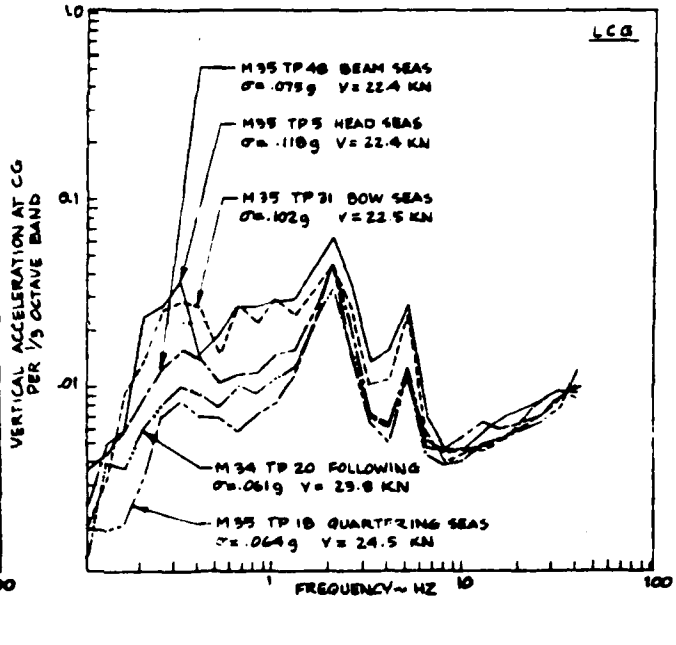

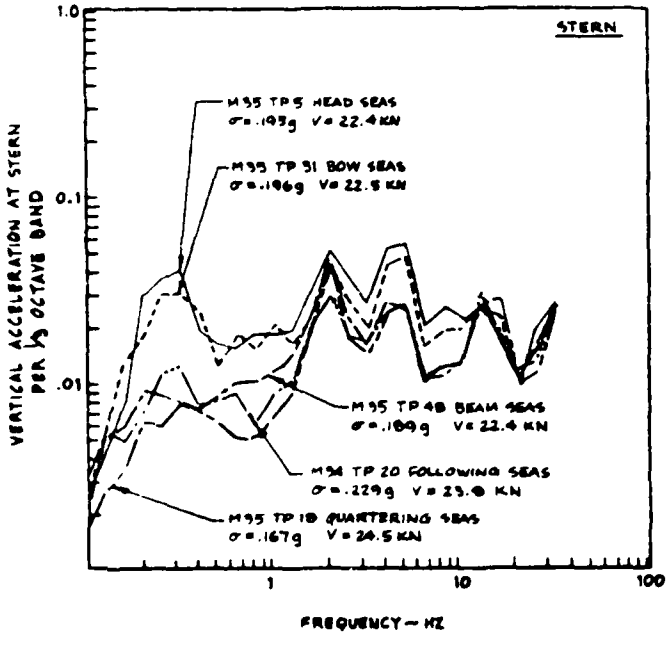

FIGURE 8-32
SEA STATE III VERTICAL ACCELERATION PER 1/3 OCTAVE BAND - MAXIMUM SPEED 1900 LIFT FAN RPM - RCS-OFF

Figure 8-14 shows the RCS effects in Sea State II to increase percentagewise as the RCS-off standard deviations increase. This is not the case in Sea State III. This can be taken as an indication that we are now being limited by the available fan airflow; if more flow were available to modulate with the RCS, greater RCS effectiveness could probably be achieved. This is also the likely reason that 1900 fan rpm was felt to give better results in Sea State III than the 1700 rpm found best for Sea State II.

The correlation of speed at fixed throttle setting again shows no significant effect of RCS operation. As for the lower sea states, this is probably due to the RCS action decreasing the magnitudes of the excursions in sidehull wetting. This, in turn, decreases the effect of the non-linear sidehull broaching tending to increase the average wetted area (see Section 8.2.3).

8.4.4 1/3-Octave Band Acceleration Data

8.4.4.1 RCS-Off Data

The 1/3-octave band data for vertical accelerations with the RCS off are shown on Figures 8-32 and 8-33. The data shown are all for on-cushion operation with 1900 fan rpm (which is judged to give the best ride in this sea state). Separate plots are given for accelerations at the bow, the LCG and the stern. Data for all headings are given on each plot.

The data for maximum speed are shown on Figure 8-32. A number of distinct, identifiable peaks are apparent in these curves. The peak near 0.3 Hz is due to the pitch mode resonance. The 2 Hz heave mode is clearly displayed in all the curves as is the first longitudinal bending mode at 5 Hz. For the bow and stern accelerations, there are additional peaks between 10 and 11 Hz and between 20 and 30 Hz. These are most likely acoustic modes.

The data tend to fall into two groups. The head and bow sea cases tend to be close together at all frequencies with the bow acceleration levels slightly lower. The data for the other headings tend to group together with beam, quartering and following seas giving about the same results beyond the heave frequency. At the heave frequency, the beam seas have lower acceleration levels than the other headings. For lower frequencies, the curves tend to spread somewhat with beam, following and quartering seas giving successively lower values. The quartering seas giving a consistently better ride than the following seas may be associated with the encounter frequencies for following seas giving more excitation around the pitch natural frequency than for quartering seas.

The LCG accelerations are dominated by the peak at the heave natural frequency. The bow and stern accelerations are more heavily influenced by pitch motions as would be expected. Also, the 5 Hz bending mode is more influential at the bow and stern as expected.

FIGURE 8-31

SEA STATE III EFFECT OF RCS ON HEAVE ACCELLERATION, CUSHION PRESSURE AND SHIP SPEED

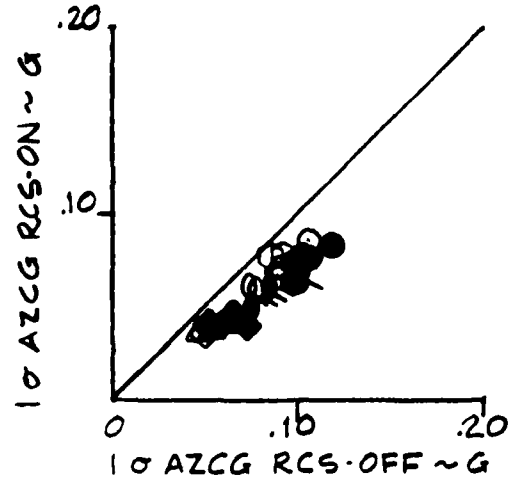

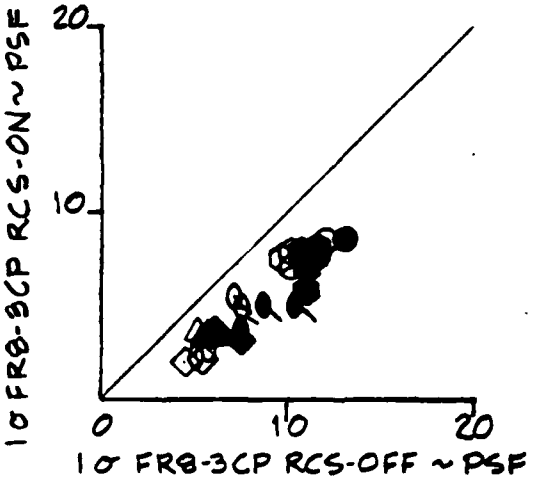

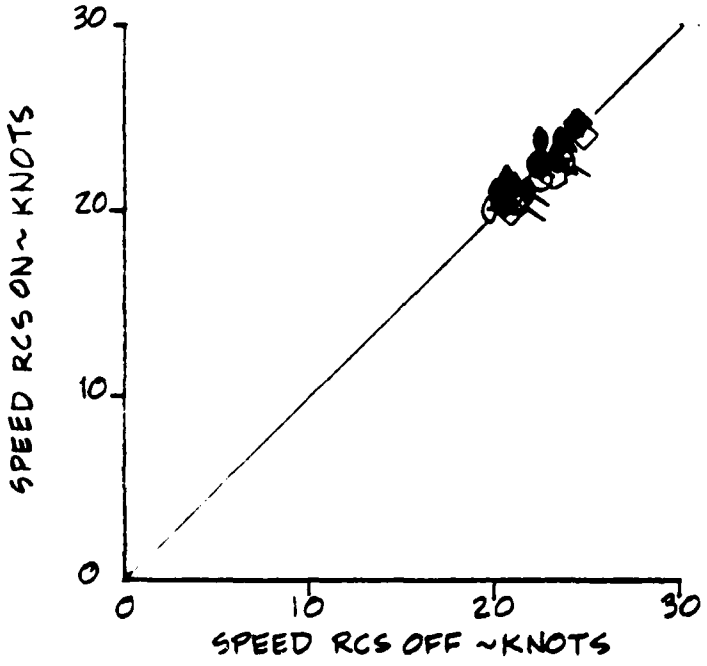

- ● 1900 LIFT RPM
- ○ 1700 LIFT RPM

- ○ HEAD SEAS
- ⬡ BOW SEAS
- ⬯ BEAM SEAS
- ◇ QUARTERING SEAS
- △ FOLLOWING SEAS – (MISSION 34 ONLY)
- ○ MISSION 35
- Q MISSION 44

8.4.3.2.2 Nominal 20 kn Conditions

Figure 8-30 presents the results for the nominal 20 kn speed. These data are quite similar to those for the maximum speed case.

The pitch data are about the same as in Figure 8-29 except the head sea responses are a bit lower and are now about the same as for the bow seas.

The roll data display the same general character as for maximum speed, but now there is an indication that the following sea standard deviations may actually be somewhat larger than those for the quartering seas. The same situation applies to the lateral accelerations.

The LCG vertical acceleration levels are about the same as for maximum speed, but now indicate a minimum for the beam sea condition. This would not be unreasonable.

The axial accelerations are also about the same as for maximum speed, but do not display such severe scatter at the beam sea condition as was shown on Figure 8-29.

8.4.3.3 RCS Effects

The effects of the RCS on the standard deviations is best seen on Figure 8-31 where we have again plotted the RCS-on data versus the RCS-off data for the same condition. Considering the variety of conditions covered on these plots and the different disturbance spectra which the RCS faces for these conditions, the strong tendency for the data to collapse to a single curve for each plot seems rather remarkable for such a simple correlation.

The RCS effect in reducing both the LCG vertical accelerations and the cushion pressures appears to be somewhat greater with 1900 fan rpm than with 1700. 1900 rpm is generally considered the best fan speed for this sea state (at least at and above 20 kn). As was the case for Sea States I and II, the acceleration level reductions are somewhat less than the reductions in cushion pressure excursions.

For the highest acceleration case (maximum speed in head seas at 1900 rpm), the LCG vertical acceleration standard deviation is reduced by about 30% of the RCS-off values while the cushion pressure standard deviations are reduced by about 35% of the RCS-off values. For cases having lower RCS-off levels, however, the cushion pressures are reduced by a larger percentage while the percentage reduction of the accelerations seems to be roughly constant. The rms vertical acceleration levels are reduced to less than 0.1 g by use of the RCS; this level is sufficiently low to permit long term operations without excessive fatigue and performance degradation on the part of the crew. The reductions achieved are very worthwhile.

The variation of roll amplitudes with heading is more difficult to understand in that the nominally symmetric head and following sea conditions give about the same roll angle standard deviations as do the quartering and bow sea conditions. We have commented in Sections 8.2 and 8.3 that some appreciable amplitude in roll in head and following seas is not surprising. It probably arises due to the short crested nature of ocean waves. Additionally, at times during testing a long period swell was observed coming from a different direction than the wind generated sea. However, this does not explain why the distinctly asymmetrical conditions of quartering and bow seas produces no greater amplitudes. We do, of course, find a much larger response in the beam sea condition, but the narrow range of heading angles over which additional roll perturbations occur is rather surprising.

The SES-200's pitch and roll periods are quite close together at around 0.3 Hz for cushionborne operation. This definitely promotes coupling between the modes, particularly in short crested sea conditions. On board observations in Sea State III suggest that, while the roll amplitudes are small, the roll damping is also low cushionborne and the ship rolls mostly at its natural roll period. The fact that the amplitudes are not significantly greater in the asymmetrical sea conditions may be due to the fact that these seas do not produce significantly greater excitation forces than were present during head sea operation. This is possible since the roll period is considerably higher than the period of maximum energy of the encountered sea spectrum, i.e., the SES-200 does not develop syncronous rolling with the waves.

The vertical accelerations at the LCG behave much as would be expected. The greatest excursions occur in the head sea case where the encounter frequencies yield greater input spectral components near the 2 Hz heave natural frequency. As the heading falls off from head seas, the acceleration levels decrease. They are relatively insensitive to heading over the range from following to beam seas.

The axial acceleration standard deviations display a similar trend but are much less sensitive to heading. There is also considerable scatter in the data for the beam sea cases. It is noted that there is a distinct tendency for the M-44 points to exhibit large standard deviations here. However, M-44 on-cushion test points were run only in beam seas and most of the beam sea data are from that mission. Therefore, it is not known whether the scatter is associated with the beam sea condition or is somehow peculiar to the M-44 test conditions.

The lateral acceleration data are similar to the roll data except that the (suspect) peak at the beam sea heading is less pronounced. Again, the lack of increased response at bow and quartering seas relative to head and following seas has not been explained.

In addition to the standard deviations, we have also shown the craft speed as a function of heading. As might be expected, the maximum speed is higher for following and quartering seas and decreases as the heading approaches the head sea condition.

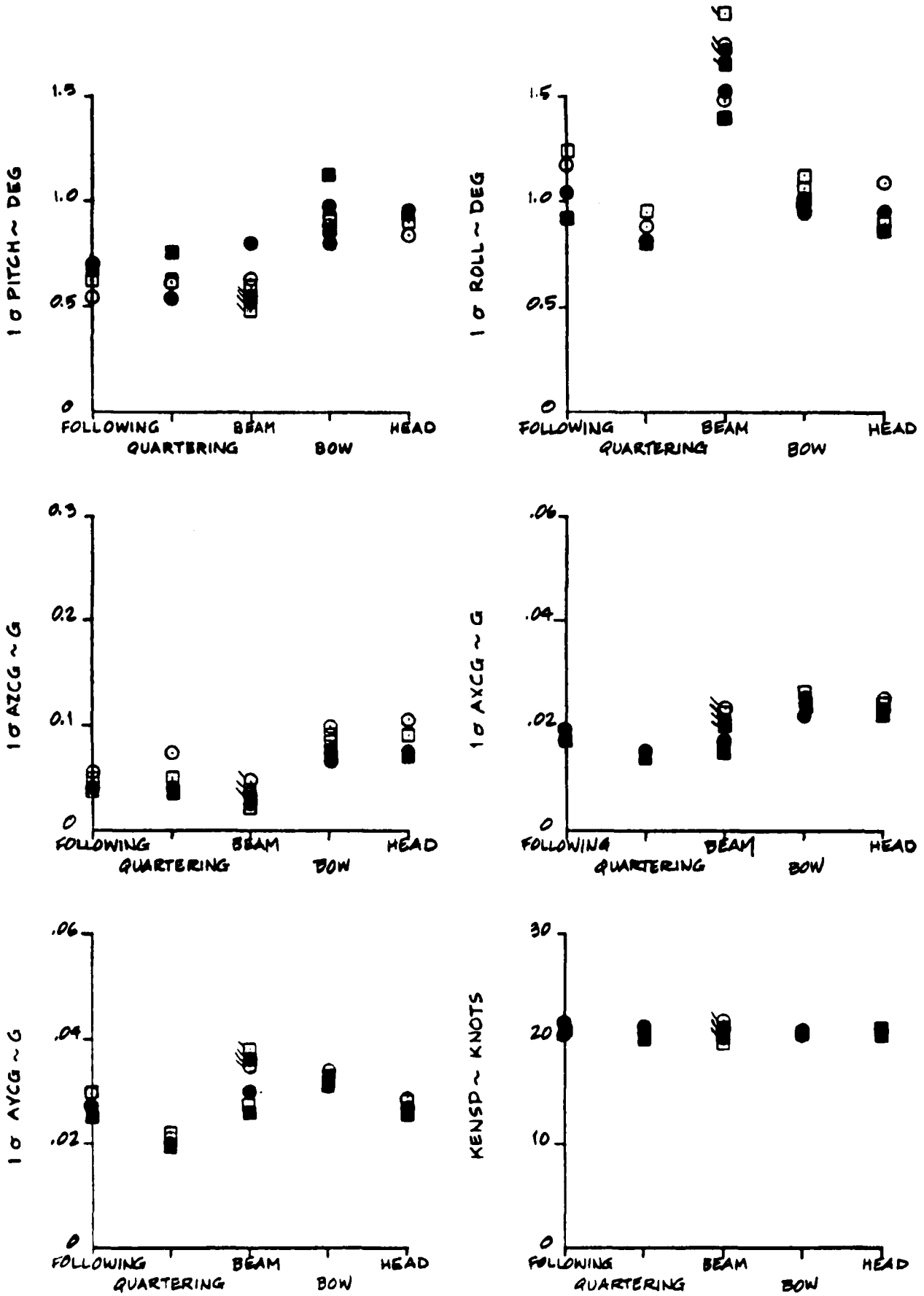

FIGURE 8-30 SEA STATE III EFFECT OF HEADING ON MOTIONS - 20 KNOTS

○ MISSION 35 ○ 1900 LIFT RPM ● RCS ON
○ MISSION 44 □ 1700 LIFT RPM ○ RCS OFF
○ MISSION 34 (FOLLOWING SEAS ONLY)

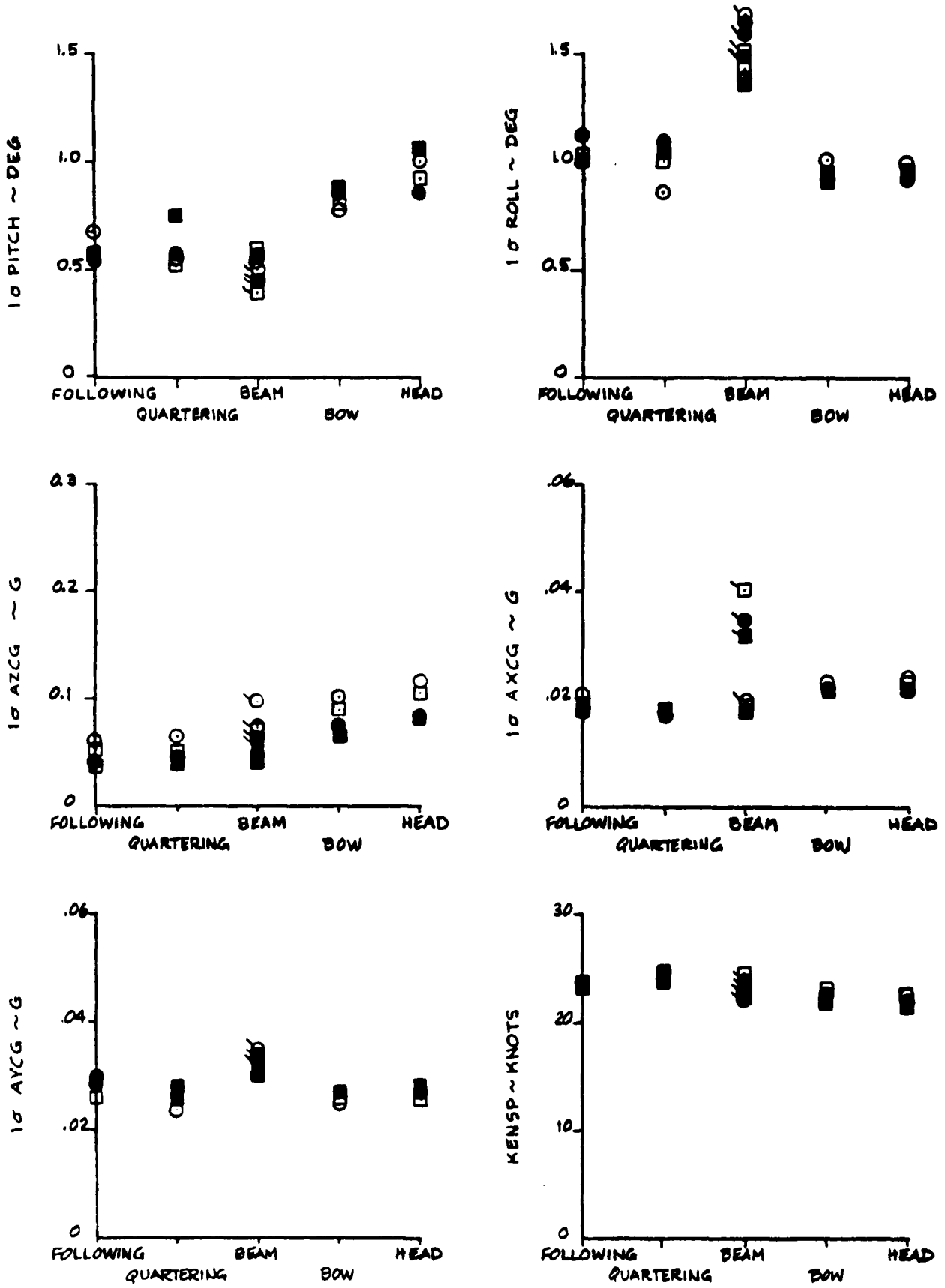

FIGURE 8-29 SEA STATE III EFFECT OF HEADING ON MOTIONS - MAX SPEED

○ MISSION 35 ○ 1900 LIFT RPM ● RCS ON
○ MISSION 44 □ 1700 LIFT RPM ○ RCS OFF
○ MISSION 54 (FOLLOWING SEAS ONLY)

The on-cushion roll standard deviations are about 50% greater than the head and bow sea values. The off-cushion values are comparable to the head seas data. This difference between on- and off-cushion results may be due in part to the lower roll damping associated with the on-cushion operation. With the larger sidehull immersion in the off-cushion case, the sidehulls (due primarily to the component of lateral velocity induced by roll rates) are capable of producing somewhat more hydrodynamic damping moments.

The pitch angle standard deviations are on the order of half those for the head sea case. This is as expected since the beam seas can produce very little in the way of pitch moments.

8.4.3.1.4 Quartering Seas

The standard deviations for quartering seas are shown on Figure 8-47. These data are very similar to the M-35 data for beam seas. The principal differences are the lower roll amplitudes for quartering seas and the slightly lower lateral accelerations. The roll angles for this condition are comparable to those for the head and bow sea case.

For the off-cushion data, the M-44 data indicate higher pitch angle amplitudes and lower roll angle amplitudes.

8.4.3.1.5 Following Seas

The standard deviation data for following seas (Figure 8-28) are much like the M-35 data for quartering seas. The principal difference is the higher values for stern accelerations at maximum speed. Stern accelerations appear to increase very rapidly with increasing speed. In fact, the maximum speed stern acceleration levels are appreciably higher in this condition than for the head sea case (Figure 8-24), whereas the bow and LCG vertical accelerations are considerably lower. No similar trend was observed in Sea State II (see Figures 8-12 and 8-13). The explanation for this is not readily apparent.

8.4.3.2 Standard Deviations as Functions of Heading

The standard deviations are plotted versus relative wave heading on Figures 8-29 and 8-30. On-cushion data points only are presented.

8.4.3.2.1 Maximum Speed Conditions

Figure 8-29 shows the results at maximum speed. The pitch angle data are about as expected. The pitch amplitudes decrease somewhat as we move from following to beam seas, then increase as we progress to the head sea case. The head seas give the largest pitch motions.

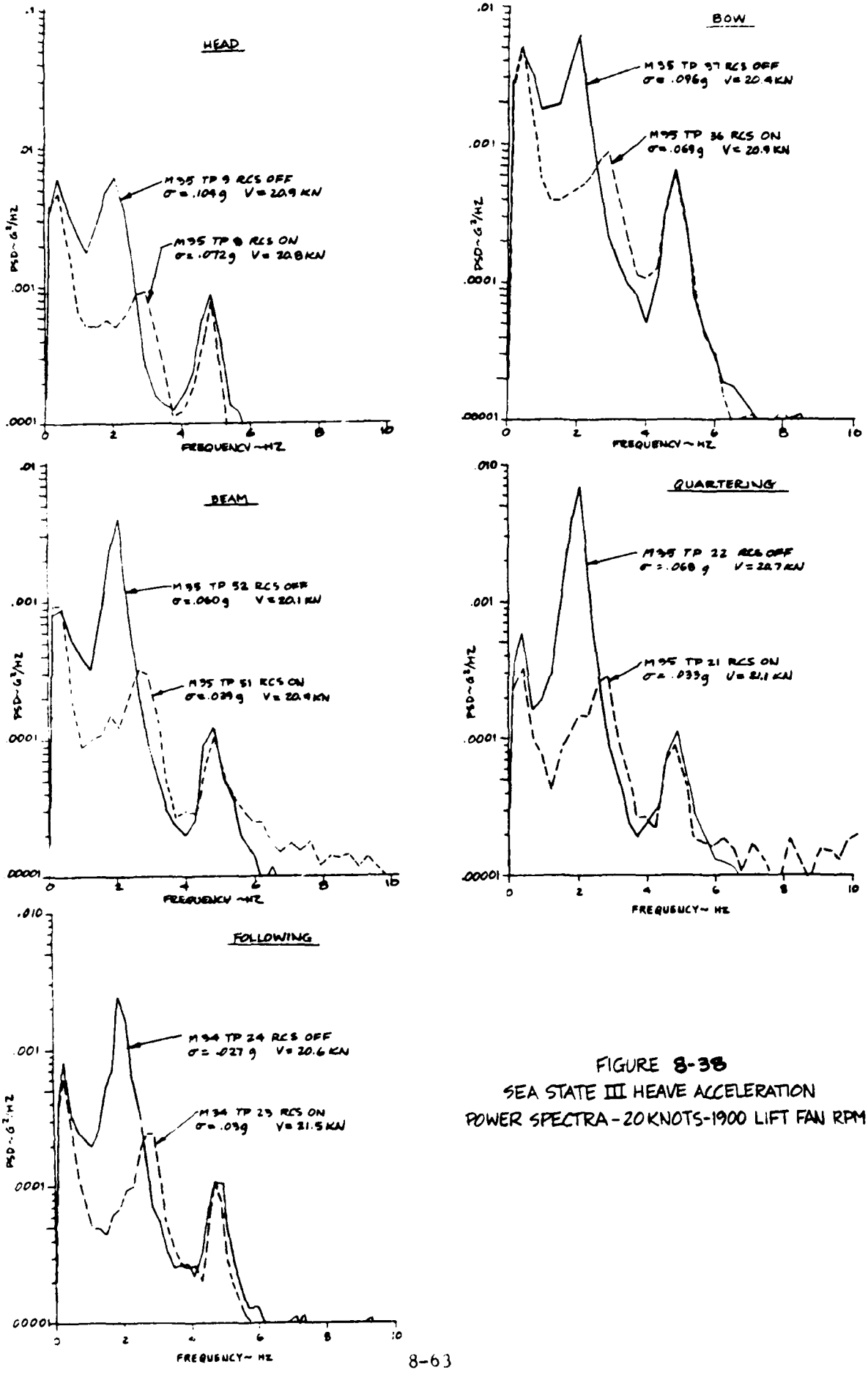

FIGURE 8-38
SEA STATE III HEAVE ACCELERATION
POWER SPECTRA - 20 KNOTS - 1900 LIFT FAN RPM

Figure 8-36 presents the RCS-off spectra for the angular rates, the cushion pressure and the LCG vertical accelerations. The pitch natural frequency is about 0.3 Hz and the concentration of the pitch rate spectral power near this frequency is evident from the figure. The pitch rate spectra are considerably higher for head and bow seas than for the other headings. This is in agreement with the pitch amplitude standard deviation data of Figure 8-30. The apparently wider bandwidth for head and bow seas is probably due to the cut-off level of the plot, leaving only the peaks for the other headings. The standard deviations are indicated on the plots. It may be noted that a simplistic effective bandwidth computation of dividing the pitch rate standard deviation by the pitch amplitude standard deviations from Figure 8-30 would indicate a bandwidth of 1.5 or 2 rad/sec. (around 0.2 or 0.3 Hz) confirming that the spectral contributions from frequencies much exceeding the pitch natural frequency are of inconsequential total power.

The roll rate spectra are similar in shape to the pitch rate spectra. The roll natural frequency is also in the neighborhood of 0.3 Hz as previously discussed. At first glance, the roll rate spectra appear suspect in that the head sea spectrum is higher than the beam sea spectrum. This is a coincidence. Only a few roll spectra were produced during the data reduction process. It turned out that the one selected for head seas had a higher standard deviation than any of the other head sea test points by 25%, indicating it was probably not the most representative test. Likewise, the spectra reduced for the beam sea case had a lower standard deviation than most of the other 20 knot beam sea runs. This choice of test conditions makes for a rather poor comparison; unfortunately, it was unavoidable as the spectra had to be requested at the same time that the data were digitized.

The yaw rate spectra tend to peak sharply at frequencies near 0.2 Hz in following seas. As the heading is progressively changed from following to head seas, the spectral peak becomes lower and, at least for head and bow seas, the spectrum tends to broaden. The highest yaw rate standard deviations occur in following seas -- a condition where it is common to have some difficulty holding a constant heading. The standard deviation drops somewhat in going to quartering seas, is higher again for beam seas, and decreases progressively through bow and head seas. This all appears reasonable.

The heave acceleration data again clearly display peaks due to the pitch and heave modes (0.3 and 2 Hz) and the first longitudinal bending mode (5 Hz). The data are similar to the Sea State II data (Figures 8-19 and 8-20) except that the pitch mode is more prominent here and the reduction in the heave mode peak in going from head to following seas is less pronounced. The behavior of the pitch mode peak with heading conforms to the pitch rate spectra behavior. This corroborates that this low frequency peak is indeed due to pitch motions. The behavior of the spectra near the bending frequency is similar to the pitch mode characteristics in that the head and bow sea conditions give large responses, while the data for the other headings tend to group together at substantially lower levels.

The cushion pressure spectra also display the peaks at the pitch and heave natural frequencies but, as in lower sea states, show no evidence of appreciable response at the bending frequency due to the small cushion volume changes associated with the mode shape. Note that there is an indication (also evident in the Sea State I and II data, see Figures 8-9, 8-19 and 8-20) of a small peak around 4.1 Hz. This has been identified as an acoustic mode; it does not influence the vertical accelerations much because it is an antisymmetrical mode, i.e., the two ends of the cushion are 180 degrees out of phase.

Figure 8-37 shows the effects of the RCS on the cushion pressure power spectra. As in the lower sea states, the RCS primarily acts to reduce the pressure excursions in a range of frequencies around the heave mode natural frequency, i.e., from about 0.3 to 2.5 Hz. There is now a very slight tendency to increase the pressure oscillations in a narrow frequency band of about 3 to 3.5 Hz; this effect was not consistently displayed in the data for lower sea states.

While the RCS is a cushion pressure feedback system and, therefore, the direct effects are most evident in the cushion pressure spectra, the true purpose of the RCS is to reduce the vertical acceleration levels. The effect on the vertical accelerations is shown on Figure 8-38. The effective bandwidth of the RCS found in the cushion pressure data is again evident here as is the tendency to amplify rather than attenuate in the 3 to 3.5 Hz range (though this range appears to extend more nearly to 4 Hz here). As was the case in lower sea states, the RCS has little effect on the bending mode responses. For the beam and quartering sea cases, there is also a tendency for the RCS to amplify at frequencies above 6 Hz. Reference to the 1/3-octave data (Figure 8-35), which extend to higher frequencies, shows that this effect is reversed at higher frequencies. This effect was not seen in the lower sea state data, but those data were only for head and following sea cases.

The general level of effectiveness of the RCS (both as shown in detail in the power spectra and 1/3-octave band data and as shown more grossly in the standard deviation data) in Sea State III is quite beneficial to the ride and habitability.

8.5 SEA STATE IV MOTIONS

8.5.1 Test Conditions

One mission (M-38) was run in Sea State IV. This was conducted for a heavy ship condition with the gross weight varying from 190.1 to 197.3 L.T. and the LCG between -1.5 and -1.7 ft. The tests were run approximately 30 n.m. east of the Chesapeake Bay Light, i.e., in the ocean but considerably closer to shore than the Sea State III tests conducted in the vicinity of the NOAA buoy.

Tests were conducted from following to head seas in 45 degree increments. All tests were done on-cushion at 1900 fan rpm. Only maximum speed runs were made since the maximum speed was about 20 kn., so no separate runs at this nominal speed were needed.

Test points of 5 minute duration were employed for the motions data. Longer data segments were employed to obtain wave data (see Section 8.5.2).

To properly evaluate the RCS effects, the test sequence of RCS-off, RCS-on, RCS-off was again generally employed.

8.5.2 Wave Measurements

Wave measurements were obtained from the boom-mounted TRT radar altimeter corrected for craft motions using vertical accelerometer mounted at the altimeter location. The Waverider buoy was not employed due to difficulties in deploying and retrieving the buoy.

The wave data were processed over a sequence of test points run at one heading. The wave data were gathered both during and between the testpoint data segments to produce a reasonably long data sample for the wave data processing.

The significant wave heights are listed in the following table.

TABLE 8-1 SEA STATE IV SIGNIFICANT WAVE HEIGHTS

Heading	Duration (Min.)	Test Points	Significant Wave Height (ft)
Head	26	1-7	6.3
Bow	10	18,19	5.5
Beam	16	14-16	7.1
Quartering	15	11-13	8.7
Following	16	8-10	5.8

The wave heights are rather more variable from one condition to another than were those for lower sea states. Some of this may be due to the generally shorter data segments employed and to the use of the boom-mounted altimeter data. However, much of the spread is certainly due to actual changes in the seaway.

The mission was conducted just after a storm, so the seaway was in a somewhat transient state. Also, unlike the situation for lower sea states, the sea was quite confused.

The particularly large wave heights for quartering and beam seas should be noted as they affect the interpretation of the motions data given in the following section. The measured wave heights generally cover the full range of Sea State IV; the quartering sea case could actually be classified as low Sea State V.

8.5.3 Standard Deviations

The standard deviations for Sea State IV are shown as functions of relative wave heading on Figure 8-39. Both RCS-on and RCS-off data are shown. The effects of the RCS are shown more clearly on Figure 8-40 to be discussed subsequently.

The pitch data do not follow the trend shown for Sea State III (Figures 8-29 and 8-30). The Sea State IV data indicate a slight increase in pitch motions as we proceed from following to beam seas and a gradual decrease in the amplitudes as we proceed to head seas. The Sea State III data definitely indicated that head and bow seas gave the most pitch.

Part of this difference in behavior is due to the larger wave heights extant during the quartering and bow sea runs. Roughly correcting for this, it would appear that the correct behavior would be a curve that peaked around bow seas and dropped off on each side of the peak. The pitch standard deviations, allowing for a correction due to varying wave height, do not appear to vary a great deal with heading. The confused seaway in which the tests were run would account for some of this effect. Except in head seas (where there is considerable data scatter), the pitch motions are somewhat larger than in Sea State III, as would be expected.

The roll angle standard deviations do not display the sharp increase for the beam sea case shown on Figures 8-29 and 8-30 for Sea State III. This may be due in part to the confused nature of the seaway. The roll motions in Sea State IV are over 2.5 times those of Sea State III. It is worth noting that, even with this large increase, the roll motions are quite small compared to those for normal monohull ships under these conditions.

It may be noted that there is a definite indication that the RCS action tends to decrease the roll motions, particularly in quartering and beam seas. Examination of Figures 8-29 and 8-30 shows that there was also evidence of this effect in Sea State III. The reason for this is not definitely known. However, it could be due to the tendency of the RCS to decrease the mean cushion pressure somewhat and, therefore, increase the mean immersion; the increase in sidehull immersion provides an increased source of hydrodynamic damping in roll arising from sidehull sway velocity components. This effect might be more pronounced in larger waves where, due to limits of fan capacity, the immersion increase would be greater.

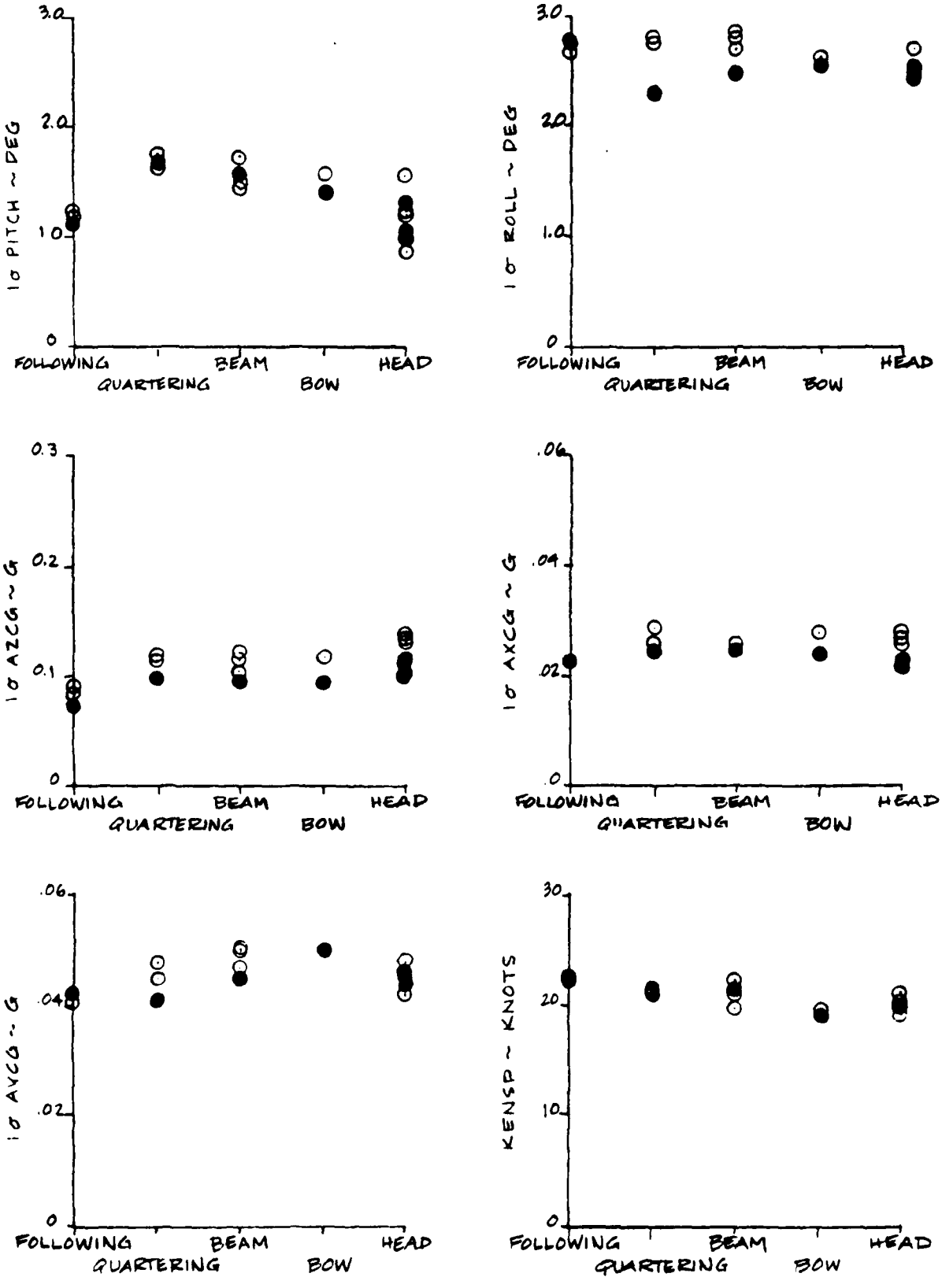

FIGURE 8-39 SEA STATE IV EFFECT OF HEADING ON MOTIONS - MAX SPEED 1900 LIFT FAN RPM

○ RCS-OFF
● RCS-ON

The vertical acceleration standard deviation data are similar to those for Sea State III but the motions are slightly larger. Head seas again give the largest acceleration levels. The resemblance to the Sea State III data is improved if one corrects the Sea State IV data for the larger wave heights in beam and quartering seas.

The axial acceleration data resemble those for Sea State III and are slightly larger. The variation with heading is even less than for Sea State III.

The lateral accelerations are over 1.5 times those of Sea State III. They are relatively insensitive to heading. The larger amplitudes for beam seas shown in the Sea State III data are not indicated here.

Also shown on Figure 8-39 are the maximum speed data. They are little affected by heading in this sea state. The maximum speed decreases slightly as we go from following to head seas.

Figure 8-40 presents the standard deviations as plots of RCS-on versus RCS-off data.

The RCS reduces the vertical acceleration levels to about 75% of the RCS-off values. This is slightly less improvement than found for Sea State III, as would be expected in view of the fan capacity limitations discussed in Section 8.4.3. As was the case in Sea State III, the accelerations are reduced by about a constant percentage rather than a percentage which increases with increasing RCS-Off values as was found in Sea States I and II.

The general level of the cushion pressure standard deviations is reduced to about 75% of the RCS-off values, i.e., the same as the accelerations. However, for head sea conditions, the reductions are to about 67% of RCS-off values; this is more in keeping with the results in lower sea states. This more pronounced effect of heading was not clearly displayed in the data for lower sea states.

The correlation of maximum speed RCS-on and -off again shows no noticeable effect of the RCS.

8.5.4 1/3-Octave Band Data

LCG vertical accelerations in Sea State IV are plotted in 1/3-octave band format in Figure 8-41. RCS-off and RCS-on conditions at full propulsion power and 1900 fan RPM are compared at each of the five (5) headings.

The data appear quite similar for all headings. This is different than the trends found in Sea State III (Figure 8-34) where the head and bow sea data were similar and showed more energy below the 2 Hz heave mode than the beam, quartering and following sea data. It is expected that this insensitivity to heading in Sea State IV is, in large part, due to the confused nature of the seas noted by the on-board observers.

FIGURE 8-40
SEA STATE IV EFFECT OF RCS ON HEAVE ACCELERATION, CUSHION PRESSURE AND SHIP SPEED MAXIMUM SPEED-1900 LIFT FAN RPM

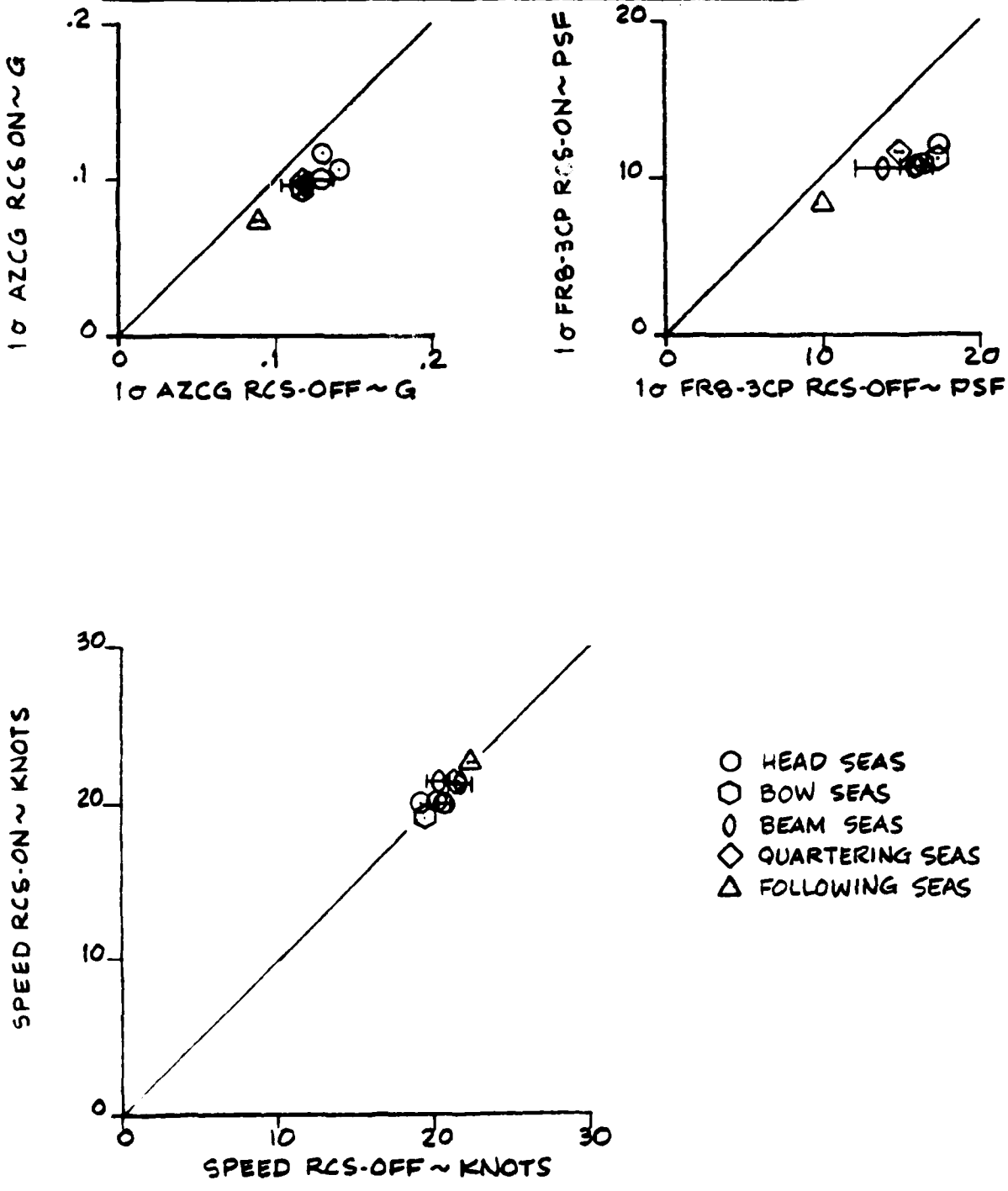

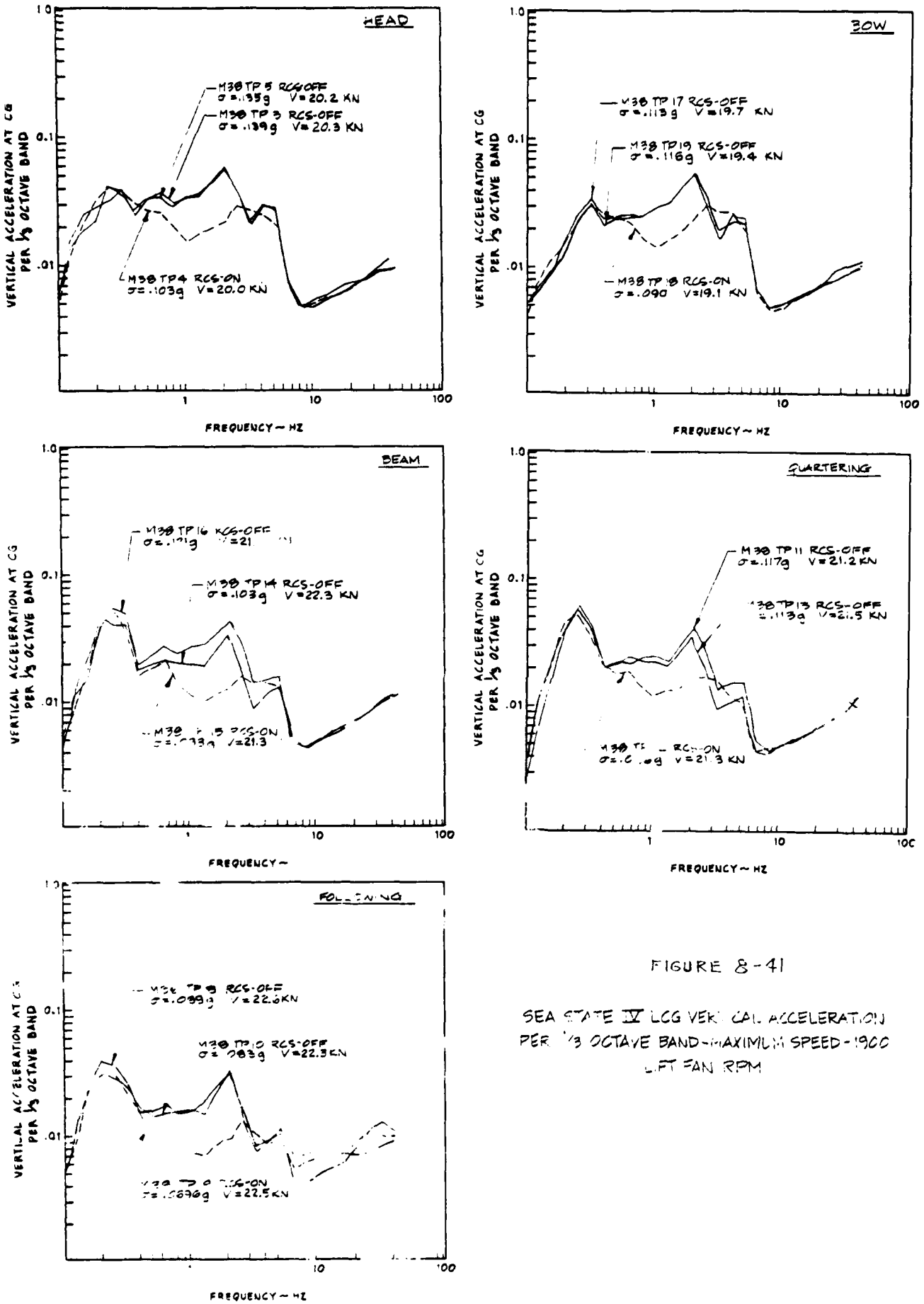

FIGURE 8-41

SEA STATE IV LCG VERTICAL ACCELERATION PER 1/3 OCTAVE BAND - MAXIMUM SPEED - 1900 LIFT FAN RPM

The RCS reduces the accelerations in the 0.8 - 2.5 Hz region around the heave natural frequency. As noted for Sea State III, the RCS effectiveness in Sea State IV is limited by the available fan flow rate; however, there is still a considerable improvement in ride quality at all headings.

8.5.5 Power Spectra

Power spectra are not presented for the Sea State IV tests.

8.6 SEA STATE V MOTIONS

One partial mission (the start of M-38) was conducted in medium-to-high Sea State V. This mission was conducted at night while loitering at about 10 kn waiting for daylight to see what kind of conditions were offered to conduct tests. As a result, the wave headings are not known. It was felt that the ship was in a bow sea condition throughout most of the night.

The gross weight was in the range 190.1 to 197.3 L.T. (heavy ship condition) and the LCG in the range of -1.5 to -1.7 ft.

Extensive data reduction (power spectra, etc.) was not attempted for this mission. Mean values and standard deviations of the greatest interest are summarized on Table 8-2. Note that, due to the sea state, the RCS was kept on during most of the mission and was off only for the last test point when the motions were less severe.

Speeds were around 10 kn and the propellers at around 2/3 speed throughout the mission. Fan speeds were nominally 1900 rpm to around 1700 rpm. The reason for this is not known; it is quite possible that the fan throttles were bumped during the night.

In comparing the standard deviation data with those for Sea State IV (Figure 8-39), it must be borne in mind that the speeds in Sea State V are about half those in Sea State IV. This is not, of course, maximum speed in Sea State V.

Except for TP-25, the pitch standard deviations are somewhat higher than in Sea State IV as would be expected due both to the larger waves and the generally reduced encounter frequencies.

For the first three test points, the roll angle standard deviations are comparable to the RCS-on data for Sea State IV. The last three test points exhibit significantly higher roll amplitudes. These standard deviations of over three degrees are appreciably higher than any previously observed values. The reason for the high values for the last three test points is not known. It is probably due to changes in the relative wave headings.

The vertical acceleration levels at the LCG are comparable to or lower than the levels for Sea State IV. This is probably due to the lower speed employed here. Again, note the decreased acceleration amplitudes for the last two test points indicating a change in relative wave heading. The bow and stern accelerations are considerably larger than those at the LCG. This reflects the contributions of the sizeable pitch motions to the accelerations.

The axial acceleration levels are comparable to those for Sea State IV, except for the last two test points which are somewhat lower. The low ship speed in Sea State V causes these levels to be lower than in a comparison at equal speeds.

TABLE 8-2

MOTIONS SUMMARY
MISSION 38 - SS V

			AVERAGE						STANDARD DEVIATION								ALT Av.1/3 High
TP -	Time Hr:Min.	RCS -	KENSP kn	*PRPMP rpm	*PRPMS rpm	**FRPMP rpm	**PRPMS rpm	FR8-3CP psf	Pitch deg.	Roll deg.	AZBOW g	AZCG g	AZSTR g	AXCG g	AYCG g	FR8-3CP psf	Wave Ht. ft
20	1:47-1:52	On	9.6	593	573	1932	1855	69.5	2.286	2.287	.242	.089	.182	.030	.033	22.306	10.0
21	2:00-2:15	On	9.3	573	551	1926	1833	69.0	2.283	2.227	.243	.093	.181	.029	.034	20.313	11.4
22	3:00-3:05	On	8.5	534	494	1922	1818	68.8	2.346	2.552	.210	.087	.164	.027	.032	19.358	No wave Data Red.
23	4:15-4:20	On	9.2	538	499	1785	1610	68.3	1.883	3.238	.181	.084	.143	.023	.034	19.441	11.3
24	5:15-5:20	On	10.4	545	501	1795	1621	75.8	2.004	3.382	.121	.065	.086	.017	.041	9.486	11.8
25	6:00-6:15	Off	10.5	554	519	1797	1623	79.3	1.618	3.083	.111	.063	.080	.016	.038	8.147	10.5

* Propeller RPM - Max. is 900.
** Fan RPM.

The lateral accelerations are considerably less than in Sea State IV except for the last two test points which are comparable to the Sea State IV data. The reduced craft speed in Sea State V contributed to the lower acceleration levels.

The trend in the cushion pressure standard deviations follows that for vertical accelerations as might be expected.

There is a general tendency observed throughout for the last two or three test points to exhibit significantly different behavior than the first three. It is strongly suspected that this may be due to a change in relative wave heading or to transition to a more short-crested seaway.

The data are insufficient to permit any evaluation of the RCS effectiveness in this sea state. However, the on-board observers felt that the system was effective even though the speeds were only in the 9-10 knot range. This is due to the fact that in large waves the cushion often vents to atmosphere under the sidehulls and seals. During subsequent recompression of the cushion, there can be a spike in the cushion pressure (and LCG vertical acceleration). It was felt that the RCS attenuated a large number of the pressure spikes that would have occurred.

Figure 8-42 shows the LCG vertical accelerations in 1/3-octave band format for the first three (3) Sea State V test points. The data are fairly consistent indicating that the seaway and the heading probably remained constant during the 1 hour period in which these test segments were recorded. Based on Figure 8-42, it appears the heave accelerations in Sea State V at 9 knots are comparable to the heave accelerations measured in Sea State IV at 20 knots (Figure 8-41). This is explained by the fact that the lower ship speed in Sea State V is compensating for the larger wave heights.

FIGURE 8-42 SEA STATE V VERTICAL ACCELERATION PER 1/3 OCTAVE BAND - 30 KNOTS - 300 LIFT FAN RPM - RCS ON

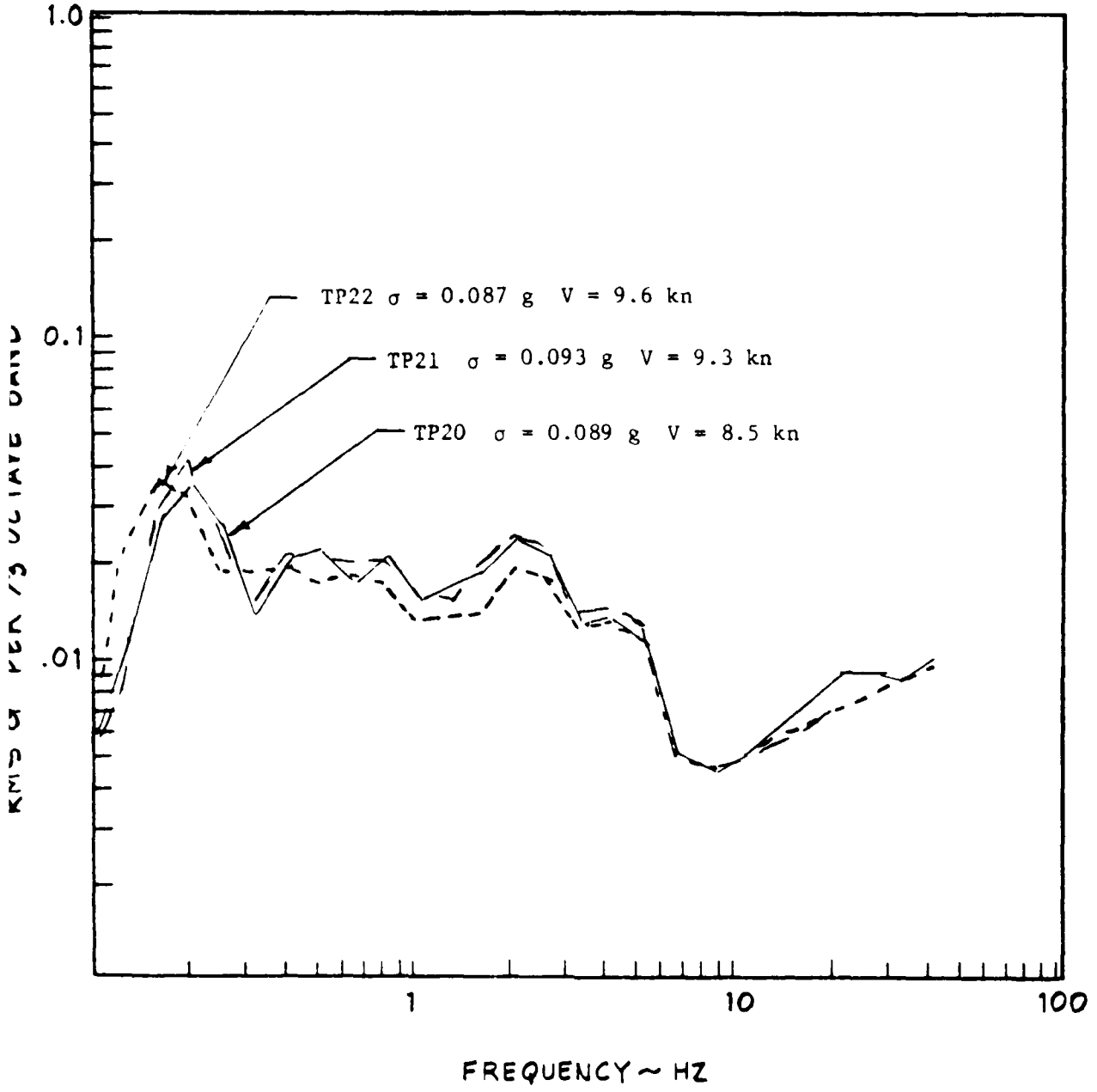

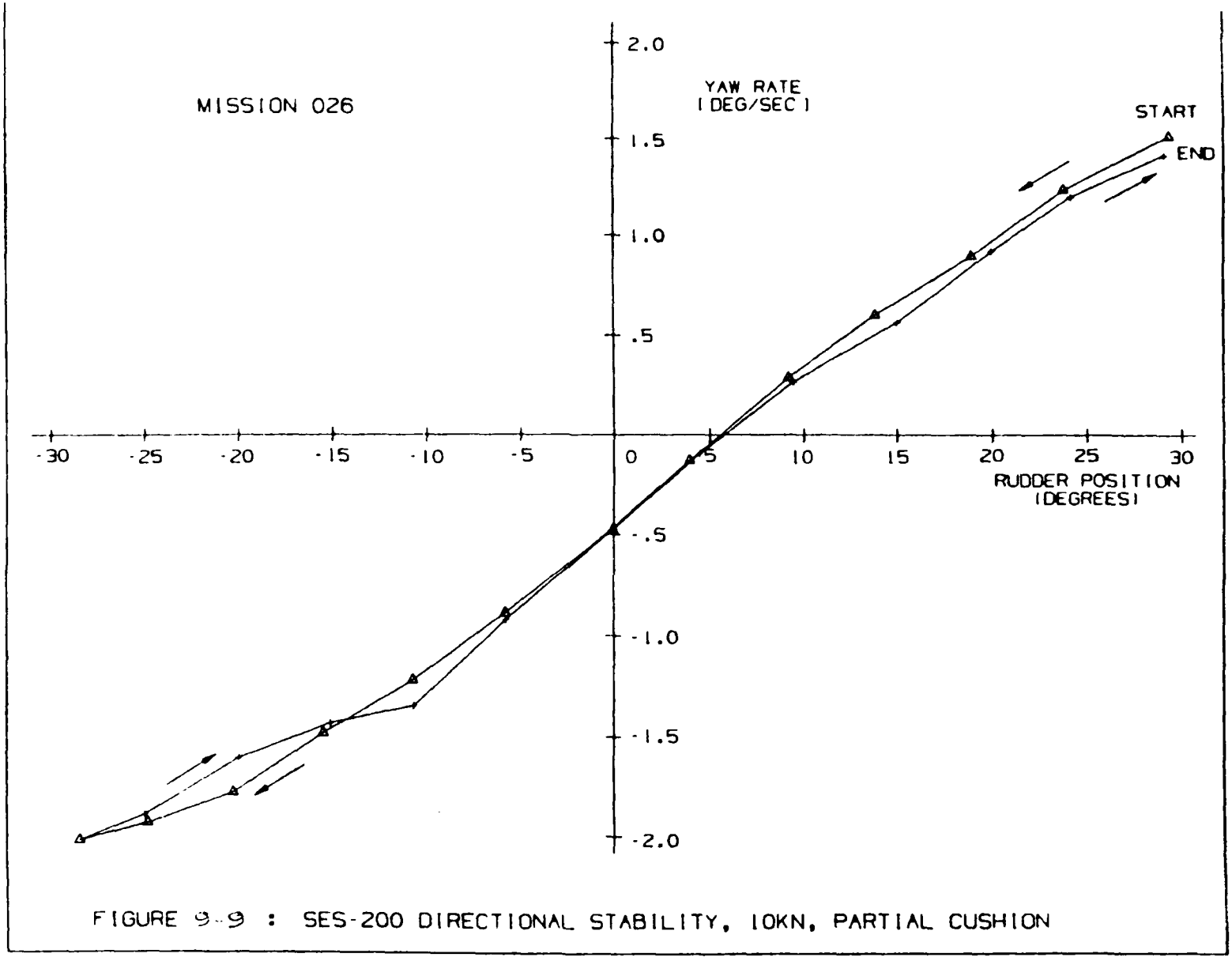

FIGURE 9-9 : SES-200 DIRECTIONAL STABILITY, 10KN, PARTIAL CUSHION

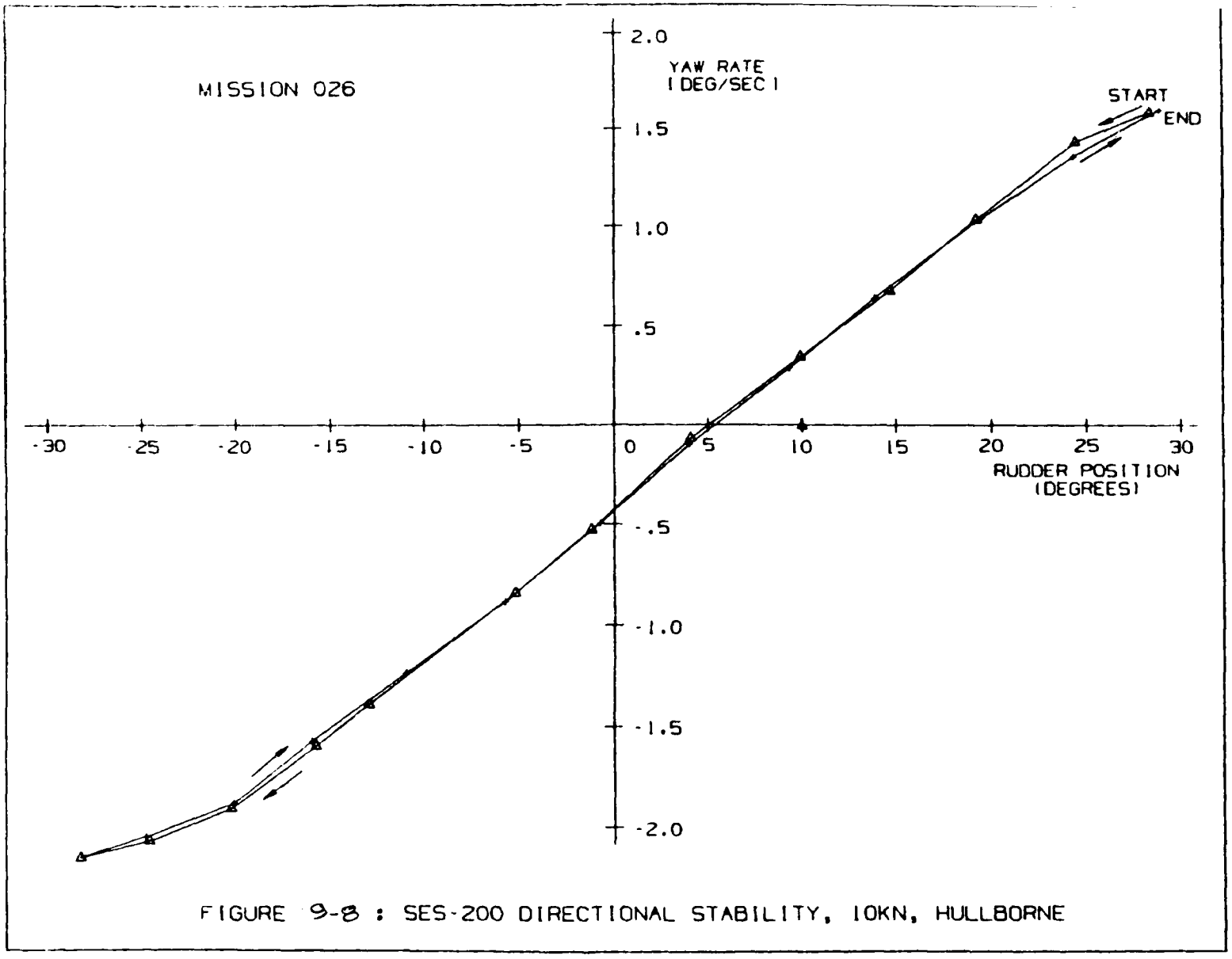

FIGURE 9-8 : SES-200 DIRECTIONAL STABILITY, 10KN, HULLBORNE

9.2 STABILITY

9.2.1 Directional Stability

The SES-200's ahead directional stability characteristics were measured by performing Dieudonne spiral maneuvers during Missions 26, 54 and 70.

In the spiral maneuver, the vessel is steadied on a straight course at preselected lift and propulsion settings. Once the steady speed condition is established, lift and propulsion power is left alone for the duration of the maneuver. The spiral is initiated by turning the rudder hard over in one direction. This position is maintained until the vessel's rate of turn reaches a constant value. In succeeding steps, the rudder is moved in 5 degree increments toward the hard over position in the opposite direction. At each step, the rudder position is held until a constant turn rate is established. Upon reaching the full opposite rudder position, the helm is returned to the original hard over position in the same increments.

The spiral maneuver provides data on the variation in ship's turn rate with rudder position from hard starboard to hard port and back to hard starboard. A plot of the vessel's yaw rate versus rudder angle from this data is indicative of a vessel's directional stability. In a directionally stable vessel, increases in rudder angle from the nominal center position will produce corresponding increases in yaw rate and decreases in rudder angle toward the center position will reduce the yaw rate.

Figures 9-8 through 9-13 are plots of SES-200 spiral maneuver data for normal ahead operation with both propulsion engines and both rudders functioning. Figures 9-8 through 9-10 show hullborne, partial cushion and full cushion spiral data, respectively, for an initial speed of 10 knots prior to starting the maneuver. Figures 9-11 and 9-12 show partial and full cushion spiral data, respectively, for an initial speed of 20 knots and Figure 9-13 shows spiral data for full cushion operation using maximum propulsion power. The partial cushion and full cushion spirals were conducted using 1300 and 1700 lift fan RPM, respectively.

Based on the data presented in these figures, the SES-200 would be judged directionally stable for normal ahead operation in the hullborne, partial cushion and full cushion operating modes. The SES-200's yaw rate response to rudder deflection from the nominal center position increases in all cases and there are no hysteresis loops or significant changes in the slope of the measured data points. There is some indication in Figures 9-10 through 9-12 that the rudder's effectiveness did not improve beyond 25 degrees deflection in the port direction. Reasons for this are not known; however, it may simply be a matter of data scatter due to failure to achieve constant turn rates.

Figures 9-8 through 9-13 show that the SES-200 requires between five (5) and eight (8) degrees of starboard rudder to achieve zero turn rate. During all tests except the maximum power spiral, the propeller RPMs were matched to try and ensure balanced propeller thrust. Therefore, it is not felt that unbalanced propeller performance is responsible for this offset.

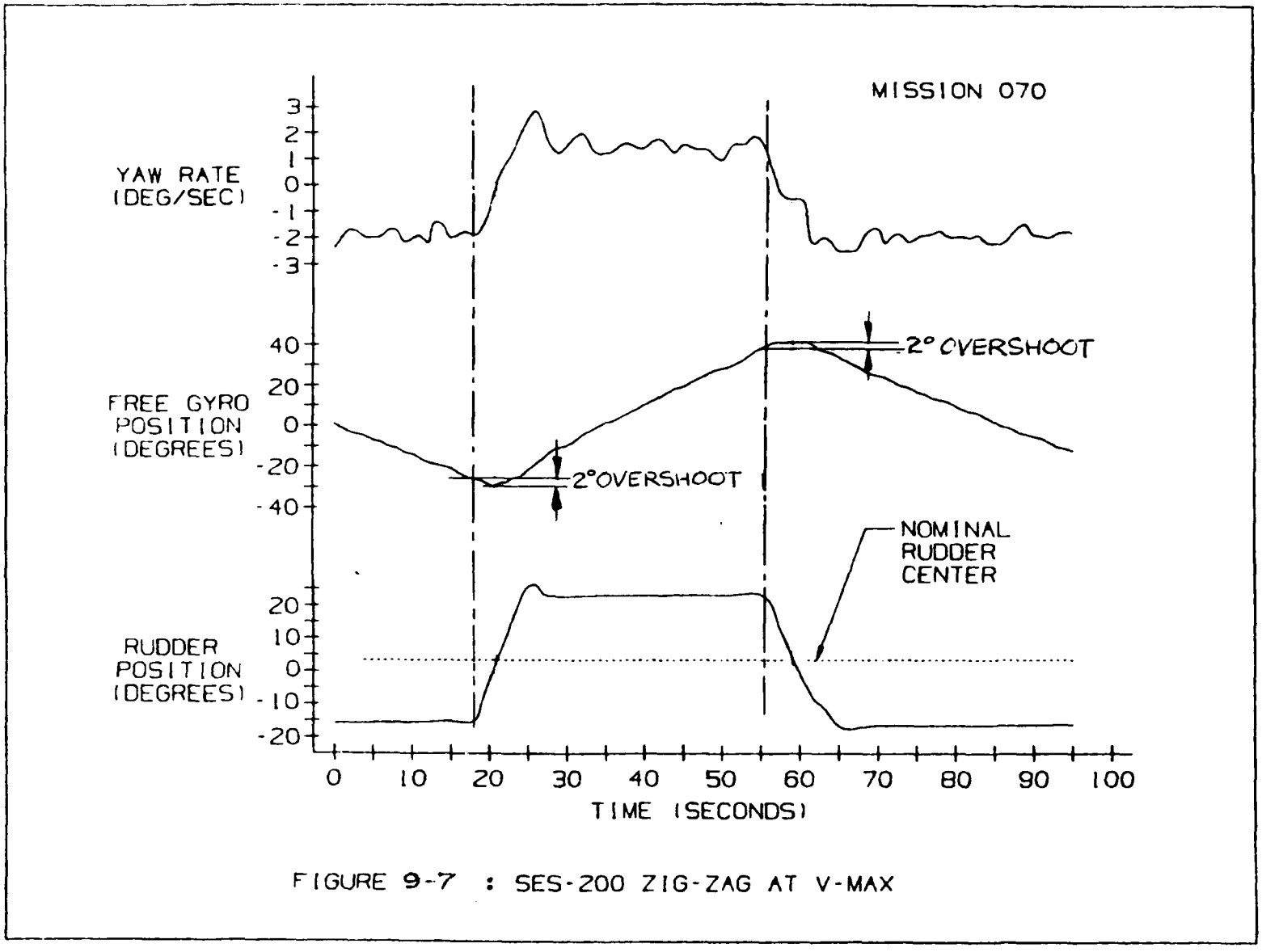

FIGURE 9-7 : SES-200 ZIG-ZAG AT V-MAX

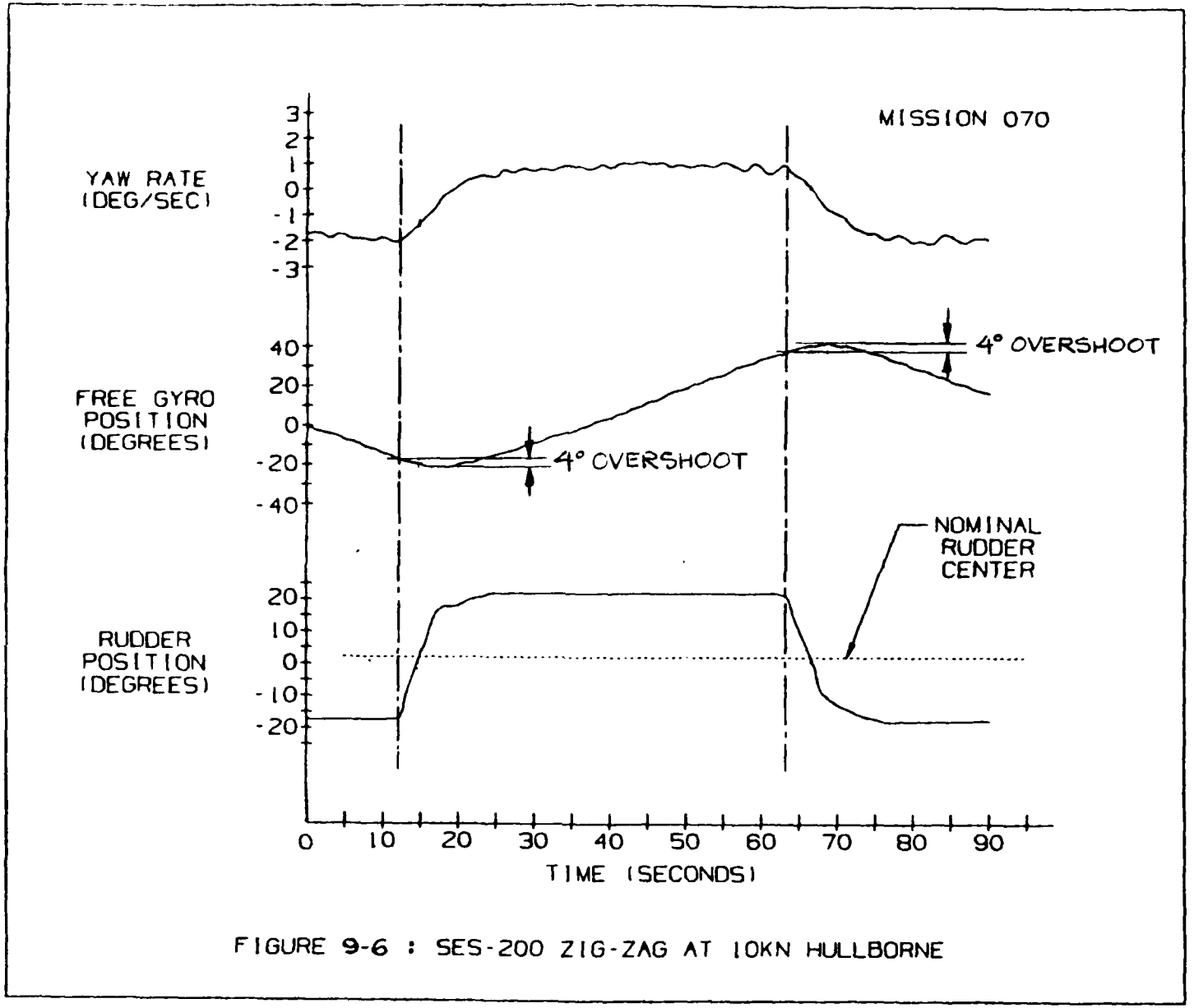

FIGURE 9-6 : SES-200 ZIG-ZAG AT 10KN HULLBORNE

9.1.3 Zig-Zag Maneuvers

Zig-Zag or Kemp maneuvers were performed during Missions 54 and 70 to measure the ship's response to the rudder. The test procedure followed is given below:

1. The SES-200 is steadied on a straight course at a preselected nominal speed. Once the steady speed is established, the lift and propulsion controls are not adjusted for the duration of the maneuver.

2. Next the rudder is deflected to starboard at maximum rate by 20 degrees from the nominal center position required to maintain a straight course.

3. This helm position is held until the gyro indicates a +20 degree course change. Then the rudder is deflected at maximum rate to port by 20 degrees from center.

4. The new helm position is held until a -20 degree change relative to the original course is indicated. Steps 2-4 are then repeated once more to complete the maneuver.

During the Mission 53 zig-zag maneuvers, the heading gyro's output to the Data Acquisition System (DAS) was found to be unuseable. Therefore, data from this mission are not presented. In Mission 70, the lack of a suitable heading measurement was corrected by installing a free gyro on the SES-200 and connecting its output to DAS.

The NATC Tracking Range was used to measure the ship's path during the zig-zag maneuvers. However, due to an oversight during Mission 70, the time code recorded on the ship's DAS was not syncronized with the tracking range. Therefore, the range data are not useable and only the DAS measurements are presented to illustrate the ship's response to the rudder.

During Mission 70, zig-zags were conducted at initial speeds of 5 and 10 knots hullborne and at 20 knots and maximum speed cushionborne using 1700 lift fan rpm. Figure 9-6 illustrates rudder position, heading and yaw rate measurements versus time during a portion of the 10-knot hullborne zig-zag. An overshoot angle of 4 degrees is indicated in the figure for this operating condition. The overshoot angle is a numerical measure of a ship's response to the helm; it is indicative of the amount of anticipation required of a helmsman while operating in restricted waters. Typically, an overshoot angle of 4 degrees is considered quite good.

Figure 9-7 illustrates a segment from the cushionborne zig-zag maneuver conducted at maximum speed. In this case, there are only 2 degrees of overshoot indicating that the SES-200 responds slightly quicker during high speed cushionborne turning than during low speed hullborne turning. Note that in both Figures 9-6 and 9-7, the helm positions were held for more than the 20 degrees of course change called for in the test procedure. This may be due to the fact that by mistake, the operators used the ship's heading gyro to judge the course change rather than the free gyro recorded on DAS. As the heading gyro was known to be in error, this would explain the lack of consistent 20-degree course changes in Figures 9-6 and 9-7.

During Mission 70, several constant power rudder turns were conducted in which the rudder position was held until the ship's compass indicated a 540 degree heading change. These tests were performed to measure the ship's final diameter in addition to the diameter of the initial 180-degree course change. The final diameter is the diameter of the ship's track after the speed and turn rate have reached constant values. Figure 9-5 illustrates the results for an initial speed of 27 knots and a rudder deflection of 30 degrees. The tactical diameter is 1264 ft (about eight ship lengths) which is comparable to the values plotted in Figure 9-4 for 30 degrees rudder deflection and maximum initial speed. Figure 9-4 shows an initial steady turning diameter of 860 ft; however, this diameter is not maintained throughout the remainder of the turn as the vessel initially slowed during the first 180 degrees and then started regaining speed. For this reason, the 860 ft diameter should not be regarded as a final turning diameter.

9.1.1.2 Constant Speed Rudder Turns

During Mission 52, several on-cushion rudder turns were conducted at constant speed. The procedure used was to set the helm at the desired position and then adjust the propulsion power to try and maintain a nominal speed of 20 knots throughout a 180-degree course change.

The results are tabulated in Table 9-1. Typically, they indicate about the same turning radius for a given rudder deflection as the constant power turns.

TABLE 9-1

SES-200 Constant Speed Turns
20 knots

RUDDER POSITION	TACTICAL DIAMETER	TIME TO TURN 180°
-10°	4430 ft	3.95 min.
-20°	2360 ft	2.17 min.
-25°	1580 ft	1.45 min.
+25°	1900 ft	1.50 min.

9.1.2 Differential Thrust Turns

Differential propeller thrust is used on the SES-200 for very low speed maneuvering such as docking. Due to the wide spacing of the propeller shafts (approximately 35 ft), the SES-200 is highly maneuverable under such low speed conditions.

At speeds above about idle ahead, differential thrust turning is typically not used as rudder turning is much more effective. An attempt was made to document the differential thrust turning performance at intermediate speed conditions during Mission 53. Tests were conducted at speeds of 10 knots hullborne and at 20 knots on-cushion using 1700 lift fan rpm.

The results from these tests are not reported as there were a number of inconsistencies in the data which could not be explained. Additionally, the operators and technical observers advised that the tests be repeated as there were a number of difficulties encountered while trying to establish the nominal differential thrust condition. These difficulties were such that they would have influenced the turn rates and diameters.

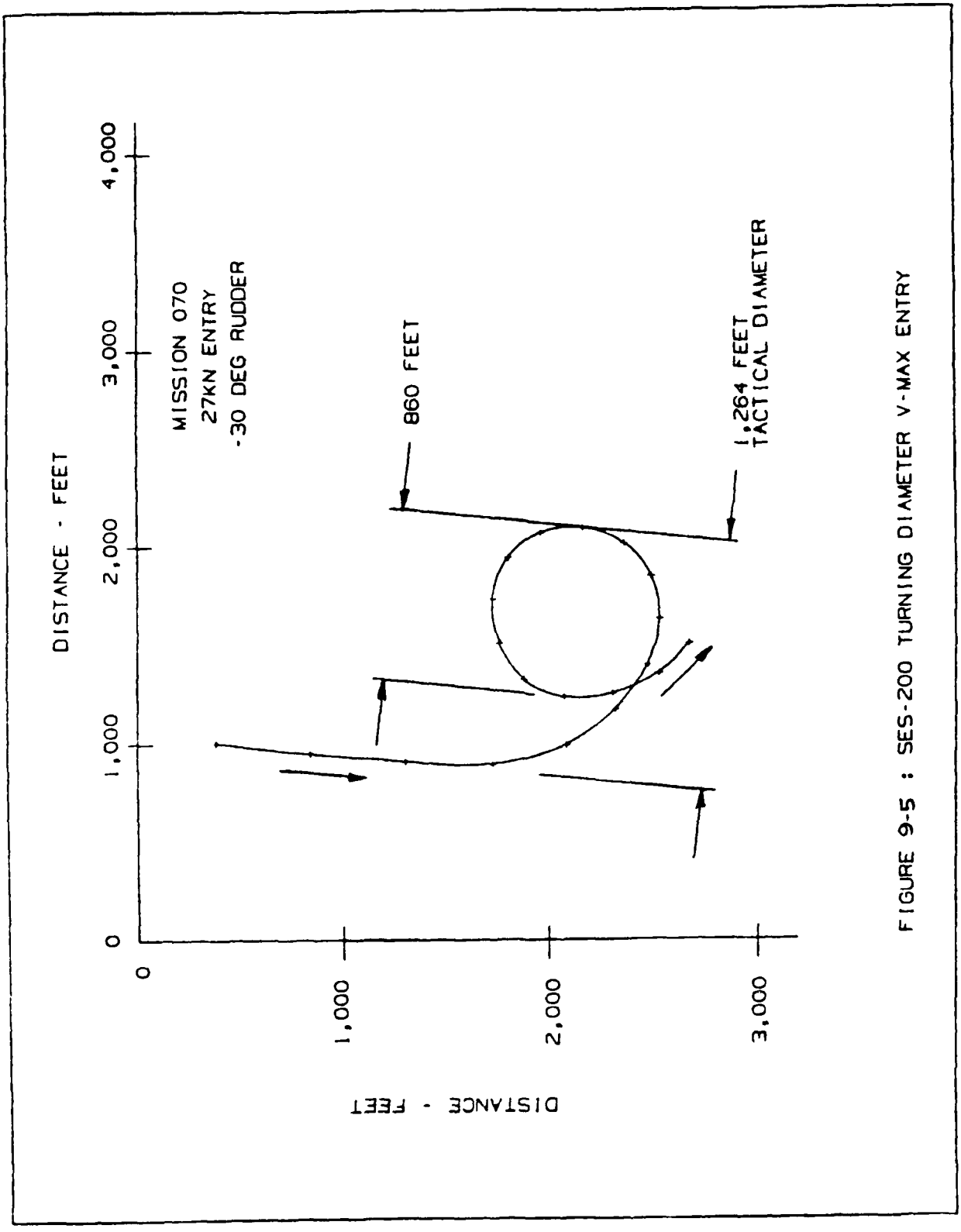

FIGURE 9-5 : SES-200 TURNING DIAMETER V-MAX ENTRY

9.1.1 Rudder Turns

9.1.1.1 Constant Power Rudder Turns

Constant power rudder turns were performed during Missions 52, 54 and 70. The procedure followed was first to set the SES-200 on a straight course at a predetermined lift setting. Next, propulsion power was adjusted to achieve a desired nominal speed. Except for the tests conducted at maximum speed, this was accomplished using matched propulsion engine RPMs. Then testing was initiated by moving the helm either 10, 20 or 30 degrees from the nominal center required to maintain a straight course. The helm was held at the new position until the ship's compass indicated a 180 degree heading change (Missions 52 and 54) or a 540 degree heading change (Mission 70). These turns are referred to as constant power as neither lift nor propulsion power is adjusted during the test point, i.e., the ship slows during the turn maneuver.

Figures 9-1 through 9-4 show the SES-200's tactical diameter (i.e., the diameter of the initial 180 degree turn) versus the change in rudder angle. The change in rudder angle is measured relative to the rudder position required to maintain a straight course. Typically, the SES-200 requires several degrees of rudder to balance asymmetries and maintain a straight course. This is not unusual for a twin screw ship of this size. Figures 9-1 through 9-4 also show the time required to turn 180 degrees versus the change in rudder angle.

Figures 9-1 and 9-2 are for hullborne turns initiated at speeds of 5 and 10 knots, respectively. At both speeds, increasing the rudder from 10 to 20 degrees significantly reduces the tactical diameter. However, increasing the helm beyond 20 degrees has no effect at 5 knots and only makes a small reduction in the turning diameter at 10 knots.

Figures 9-1 and 9-2 indicate slightly smaller tactical diameters for pots turns than starboard turns for the initial 10 degree change of rudder position. As the rudder effectiveness changes rapidly with position in this region, any small errors in the rudder position calculation could account for the differences in port and starboard tactical diameters shown in the figures.

The results shown in Figures 9-1 and 9-2 indicate that for hullborne operation at and above 5 knots, the minimum tactical diameter for constant power turning using the rudders is about 1000 ft, i.e., about six (6) ship lengths. Due to lack of test time, no low speed cushionborne turning tests were performed for comparison.

Figures 9-3 and 9-4 are for cushionborne turns initiated at 20 and 29 knots (maximum speed), respectively. The lift fan speeds were matched at 1700 RPM for all test points. At both ship speeds, rudder effectiveness varies more uniformly with angle than it did for the hullborne turns. That is, increasing the rudder angle reduces the tactical diameter over the full range of rudder travel. For the initial 10 degrees of rudder deflection, these figures confirm the hullborne results in that they also indicate smaller tactical diameters for port turns than for starboard. Again, small errors in the rudder calibrations may account for these trends. At the higher rudder angles (20 and 30 degrees), the port turns still appear slightly tighter; however, the differences are within the scatter that would be expected for this type of test.

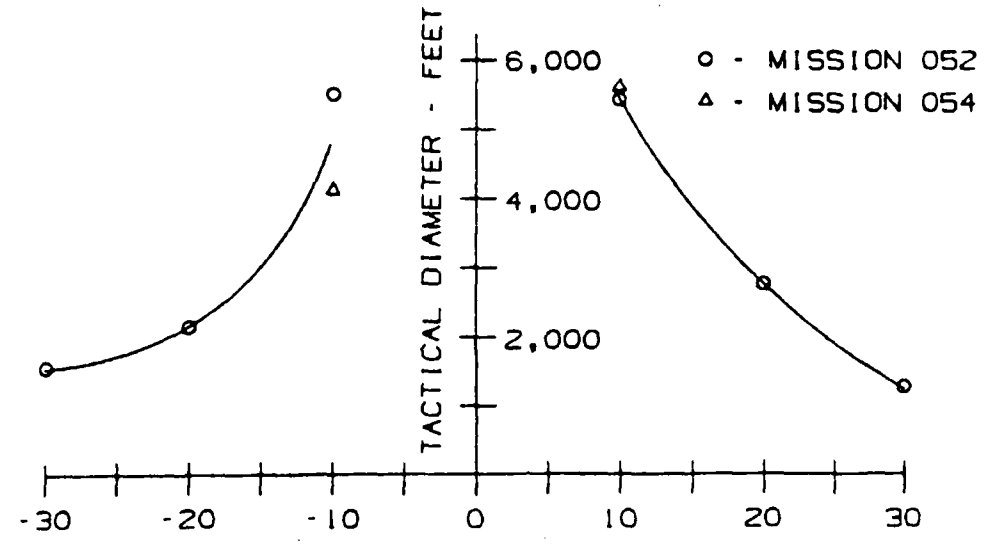

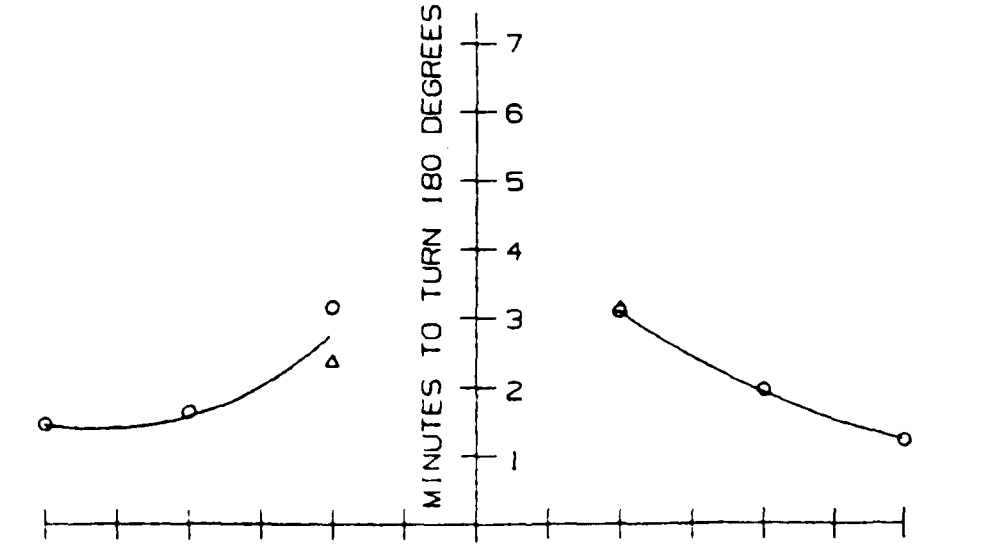

FIGURE 9-4 : SES-200 RUDDER TURNS, 29 KNOTS FULL CUSHION

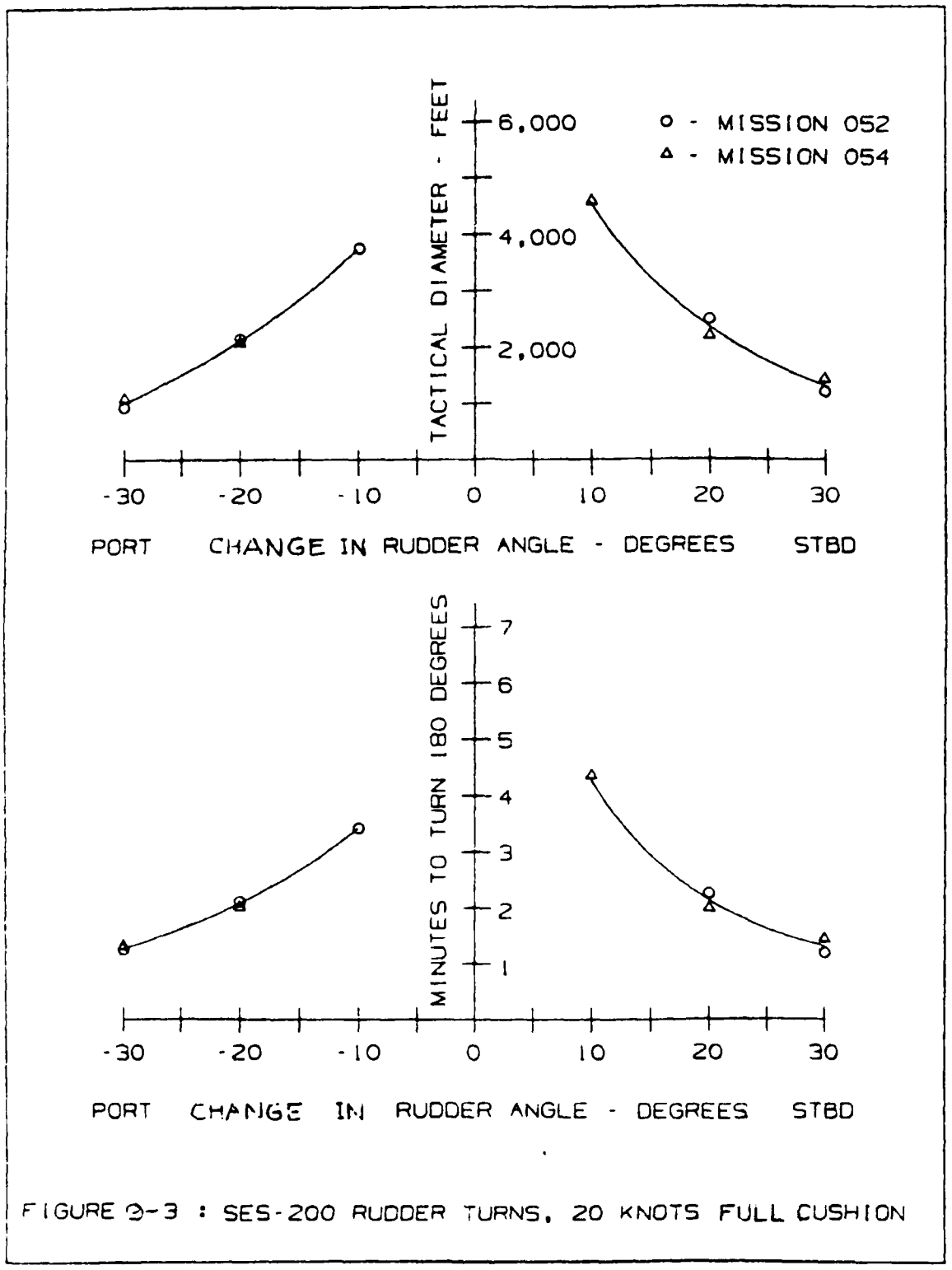

FIGURE 9-3 : SES-200 RUDDER TURNS, 20 KNOTS FULL CUSHION

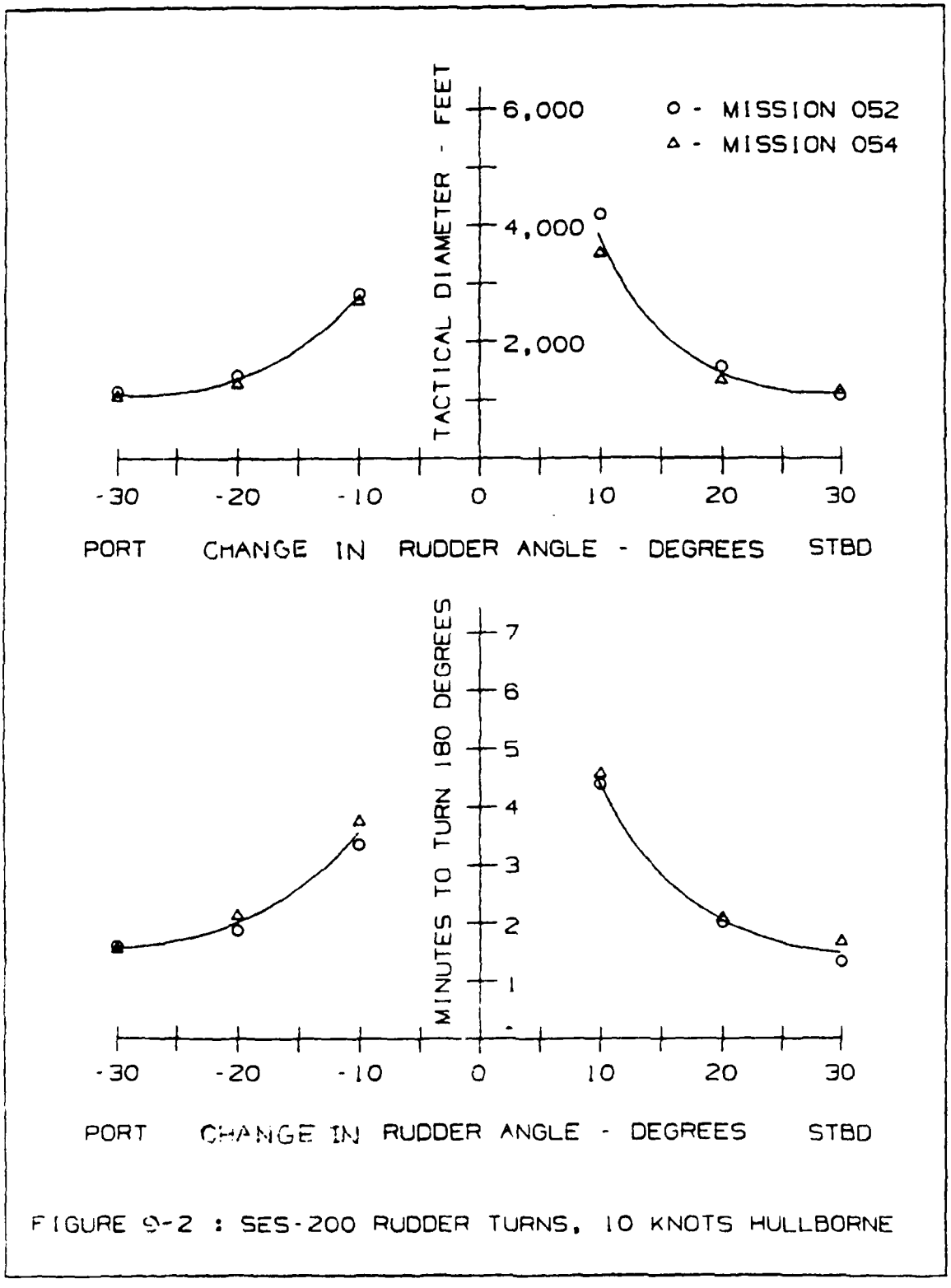

FIGURE 9-2 : SES-200 RUDDER TURNS, 10 KNOTS HULLBORNE

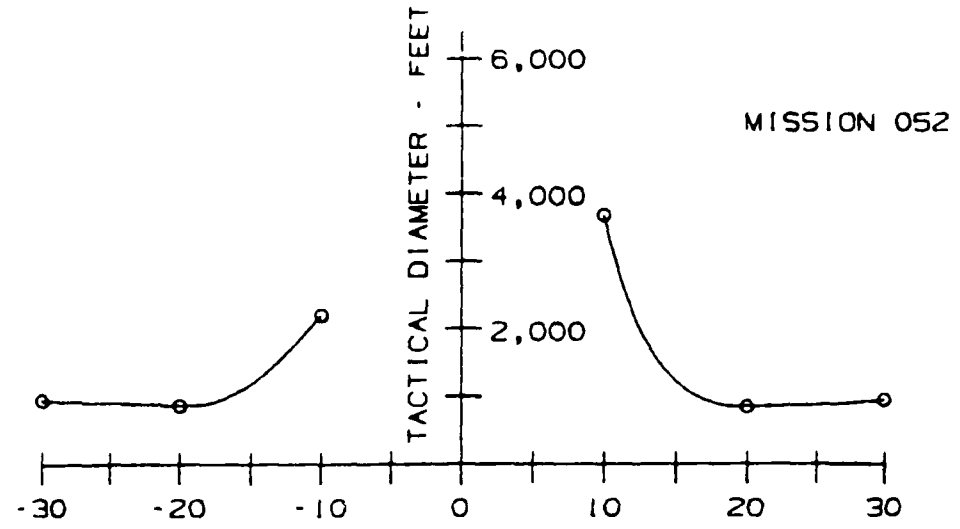

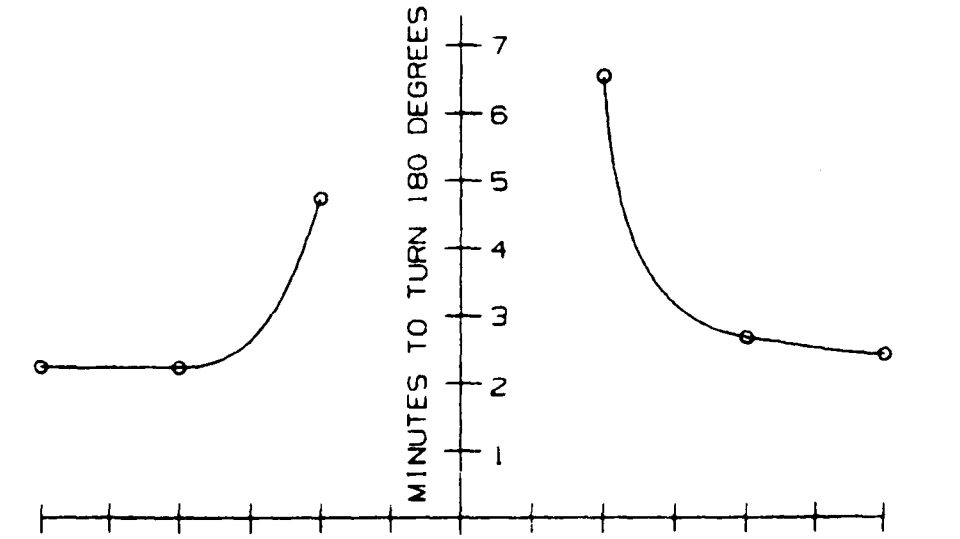

FIGURE 9-1 : SES-200 RUDDER TURNS, 5 KNOTS HULLBORNE

9. MANEUVERING AND STABILITY

Maneuvering and stability data were collected during Missions 26, 52, 53, 54, 60, 69 and 70. These missions were conducted in Chesapeake Bay in calm water and low Sea State I conditions. Tables 6-3 and 6-4 identify the types of tests conducted during each mission. Except for the Pitch Stability Tests conducted during Mission 60 and the Roll Stability Tests completed during Missions 69 and 70, all tests were conducted at the light ship test condition. Mission 60 was conducted at the heavy ship test condition. The displacement during the Roll Stability Tests was between 170 L.T. and 183 L.T., which is intermediate between the light and heavy ship test conditions.

During all maneuvering and stability tests except Mission 70, the rudders tended to drift off the position held at the start of a test point. When this drift exceeded the 4-6 degree deadband in the feedback loop, the rudders would be automatically reset at the commanded position after which they would start drifting again. This sequence was repeated on the order of once every minute or about 2-3 times during a 180° turn initiated at 20 knots. Regardless of the initial rudder position, the drift was always toward the positive rudder direction in the SES-200's sign convention, i.e., the direction that would increase the diameter of port turns and reduce the diameter of starboard turns. As the drift was continuously corrected by the feedback loop, there is no accurate means of assessing its effect on the test results and therefore the problem is not discussed relative to the various maneuvering and stability tests. It is expected that this drift primarily contributes to increasing the scatter in the test data. Prior to Mission 70, the problem was corrected; however, as this was at the end of the test program, there was no opportunity to repeat any tests.

9.1 MANEUVERING TESTS

All maneuvering tests were confined to the area of the bay covered by the Naval Air Test Center's Chesapeake Test Range. Radar tracking equipment at the range recorded the ship's position and track heading versus time during all maneuvers performed.

The output of the tracking equipment consists of an X-Y plot of the ship's position, and a tabular printout of the ship's X and Y coordinates and the track heading versus time. The points are computed from raw data using a second order smoothing algorithm. The algorithm uses raw data recorded over the previous twenty (20) second interval at 5 pps. Every fifth solution of the smoothing algorithm is plotted and tabulated which means the plot and printout are updated once a second. The time associated with each output is the midpoint of the smoothing interval.

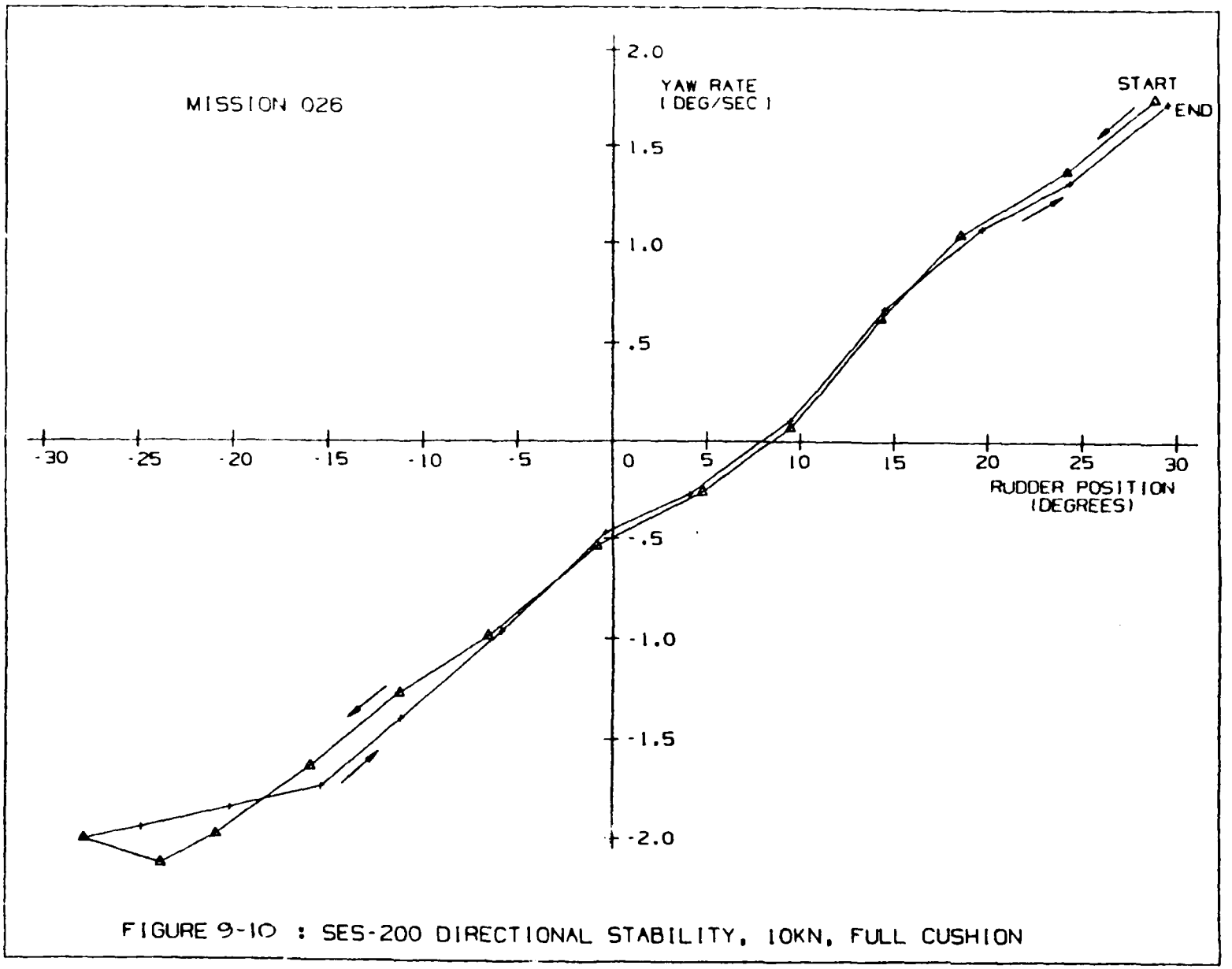

FIGURE 9-10 : SES-200 DIRECTIONAL STABILITY, 10KN, FULL CUSHION

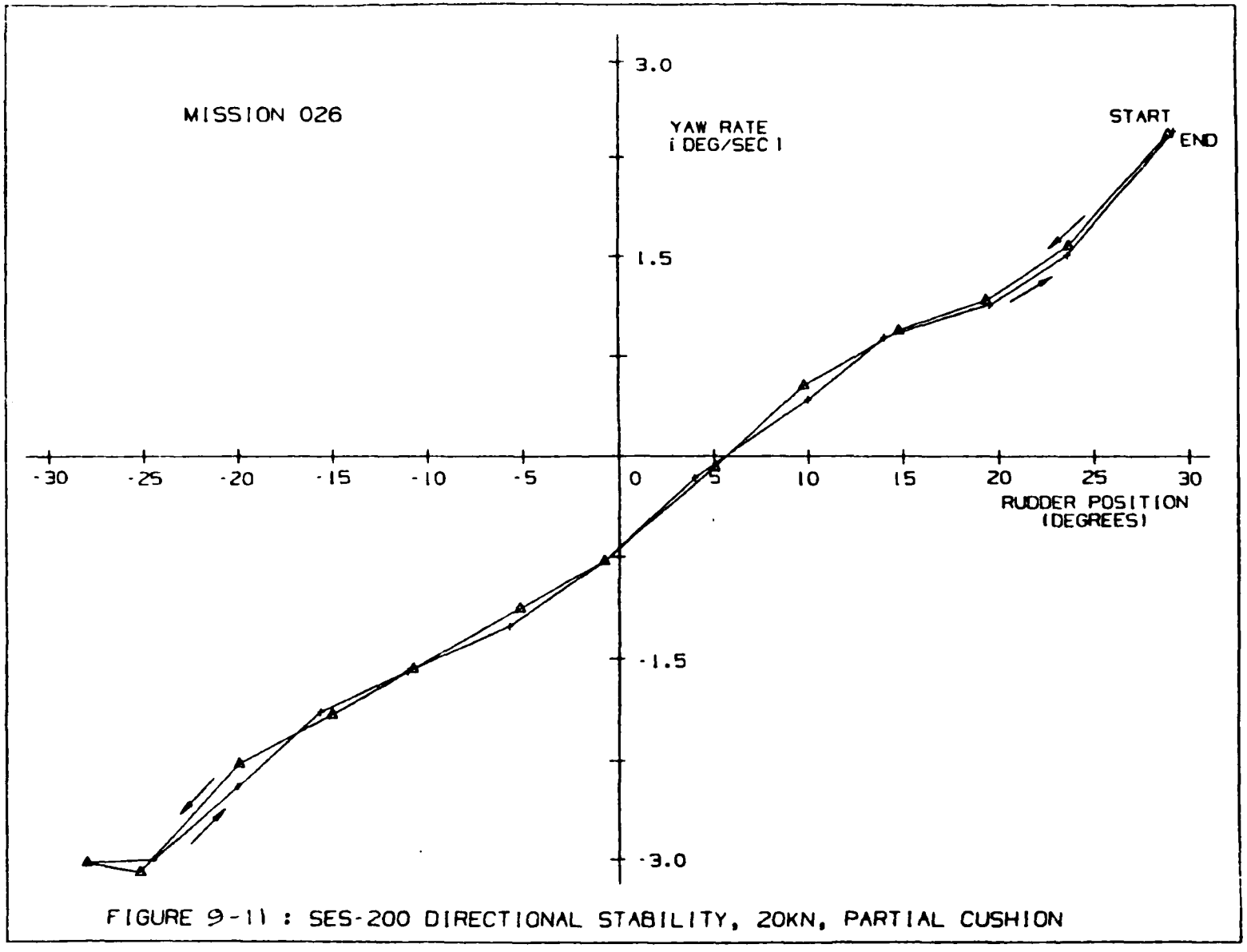

FIGURE 9-11 : SES-200 DIRECTIONAL STABILITY, 20KN, PARTIAL CUSHION

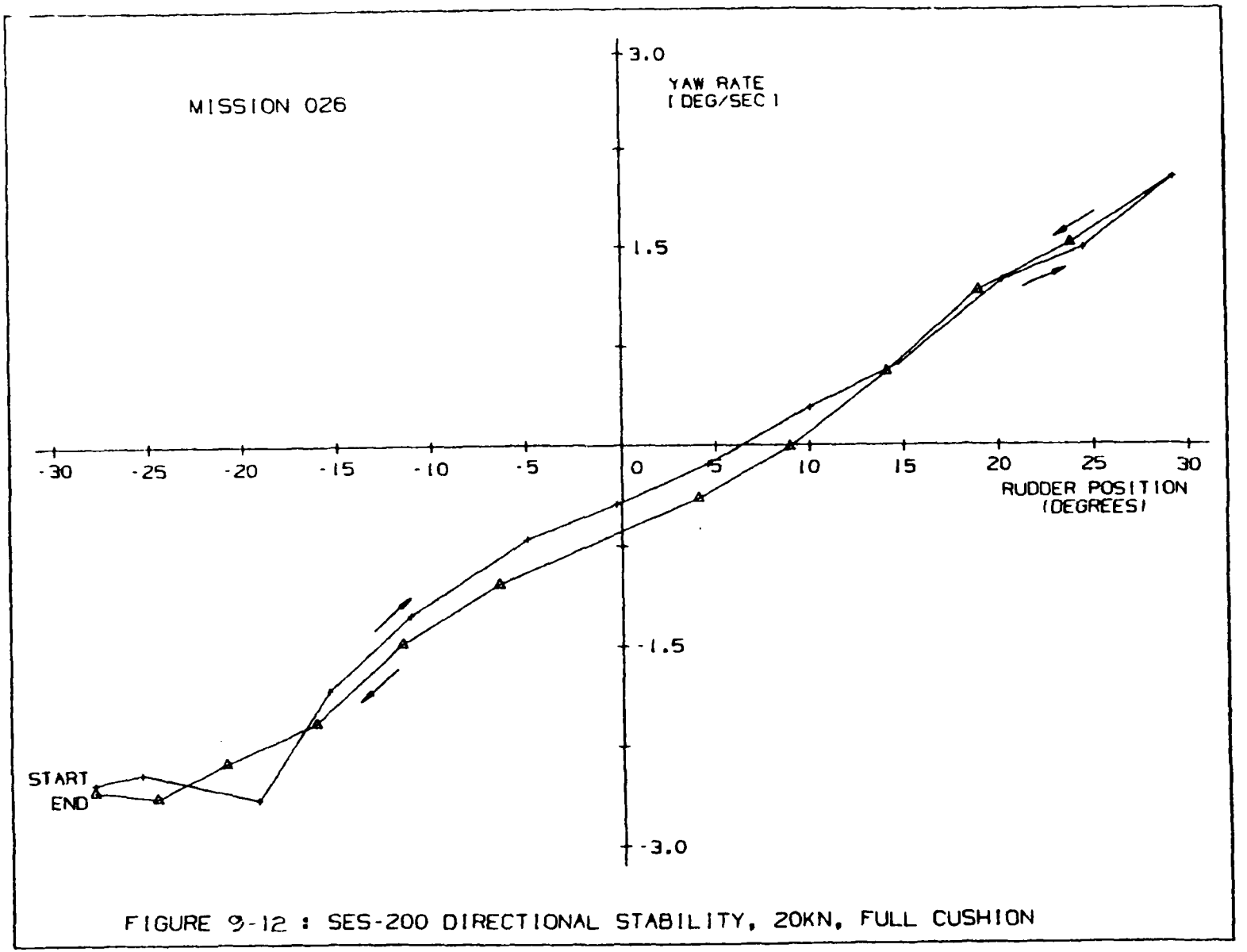

FIGURE 9-12 : SES-200 DIRECTIONAL STABILITY, 20KN, FULL CUSHION

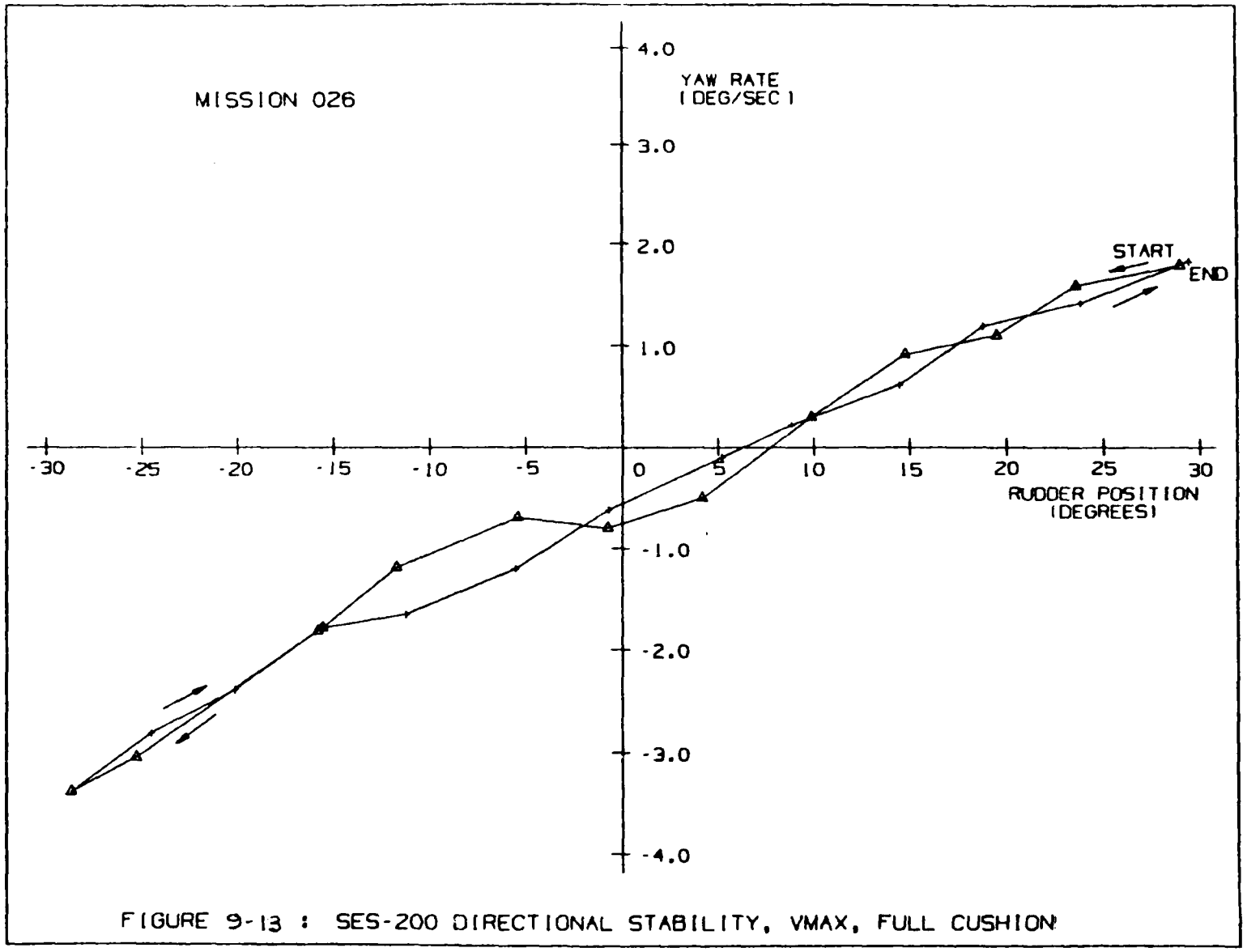

FIGURE 9-13 : SES-200 DIRECTIONAL STABILITY, VMAX, FULL CUSHION

It is likely that a dynamic or geometric asymmetry below the waterline is responsible. Since the propellers rotate in opposite directions, the presence of a lateral thrust component was ruled out. During the tests, the vessel carried a small amount of port list (less than .75 degrees). This could cause the offset as the added drag on the port sidehull would require a small amount of starboard rudder to maintain a straight course. It is also possible that the rudder calibrations are in error and therefore it was planned to measure the actual rudder positions versus the bridge and DAS indicators when the SES-200 was lifted at the conclusion of the Technical Evaluation. However, weight considerations during the lift necessitated removing the DAS and therefore this check was not performed.

Regardless of the reason for this offset, it is not considered serious and its presence does not detract from the conclusions drawn regarding the ship's directional stability. It is fairly common for a twin screw ship of the SES-200's size to carry a small amount of rudder to balance asymmetries.

Two spiral maneuvers were conducted to judge the SES-200's directional stability for impaired conditions. The results presented in Figure 9-14 illustrate the spiral data for operation using one propulsion engine (the port side) and both rudders. The data were taken for an initial speed of 10 knots using 1700 lift fan RPM. The data show that the ship would be judged directionally stable for single-engine operation. There is more scatter in the data in Figure 9-14 than in the tests using both engines. This may be due to the fact that with one engine secured, it was harder to judge when the vessel's turn rate had sufficiently stabilized to take a data point.

Figure 9-15 illustrates spiral data for operation using one propulsion engine and one rudder. In this case, both the port rudder and the port propulsion engine were secured. The data were taken for an initial speed of 10 knots using 1700 lift fan RPM. Based on the plot, the vessel would be judged directionally stable for this impaired condition also. The comments made regarding data scatter in Figure 9-14 are applicable here also.

9.2.2 Pitch Stability

During Mission 60, pitch stiffness tests were conducted to measure the variation in mean trim angle with longitudinal center of gravity (LCG) position. The results obtained are indicative of the ship's static pitch stability. Tests were conducted by shifting ballast water to vary the LCG position from 1 ft forward to 4 ft aft of amidships. At each LCG position, data were recorded for three speeds (15, 20 and 25 knots) and two fan RPMs (1700 and 1900).

Figure 9-16 shows a plot of the measured trim angle versus LCG position for speeds of 17 to 18 knots and 23 to 24 knots using 1700 fan RPM. Each data set was fitted with a straight line using a linear least squares fit. These lines indicate a static pitch stiffness of 550 ft-ton per degree for 17 to 18 knot operation and 690 ft-ton per degree for 23 to 24 knot operation. In both cases, the results indicate the ship is statically stable in pitch over the range of LCG positions tested.

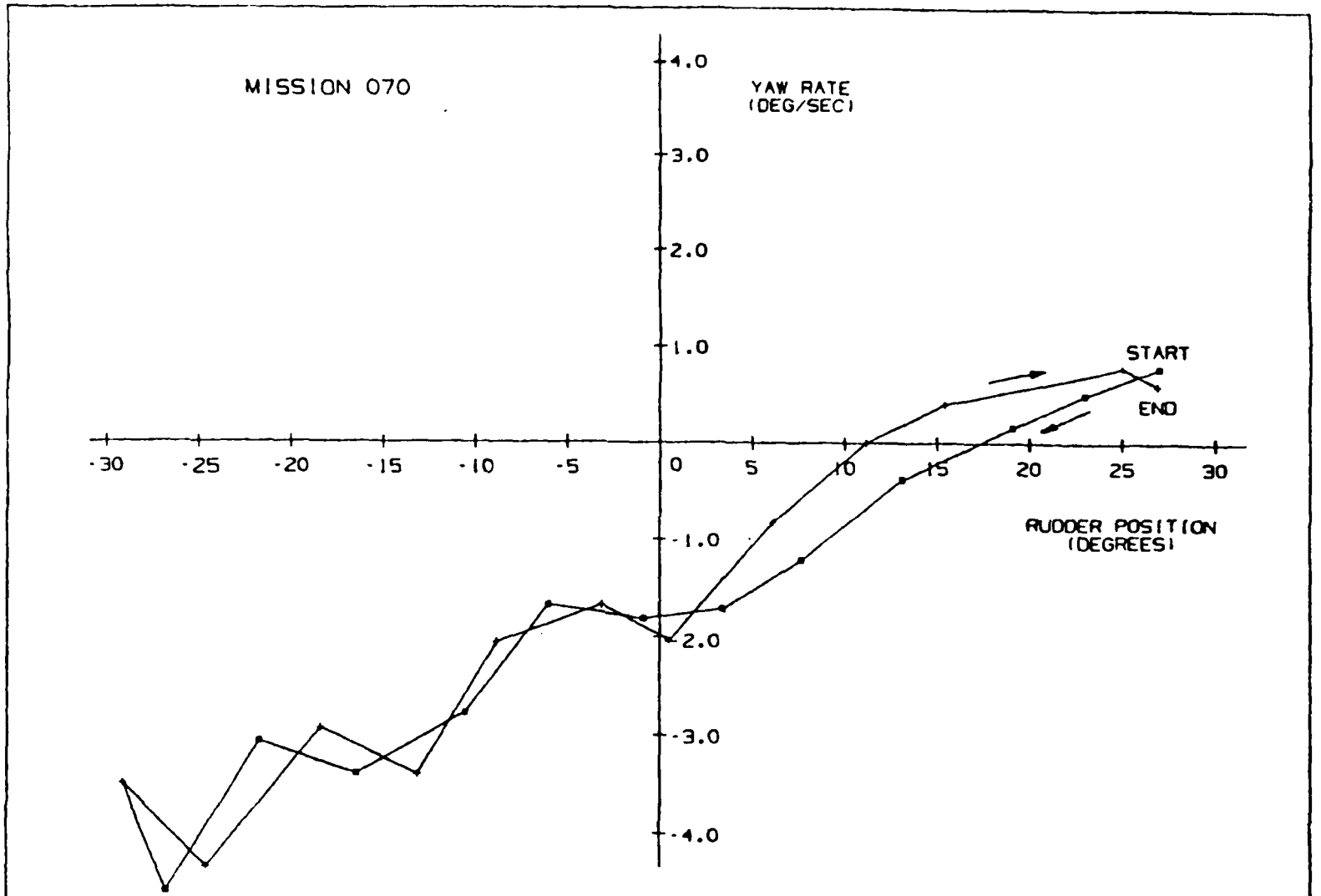

FIGURE 9-14 : SES-200 DIRECTIONAL STABILITY, 10KN, FULL CUSHION, STARBOARD PROPULSION ENGINE SECURED.

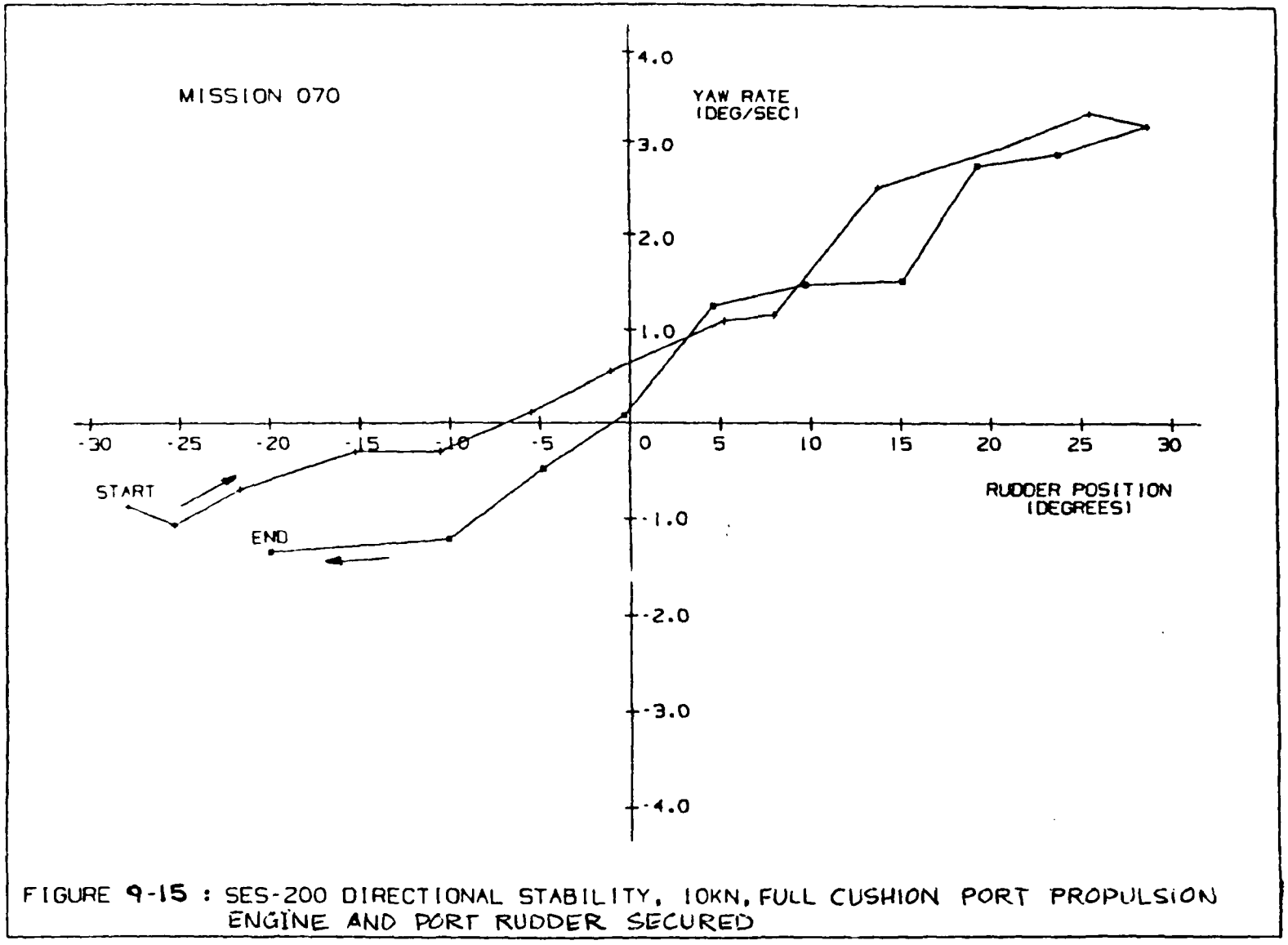

FIGURE 9-15 : SES-200 DIRECTIONAL STABILITY, 10KN, FULL CUSHION PORT PROPULSION ENGINE AND PORT RUDDER SECURED

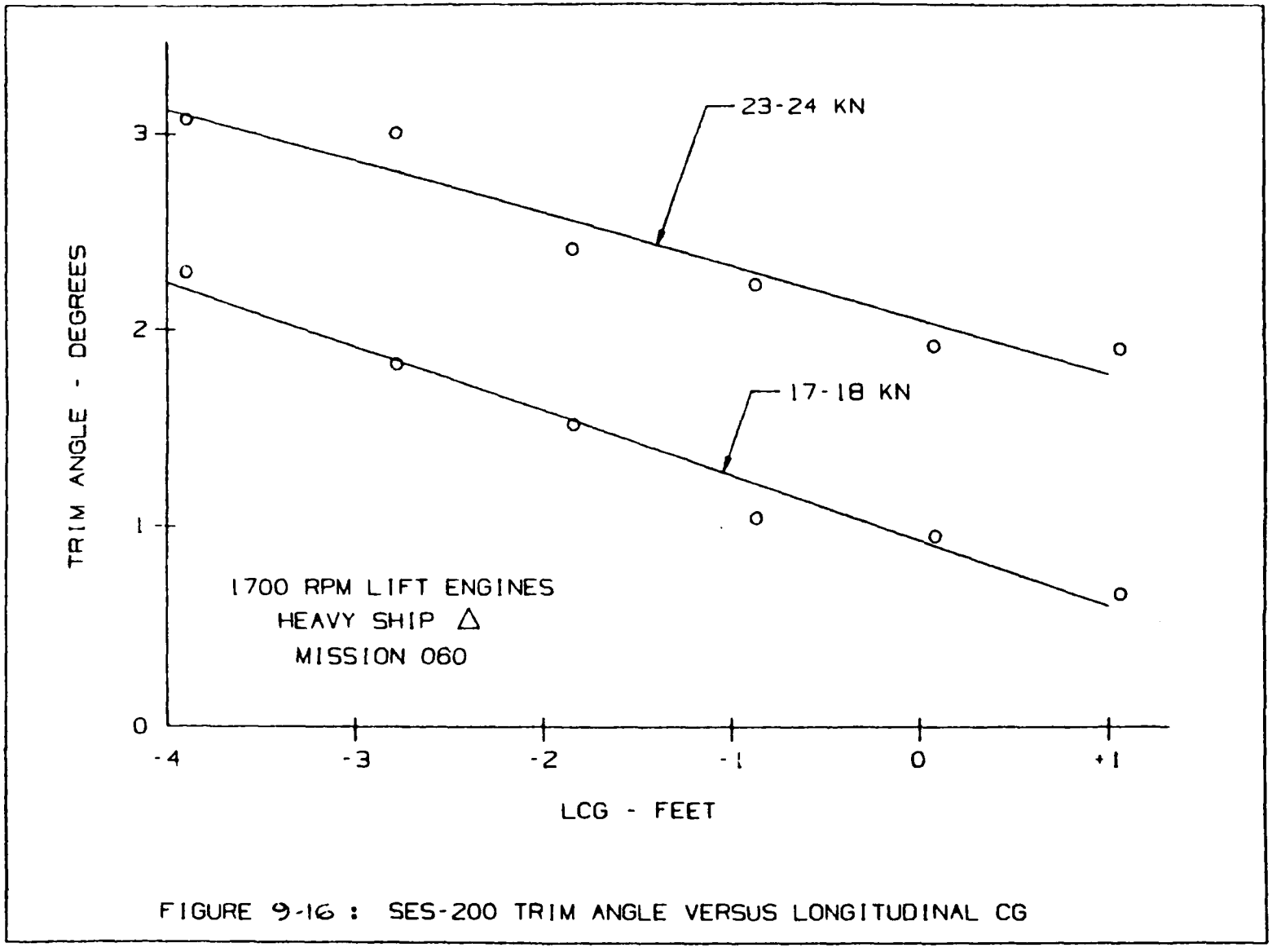

FIGURE 9-16 : SES-200 TRIM ANGLE VERSUS LONGITUDINAL CG

9.2.3 Roll Stability

During Missions 69 and 70, Roll Stiffness Tests were conducted to measure the variation in mean roll angle with transverse center of gravity (TCG) position. The tests were conducted by shifting ballast water between the Number 2 Starboard Ballast Tank and the Number 2 Port Ballast Tank to shift the TCG by .15, .33 and .47 ft off the centerline. At each TCG position, data were recorded for three speeds (18, 21 and 25 knots) and two fan RPMs (1700 and 1900).

Figure 9-17 shows a plot of the measured roll angle versus TCG position for the 21 knot speed condition at both lift fan RPMs. The lines fitted to the data using a linear least squares fit indicate a static roll stiffness of 61 ft-tons per degree at 1700 fan RPM and 41 ft-tons per degree at 1900 fan RPM. The lower roll stiffness at the higher fan speed results from the fact that the less weight is supported by the sidehulls and therefore they provide less roll restoring force. In both cases, the results indicate the ship is statically stable in roll over the range of TCG positions tested.

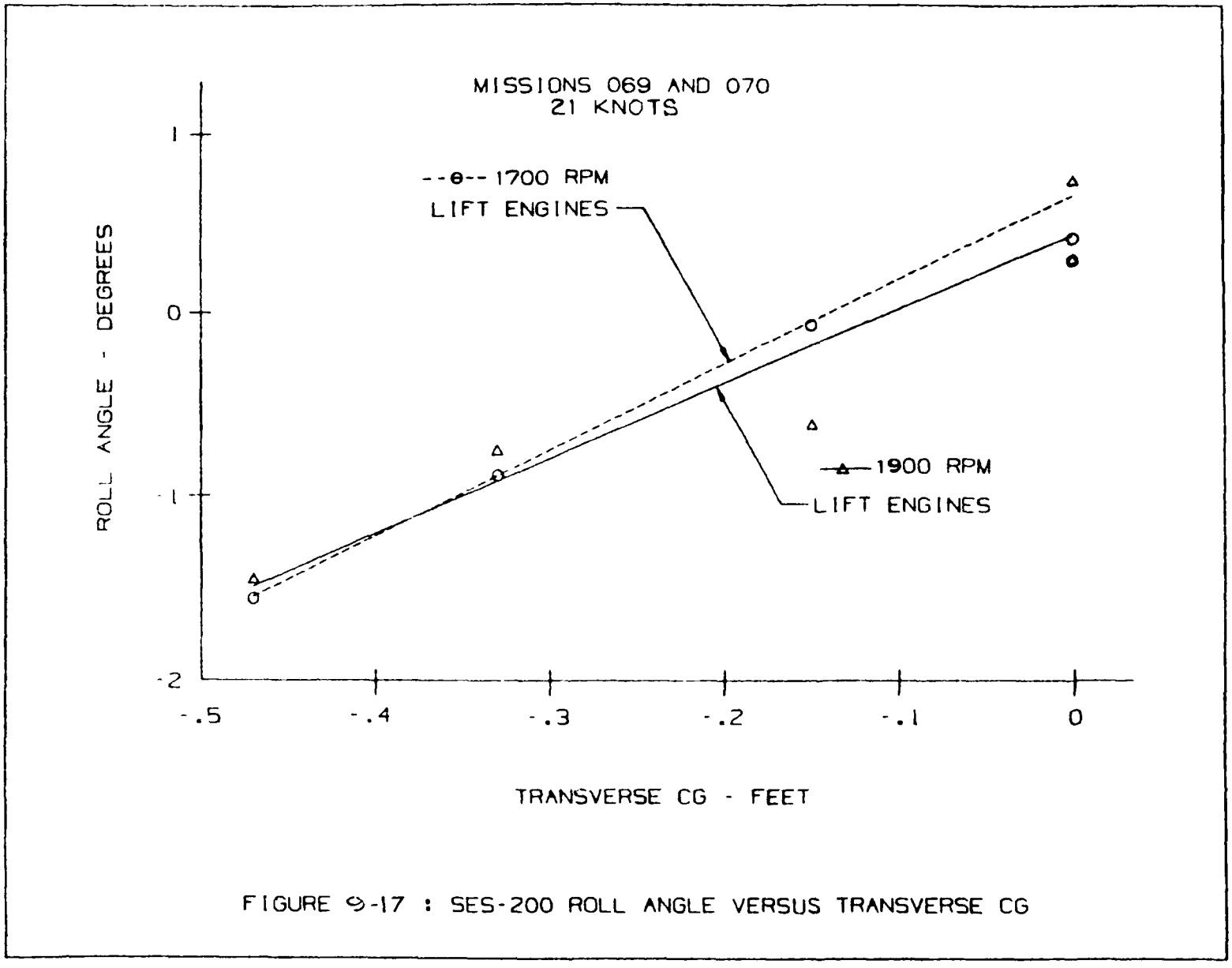

FIGURE 9-17 : SES-200 ROLL ANGLE VERSUS TRANSVERSE CG

10. REFERENCES

1-1 SES-200 Technical Evaluation Executive Summary Report, MD-R-1199-1, Maritime Dynamics, Inc., September, 1983.

2-1 Test and Evaluation of the Bell-Halter 110-ft Surface Effect Ship Demonstration Craft, P. K. Spangler, Report No. 6660-60, Naval Sea Systems Command Detachment, Norfolk, VA, February, 1981.

2-2 SES-110 Acceptance and Evaluation Trials, May-June, 1981, SESTF Report No. 183, Surface Effect Ship Test Facility, Patuxent River, MD.

2-3 Technical and Operational Evaluation of USCG DORADO (WSES-1), Report No. CG-D-44-82, USCG Research and Development Center, Avery Point, Groton, CT, August, 1982.

4-1 High Length-to-Beam Ratio Surface Effect Ship, A. G. Ford, R. N. Wares, W. F. Bush, S. J. Chorney, Report No. DTNSRDC-78/064, David Taylor Naval Ship Research and Development Center, Bethesda, MD, July 1978.

4-2 The Wave Resistance of an Air Cushion Vehicle, L. J. Doctors, University of Michigan, Ann Arbor, MI, December 1970.

4-3 Powering Predictions for Surface Effect Ships Based on Model Results, R. A. Wilson, N. King, C. E. Heber, J. A. DiJoseph, Report No. DTNSRDC-78/602, David Taylor Naval Ship Research and Development Center, Bethesda, MD, July 1978.

4-4 Wave and Sea Scale for Fully Arisen Seas, Neumann Wind/Wave Relationship, Wilbur Marks, David Taylor Model Basin.

4-5 Seakeeping by Design, Comstock & Keane, Naval Engineers Journal, Vol. 92, No. 2, April, 1980.

6-1 SES-200 Test Plan, Surface Effect Ship Test Facility, Naval Air Station, Patuxent River, MD, November, 1982.

6-2 Statement of Work, Technical Evaluation of the SES-200, U. S. Coast Guard, Office of Research and Development, Washington, DC.

6-3 SES-200 Operational Test Matrices, Surface Effect Ship Test Facility, Naval Air Station, Patuxent River, MD, March, 1983.

6-4 SES-100A Ride Control System Test Requirements, TN-1048-002, Maritime Dynamics, Inc., Tacoma, WA, October, 1976.

6-5 Bendat, Julius S. and Piersol, Allan G., Random Data: Analysis and Measurement Procedures, Wiley-Interscience, 1971.

6-6 Brady, J. J. and Cosgrove, W. J., Methods and Formulation of the SESTF Power Spectral Density Computer Routine, Dept. of the Navy, Surface Effect Ship Test Facility, Naval Air Station, Patuxent River, MD, October, 1975.

6-7 Burington, Richard Stevens and May, Donald Curtis, Handbook of Probability and Statistics with Tables, McGraw-Hill, New York, NY, 1970.

6-8 Crow, Edwin L., Davis, Frances A. and Maxfield, Margaret W., Statistics Manual, Dover Publications, Inc., New York City, NY, 1960.

6-9 Bloomfield, Peter, Fourier Analysis of Time Series: An Introduction, John Wiley & Sons, New York City, NY, 1976.

6-10 Surface Effect Ship Test Facility, Statistical and Histogram Program Documentation

6-11 Eykhoff, Pieter, System Identification, Wiley-Interscience, New York, NY, 1977.

6-12 SES-100A Wave Height Sensor Performance Requirements, MDR 1049-53, Maritime Dynamics, Inc., Tacoma, WA, March, 1977.

7-1 The Wave Resistance of an Air Cushion Vehicle, L. J. Doctors, Dept. of Naval Architecture and Marine Engineering, University of Michigan, December, 1970.

7-2 SES-200 Operator's Manual, Bell-Halter, Inc., New Orleans, LA.

7-3 Test and Evaluation of the Bell-Halter 110-Foot Surface Effect Ship Demonstration Craft, P. K. Spangler, Report No. 6660-60, Naval Sea Systems Command Detachment, Norfolk, VA, February, 1981.

APPENDIX A

SES-200 HULL MATERIALS/MACHINERY/OUTFIT

HULL MATERIALS	
n Deck Forward	3/16-inch 5086 aluminum
n Deck Aft	1/4-inch 5086 aluminum
e Plating	1/4-inch and 5/16-inch 5086 aluminum
tom Plating	1/2-inch 5086 aluminum
Deck Plating	1/2-inch, 3/16-inch, 1/4-inch 5086 aluminum
kheads	1/8-inch, 3/16-inch, 1/4-inch 5086 aluminum
FRAMING	
gitudinal Framing with Subdivision Bulkheads	
LOWER DECKHOUSE	
ting (Sides)	1/8-inch and 3/16-inch aluminum
ting (Roof)	1/8-inch and 3/16-inch 5086 aluminum
UPPER DECKHOUSE	
ting (Sides)	1/8-inch and 3/16-inch aluminum
ting (Roof)	1/8-inch 5086 aluminum
DECK FITTINGS	
minum Bitt	One twin-post, 5-inch, heavy-duty
Bitts	Two twin-post, 4-inch, heavy duty aluminum
Beam	Two single-post, 5-inch, heavy-duty aluminum
rter Bitts	Two twin-post, 4-inch, heavy-duty aluminum
ern Bitts	Two twin-post, 4-inch, heavy-duty aluminum
SOLE PLATING	
cond Deck	1/8-inch and 3/16-inch 5086 aluminum

AD-A152 344 SES-200 (SURFACE EFFECT SHIP) TECHNICAL EVALUATION TEST REPORT(U) MARITIME DYNAMICS INC TACOMA WA J D ADAMS ET AL. JAN 84 MD-R-1199-2 USCG-D-1-85 3/3

UNCLASSIFIED N00167-83-C-0047 F/G 13/10 NL

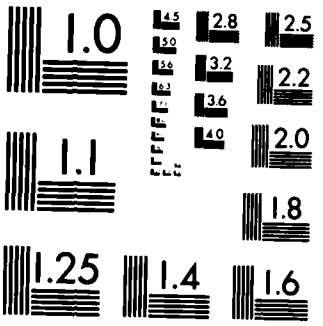

MAIN MACHINERY	
Main Engines	Two GM 16V-149TI engines, diesel, turbo-charged, intercooled, heat exchanger cooled, air start, 180-mm injectors, 1600 hp at 1900 rpm.
Gears	Two Reintjes WAV-800 reverse reduction gears. Input shafts, identical rotation; output shafts, opposite rotation.
Lift Engines	Two GM 8V-92TI engines, diesel, turbo-charged, intercooled, heat exchanger cooled, air start, 445 hp at 2100 rpm.
Lift Fans	Two Bell Textron 42-inch welded aluminum, centrifugal fans--direct driven from engines.
Generator (Primary)	One GM 3-71 55-kW, heat exchanger cooled, 24-V starting - 208 Vac.
Generator (Standby)	One KATO KAMAG 14 40-KW, clutch-driven off port lift engine.
Steering	Four-station system: One pilothouse forward One pilothouse astern Two bridge wings
Engine Controls	Main engine throttle and gear selector at each station. Lift engine throttle and clutch at pilothouse forward station.
Ride Control System	Four MariDyne Vent Valves mounted on the main deck, 32 gpm hydraulic system clutch-driven off the STBD lift engine, MariDyne Electronic Control Unit on the bridge.
UNDERWATER GEAR	
Propellers	Gawn Burrill three-bladed bronze, 40-inch-dia. x 51 inch pitch.
Shafts	4-inch dia. Aquamet 17 stainless steel.
Couplings	Ringfedder locking assembly, Series RFN 7012N.
Bearings	4-inch B.J. Byplex rubber bearings.

MAIN MACHINERY (Cont.)	
Bilge Pumps	One Crown 2-inch, 7.5-hp electric motor. Two Jabsco 1.5-inch, belt-driven off main engines. Two Rule 5-year - stuffing box void. Two Shur-Dri-Electrical - Rudder Compartments.
Fire Pump	One Crown 2-inch, 7.5-hp electric motor.
Air Compressors	One Quincy Model D-310 with 2-hp electric motor. One Quincy Model D-310 with 1.5-hp electric motor.
Air receiver	One Manchester, 120-gallon, 250-lb/in^2 working pressure.
Desalinization Plant	One Standard Communications Model HRO 400 - 400 gal/day reverse osmosis system.
Potable Water Pump	One Myers Ejecto 208-volt unit with 21-gallon pressure tank.
Sanitary Water Pump	One Myers Ejecto 208-volt unit with 21-gallon pressure tank.
Anchors	Two 90-pound Danforth with 360-ft of 5/8-inch stainless wire rope.
Anchor Windlass	One Vetus Electric Model "Titan" 2205-lb lifting power at 30-ft/min.
Heating and Air Conditioning	Two 5-ton Carrier units with water-cooled compressors, units equipped with 12-kW heating strips; thermostat controlled.
Hot-Water Heaters	Three 9-kW Crane Silver Monitor, two at 30-gallon capacity, one at 17-gallon capacity.

ELECTRICAL	
Generator	55-kW - 208 Vac generator set - Primary 40 kW engine-driven backup.
Generator Control Panel	One Continental Electric Services Corp. 3-phase unit.
Lighting	Incandescent and fluorescent, as required.
Batteries	Two 12-volt batteries, 24 volts for generator starting. One 12-volt, 100-ampere-hour battery for navigation lights and general alarm.
Engine Alarms	Low-lube oil, high-water temperature, all engines gear oil contamination, Reintjes gears. High bilge water levels in engine room. All alarms in pilothouse and engine room.
Windshield Wipers	Four Sprague Air-Push, compressed air driven; three on forward facing pilothouse windows and one aft facing.
ELECTRONICS	
Radio (VHF)	Decca STR-25
Radio (SSB)	Drake TRM-1
Fathometer	Morrow DS-200
Compass	Ritchie 5-inch Globe Master Series
Loran C	Decca 1024
Radar	Decca 916 TRNP
Speedometer	Kenyon KS-245 Knotmeter

GALLEY EQUIPMENT	
Stove	One Sears Kenmore electric, four-element with oven.
Refrigerators	One Sears Kenmore Model 106-7690211 side-by-side refrigerator/freezer unit.
	One Sears Kenmore Model 46H61901H refrigerator/freezer.
Freezer	One Sears Kenmore Model 47H10098N chest freezer.
INTERIOR SHEATHING	
Insulation	Foil-backed fiberglass, 3 inches thick.
Paneling	Vinyl coverings or vinyl-clad aluminum.
	Sheet coverings on bulkheads.
	Perforated metal overheads.
	Formica accents.
WATER CLOSETS	
Water Closets	Two on main deck with toilet, lavatory, and shower.
	Two on second deck with toilet, lavatory, and shower.
OUTFITTING	
Control Console	Gauges housed in Rosewood Formica in pilothouse.
Helmsman's Stool	One helmsman's stool with Naugahyde cushions.
Toilets	Four JABSCO Model 18100-0101.

OUTFITTING (Cont.)	
MSD - Type II	Two Humphrey Model 10.
Floor Coverings	Accommodations and lounge - Nylon indoor/ outdoor carpeting; pilothouse, public areas, and water closets - vinyl tile.
Windows	Fixed Lexan and safety plate in rubber and rigid frames.
Interior Doors	Varnished wood with lock sets.
SAFETY EQUIPMENT	
Fire Extinguishers (Portable)	Four 15-pound CO_2.
	Seven 10-pound dry chemical units.
	One 2.75-pound dry chemical unit.
Fire Extinguishing System (Fixed)	One 500 pound CO_2 in engine room.
Fire Detection System	Two thermal sensors in engine rooms, alarm panels in wheelhouse and galley.
Life Floats	Two 25-person inflatable life rafts with paddles.
Life Jackets	USCG-approved jackets for 21 persons.
	All required safety equipment.
HULL PROTECTION	
Anodes	Installed as required to ward off electrolytic action.

METRIC CONVERSION FACTORS

Approximate Conversions to Metric Measures

Symbol	When You Know	Multiply by	To Find	Symbol
	LENGTH			
in	inches	*2.5	centimeters	cm
ft	feet	30	centimeters	cm
yd	yards	0.9	meters	m
mi	miles	1.6	kilometers	km
	AREA			
in^2	square inches	6.5	square centimeters	cm^2
ft^2	square feet	0.09	square meters	m^2
yd^2	square yards	0.8	square meters	m^2
mi^2	square miles	2.6	square kilometers	km^2
	acres	0.4	hectares	ha
	MASS (weight)			
oz	ounces	28	grams	g
lb	pounds	0.45	kilograms	kg
	short tons (2000 lb)	0.9	tonnes	t
	VOLUME			
tsp	teaspoons	5	milliliters	ml
Tbsp	tablespoons	15	milliliters	ml
fl oz	fluid ounces	30	milliliters	ml
c	cups	0.24	liters	l
pt	pints	0.47	liters	l
qt	quarts	0.95	liters	l
gal	gallons	3.8	liters	l
ft^3	cubic feet	0.03	cubic meters	m^3
yd^3	cubic yards	0.76	cubic meters	m^3
	TEMPERATURE (exact)			
°F	Fahrenheit temperature	5/9 (after subtracting 32)	Celsius temperature	°C

*1 in = 2.54 (exactly). For other exact conversions and more detailed tables, see NBS Misc. Publ. 286, Units of Weights and Measures, Price $2.25, SD Catalog No. C13.10:286.

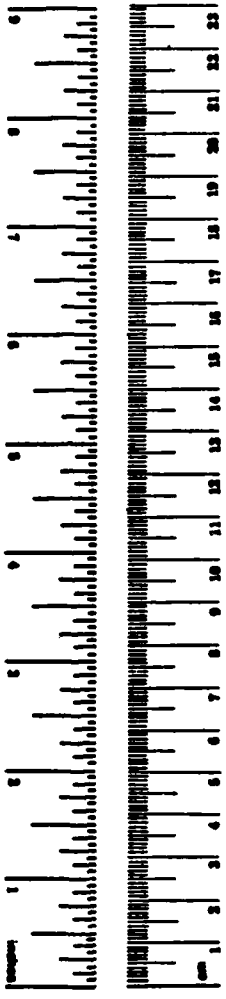

Approximate Conversions from Metric Measures

Symbol	When You Know	Multiply by	To Find	Symbol
	LENGTH			
mm	millimeters	0.04	inches	in
cm	centimeters	0.4	inches	in
m	meters	3.3	feet	ft
m	meters	1.1	yards	yd
km	kilometers	0.6	miles	mi
	AREA			
cm^2	square centimeters	0.16	square inches	in^2
m^2	square meters	1.2	square yards	yd^2
km^2	square kilometers	0.4	square miles	mi^2
ha	hectares (10,000 m^2)	2.5	acres	
	MASS (weight)			
g	grams	0.035	ounces	oz
kg	kilograms	2.2	pounds	lb
t	tonnes (1000 kg)	1.1	short tons	
	VOLUME			
ml	milliliters	0.03	fluid ounces	fl oz
l	liters	2.1	pints	pt
l	liters	1.06	quarts	qt
l	liters	0.26	gallons	gal
m^3	cubic meters	35	cubic feet	ft^3
m^3	cubic meters	1.3	cubic yards	yd^3
	TEMPERATURE (exact)			
°C	Celsius temperature	9/5 (then add 32)	Fahrenheit temperature	°F

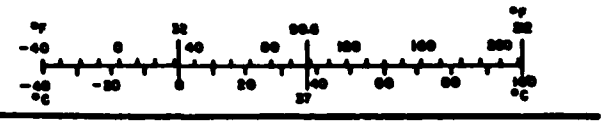

END

FILMED

5-85

DTIC